# Acid Deposition in Colorado – A Potential or Current Problem; Local Versus Long-distance Transport Into the State

A Compendium of Papers
Presented at a Workshop Sponsored by the

**Cooperative Institute for Research in the Atmosphere**

Roger A. Pielke, Editor

Colorado State University, Ft. Collins, CO

August 13-15, 1986

CIRA

Colorado State University

## PREFACE

Roger A. Pielke

The purpose of the CIRA workshop held on August 14 and 15, 1986 was to solicit information as to whether Colorado currently has an environmental problem associated with acid deposition, and whether sources of the acidic material are predominantly from outside the state or within Colorado. The list of attendees to the Workshop is presented as Appendix A. Each of the attendees was invited to prepare a written contribution for incorporation into this publication.

The consensus of the Workshop was that the Alpine lakes within the state are the locations most at risk from acid deposition. Of particular concern is the "acid flush" mechanism in which strong acids build up in snowpacks, only to be suddenly released into the watershed during spring runoff. The transport of urban pollution by summer thermally-forced daytime upslope flow, and by winter upslope storms from the Front Range cities of Colorado into the adjacent mountains is also of concern. National Forest Wilderness Areas and Rocky Mountain National Park, federally mandated Class I areas, are situated close to this urban source of acid materials.

Except for the urban regions and a few in-state power plants, much of the acid pollutants are transported into the state from elsewhere. The smelters in southern Arizona and northern Mexico are of special concern because of their large volume of effluent.

It was generally agreed at the Workshop that while permanent damage to the environment has not yet occurred, continued and/or increased transport of acidic pollution into the mountains of Colorado could soon cause irreversible damage. It is, therefore, in the best interest of the state to reduce pollution effluent from within Colorado, and to work with federal land managers to minimize the contribution of pollutants transported into the state from outside sources.

## ACKNOWLEDGEMENTS

The Editor of and Contributors to this volume appreciatively acknowledge the able typing of the papers into the LaTex typesetting format by Mrs. Loretta Wilson. The coordination of the typing and correspondence with the authors was competently handled by Ms. Joanne Williams.

## TABLE OF CONTENTS

# Session I

# Effects of Wet and Dry Deposition in Colorado

# The Acidification Status of Colorado Lakes
# A Chemical Classification

Willard R. Chappell*
Robert R. Meglen
Glenda A. Swanson
Lynne A. Taylor
Robert J. Sistko
Robert B. McNelly
Center for Environmental Sciences
University of Colorado at Denver

Emily L. Hartman
Mary Lou Rottman
Department of Biology
University of Colorado at Denver

Ronald W. Klusman
Todd D. Margulies
Department of Chemistry and Geochemistry
Colorado School of Mines

August 13, 1986

**Abstract**

During 1984 and 1985 water samples were obtained from approximately 231 different lakes in the State of Colorado. Over a hundred of these lakes were sampled twice in 1984 and thirty two were sampled twice in 1984 and once in 1985. In 1985 soil and sediment samples were collected from thirty two target lakes. Vegetation maps were also developed for the drainage basins of these lakes.

The water samples were analyzed for about thirty parameters. This chemical data and the vegetation data have been subjected to multivariate pattern recognition statistical analysis. This analysis reveals that there are four major factors which discriminate between the lakes in Colorado. These are a bedrock factor, a vegetation factor, a lake morphology/soil development factor, and a trace elements factor. These allow the lakes to be classified into different groups. The soil and sediment samples were analyzed for CEC, organic carbon and pH. The soil and sediment data support the lake classification scheme.

*Also, Department of Physics, University of Colorado at Denver

## INTRODUCTION

I would like to briefly describe a collaborative study involving the Center for Environmental Sciences at the University of Colorado at Denver and the Colorado School of Mines. In 1982 Bob Meglen, Ron Klusman and I designed a synoptic survey of Colorado lakes. The purposes of the survey were:

- To establish a chemical characteristics baseline for comparison with future studies.
- To use pattern recognition to develop and test surrogate measures of acidification.
- To identify key variables (chemical, biological and geological) which classify or distinguish Colorado Lakes.
- To develop a lake classification scheme.

The need for a baseline is relatively obvious. The development of surrogates relates to the question of whether there might be more reliable and sensitive measures (perhaps multivariate indices) than pH and alkalinity for acidification status and sensitivity. The classification of lakes would lead to the ability to generalize research results from single lakes to classes represented by these lakes and to choose appropriate variables for monitoring.

One of the main reasons for conducting the study was to determine the range of lake chemistries in Colorado and to compare the Colorado lakes to those from other geographical areas which have been studied more intensely than the lakes in Colorado. We were recently aided in this cause when we received funding from EPA to apply the statistical methods we have been using to the eastern U.S. lake survey data base which consists of approximately 1600 lakes.

Although the concept of the Colorado survey was developed in 1982, we did not obtain the necessary funding until early 1984. As a result, our initial sampling took place in 1984. We received additional funding which enabled us to conduct another sampling in 1985. We have recently obtained support that will allow us to conduct yet another sampling in 1986.

## EXPERIMENTAL DESIGN - 1984 STUDY

In 1984 a list of all named (or numbered) lakes in Colorado was assembled from the 1972 Colorado Fish and Wildlife Inventory and the U.S.G.S. Geographic Names Information System of Lakes and Tanks of Colorado. The lakes were checked to avoid duplicate lakes. The master list of 4069 lakes contains names (including alternate names), altitude, drainage basin, U.S.G.S. map number, surface area, source list county, latitude and longitude. The four major U.S.G.S. drainage basins were subdivided into 12 smaller basins which are listed below:

| | |
|---|---|
| Colorado - Blue | Rio Grande |
| Yampa - White | Arkansas (above 6000 feet) |
| Eagle - Roaring Fork | Arkansas (below 6000 feet) |
| Gunnison | North Platte - Laramie |
| Delores - San Miguel | South Platte (above 6000 feet) |
| San Juan - Las Animas - La Plata | South Platte (below 6000 feet) |

The Arkansas and South Platte altitude division was based on geologic differences that occur at approximately 6000 feet. Each lake was then assigned to one of these basins. In order to include sufficient representation among the various geological, climatic and vegetation characteristics we drew equal sample sizes from each of the twelve basins.

Twenty lakes were selected randomly from each of the twelve basins. Since primary sampling was by helicopter, we had to separate out the wilderness area lakes because of the lack of helicopter access. We finally arrived at a list of 144 lakes (12 in each basin) for which we obtained permission for helicopter access.

The helicopter sampling in 1984 was conducted twice, once in early June and again in early October. The purpose of two samplings was to discern any seasonal variation which may exist. The sampling was accomplished by hovering above the lake surface and lowering a self-rinsing plastic/teflon Van Dorn sampling device to below the surface which was then sealed and retrieved, thereby obtaining a vertical column of water from the top two feet of the lake.

In situ measurements were made of temperature at the time of sampling. The mean hovering time was thirty seconds. During travel to the next site samples were transferred to acid washed bottles on board the helicopter. This protocol was very efficient. The July sampling of 139 lakes was accomplished in six days (30.1 flight hours). The October sampling of 130 lakes was less efficient and required 35 helicopter hours and some extra days because of adverse weather.

Ten percent of the lakes were selected at random for duplicate sampling. Periodically 2 liter blanks of doubly-distilled, deionized water was given to the crew for transfer to the lake water sample bottles on board the helicopter. The duplicates and blanks were treated as "blind" during the analytical protocols.

The field sampling crew consisted of seven members. On board the helicopter were the pilot, the geologist/navigator (Ron Klusman) and the chemist/sampler. In a van which served as a field lab were three chemists from the Center's Analytical Laboratory, and in the fueling vehicle was the helicopter mechanic. The support vehicles would rendezvous at convenient locations with the helicopter. Samples were transferred to the field lab for immediate measurement of pH and conductivity.

Field observations recorded by the flight crew included bedrock type, vegetation, color and surrounding use/presence of human activity. Three 35mm color transparencies and two color prints were taken.

At the end of each day the samples were subjected to further analysis and preservation. Four separate aliquots were prepared of each sample. These were either filtered or unfiltered and acidified or unacidified. The filter residues were retained. Field measured parameters include pH, conductivity, and alkalinity (Gran titrations) which were performed on unfiltered samples.

The samples were then brought back to the Center's Analytical Laboratory for further analysis of an additional 25 to 30 chemical parameters. These are shown in Table I with the method used and the aliquote analyzed. The details of the analytical methods, operating conditions and QC/QA procedures used are given in reference 1.

As indicated earlier, we were unable to obtain access to wilderness area lakes for helicopter sampling. We augmented the sampling program to include several lakes selected at random from seven wilderness areas. These lakes were sampled by our research team by hiking into each selected lake and sampling near the shore. A total of 25 lakes were sampled during the months of July/August. Because of the different protocol and extended period the data was treated independently from the other lakes. However, multivariate pattern recognition showed that this separate treatment was not necessary, i.e. there was no sampling bias.

## PATTERN RECOGNITION

Approximately 10,000 pieces of data were generated from the lake samples. This is not uncommon in environmental studies because of the recent advances in analytical methodology. These advances have allowed the generation of data at a rate that can, and often does, exceed the capacity to evalute

Table I

| SPECIES | METHOD | ALIQUOT |
|---|---|---|
| Al (Total) | HGA | UFA |
| Al (Diss.) | HGA | FA |
| As | HGA | FA |
| B | HGA | FA |
| Ba | ICP | FA |
| Ca | ICP | FA |
| Cd | HGA | FA |
| Cl | IC | FUA |
| Cr | HGA | FA |
| Cu | HGA | FA |
| F | COL | FUA |
| Fe | ICP | FA |
| Fluoresc. | EM | FUA |
| $HCO_3$ (Alk.) | COL/GRAN | UFUA |
| K | AAS | FA |
| Li | ICP | FA |
| Mg | ICP | FA |
| Mn | ICP | FA |
| Mo | HGA | FA |
| Na | ICP | FA |
| $NO_3$ | IC | FUA |
| Pb | HGA | FA |
| pH | ELEC | UFUA |
| $PO_4$ | IC | FUA |
| Si | HGA | FA |
| Spec. Cond. | ELEC | UFUA |
| $SO_4$ | IC | FUA |
| Zn | HGA | FA |

METHOD ABBREVIATIONS

ICP Inductively Coupled Plasma Atomic Emission Spectroscopy
AAS Flame Atomic Absorption Spectrophotometry
HGA Graphite Furnace Atomic Absorption Spectrophotometry
IC Ion Chromatography
COL Colorimetric
GRAN Gran titration and Technicon
EM Fluorescence by molecular emission
ELEC Electrochemical/Potentiometric

PRESERVATION TREATMENT ALIQUOT ABBREVIATIONS

FA Filtered and Acidified
UFA Un-filtered and Acidified
FUA Filtered and Un-acidified
UFUA Un-filtered and Un-acidified

the data. Chemists recognized this problem several years ago. They responded by developing a new subdiscipline of chemistry called chemometrics (2). This particular subdiscipline uses mathematical and statistical methods:

- To design or select optimal measurement procedures and experiments.
- To provide maximum chemical information by analyzing chemical data.

One particular set of techniques that is used by chemometricians is called Pattern Recognition. Many of the tools used by this approach are familier, e.g. factor analysis. The pattern recognition approach consists of two phases; exploratory data analysis and applied pattern recognition (classification model development). The purpose of the exploratory phase is to uncover the basic relationships that exist among the variables and between samples. The applied pattern recognition phase tests the strength of these relationships and other presumed relationships by developing predictive models. One strength of these techniques is that it is possible to look at the entire data set of approximately 10,000 entries simultaneously and that no prior assumptions are made.

It is not possible to go into a detailed description of the multivariate statistical methods which are the tools of pattern recognition. Suffice it to say that if 30 parameters are measured on 294 water samples we can think of each sample as represented by a point in 30 dimensional space. The "distance" between points in 30 dimensional space is a measure of their similarity. We can think of these points as fingerprints. If several lakes have very similar fingerprints and cluster in one part of 30-space and another group clusters in another part of 30-space and the intragroup separations are much less than then intergroup separations, we can say that these are two distinct classes. We can then look for similarities in geology, vegetation or other features which the lakes in each group have in common with each other and which distinguish the two groups from each other as explanations for the classification.

An underlying hypothesis of the study which was designed as a multivariate approach was that

- The lakes of Colorado can be classified by their chemical fingerprint and that these fingerprints reflect the landscape components such as bedrock geology.

Of particular interest is the fact that the fingerprint is multivariate in nature. As a result a change in the fingerprint of a lake can reflect subtle effects that slightly affect several variables simultaneously and which would never be noticed with a univariate approach.

## RESULTS – 1984 SAMPLING

The results from the 1984 sampling will be only briefly noted. They are described in detail in reference 1.

- While the concentrations of the individual chemical species in a given lake showed seasonal variations, the multivariate fingerprints for the vast majority of lakes do not change significantly. However, the variance was larger in the July than the October samples. The larger variance in the July samples may reflect heterogenieties not present after fall overturn.
- Remote alpine, non-wilderness area lakes have fingerprints which are indistinguishable from remote wilderness area lakes. Even though the sampling was different.
- Wilderness area lakes which receive frequent human use have fingerprints that are indistinguishable from non-wilderness area lakes subject to moderate recreational use.
- The lakes can be classified in terms of their multivariate chemical fingerprints and these fingerprints reflect the bedrock, vegetation, soil and human use in the watershed.

- The application of a classification model SIMCA (Soft Independent Modelling by Class Analogy) gave rise to a geology–vegetation classification system which involved nine classes with an overall predictive capability of 90%.

The relationship of lake water chemistry to geology and vegetation revealed by the 1984 data involved only qualitative descriptions of vegetation and geology. In order to further understand the strength of these relationships and their biogeochemical origins, the research team felt that quantitative measures were needed. The generation of these quantitative measures thus became one of the primary objectives of the 1985 effort.

In addition, the prototype classification model provided a basis for selecting additional lakes to test the classification scheme. Of particular interest was the firmness of the class boundaries – whether these are sharp or diffuse. We also wished to closely examine the bedrock influence on alpine lake water chemistry because there were too few such lakes in the 1984 sample to show such distinctions. Other lakes were selected to test the hypothesis that the presence or absence of inlet and outlet streams affects lake water chemistry.

## EXPERIMENTAL DESIGN – 1985 SAMPLING

The objectives of the 1985 sampling were:

- To obtain quantitative measures of geologic and vegetative characteristics of a subset of the lakes sampled in 1984 in order to test the strength of the relationships between lake water chemistry and landscape characteristics.
- To sample additional lakes to test the adequacy of the 1984 sampling in representing the geologic and vegetative variability of the region.
- To obtain additional helicopter samples from lakes sampled in 1984 to obtain a measure of annual variability.

In order to accomplish these objectives, two sets of lakes were identified.

- Target Lakes – Thirty two lakes which were sampled twice in 1984 were selected for resampling and geologic and vegetative studies by teams of geologists and biologists. The criteria for selection were representativeness of each of the nine classes identified in the prototype model (representativeness was measured by the distance from the centroid of the class in multi-space) and accessibility for helicopter and ground-based sampling.
- Hypothesis Testing Lakes – These lakes were selected to test the validity and generality of the classification scheme. Geologic and topographic maps were used to select lakes underlain by the major geologic bedrock types. Additional candidate alpine lakes were selected. Several sets of lakes connected by streams were selected to test the effect of inlet/outlet status on lake water chemistry.

The protocol for the helicopter sampling was the same as in 1984. The fewest number of lakes sampled in any day was six, the maximum was 21. The helicopter sampling of 92 lakes was accomplished in six days (25.1 flight hours). Three wilderness area lakes were sampled by the geology crew from the shore. Fortunately, the weather was more favorable than it had been in October, 1984.

During the summer of 1985 a biology field crew and geology field crew visited the target lakes. The biology crew consisted of Drs. Emily Hartman and Mary Lou Rottman of the University of Colorado, accompanied by two biology graduate students. The geology crew consisted of Dr. Ron Klusman and his graduate student.

The biologists conducted surveys of vegetation types and percent cover in the drainage basins of the target lakes. Vegetation maps were constructed by using aerial photos and running intersecting 0.5 meter belt transects in each basin. The cover type categories were a modification of those used in the San Juan Ecology Project and by the Soil Conservation Service. The initial list of 36 cover types was reduced to ten: meadow, dry shrub, wet shrub, ponderosa, lodgepole, spruce-fir, mixed coniferous, deciduous coniferous, aspen and unvegetated.

The geologists were able to visit only 30 of the 32 lakes. Ten soil samples were taken around each lake with soils from all vegetation types represented. Samples were taken at a depth of six to eight inches or in the B horizon where it was possible to identify horizons. The samples were sieved to less than 2mm, labeled and stored. Three sediment samples were taken around each lake and were sieved and stored in the same manner as soil samples. Additional observations were recorded regarding geology, vegetation and human impacts. A photographic record was also kept.

The samples were dried and split into two halves and one half was ground to less than 200 mesh (0.5mm). Then pH, organic carbon and cation exchange capacity (CEC) were determined for the soils and sediments.

## RESULTS – 1985 SAMPLING

To date the chemical data from the 1985 samples and the vegetation data from the target lakes have been subjected to pattern recognition analysis. The soil analyses were only recently completed and statistical analyses have only been done on the soil data itself.

- The univariate analyses on the soil data indicated that the distributions were approximately log normal except for pH.
- The mean pH of all sediments is 6.38 (range 4.3–8.3) compared to 5.91 (range 3.5–9.6) for the soils.
- The mean CEC for the soils is 40.7 (range 6.2–159) compared to 29.5 (range 0.4–83) for the sediments (units of meq/100g).
- The strongest correlation between pairs of measured parameters is between organic carbon and CEC.
- Analysis of Variance (ANOVA) calculations show that most of the variance in the measured parameters for soils can be attributed to differences between the classes identified in the prototype model as opposed to intra-class differences and that these between class differences are highly significant. Thus the soil measurements strongly support the existence of lake classes based on water chemistry.
- ANOVA results for sediments show that the pH variances support the hypothesized classes but the organic carbon and CEC data do not show any significance in the differences between classes or within classes. This may be due to a greater heteorgeneity in the sediments which would be consistent with field observations. Thus the three samples obtained from each lake may be inadequate.
- Factor analysis of the lake chemistry and vegetation data further supports the hypothesis that the lake chemistry is a reflection of the bedrock, vegetation and land use in the lake drainage basin. It also shows that lake morphology such as inlet/outlet status (permanent, intermittent, etc.) affects lake chemistry in a predictable manner. There are four factors accounting for most of the variance in the data. These have been named the "bedrock" factor, "biological" factor, "lake morphology/soil development" factor and "trace element" factor.

- The "bedrock" factor is the major separator of lakes accounting for most of the variance in the data. It is related to bedrock solubility and the most important variables are Ca, Ba, alkalinity, Mg, specific conductance and Sr. When this factor increases all of the above parameters increase. This identification with bedrock solubility is made because lakes which are low on this factor are located on Precambrian metamorphic and igneous bedrock. Lakes high on this factor are on Cretaceous and Tertiary sedimentary rock, while lakes intermediate on this factor lie on Tertiary igneous and Pennsylvanian sedimentary bedrock. One resampled lake showed an unusually large shift along the bedrock factor between the Fall 1984 and 1985 samples. Field observations indicated that a large talus slide had apparently occurred between the two visits. We propose that this slide accounted for the significant change in the geologic component of chemical inputs to the lake.

- A secondary factor accounting for less total variance than the bedrock factors is the "biologic" factor. This factor is a reflection of the amount of vegetation and decaying biological matter in the vicinity of the lake. Chemical variables with high factor loadings include Fe, fluorescence, dissolved Al and Mn. These variables have an inverse relationship with the percentage of the drainage area that does not contain vegetation. The lakes which are low on this factor are alpine and sub-alpine lakes. The lakes high on this factor are those surrounded by heavy coniferous vegetation. Lakes surrounded by mixed vegetation (e.g. aspen, meadows and spruce-fir) or by grasslands or dry shrub are intermediate on this factor.

  The data set consisting of all the lake water chemistry for the 95 lakes sampled in 1985 also shows that nitrate loads inversely with iron and fluorescence on the biologic factor, i.e., lakes which are high in the vegetation factor are low in nitrate. This suggests that nitrate is taken up by the vegetation and is not available for leaching. Sulfate also loads in the opposite direction to iron and fluorescence.

- Another secondary factor which contributes approximately the same to the variance as the biologic factor is the "lake morphology/soil development" factor. Chemical features loading on this factor are F, Si and sulfate. These features are consistent with the interpretation that the extent of soil development and soil–water contact time affects their release and transport to the lake. Those lakes which are low on this factor (i.e., have low Si, F, etc. in their waters) are the smaller lakes with intermittent or no permanent inlets and outlets. Those high on this factor are reservoirs, lakes with permanent inlets and outlets, and lakes which have indications of considerable soil–water contact.

- A tertiary factor which explains a smaller amount of the variance than the three just mentioned is called the "trace element" factor. This factor generally includes Cd, Zn, Mn and pH, with pH loading inversely with the metals. The heavily vegetated lakes generally lie lower on this factor than the alpine lakes with more bedrock exposure, indicating that vegetation may immobilize the trace metals.

- The classification modelling of the 1985 data shows that the Target lakes were indeed "typical" lakes within the 1984 prototype model categories. There were only four misclassified lakes. Three of these were on mixed or borderline bedrock geology and the other one was the lake which had the landslide and was mentioned earlier.

- However, the hypothesis testing lakes showed the the 1984 model categories have diffuse and overlapping boundaries. Thus while the centroids of the classes are well separated in multispace, their boundaries overlap leading to a more continuous behavior in the factor which separates one class from another.

- In spite of the fact that the classes developed in the 1984 model overlap, Figure I illustrates that clear class distinctions are possible when both the bedrock (F1) and biologic (F2) axes are used. The dots correspond to the 1984 and 1985 data for the target lakes (representing 96 lakes and 31 water chemistry variables). Four major classes are shown with two of them having subclasses of different bedrock types. Rito Alto is the lake where the landslide occurred.

- The application of pattern recognition to the eastern lake data from the EPA National Surface Water Survey has revealed that the major factor is very similar to the bedrock factor found for the Colorado lakes. It involves variables such as alkalinity, Ca, DIC, pH, Cl and Mg. The second most important factor is similar to the biologic factor and involves DIC, color, total P, Fe and Mn. The eastern data indicates that neither alkalinity nor acid neutralizing capacity are adequate measures of sensitivity.

- The factor that appears to separate the "acidified" lakes from others in the eastern data base has large loadings from Al (extractable and total) and sulfate. We have not identified a similar factor or chemical association in the Colorado data.

## DISCUSSION

The data from 1984 and 1985 show that inorganic constituents of lake water are related in a predictable way to the landscape surrounding the lake. The data developed by EPA from the eastern lake survey shows similar characteristics. Our results indicate that for the eastern lakes those that have been "acidified" have a characteristic multivariate chemical "fingerprint". The use of pattern recognition techniques may provide a convenient and sensitive device for detecting a change if one were to occur. We are hopeful that with further work our study will lead to sensitive and reliable multivariate indices to characterize both sensitivity and acidification states.

## ACKNOWLEDGEMENTS

The authors wish to acknowledge the financial support of the University of Colorado, Adolph Coors Company, Anaconda Minerals Company, City of Colorado Springs, Colorado Ute Electric Association, ColoWyo Coal Company, Pittsburgh Midway Coal and Mining Company, Platte River Power Authority, Public Service Company of Colorado, Rocky Mountain Energy, Salt River Project, Stone and Webster, Tri-State Generation and Transmission, and West Associates. The authors also express their appreciation to the helicopter pilots Robert Greeno (1984) and Richard Van Dusen (1985) and the helicopter mechanic Robert Patrick.

## REFERENCES

1. Chappell, W.R., R.R. Meglen, G.A. Swanson, L.A. Taylor, R.J. Sistko, and R.B. McNelly, 1985. Acidification status of Colorado lakes: Part I Chemical classification. Center for Environmental Sciences, University of Colorado at Denver, May, 1985.

2. Kowalski, B.R., ed. Chemometrics: Theory and Applications. ACS Symposium Series No. 52, American Chemistry Society, Washington, DC.

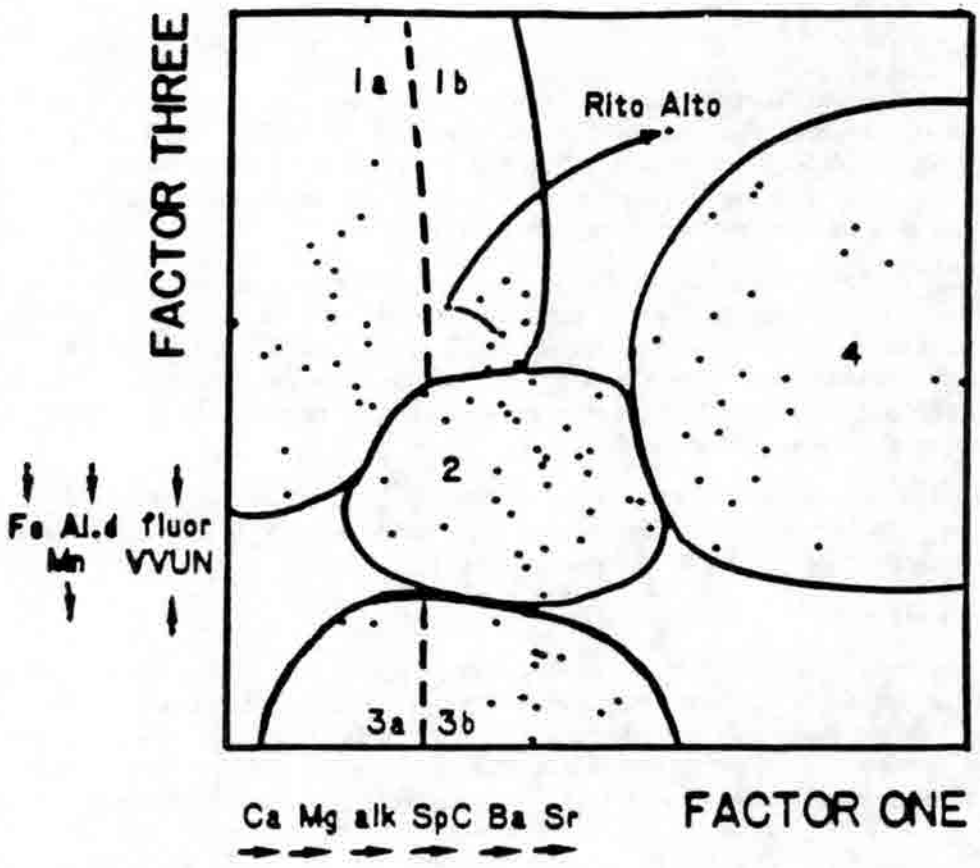


| | | |
|---|---|---|
| 1a | Alpine/subalpine | MPc and IgPc bedrock |
| 1b | Alpine/subalpine | IgT and SdPn bedrock |
| 2 | Mixed vegetation - aspen, meadows, spruce-fir, ponderosa | MPc, IgPc, IgT, and SdPn bedrock |
| 3a | Heavy coniferous vegetation - spruce-fir, lodgepole, ponderosa | MPc bedrock |
| 3b | Heavy coniferous vegetation - | IgT bedrock |
| 4 | Grasslands, dry shrub | SdK, SdT bedrock |

Figure I. Factor score plot of Data Set C showing localization of vegetation types along bedrock and vegetation factor axes. Key to vegetation and geologic characteristics are shown above.

# The Influence of Eolian Dust on the Buffering Capacity of Alpine Soils in Front Range, Colorado*

M. Iggy Litaor
Institute of Arctic & Alpine Research
University of Colorado

August 13, 1986

**Abstract**

The alpine soil system in the Colorado Front Range has been affected by wind-blown calcite that has raised the pH of the soil solutions and maintained high base saturation especially in the topsoil horizons. Such natural liming presumably increases the ability of the alpine soil environment to buffer acid deposition. These findings and soil and interstitial waters chemistry results suggest that the current load of acid deposition had little or no effect on the terrestrial system during the study period (1983–1985).

## INTRODUCTION

Burns (1980) attributed the development of soils in the Colorado Front Range to topographic setting and alpine loess accumulation. He postulated that eolian loess is an extremely important factor in the pedogenesis of alpine soils and hypothesized that the relatively high exchangeable calcium content has been derived from calcium-rich, wind-blown material. He also suggested that the fine particles of alpine loess have their origin from distant sources during the winter and local sources during the summer. Litaor (1986) showed that surface horizons of soils in the Colorado Front Range are maily eolian dust accumulation and sub-surface horizons are mainly weathered parent material. The importance of eolian-derived materials in several alpine ecosystems has also been recognized by Caine (1974), and Thorn and Darmody (1980). Grant and Lewis (1982) found high amounts of $Ca^{2+}$ in precipitation measured in Como Creek, Colorado. They suggested that terrestrial sources are a major contributor of the alkaline material in precipitation. But they did not provide direct observations to support this notion.

The objective of this report is to evaluate the mineralogical and chemical composition of eolian dust and its contribution to soil-buffering capacity in the Colorado Front Range.

## DESCRIPTION OF THE STUDY AREA

The Green Lakes Valley is located 35 km west of Boulder, Colorado, on the eastern side of the Continental Divide (Fig. 1). The Green Lakes Valley alpine watershed was chosen to be the major site for the University of Colorado Long-Term Ecological Research (CULTER) program, mainly because of the wide range of conditions within it. The valley has an area of 5.64 $km^2$, of which 0.4 $km^2$ is in permanent lakes. These lakes are part of the water systems for the city of Boulder. The study area

*Contribution from the University of Colorado Long-Term Ecological Research Program. University of Colorado, Boulder. Supported by the National Science Foundation, Washington, D.C., under grant No. BSR–8012095.

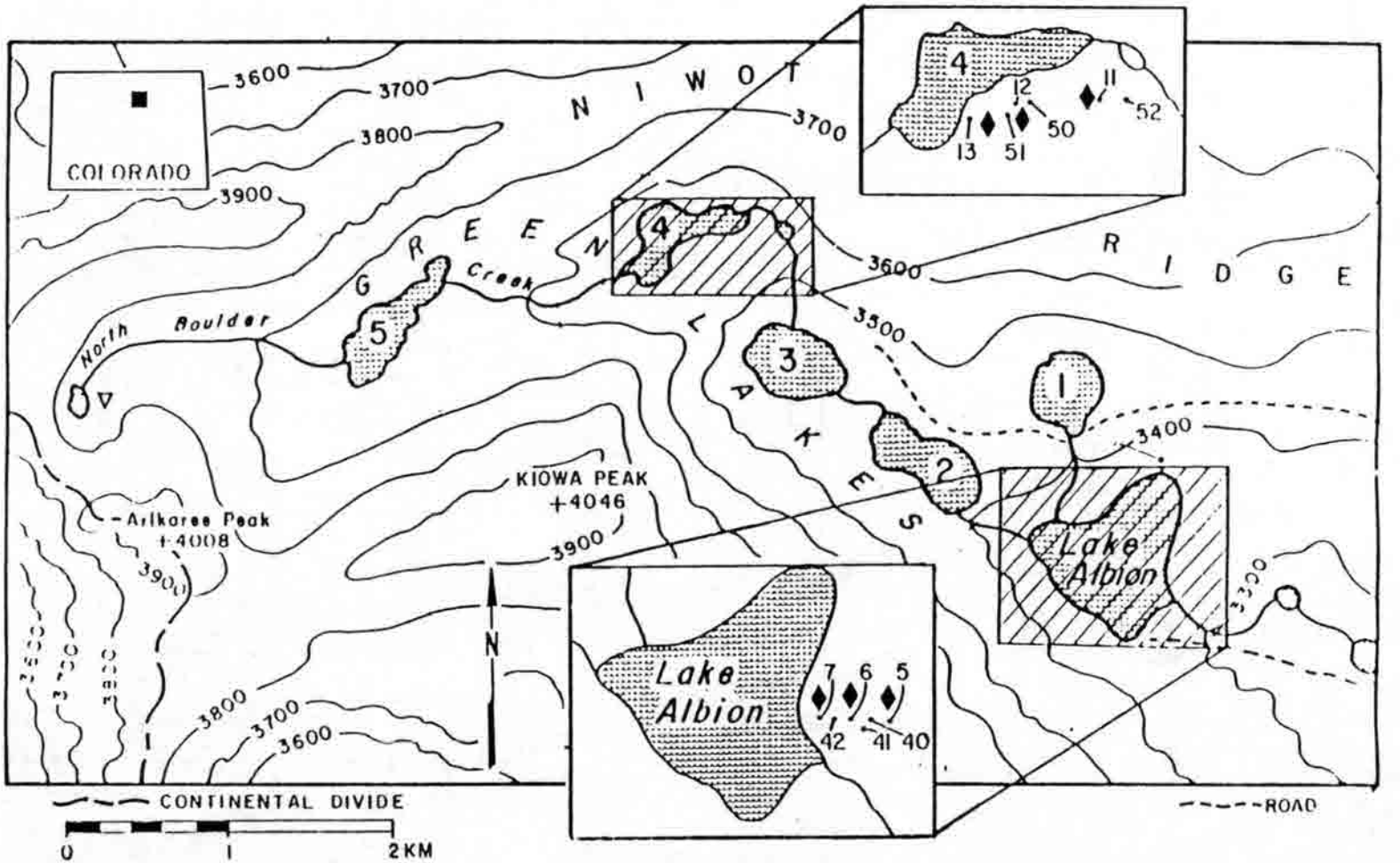


Figure 1. Soil eolian and lysimeter sites in the Green Lakes Valley. Numbers indicate soil pits. The locations of eolian dust traps are indicated by triangles, whereas diamonds represent ceramic porous cup lysimeters.

in the Green Lakes Valley consists of three different ecological landscapes: (i) the higher alpine zone of Arikaree cirque; (ii) the alpine zone (Green Lake 4); and (iii) the forest-tundra ecotone adjacent to Lake Albion. Two main ecological gradients within the study area are those caused by altitudinal change and topoclimatic variations. The altitudinal gradient runs from Lake Albion, with a mosaic of alpine turf, wet meadows, dense willow meadows, krummholz, and subalpine conifer forest, to Arikaree Cirque where a few plants exist in small wind-protected soil sites on the cirquewall. The topoclimatic aspect gradient controls variation in vegetation between north facing and south facing slopes. In general, the vegetation formations are higher on the south facing slopes than on the north facing slopes. The alpine turf meadow is usually confined to areas with a higher water table, and willow meadow is confined to stream channels and bogs. The confiers of the subalpine forest and krummholz prefer drier sites. The principal parent materials are Albion monzonite, Boulder Creek granite, and biotite gneiss.

## FIELD AND LABORATORY METHODS

On the basis of a preliminary soil survey, two relatively simple slopes were chosen as sites for a detailed study of eolian dust and soil chemistry and mineralogy. An additional site was chosen for a study of eolian dust accumulation in Arikaree Cirque (Fig. 1). The sites are referred to as Albion Lake soil catena, Green Lake 4 soil catena, and Arikaree Cirque. In order to examine the soil properties, the pits were excavated to bedrock, or to a depth of 1.2 m below the soil surface. The morphological, chemical and physical characteristics of the soils are given in Litaor (1986).

Soil interstitial waters were sampled by ceramic porous cup samplers at three soil sites along each catena, during three summers from 1983 to 1985. Two samplers were installed at each soil site: the first to collect water from O/A horizon interface, and the second to collect water from the 2Bw horizon. The chemical characteristics of the soil interstitial waters are given in Litaor (1986).

## EOLIAN DUST COLLECTION

One dust trap was installed at each of the soil study sites following the procedure described by Gile and Grossman (1979). There is no standard method for collecting eolian dust. The method by Gile and Grossman was designed for a desert condition, but it has been used in other environments (Reheis, 1984). Furthermore, the cost of these traps is minimal, and they are easy to install and maintain. These dust traps consisted of detachable pans filled flush to the top with glass marbles each about 1 cm in diameter. The pans were 30 cm in square and 7 cm deep. They were constructed from 16 gauge galvanized iron with folded edges and watertight seams. A threaded base plate was attached to the bottom of the pan so that it could be screwed onto or off a 2.5 m rod mounted to the ground. A double thickness of 10 mil vinyl sheeting covered the inside and outside of the pans. Nylon tape fastened the sheeting tightly to the sides of the traps. The glass marbles were thoroughly washed with distilled water before filling the pans.

Eolian dust was collected twice a year—once in early spring and once in late summer during the field seasons of 1982 to 1984. As a first step in removing the dust, a small quantity of distilled water was poured over the marbles in the pan. The marbles were gently rolled and stirred in this water, then transferred to another Nalgene container for analyses.

Snow covered the eolian dust traps most of the winter, so the total weight of eolian dust collected during the three summer months was equal to or greater than that collected during the rest of the year. Although the dust traps were high above the local snow cover, snow that fell directly on the traps prevented some of the dust from reaching the trap. When the snow was blown away, it carried the dust with it. Further, there are no standard methods for sampling eolian dust, principally because rates of eolian deposition depend strongly on the nature of the receivingt surface (Roth and

others, 1985). For example, measurements using buckets as collectors yield different results from those using flat-plat collectors. It is unlikely that the collection devices collect eolian particulates at the same rate as do tree leaves or other natural surfaces. In addition, most attempts to collect eolian particulates have experienced problems with contamination (Reheis, 1984). Nonetheless, I assumed that the total chemistry and clay mineralogy data reflect the chemistry and clay mineralogy of eolian dust.

## RESULTS AND DISCUSSION

The chemistry and clay mineralogy of the eolian dust are presented in Tables 1 and 2. The eolian dust has a mean pH value of 6.2 and has an average of 21.8% organic carbon content (Table 1). Calcite was observed in two dust samples (Table 2). Because x-ray peaks of calcite are rather subdued, 0.1N HCl was applied for a few hours until the effervescence completely ceased, and then the sample was x-rayed again. The calcite peak essentially disappeared.

Inorganic carbon and high base saturation percentages were found in topsoil horizons, whereas no inorganic carbon and small base saturation percentages were observed in subsurface horizons (Table 3). These finding support the hypothesis that eolian material containing calcium has been deposited in the alpine zone of the Colorado Front Range.

To further test the findings that eolian dust exert an important role in the buffering capacity of alpine soils, six soils and the eolian dust were analyzed for elemental composition by x-ray fluorescence (Table 4). The topsoil horizons have mean amounts of CaO of 2.51%±0.54, whereas the eolian dust had 2.72%±0.15. The subsurface horizons have considerably smaller amounts of CaO (x=0.85%±0.19). These results strongly support the notion that eolian dust which contain $CaCO_3$ affects the levels of calcium in the topsoil horizons of alpine soils in the Colorado Front Range.

Soil interstitial waters were studied at six soil sites along two catenas during summer 1983 and 1985. The concentrations of major soil water constituents and pH are summarized in Table 5. Analysis of variance was performed to test the significance of the temporal variations in the soil interstitial waters between 1983 and 1985 (Table 6). None of the major soil water substances such as alkalinity, calcium, nitrate, sulfate, and pH have changed significantly during the study period. Indeed, the soil system in the study area is well buffered. Eolian dust which contains calcite regulates the level of $Ca^{2+}$ on the ion exchange sites and consequently controls the amount of $Ca^{2+}$ in the soil solution. Calcite dissolution product ($HCO_3$-) and organic acids (Litaor, 1986) regulate the pH of the soil system. These findings strongly suggest that the current load of acid deposition had little or no effect on the terrestrial system during the study period.

## SOURCE AND PATHWAYS OF ALKALINE MATERIAL

Few recent papers have studied the source of alkaline material in precipitation in Colorado and Utah. Nagamoto and others (1983) found that snow in the eastern foothills of the Front Range is much less acidic than rain. They explained this phenomenon by noting that snow crystals have a greater scavenging efficiency than rain drops for capturing atmospheric soil particles which are alkaline in the area. The capturing of alkaline material has also been noted as an important phenomenon in the mountains of northern Utah (Messer, 1983). Sequeira (1982) suggested that the high values of $Ca^{2+}$ and $SO_4^{2-}$ in composite deposition (dry and wet) at Alamosa, Colorado were originated from the deserts of the southwest. However, no $CaSO_4$ was found in the eolian dust of the present study. Pollen study in the Green Lakes Valley (S.K. Short, personal communication, 1985) showed that desert species from western Colorado are an important fraction of the pollen collection. It is clear from the preceding discussion that the origin of alkaline material in precipitation in the Front Range area might be originated from eastern and/or western Colorado. Therefore, further

Table 1. Eolian dust analyses (1983)

| Location | Organic matter | pH | sand | silt | clay |
|---|---|---|---|---|---|
| | % | | g | | |
| Albion Lake | 17.5 | 6.5 | 0.079 | 0.06 | 0.11 |
| Green Lake 4 | 30.3 | 5.5 | 0.048 | 0.02 | 0.08 |
| Arikaree Cirque | 17.1 | 6.8 | 0.119 | 0.03 | 0.10 |

Table 2. Relative abundance of clay minerals in eolian dust.*

| Location | K | C | M | Quartz | Feldspar | Calcite |
|---|---|---|---|---|---|---|
| Albion Lake | 2 | 1 | 2 | 3 | 2 | 1 |
| Green Lake 4 | 2 | 1 | 2 | 3 | 2 | 1 |
| Arikaree cirque | 2 | 1 | 2 | 3 | 2 | 2 |

* Expressed as relative quantities: 1 = trace (0-10%); 2 = minor (10-35%); 3 = major (35-65%). K = kaolinite C = chlorite, and M = mica.

Table 3. Inorganic carbon and base saturation percentages of selected soils in the study area

| Horizon | Inorganic Carbon $CaCO_3$ % | Base Saturation % |
|---|---|---|
| Lake Albion (Spodosolic Cryochrept, GRL 5) * | | |
| Oe | 0.55 | 98.5 |
| A | 0.51 | no sample |
| 2Ej | 0.32 | 83.9 |
| 2Bw | 0.0 | 27.0 |
| 3B | 0.0 | 31.0 |
| Lake Albion (Spodosolic Cryochrept, GRL 40) * | | |
| Oe | 0.64 | 99.7 |
| A | 0.34 | 99.9 |
| Ej | 0.25 | 89.5 |
| 2Bw1 | 0.05 | 76.4 |
| 2Bw2 | 0.0 | 37.6 |
| 3B | 0.0 | 23.4 |
| 3BC | 0.0 | 20.2 |
| Green Lake 4 (Typic Cryumbrept, GRL 11) * | | |
| Oe | 0.35 | 99.2 |
| A1 | 0.31 | 98.0 |
| 2A2 | 0.19 | 70.8 |
| 2Cox | 0.09 | 58.2 |
| 2Cn | 0.0 | 49.4 |
| Green Lake 4 (Typic Cryumbrept, GRL 12) * | | |
| A | no sample | 85.5 |
| 2Bw | no sample | 38.8 |
| 2BC | no sample | 37.1 |

* GRL = Green Lakes, see Fig. 1 for exact location of these soil pits

Table 4. Weighted mean of elemental composition of six selected soils and eolian dust using x-ray fluorescence.

| Horizon | $K_2O$ | CaO | $Fe_2O_3$ | MgO | $Al_2O_3$ | $SiO_2$ |
|---|---|---|---|---|---|---|
| | | | Albion Lake Soil Catena | | | |
| Oe | 2.75 | 2.68 | 3.64 | 2.51 | 16.86 | 68.4 |
| A | 2.53 | 2.07 | 3.74 | 2.92 | 18.28 | 68.4 |
| 2Ej | 3.56 | 2.05 | 3.84 | 7.24 | 17.43 | 63.5 |
| 2Bw | 1.00 | 0.94 | 3.47 | 3.28 | 21.34 | 56.6 |
| 3Bw | 2.04 | 1.04 | 3.72 | 2.61 | 22.10 | 67.4 |
| | | | Green Lake 4 Soil Catena | | | |
| Oe | 2.17 | 2.19 | 3.92 | 2.78 | 17.0 | 71.16 |
| A | 2.54 | 1.35 | 3.66 | 2.54 | 15.95 | 69.84 |
| 2Bw | 2.13 | 0.59 | 3.65 | 3.83 | 20.2 | 70.42 |
| 2BC | 3.35 | 0.91 | 3.38 | 2.63 | 17.75 | 67.30 |
| Eolian material collected during summers 1983 and 1984 | | | | | | |
| | 2.16 | 2.72 | 3.33 | 1.35 | 17.47 | 55.09 |

Table 5. Mean and standard deviation of selected soil water constituents from 1983 to 1985 (n = 120).

| Ion | mg/l |
|---|---|
| $Ca^{2+}$ | 4.25 $\pm$ 3.6 |
| $HCO_3^-$ | 4.4 $\pm$ 3.3 |
| $NO_3^-$ | 1.6 $\pm$ 0.9 |
| $SO_4^{2-}$ | 2.8 $\pm$ 1.7 |
| pH (log units) | 6.3 $\pm$ 0.4 |

Table 6. Analysis of variance. Test of significance for soil water using sequential sum of squares (n =120).

| Source of Variation | Soil Water Constituent | F | Sig. of F |
|---|---|---|---|
| Year | $Ca^{2+}$ | 1.69 | 0.28 |
| | $HCO_3^-$ | 1.46 | 0.23 |
| | $NO_3^-$ | 1.33 | 0.27 |
| | $SO_4^{2-}$ | 1.02 | 0.36 |
| | pH | 0.46 | 0.49 |

Year = 1983 to 1985.

research is needed to establish the source and the magnitude of the calcite in the eolian dust through incorporation of chemical, mineralogical and pollen studies.

## REFERENCES


Burns, S.F., 1980: Alpine soil distribution and development, Indian Peaks, Colorado Front Range. Ph.D. thesis, University of Colorado, Boulder, 360 p.

Caine, N., 1974: The geomorphic processes of the alpine environment. In Arctic and Alpine Environments, J.D. Ives and R.G. Barry, eds., Methuen, London.

Gile, L.H., and R.B. Grossman, 1979: The desert project monograph. USDA Soil Conservation Service.

Grant, M.C., and W.M. Lewis, 1982: Chemical loading rates from precipitation in the Colorado Rockies. *Tellus*, **34**, 74-88.

Litaor, M.I., 1986: Geochemistry of alpine soils in the Colorado Front Range, with special reference to acid deposition. Ph.D. thesis, University of Colorado, Boulder, 250 p.

Messer, J.J., 1983: Geochemically alkaline snowpack in Northern Utah mountains in spring of 1982. *Atmos. Environ.*, **17**, 1051-1054.

Nagamoto, C.T., F. Parungo, R. Reinking, R. Pneschel, and T. Gerish, 1983: Acid clouds and precipitation in eastern Colorado. *Atmos. Environ.*, **17**, 1073-1082.

Reheis, M.C., 1984: Chronological and climatic control on soil development, northern Bighorn Basin, Wyoming and Montana. Ph.D. thesis, University of Colorado, Boulder, 346 p.

Roth, P., C. Blanchard, J. Harte, H. Michaels, and M. El-Asbry, 1985: The American West's acid rain test. Research Report #1, World Resources Institute, University of California, Berkeley.

Sequeira, R., 1982: Chemistry of precipitation at high altitudes: inter-relation of acid-base components. *Atmos. Environ.*, **16**, 329-335.

Thorn, C.E., and R.G. Darmody, 1980: Contemporary eolian sediments in the alpine zone, Colorado Front Range. *Phys. Geog.*, **1**, 161-171.

# Session II
# Emissions

# A Utility Perspective on Western Acid Rain

Robert L. Pearson
Public Service Company of Colorado
P.O. Box 840
Denver, Colorado 80201

August 13, 1986

The current state of knowledge about acid deposition in the West and its environmental consequences is more limited than that regarding Europe and eastern North America. Principle deficiencies include; data describing regional, spatial and temporal distributions of deposition, particularly dry deposition; historical knowledge of surface water chemistry and forest conditions relevant to effects assessment, and; knowledge of western ecosystem processes and their resilience to chemical change.

The available knowledge indicates that the deposition of acid-forming substances varies widely, but is generally far lower than found in the East. In analogy to eastern North America, areas considered by others to be susceptible to possible effects were studied. These areas include certain low alkalinity surface waters and forest or vegetation systems located on soils with low buffering capacity. These are almost exclusively located in climatologically severe alpine and subalpine areas. The western region is highly variable in climate. A few areas of high precipitation exist along the Pacific Rim, but most of the region is arid and desert-like, separated by high mountain ranges. Pollutant emission levels of $SO_x$ and $NO_x$ are changing graphically, but temporally decreasing or remaining approximately steady. Despite more than 50 years of exposure to pollutant emissions and concentrations much greater than those found today in some areas, the western United States does not show any credible evidence of adverse effects on a regional scale associated with deposition of sulfur and nitrogen compounds. Except as noted, available information indicates that it is unlikely that one would expect to find such evidence for the western environment.

To provide a margin of safety, increased effort should be devoted to acquiring scientific information about western atmospheric deposition processes and possible environmental effects. However, based on available information, there is no urgency or even a scientific rationale for additional regulatory action in the West. In fact, is is questionable whether adverse effects will be found at all in the context of naturally occurring acidification processes in ecosystems. Evidence supporting this view exists in the scientific literature as discussed below. If verified by ongoing studies, this result is very important. It essentially eliminates the deposition phenomenon as an environmental issue, and relegates its significance on to an efficient, geographically distributed means of pollution removal from the air.

There is no credible scientific evidence of adverse, regional scale ecological affects associated with acid deposition in the West. None are expected at current deposition levels if ecosystem information is used to assess the potential for changes in soil, vegetation, and water chemistry. The area extent of terrestrial and aquatic resources said to be at risk is confined mainly to specific

alpine and subalpine areas, which are generally smaller than those previously reported. There are no comparative studies to indicate that western ecosystems are more susceptible to acid deposition than elsewhere. Consequently, regulatory action to add incremental emission controls is unwarranted.

Information about the ecological processes affected by acid deposition is limited for western conditions. However, the information available is sufficient to define ecosystem resources at risk with only minimal use of analogies derived from experience in other regions. Although similarities exist, the differences in western climate, ecosystem characteristics and deposition chemistry make extrapolation of acidity impacts from other areas questionable.

Wet deposition of sulfate in the West is well below that associated with adverse ecological effects even if the proposed threshold was relevant.

Unlike eastern North America, sulfate is not an adequate surrogate of acidity in the West because it is correlated strongly with non-acidic, soil-derived materials. Because of the lack of acidity production, a wet sulfur deposition threshold level for acidity per se or for nitrate exists for deposition effects, which is applicable anywhere.

Dry deposition, often mentioned as uniquely large in the West compared to wet deposition, is not necessarily large in susceptible alpine and subalpine areas where precipitation is high, because of the very low ambient concentrations of acidic gases and particles.

The acid deposition levels associated with man's activities should not significantly increase in the West, reducing the chance of unidentified environmental effects in the future. Man-made $SO_2$ and $NO_2$ in the West are projected to be less in the year 2000 than the total was in 1970.

Systematic study in the West is needed to enhance the understanding of acid deposition on ecological processes in potentially susceptible regions.

# Sulfur Dioxide Emissions and Acid Deposition: An Empirical Source-Receptor Relation from Monthly Data

Charles B. Epstein
Michael Oppenheimer
Environmental Defense Fund, Inc.
444 Park Avenue South
New York, New York 10016

August 15, 1986

The relation between sources of $SO_2$ and precipitation sulfate concentrations at distant receptors is the subject of intensive empirical and theoretical investigation (1,2). This relation provides a probe of atmospheric chemistry, physics, and meteorology, and insight into the effectiveness of potential acid deposition reduction strategies. Large variations in emissions of $SO_2$ by southwestern U.S. copper smelters, the major regional sulfur source, between 1980 and 1984 provide a unique opportunity for study of the source–receptor relation, as the National Atmospheric Deposition Program (NADP) simultaneously monitored wet precipitation sulfate concentrations on a weekly basis at Rocky Mountain locations. In this article we build on our earlier analysis of annual average data (2), by examining monthly sulfate concentration and emissions data for 1980–84. We show that monthly data are consistent with a linear relation between emissions and concentration, possessing the expected properties of a source–receptor relation. We then predict concentration changes resulting from the addition of a new smelter at Nacozari, Mexico, expected to be the second largest $SO_2$ source in North America.

$SO_2$ emissions from eleven copper smelters in Arizona, New Mexico, Utah, and Nevada were summed to yield monthly regional emissions by the smelter source sector (Table 1, Figure 1). The uncertainties in the emissions inventory are estimated at about $\pm$ 5% (2). Ionic concentrations in wet precipitation have been measured weekly at five Colorado monitoring stations (Sand Spring, Pawnee, Rocky Mountain National Park, Alamosa and Manitou; cf. Figure 1, reference 2) since mid-1980 (3). In NADP data, the error due to imprecision in sampling and anlysis is less than 15% (4).

Weekly observations from the five Colorado stations were combined and averaged over each month to produce volume weighted mean (VWM) concentrations which are shown in Table 1 and Figure 1. Valid samples were available for over 80 percent of the station-weeks during the 6/80–12/84 period. Monthly averages from the combined weekly records of five stations are studied because they are subject to a smaller standard error than are monthly station specific averages. We use volume weighted averages in order to reduce the effect of low volume events, for which concentration is volume-dependent (5). We have restricted ourselves to this set of the five longest recording stations

Table 1: Monthly Smelter Sulfur Dioxide Emissions, and Precipitation Sulfate Concentrations.

| Date | Total Emissions | Concentration | Deseasonalized Concentration |
|---|---|---|---|
| 1980 | | | |
| J | 88.35 | 2.86 | 2.55 |
| J | 11.02 | 1.69 | 1.09 |
| A | 6.83 | 1.17 | 1.15 |
| S | 13.43 | 1.18 | 0.86 |
| O | 61.76 | 1.39 | 1.29 |
| N | 83.74 | 2.18 | 1.53 |
| D | 84.03 | 0.94 | 1.43 |
| 1981 | | | |
| J | 92.05 | 0.52 * | 1.97 |
| F | 84.50 | 1.43 | 1.27 |
| M | 101.14 | 1.15 | 1.59 |
| A | 92.94 | 1.88 | 1.50 |
| M | 95.75 | 1.67 | 1.68 |
| J | 90.98 | 1.94 | 1.71 |
| J | 101.10 | 2.12 | 1.67 |
| A | 97.92 | 1.77 | 1.62 |
| S | 95.68 | 2.09 | 1.88 |
| O | 91.24 | 1.45 | 1.45 |
| N | 95.99 | 1.59 * | 1.35 |
| D | 91.05 | 1.10 | 1.62 |
| 1982 | | | |
| J | 91.28 | 0.56 | 0.99 |
| F | 77.05 | 1.68 | 1.61 |
| M | 70.64 | 0.80 * | 1.25 |
| A | 61.69 | 1.70 | 1.47 |
| M | 44.36 | 0.92 | 0.95 |
| J | 41.64 | 1.07 * | 0.92 |
| J | 52.31 | 0.67 * | 0.37 |
| A | 52.13 | 1.36 | 1.07 |
| S | 52.06 | 0.93 | 0.83 |
| O | 50.32 | 1.08 | 1.19 |
| N | 33.79 | 0.86 | 1.04 |
| D | 27.32 | 0.38 | 0.94 |
| 1983 | | | |
| J | 37.53 | 1.14 | 0.53 |
| F | 49.53 | 1.33 | 1.37 |
| M | 53.80 | 0.56 | 1.03 |
| A | 71.54 | 0.90 * | 0.81 |
| M | 74.58 | 1.15 | 1.20 |
| J | 69.43 | 1.15 | 1.08 |
| J | 43.26 | 1.09 | 0.94 |
| A | 47.53 | 1.46 | 1.04 |
| S | 68.13 | 1.18 | 1.19 |
| O | 64.32 | 1.06 | 1.28 |
| N | 64.51 | 0.63 | 1.22 |
| D | 55.62 | 0.56 * | 1.15 |
| 1984 | | | |
| J | 49.54 | 3.88 * | 2.21 |
| F | 47.06 | 0.83 * | 0.98 |
| M | 53.66 | 1.03 | 1.51 |
| A | 52.89 | 1.38 | 1.43 |
| M | 58.14 | 1.28 * | 1.35 |
| J | 55.34 | 1.38 | 1.39 |
| J | 54.39 | 1.43 | 1.42 |
| A | 51.85 | 1.01 | 0.46 |
| S | 53.51 | 1.07 * | 1.20 |
| O | 63.32 | 0.65 * | 0.98 |
| N | 63.94 | 1.20 * | 2.20 |
| D | 59.90 | 0.62 | 1.24 |

(see narrative, following page)

Arizona emissions figures are from the Arizona Department of Health Services, Phoenix. Emissions figures for all non-Arizona Kennecott Sources (in Utah, Nevada, and New Mexico) are from the Kennecott Minerals Company, Salt Lake City, Utah. Due to malfunctioning monitors at the Hurley, NM smelter during 1980 and the last quarter of 1984, emissions for these months are estimated from available monthly data and a knowledge of operating days per month at this site. Annual and quarterly emissions for the Phelps Dodge Smelter in Hidalgo, New Mexico, were obtained from the Air Quality Bureau, New Mexico Department of Health and Environment, Santa Fe. Monthly emissions were estimated as one third of quarterly during the corresponding quarter, except for late 1980, when they were estimated as one twelfth of annual.

Monthly sulfate concentrations were calculated as the volume weighted mean of weekly observations, combined from five Colorado stations of the NADP (Sand Spring, Pawnee, Rocky Mountain National Park, Alamosa, Manitou). Months failing to meet the NADP quality control criterion that chemical data be available from at least 75% of the station-weeks in the averaging period are indicated by an asterisk.

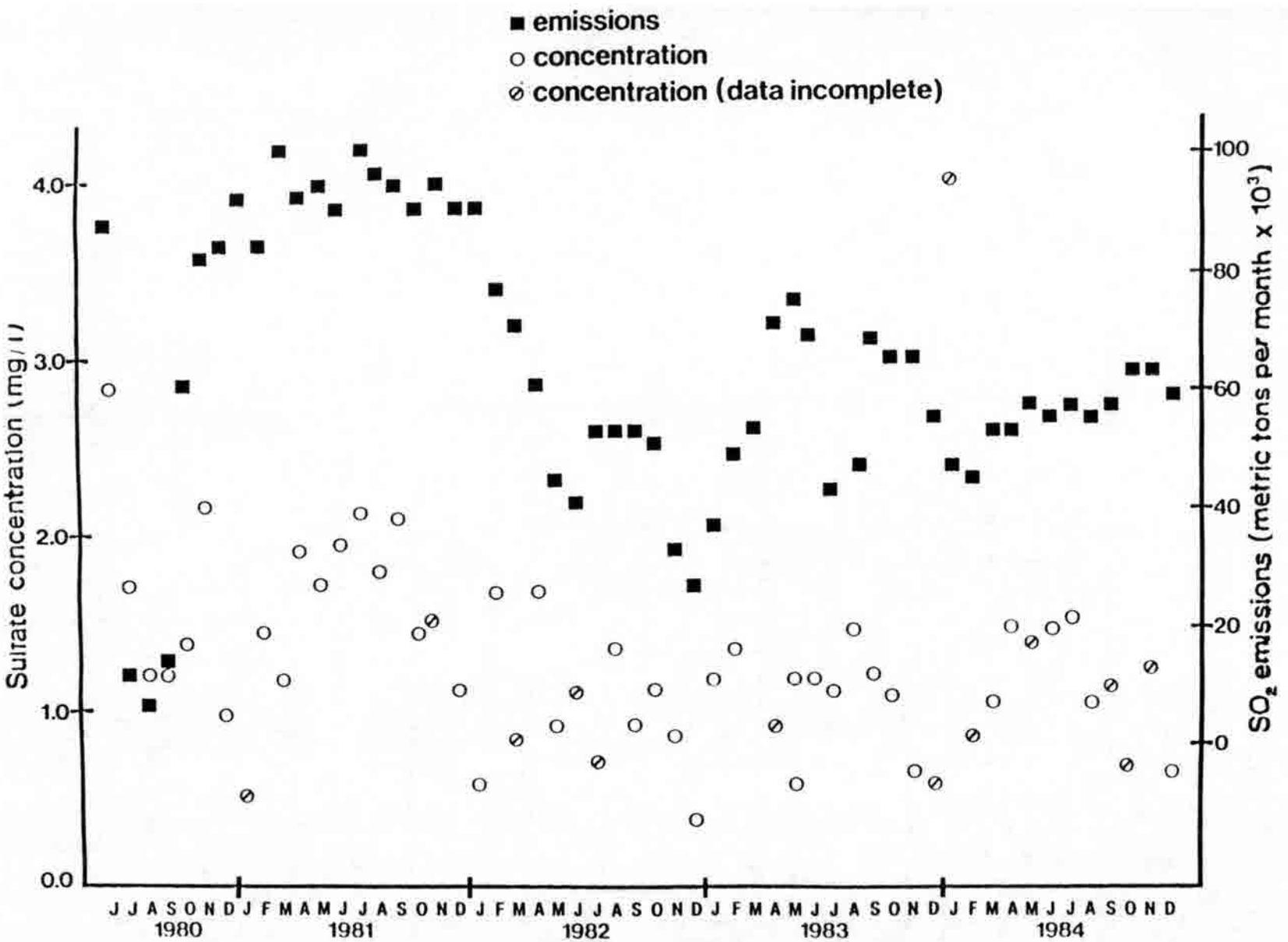


Figure 1: Smelter $SO_2$ emissions and VWM sulfate concentrations from 5 Colorado stations, combined, for June 1980 - December 1984. Emissions -■, concentration -○, incomplete concentration data -⊘. (ie. chemical data available from fewer than 75% of the station-weeks in the month)

in a single state because the use of data from more widely separated stations adds an element of geographic variability, increasing the standard error of the VWM concentrations.

To investigate the relation between emissions and sulfate concentration, we employ the model of linear regression. A regression of 55 consecutive months of VWM sulfate concentration data on total smelter $SO_2$ emissions explains little of the variation in sulfate and is marginally insignificant (cf. Table 2, line 1). However, 13 of the 55 months fail to meet the NADP quality control criterion that chemical data be available from at least 75% of the station-weeks in an averaging period. If these 13 months are omitted from the data set, then regression of VWM sulfate on smelter $SO_2$ explains 18% of the concentration variability ($p < .01$, t-test, cf. Table 2, line 2).

By inspection, Figure 1 reveals annual periodicity in VWM sulfate concentration variability, with higher concentrations in the spring and summer months. Since this periodic variation is due to seasonal changes in regional photochemistry and meteorology, and not to periodic variation in smelter emissions, we have employed a computer algorithm (6) to remove the annually periodic component of VWM sulfate concentration variability. The algorithm partitions a monthly time series into trend, seasonal, and irregular components, using a series of moving median, moving average, and weighted moving least-squares-regression filters. The seasonal component is allowed to evolve over time. The deseasonalized series (Table 1) is the sum of the trend and irregular components, and is calculated from the entire 55 month series.

Regression of quality controlled deseasonalized sulfate on smelter emissions explains 41% of the variation in the sulfate series ($p < .001$, t-test, cf. Table 2, where regression of non-quality controlled deseasonalized data is also displayed). Addition of a quadratic term to the regression model did not significantly increase the proportion of variance in deseasonalized sulfate explained, indicating that the $SO_2 - SO_4$ relation is insignificantly non-linear. The linear regression of deseasonalized, quality controlled sulfate on smelter emissions is plotted in Figure 2. Concentration residuals from the regression of deseasonalized concentration on emissions lack significant first order autocorrelation, whether ordered as a time series or by emissions.

Does the statistical relation between Colorado precipitation sulfate and smelter $SO_2$ possess the expected physical properties of a true source–receptor relation? Sulfate concentration, C, may be expressed as a function of $E_s$ and $E_b$, smelter and background emissions, respectively: $C = k_s E_s + k_b E_b$, where $k_s$ and $k_b$ are proportionality constants. From Figure 2, the x-intercept ($E_s$ at $C = 0$, or $-(k_b/k_s)$ is $-71,000$ tons (confidence limit, CL $= -33,000, -157,000$), calculated as the y-intercept divided by the slope. $E_b$ is estimated at 33,000 metric tons per month for U.S. sources (7,8,9). Thus, the slope and intercept of the line in Figure 2 are consistent with an independent estimate of background emissions, since the relative distances of smelter and background sources from Colorado receptors leads us to expect that $k_b > k_s$. $E_b$ is treated as a constant here because background emissions are dominated by electric power plant emissions, which deviate from their annual mean values during any given month by no more than 10% of total regional emissions, and are constant to within a few percent from year to year (9). Natural sulfur sources such as airborne soil sulfate also may affect the intercept.

The slope and intercept of the regression line in Figure 2 imply that in 1981, the period of highest smelter emissions, the contribution of average smelter emissions to sulfate concentrations was 57% (95% CL: 38%, 74%). By comparison, a theoretical long range transport model based on regional meteorology estimated up to a 46% smelter contribution to Colorado precipitation sulfate in 1981 (10). Furthermore, a regional mass budget study concluded that most wet sulfate deposited in Colorado in 1981 originated in out-of-state emissions (11).

The Arizona smelters are the largest single state source of $SO_2$, whether compared with smelters in New Mexico, Utah, and Nevada, or with electric utility emissions (inventory available through

**Table 2: Statistical Properties of Regressions of Sulfate against Total Smelter $SO_2$ Emissions. Regressions based on 42 points have omitted months with incomplete concentration data. The last two regressions are based on seasonally adjusted data.**

| Dependent Variable | N (months) | Explained sum of squares as % of total | p < | Slope (95% CL) (mg/l/kiloton/month) | y-Intercept (95% CL) (mg/l) |
|---|---|---|---|---|---|
| Monthly VWM ($SO_4$) | 55 | 6 | 0.100 | 0.0064 (-0.0005, 0.0133) | 0.87 (0.40, 1.33) |
| Monthly VWM ($SO_4$) | 42 | 18 | 0.010 | 0.0083 ( 0.0026, 0.0140) | 0.78 (0.39, 1.17) |
| Deseasonalized ($SO_4$) | 55 | 28 | 0.001 | 0.0094 ( 0.0053, 0.0135) | 0.69 (0.41, 0.97) |
| Deseasonalized ($SO_4$) | 42 | 41 | 0.001 | 0.0094 ( 0.0058, 0.0130) | 0.69 (0.44, 0.94) |

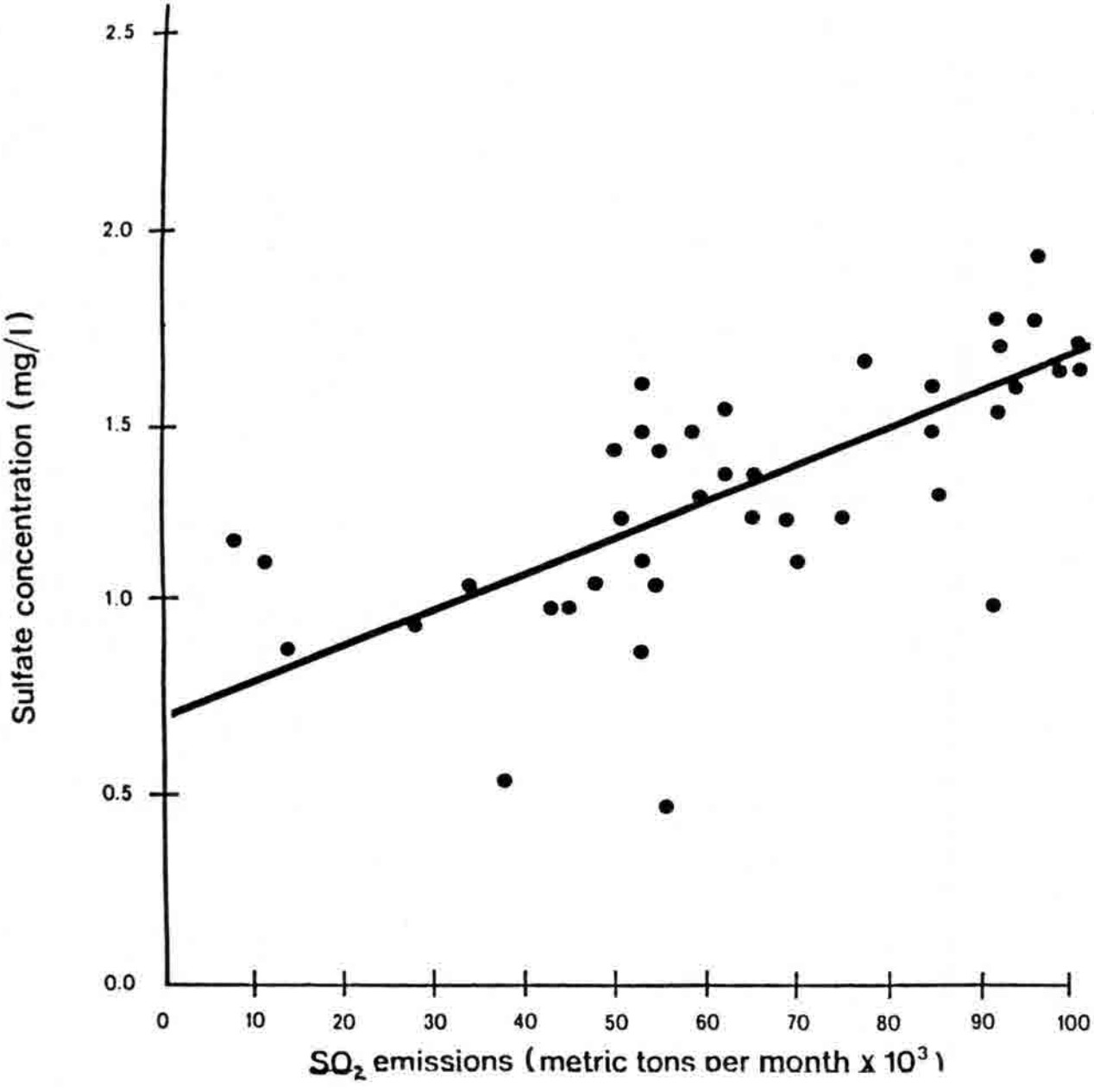


Figure 2: Deseasonalized VWM monthly sulfate concentrations for 5 Colorado stations, combined, versus total smelter $SO_2$ emissions in the intermountain region for June 1980 - December 1984 using quality-control data set (N = 42). Regression line is indicated.

1983) from Colorado, Utah, Arizona, New Mexico, Nevada or Wyoming (9,12). Consistent with this distribution of source magnitudes, when deseasonalized sulfate is multiply regressed on the ten source categories (four smelter states plus six electric utility states), only Arizona smelter $SO_2$ explains a significant portion of the variation in sulfate (N = 36 months for which quality controlled NADP data are available between 6/80 and 12/83; $p < 0.01$, F-test).

Three additional points of physical interpretation deserve mention. First, photochemical processes are slower in the winter and upper level wind trajectories arise less often from the south and west in winter than in summer, so one expects a weaker relation in winter. In fact, we find significant relations for the 2nd, 3rd and 4th quarters of the year but not the first quarter. Second, a decreasing regression coefficient (slope) with increasing distance from smelter sources has been demonstrated when all NADP stations in the region are examined (13). Thus, the relation possesses the expected geographical structure. An exponential scale of transport for sulfur may be derived from concentration gradients or slope gradients. This value is nearly 1000 km (2,13). Third, in addition to sulfate, magnesium concentrations, but no other ion concentrations, are related to $SO_2$ emissions. This relation may reflect $SO_2$ control of soil dust solubility in droplets.

Considerable variance remains in monthly sulfate, unexplained by smelter emissions. Meteorological fluctuations in wind trajectories and precipitation amounts influence precipitation concentrations. Other sources of variation in VWM sulfate include changes in background emissions, lagged responses due to sulfur transport times, and shifts in the geographic balance represented by the VWM concentration due to changes in monthly precipitation volume at each station.

A test of this source–receptor relation will be provided shortly as a copper smelter at Nacozari, Mexico, 55 miles south of the Douglas, Arizona smelter, has recently begun operation. If uncontrolled, the smelter will emit 500,000 tons of $SO_2$ per year under full operation. From Figure 2, we predict an increase in long-term monthly average precipitation sulfate concentrations at these five Colorado stations to nearly 1.60 mg/l (95% CL: 1.45, 1.75) if background emissions, meteorology, and oxidant levels resemble those for the 1980–1984 period, and domestic smelters emit at their 1984 level. An indistinguishable prediction is obtained if the regression is based on Arizona smelter emissions only. This predicted concentration approaches the highest average values observed over the period. Observation of the response of the atmosphere in this inadvertent experiment will provide a unique opportunity for studies of regional atmospheric chemistry and transport. It is imperative that coordinated deposition, cloud chemistry, aerosol, gaseous concentration, tracer and surface water chemistry measurements be planned around this source modulation as the smelter increases production in the coming few years.

The authors thank the members of the "November 8th Group" for constructive criticism, G. Oehlert and R. Goldburg for advice on statistical analysis, and J. Tyroler and K. Anderson for help with statistical software.

## REFERENCES

1. Work Group 2. U.S.–Canada Memorandum of Intent on Transboundary Air Pollution (October, 1982).

2. Oppenheimer, M., C.B. Epstein, and R.E. Yuhnke. *Science*, **229**, 859–862 (1985).

3. National Atmospheric Deposition Program Data Reports, Precipitation Chemistry. Natural Resource Ecology Laboratory, Colorado State University (1980–1984).

4. Stenslund, G.J., et al. NADP Quality Insurance Report, Central Analytic Laboratory. Illinois State Water Survey, Urbana (December 1979).

5. Junge, C.E. Air Chemistry and Radioactivity. Academic Press, New York (1963), Ch. 4.

6. Cleveland, W.S., S.J. Devlin, and I.J. Terpenning. The SABL Seasonal and Calendar Adjustment Package, Bell Laboratories, Murray Hill, New Jersey (1982).

7. Yuhnke, R., and M. Oppenheimer. Safeguarding Acid-Sensitive Waters in the Intermountain West. Environmental Defense Fund, Inc., New York (1984).

8. Work Group 3B. U.S.–Canada Memorandum of Intent on Transboundary Air Pollution (June, 1982).

9. Pechan, E.H., and J.H. Wilson, Jr. *J. Air Pollution Control Assoc.*, **34**, 1075–1078 (1984).

10. Modeling Regional Haze in the Southwest: A Preliminary Assessment of Source Contributions. Systems Applications, Inc., San Rafael, California (February, 1984).

11. Oppenheimer, M. *Atmos. Environ.*, **19**, 1439–1443 (1985).

12. Knudson, D.A. An inventory of monthly sulfur dioxide emissions for the years 1975–1983. Argonne National Laboratory Publication ANL/EES-TM-277.

13. Dupuis, L.R., and F.W. Lipfert. Multivariate analysis of acid deposition, smelter emission and the linearity issue in the Western U.S. Draft report, Brookhaven National Laboratory (1985).

# Session III

## Chemistry, and Wet and Dry Deposition of Pollution in Colorado

# Colorado Data Available Through the National Atmospheric Deposition Program

David S. Bigelow
Natural Resources Ecology Lab
Colorado State University
Fort Collins, Colorado

August 14, 1986

## BACKGROUND

The National Atmospheric Deposition Program (NADP) established in 1978 by the North Central Region of the State Agricultural Experiment Stations, has grown into a nationally distributed network of over two hundred monitoring sites, and includes the 150 stations that are designated as the National Trends Network (NTN). All of the NADP/NTN monitoring stations use an Aerochem Metrics Wet/Dry Precipitation Collector and a Belfort 5-780 Universal Rain Gage equipped with a precipitation event pen, to make two independent measures of rainfall amount and to collect a cumulative, weekly representative sample of precipitation. In addition to the use of standardized sampling equipment, the sites utilize a standard set of operating protocols, use one centralized laboratory to determine the chemical composition of the weekly rain samples and maintain one centralized data depository (3,4,6). Another feature of network data is the standardized set of data quality codes which describe conditions of sample collection and use for each weekly sample (2).

Sites are maintained as long-term (decades) monitoring stations through the sponsorship of cooperating agencies. Each agency volunteers resources (manpower, equipment, analytical costs, etc.) and agrees to utilize them according to the network's standard established procedures. Technical direction for the program comes from a technical committee of knowledgeable scientists who are active in the disciplines involved in, related to, and/or dependent upon atmospheric deposition research. Day to day network operations are coordinated by a scientific management team at Colorado State University. This group, known at the NADP/NTN Coordinator's Office, also has specific responsibility for data dissemination.

## LOCATION OF COLORADO SITES

Currently, the NADP/NTN monitoring network operates sites at ten locations in Colorado. These include stations at Mesa Verde National Park, Alamosa, Craig, Buffalo Pass (above Steamboat Springs), Pawnee National Grasslands, two at Rocky Mountain National Park, Niwot Saddle (above Ward), Manitou Springs, and Las Animas. The stations are located on the map in Figure 1. Station locations of sites in Colorado's neighboring states are also given. One additional Colorado site, in the San Juans, is scheduled to start operations in the fall of this year.

Future plans also call for the establishment of three additional stations in close proximity to the Niwot Saddle, Buffalo Pass, and the San Juan sites, to study, in part, the effect elevation has on atmospheric deposition.

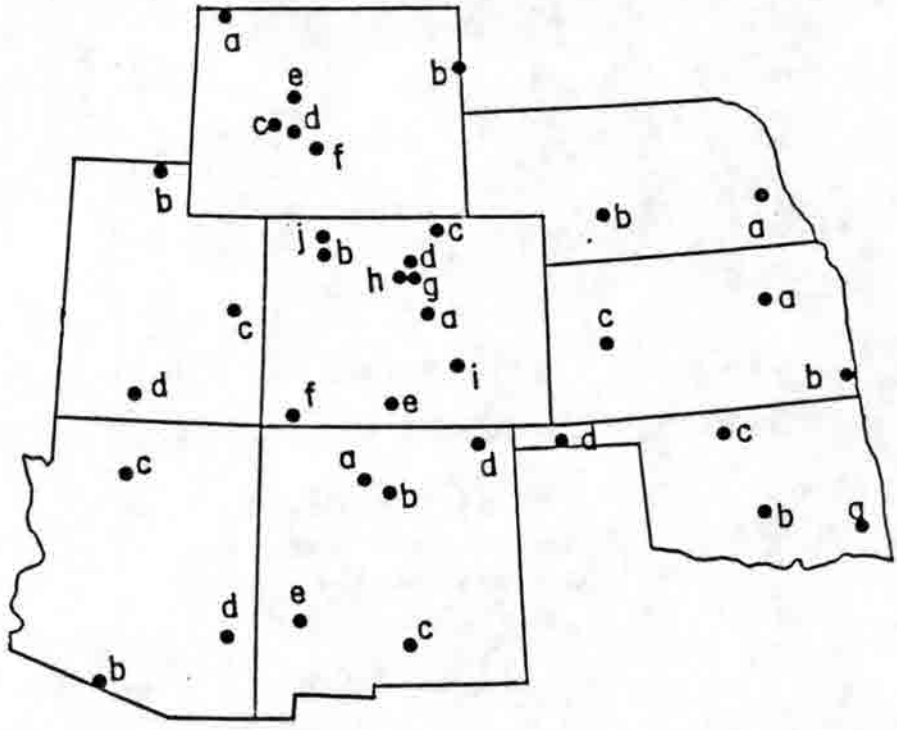

| State Key | State Code | Network | Site Name | County | Agency | Individual | Latitude | Longitude |
|---|---|---|---|---|---|---|---|---|
| **Arizona** | | | | | | | | |
| B | AZ 06 | NADP/NTN | Organ Pipe Cactus Nat'l Monument | Pima | NPS | W. Mikus | 31° 57′ | 112° 48′ |
| C | AZ 03 | NADP/NTN | Grand Canyon Nat'l Park | | NPS | R. Ernewyn | 36° 04′ | 112° 09′ |
| D | AZ 99 | NADP/NTN | Oliver Knoll | Graham | BLM | D. Molitor | 33° 04′ | 109° 52′ |
| **Colorado** | | | | | | | | |
| A | CO 21 | NADP/NTN | Manitou | Teller | USFS | D. G. Fox | 39° 06′ | 105° 06′ |
| B | CO 15 | NADP/NTN | Sand Spring | Moffat | BLM | O. Olsen | 40° 30′ | 107° 42′ |
| C | CO 22 | NADP/NTN | Pawnee | Weld | SAES-Colorado State Univ. | J. H. Gibson | 40° 48′ | 104° 45′ |
| D | CO 19 | NADP | Rocky Mtn Nat'l Park-Beaver Meadows | Larimer | NPS | D. R. Stevens | 40° 22′ | 105° 34′ |
| E | CO 00 | NADP/NTN | Alamosa | Alamosa | NOAA | R. Artz | 37° 27′ | 105° 52′ |
| F | CO 99 | NADP/NTN | Mesa Verde Nat'l Park | Montezuma | NPS | R. Heyder | 37° 11′ | 108° 29′ |
| G | CO 02 | NADP | Niwot Saddle | Boulder | Univ. of Colorado - INSTAAR | J. Halfpenny | 40° 03′ | 105° 35′ |
| H | CO 98 | NADP | Rocky Mtn Nat'l Park-Loch Vale | Larimer | NPS | J. Baron | 40° 17′ | 105° 39′ |
| I | CO 01 | NADP/NTN | Las Animas Fish Hatchery | Bent | USGS | R. Steger | 38° 07′ | 103° 14′ |
| J | CO 97 | NADP | Buffalo Pass | Routt | EPA/USFS | D. Hackett | 40° 32′ | 107° 41′ |
| **Kansas** | | | | | | | | |
| A | KS 31 | NADP/NTN | Konza Prairie | Riley | Kansas State University | G. R. Marzolf | 39° 06′ | 96° 36′ |
| B | KS 07 | NADP/NTN | Farlington Fish Hatchery | Crawford | USGS | L. R. Shelton | 37° 38′ | 94° 48′ |
| C | KS 32 | NADP/NTN | Lake Scott State Park | Scott | USGS/KS State Park Authority | L. R. Shelton | 38° 40′ | 100° 48′ |
| A | NE 15 | NADP/NTN | Mead | Saunders | SAES-Univ. of Nebraska | S. B. Verma | 41° 09′ | 96° 30′ |
| B | NE 99 | NADP/NTN | No. Platte Ag Exp. Station | Lincoln | USGS | G. Engel | 41° 04′ | 100° 45′ |
| **New Mexico** | | | | | | | | |
| A | NM 09 | NADP/NTN | Cuba | Sandoval | BLM | C. Anderson | 36° 02′ | 106° 58′ |
| B | NM 07 | NADP | Bandelier Nat'l Monument | Los Alamos | Los Alamos Nat'l Lab | R. Ferenbaugh | 35° 47′ | 106° 16′ |
| C | NM 08 | NADP | Mayhill | Otero | BLM/USFS | C. Anderson | 32° 54′ | 105° 28′ |
| D | NM 12 | NADP | Capulin Mountain Nat'l Mon. | Union | NM Env. Imp. Div./NPS | K. E. Peyton | 36° 47′ | 103° 58′ |
| E | NM 01 | NADP | Gila Cliff Dwellings Nat'l Mon. | Catron | NM Env. Imp. Div./USFS | K. E. Peyton | 33° 13′ | 108° 14′ |
| **Oklahoma** | | | | | | | | |
| A | OK 25 | NADP | Clayton Lake | Pushmataha | SAES-Oklahoma State Univ. | P. J. Wigington, Jr. | 34° 32′ | 95° 21′ |
| B | OK 17 | NADP/NTN | Great Plains Apiaries | McClain | NOAA | J. Carter | 97° 31′ | 34° 59′ |
| C | OK 00 | NADP/NTN | Salt Plains Nat'l Wildlife Refuge | Alfalfa | USGS/U.S. Fish & Wildlife | J. H. Irwin | 36° 48′ | 98° 12′ |
| D | OK 29 | NADP/NTN | Goodwell Research Station | Texas | USGS/NOAA | L. Hauth | 36° 35′ | 101° 37′ |
| **Utah** | | | | | | | | |
| B | UT 01 | NADP/NTN | Logan | Cache | NOAA/SAES-Utah State Univ. | G. L. Wooldridge | 41° 39′ | 111° 54′ |
| C | UT 98 | NADP/NTN | Green River | Emery | BLM/Green River High School | W. W. Wagner | 38° 59′ | 110° 10′ |
| D | UT 99 | NADP/NTN | Bryce Canyon Nat'l Park | Garfield | BLM/NPS | W. W. Wagner | 37° 37′ | 112° 11′ |
| E | UT 08 | NADP | Murphy Ridge | Rich | Amoco Production Company | K. Bauman | 41° 22′ | 111° 02′ |
| **Wyoming** | | | | | | | | |
| A | WY 08 | NADP/NTN | Yellowstone Nat'l Park-Tower Falls | Park | NPS | W. Hamilton | 44° 55′ | 110° 25′ |
| B | WY 99 | NADP/NTN | Newcastle | Weston | BLM | A. L. Riebau | 43° 52′ | 104° 12′ |
| C | WY 06 | NADP/NTN | Pinedale | Sublette | BLM | A. L. Riebau | 42° 56′ | 109° 47′ |
| D | WY 02 | NADP | Sinks Canyon | Fremont | BLM | A. L. Riebau | 42° 45′ | 108° 48′ |
| E | WY 98 | NADP | Gypsum Creek | Sublette | Exxon Company, USA/USFS | R. D. Goddard | 43° 15′ | 109° 15′ |
| F | WY 97 | NADP | South Pass City | Fremont | Chevron Chemical Co./USFS | A. Galbraith | 42° 30′ | 108° 50′ |
| G | WY 00 | NADP | West Glacier Lake | Albany | WY Water Res. Center/USFS | R. W. Brocksen | 41° 23′ | 106° 15′ |

**Figure 1. Location Of Colorado NADP/NTN Monitoring Stations**

## NADP DATA PRODUCTS

One of the first pieces of information that becomes available when a site is established is a Site Description Questionnaire. The questionnaire describes, in a standard format and in some detail, the location, administration, equipment and potentional emission source characteristics of each site (6). An example Site Description Questionnaire is given in Appendix A. The location and emission characteristics are unique in that they describe the site at three concentric distance intervals. The information gathered for each distance is built upon the premise that beyond the cutoff distance, the type of source identified becomes part of the regional makeup of the area. Within the cutoff, mentioned sources *may* be a significant source of bias in assuming regional representativeness. The distance intervals are: within 30 meters, which is considered the immediate site itself; 30 meters to 1 kilometer, which is designated as the area of local influence; and 1 kilometer to 50 kilometers, which is assumed to be the area of regional influence. Characteristics beyond 50 kilometers are not routinely described. A summary of critical distances for primary sources of interest to the NADP/NTN monitoring program is given in Table 1.

The Site Description Questionnaires are maintained as ASCII computer files, one per station, and are available for distribution. A subset of the information contained in these files is scheduled for publication by the U.S. Geological Survey this fall. This report will also contain some of the emission maps and topographical maps referenced in the Site Description Questionnaires.

The Weekly Field Observer Report Form (FORFs), shown in Figure 2, is the primary means of collecting weekly sample quality information and measured precipitation amounts in the NADP/NTN monitoring network. This information is merged with chemical analysis results, and, based upon quality control assurance reviews, is assigned codes which document data quality characteristics of each weekly sample (2). All of the primary information available from the weekly samples and QC/QA reviews are maintained in an interactive, on-line INGRES, relational database. It is from this database that data tapes and NADP/NTN Quarterly Reports of Precipitation Chemistry are produced. The attributes of this part of the NADP/NTN Network Database are listed in Table 2. Table 3 lists the availability of this information for Colorado sites. The information is updated monthly.

Some of the uses of this data are illustrated in Figures 3 through 5. Figure 3 shows a plot of weekly data for selected elements for the Loch Vale NADP/NTN Station. The data used to create plots like these, can be used to demonstrate temporal trends, compute statistical distributions, or determine correlations to other stratified data. Weekly data can be supplied in a variety of ways to data users including data tapes, floppy discs, interactively with a modem, or as hard copy reports such as shown in Figure 4. Figure 5 demonstrates the use of the daily precipitation TYPE values in conjunction with $NO_3$ values, both of which are supplied with standard data tapes of NADP/NTN network data.

Another type of information routinely distributed by the NADP/NTN monitoring program is seasonal and annual summaries of precipitation chemistry. The summaries consist of precipitation weighted averages for meteorological seasons (10) and annual (January through December) intervals, each season or interval being accompanied by a unique set of data completeness estimates. The data completeness estimates provide data users with a measure of data comparability with other sites as well as data from other precipitation chemistry networks. The estimates were developed during the production of the 1982 NADP Annual Data Summary of Precipitation in the United States (7) to establish minimum guidelines for utilizing summarized weekly NADP/NTN data. The estimates specify the percentage of days for which a site has valid samples, the percentage of days a site has an accountability of precipitation, the amount of valid samples for which there is also valid precipitation and finally, the percentage of the precipitation, as measured by the standard rain

Table 1. Critical Distances for Siting NADP/NTN Monitoring Stations

| Potential Sources | Distance From The Collector Minimum | | Background |
|---|---|---|---|
| Heavy Industry | 10 km | (20 if upwind) | 50 km |
| Suburban/Urban Areas | 10 km | (20 if upwind) | 50 km |
| Populations > 75,0000 | 20 km | (40 if upwind) | 50 km |
| Moving Sources | 100 m | | 10 km |
| Feedlots/Dairies, etc | 500 m | | 1 km |
| Grazing Animals | 20 m | | 1 km |
| Surface Storage | 100 m | | 1 km |
| Parking Lots | 100 m | | 200 m |
| Rain Gage | 5 m | | 30 m |

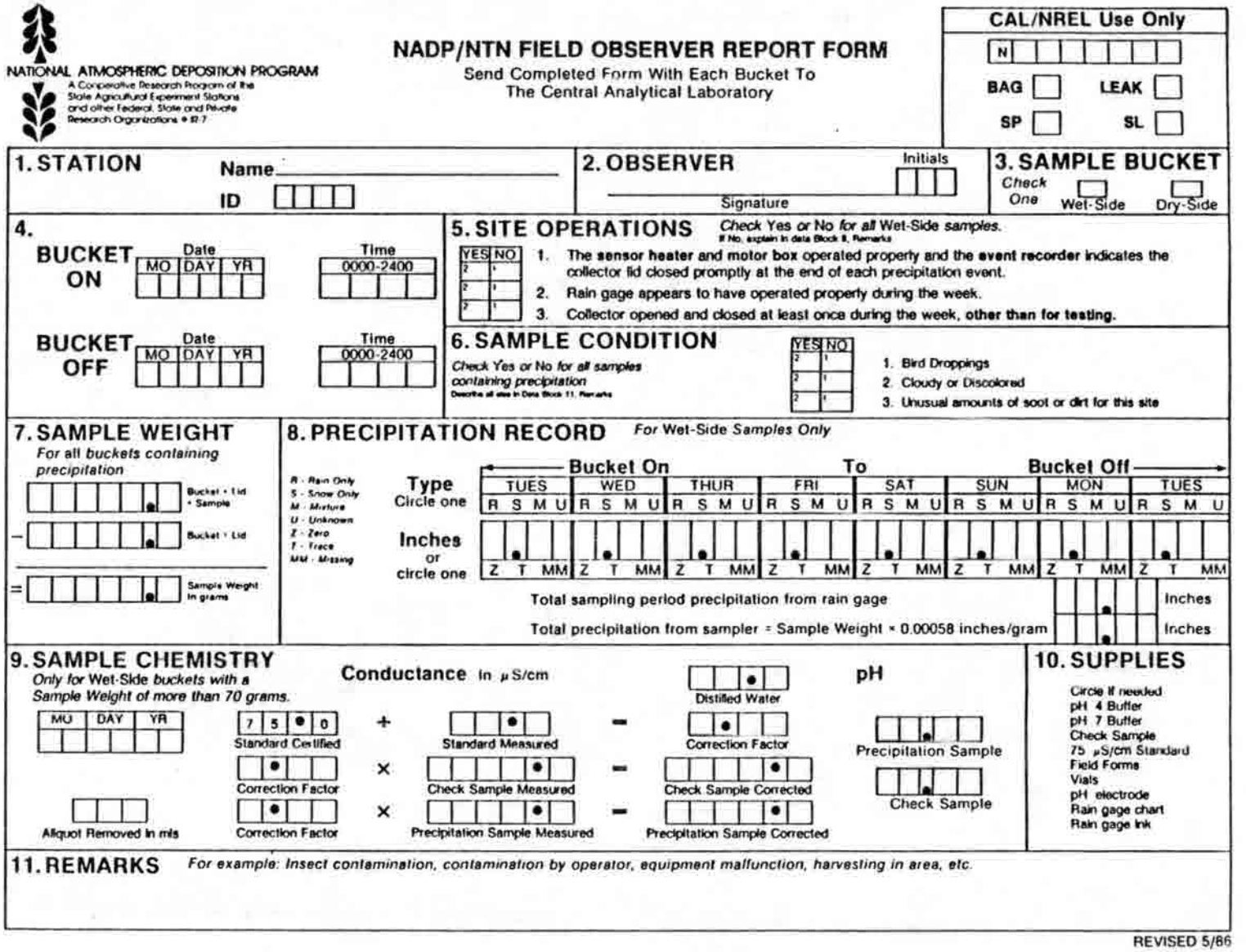


Figure 2. NADP/NTN Weekly Field Observer Report Form

Table 2. Attributes of NADP/NTN Weekly Data

| Attribute | Explanation |
|---|---|
| number | 'saroad' code |
| side | w-wet or d-dry |
| dateon | year month day |
| dateoff | year month day |
| timeon | hour minutes (Zulu or GMT) |
| timeoff | hour minutes (Zulu or GMT) |
| jdton | year,julian day |
| jdtoff | year,julian day |
| dayon | e. g. Tue-Tuesday |
| obs | observer's initials |
| calnum | nnnna, e.g. 0143b |
| seques | blank or q(quality assurance) or r(restricted) |
| calqa | CAL lab QA codes |
| modified | date data modified - year month day |
| svol | sample volume in ml |
| ppt | gage precip. in mm |
| eff | collection efficiency: sampler depth/gage depth |
| labtype | lab analysis code, e.g. wa |
| notes | field (or NREL) notes, separated by ,'s |
| checks | 1 - collector operated correctly (y or n) |
| | 2 - rain gage operated correctly |
| | 3 - collector opened and closed at least once |
| | 4 - sample contains bird droppings |
| | 5 - sample cloudy or discolored |
| | 6 - sample has lots of soot or dirt |
| pHlab | -log hydrogen ion concentration - laboratory value |
| pHfield | -log hydrogen ion concentration - field value |
| conduclab | conductivity, $\mu$S/cm - laboratory value |
| conducfield | conductivity, $\mu$S/cm - field value |
| Ca | Ca concentration in mg/l |
| Mg | Mg concentration in mg/l |
| K | K concentration in mg/l |
| Na | Na concentration in mg/l |
| $NH_4$ | $NH_4$ concentration in mg/l |
| $NO_3$ | $NO_3$ concentration in mg/l |
| Cl | Cl concentration in mg/l |
| $SO_4$ | $SO_4$ concentration in mg/l |
| $PO_4$ | $PO_4$ concentration in mg/l |
| limdetec | non-blank limit of detection symbol for Ca,Mg,K,Na,$NH_4$,$NO_3$,Cl,$SO_4$ |
| dailyrain | 8 daily rain amounts, each followed by type code [8(f5.2,a1)] |
| conducdist | field conductivity on distilled water |
| conduccor | field conductivity correction factor |
| pHcheck | field pH on check sample |
| datefld | date of field pH, etc. analysis (year month day) |

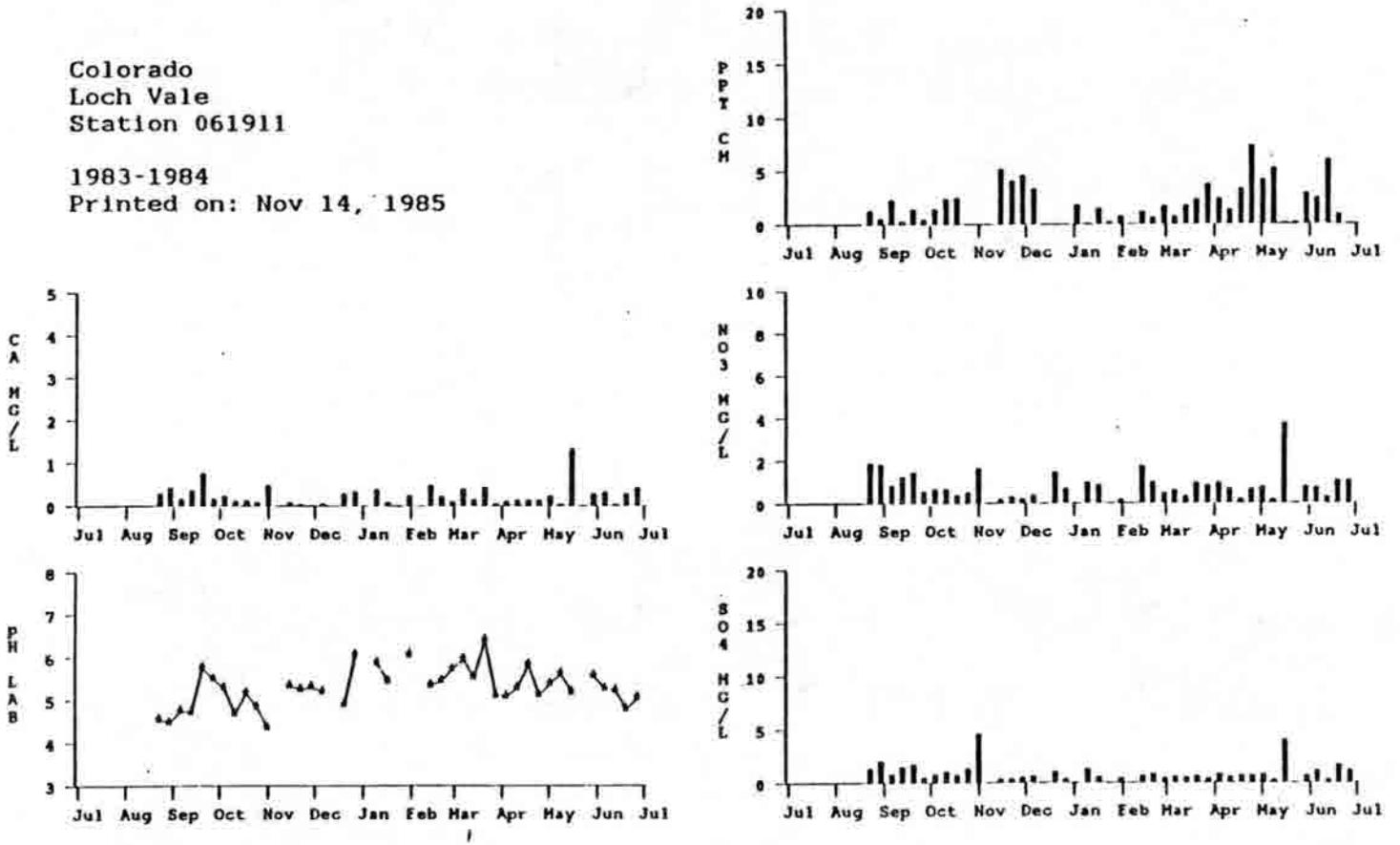


Figure 3. Weekly Data For Selected Elements at Loch Vale NADP/NTN Station

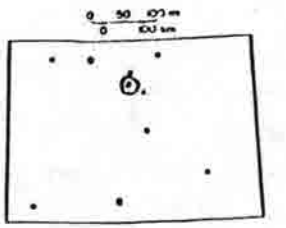

| | |
|---|---|
| State | Colorado |
| Site | Loch Vale |
| County | Larimer |
| Operation | NPS-WRFSL |
| Funding | NPS-WRFSL |
| Network | NADP |

| | |
|---|---|
| Number | 061911 |
| Longitude | 105:39:17 |
| Latitude | 40:17:16 |
| Elevation | 3159 meters |
| Printed | Nov 8, 1985 |

| date on modayr | date off modayr | pH lab | pH field | pH check | conductivity lab micro S/cm | conductivity field micro S/cm | sampler vol L | sampler dep cm | rain gage cm | coll eff | lab type | notes | time on GMT | time off GMT | obs |
|---|---|---|---|---|---|---|---|---|---|---|---|---|---|---|---|
| 032784 | 040384 | 5.10 | 4.86 | 4.34 | 7.8 | 8.8 | 1.041 | 1.53 | 2.44 | 0.63 | w | | 1830 | 1830 | saz |
| 040384 | 041084 | 5.30 | 5.04 | 4.25 | 5.6 | 5.9 | 0.604 | 0.89 | 1.37 | 0.65 | w | | 1830 | 1830 | saz |
| 041084 | 041784 | 5.85 | 5.84 | 4.27 | 2.9 | 3.9 | 0.576 | 0.85 | 3.35 | 0.25 | w | | 1830 | 1830 | saz |
| 041784 | 042484 | 5.13 | 5.03 | 4.34 | 6.3 | 7.4 | 2.286 | 3.37 | 7.39 | 0.46 | w | | 1830 | 1830 | saz |
| 042484 | 050184 | 5.39 | 5.00 | 4.35 | 5.7 | 6.8 | 1.273 | 1.87 | 4.22 | 0.44 | w | | 1830 | 1730 | saz |
| 050184 | 050884 | 5.62 | 5.34 | 4.35 | 2.3 | 2.7 | 1.265 | 1.86 | 5.26 | 0.35 | w | | 1730 | 1730 | saz |
| 050884 | 051584 | 5.19 | 4.42 | 4.23 | 24.7 | 32.3 | 0.130 | 0.19 | 0.18 | 1.08 | w | | 1730 | 1730 | saz |
| 051584 | 052284 | -- | -- | 4.24 | -- | -- | 0.088 | 0.13 | 0.23 | 0.57 | w | ns | 1730 | 1730 | saz |
| 052284 | 052984 | 5.57 | 4.86 | 4.23 | 5.9 | 7.9 | 1.999 | 2.94 | 2.95 | 1.00 | w | | 1730 | 1730 | saz |
| 052984 | 060584 | 5.27 | 4.59 | 4.22 | 8.3 | 11.6 | 1.625 | 2.39 | 2.51 | 0.95 | w | | 1730 | 1730 | saz |
| 060584 | 061284 | 5.23 | 4.91 | 4.23 | 3.9 | 4.7 | 2.745 | 4.04 | 6.10 | 0.66 | w | | 1730 | 1700 | saz |
| 061284 | 061984 | 4.79 | 4.40 | 4.20 | 13.2 | 17.7 | 0.667 | 0.98 | 0.99 | 0.99 | w | | 1700 | 1700 | saz |
| 061984 | 062684 | 5.05 | 4.65 | 4.36 | 10.7 | 14.8 | 0.253 | 0.37 | 0.10 | 3.66 | w | | 1700 | 1600 | saz |
| 062684 | 070384 | 4.99 | 4.50 | 4.36 | 8.5 | 13.5 | 0.979 | 1.44 | 1.40 | 1.03 | w | | 1600 | 1700 | saz |

| date on modayr | date off modayr | Ca mg/L | Mg mg/L | K mg/L | Na mg/L | NH4 mg/L | NO3 mg/L | Cl mg/L | SO4 mg/L | PO4 mg/L | H mg/L | cation micro eq/L | anion micro eq/L | ratio |
|---|---|---|---|---|---|---|---|---|---|---|---|---|---|---|
| 032784 | 040384 | 0.13 | 0.023 | 0.008 | 0.040 | 0.28 | 0.98 | 0.08 | 0.87 | <0.003 | 0.794e-02 | 33.8 | 36.3 | 0.9 |
| 040384 | 041084 | 0.15 | 0.030 | 0.006 | 0.057 | 0.14 | 0.72 | 0.05 | 0.63 | <0.003 | 0.501e-02 | 25.4 | 26.2 | 1.0 |
| 041084 | 041784 | 0.16 | 0.022 | 0.010 | 0.057 | < 0.02 | 0.24 | 0.07 | 0.74 | <0.003 | 0.141e-02 | 15.1 | 21.3 | 0.7 |
| 041784 | 042484 | 0.15 | 0.041 | 0.011 | 0.045 | 0.21 | 0.68 | 0.05 | 0.73 | 0.005 | 0.741e-02 | 32.2 | 27.7 | 1.2 |
| 042484 | 050184 | 0.24 | 0.039 | 0.016 | 0.049 | 0.18 | 0.78 | 0.09 | 0.84 | 0.004 | 0.407e-02 | 31.8 | 32.7 | 1.0 |
| 050184 | 050884 | 0.06 | 0.019 | 0.005 | 0.020 | 0.06 | 0.22 | 0.10 | 0.31 | <0.003 | 0.240e-02 | 11.3 | 12.9 | 0.9 |
| 050884 | 051584 | 1.34 | 0.234 | 0.082 | 0.430 | 0.84 | 3.77 | 0.34 | 4.01 | 0.006 | 0.646e-02 | 160.0 | 154.1 | 1.0 |
| 051584 | 052284 | -- | -- | -- | -- | -- | -- | -- | -- | -- | -- | -- | -- | -- |
| 052284 | 052984 | 0.29 | 0.046 | 0.048 | 0.067 | 0.16 | 0.82 | 0.12 | 0.74 | <0.003 | 0.269e-02 | 34.0 | 32.1 | 1.1 |
| 052984 | 060584 | 0.34 | 0.103 | 0.049 | 0.059 | 0.28 | 0.77 | 0.13 | 1.20 | <0.003 | 0.537e-02 | 50.2 | 41.2 | 1.2 |
| 060584 | 061284 | 0.06 | 0.010 | 0.014 | 0.026 | 0.08 | 0.33 | 0.09 | 0.36 | <0.003 | 0.589e-02 | 15.6 | 15.5 | 1.0 |
| 061284 | 061984 | 0.30 | 0.052 | 0.054 | 0.094 | 0.22 | 1.11 | 0.19 | 1.74 | <0.003 | 0.162e-01 | 53.2 | 59.6 | 0.9 |
| 061984 | 062684 | 0.44 | 0.069 | 0.128 | 0.113 | 0.13 | 1.12 | 0.18 | 1.30 | <0.003 | 0.891e-02 | 52.0 | 50.3 | 1.0 |
| 062684 | 070384 | 0.12 | 0.031 | 0.061 | 0.024 | < 0.02 | 0.67 | 0.10 | 0.81 | <0.003 | 0.102e-01 | 22.5 | 30.6 | 0.7 |

-- Indicates missing data

Figure 4. NADP/NTN Quarterly Report Of Precipitation Chemistry: Loch Vale

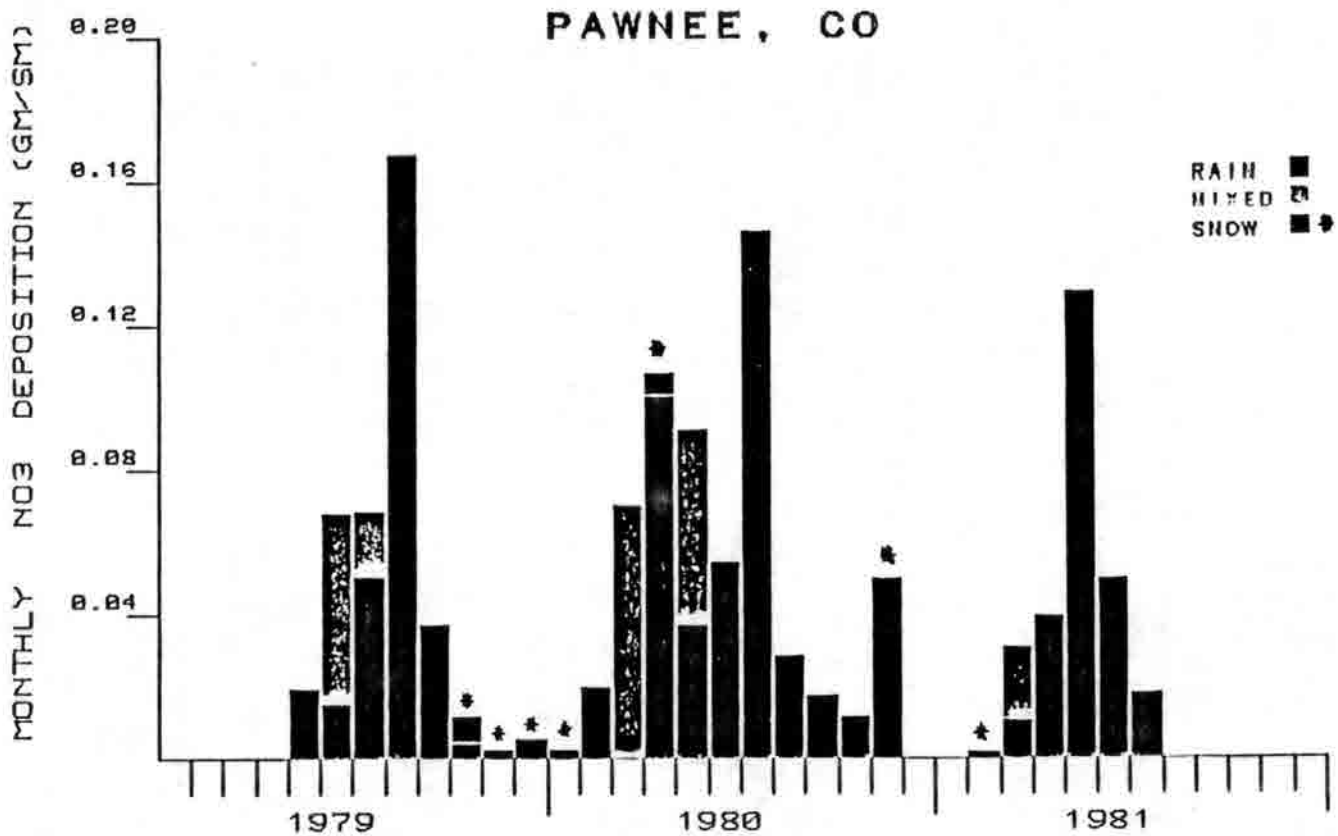


**Figure 5. Monthly $NO_3$ Deposition By Precipitation Type At The Pawnee NADP/NTN Station** (Figure courtesy of the United State Military Academy)

gage, that is represented by the collected chemistry sample. The seasonal and annual averages and data completeness estimates form the basis for producing temporal trend plots and isopleth maps distributed by the program. Since these averages and estimates are also maintained in the interactive, on-line database they too can be distributed in a variety of ways. The averages are available in units of mg/L or $\mu$ueq/L. Other units such as deposition units, can be furnished upon request.

Table 3 gives the annual data completeness estimates for Colorado sites for each year they operated for a complete annual time period. Notice the differences between the number of valid samples collected by the Manitou station in 1979 and 1980 as compared to other years. The increased uncertainty in this early data as compared to data collected in other years would most certainly want to be addressed should differences reflect a change in chemistry over the 6 year record at the site.

In addition to the data quality attributes distributed in standard NADP/NTN reports and data tapes, and data completeness estimates available with seasonal summaries, the quality of NADP/NTN data may be further assessed by evaluating data generated by external quality assurance audits conducted by the U.S. Geological Survey and the U.S. Environmental Protection Agency. Since NADP/NTN monitoring data can be used for a variety of scientific investigations, NADP is committed to the presentation of quality assurance information in much the same way it is committed to presenting precipitation chemistry data. The program recognizes that quality assurance conclusions can only be reached by data users who know to what use the data will be put.

Figure 6 is an abbreviated NADP/NTN Station Quality Assurance Report containing selected results of the NADP/NTN Site Visitation Program and the U.S. Geological Survey's Intersite Comparison Program. The first portion of the report addresses site representativeness by describing the NADP/NTN station in terms of problems that typically compromise a site's regional representativeness. These 'problems' form an agreed upon set of criteria that describe potential compromises to a site's representativeness. The report is arranged so as to describe potential site bias according to the three previously mentioned concentric distance intervals from the site. The actual criteria is given in Appendix B. In this example, the Alamosa site is noted to have been located within 100 meters of a parking lot.

The second part of the report presents audit results of the field chemistry measurements performed at the site. These numbers can be used to determine accuracy and precision of the field measurements. More complete precision and accuracy estimates of all NADP/NTN data have been published as U.S. Geological Survey Open File Reports (1,8,9).

Though not a data product per se, one addition NADP publication deserves mention. This is a map of the Distribution of Surface Waters Sensitive to Acidic Precipitation. In this NADP Technical Report (5), Norton and others have produced state maps which categorize surface water sensitivity at four levels of risk. The map for Colorado is presented as Figure 7.

## NADP DATA SERVICES

As mentioned previously, most NADP/NTN monitoring network data is stored and maintained with a commercially available, on-line interactive database management software package called INGRES. This 4GL database tool resides on a VAX 11-730 at the Natural Resource Ecology Laboratory at Colorado State University. Because of its report writing and powerful query language capability, data reports can be easily customized for specific uses. The NADP program supports a half-time person to field data requests and provide technical guidance to data users with special needs.

In addition to the database tools, the program has continued to develop mapping and plotting capabilities using the mapping packages SURFACE II, originally developed by the Kansas State

Table 3. Start Dates and Annual Data Completeness Statistics
For Colorado NADP/NTN Stations

| Station | Start Date: Year | Total Precip. | Percent of Days There is: Valid Samples | Precip. Coverage | Valid Samples And Precip. | Catch Efficiency |
|---|---|---|---|---|---|---|
| Manitou | October 17, 1978: | | | | | |
| | 1979 | 37.241 | 67.6 | 98.1 | 71.3 | 69.9 |
| | 1980 | 41.525 | 61.5 | 98.1 | 57.7 | 80.1 |
| | 1981 | 39.969 | 86.5 | 100.0 | 74.7 | 97.4 |
| | 1982 | 45.579 | 81.1 | 100.0 | 82.8 | 88.5 |
| | 1983 | 48.718 | 94.2 | 100.0 | 92.9 | 81.0 |
| | 1984 | 41.541 | 90.4 | 100.0 | 96.0 | 91.0 |
| Sand Spring | March 20, 1979: | | | | | |
| | 1980 | 30.679 | 88.7 | 99.7 | 95.6 | 83.7 |
| | 1981 | 41.725 | 90.4 | 98.1 | 99.7 | 89.9 |
| | 1982 | 37.166 | 92.5 | 100.0 | 97.2 | 89.0 |
| | 1983 | 42.736 | 90.4 | 100.0 | 83.0 | 96.4 |
| | 1984 | 46.317 | 77.0 | 100.0 | 83.9 | 87.2 |
| Pawnee | May 22, 1979: | | | | | |
| | 1980 | 32.990 | 86.5 | 100.0 | 97.8 | 79.2 |
| | 1981 | 34.380 | 90.4 | 100.0 | 92.2 | 94.3 |
| | 1982 | 41.414 | 90.6 | 100.0 | 98.3 | 96.9 |
| | 1983 | 37.275 | 90.4 | 100.0 | 97.6 | 85.6 |
| | 1984 | 41.484 | 86.6 | 100.0 | 98.2 | 80.8 |
| Alamosa | April 22, 1980: | | | | | |
| | 1981 | 22.695 | 88.5 | 100.0 | 99.2 | 93.1 |
| | 1982 | 12.509 | 71.7 | 81.1 | 80.0 | 81.9 |
| | 1983 | 18.491 | 75.0 | 100.0 | 68.7 | 85.1 |
| | 1984 | 18.036 | 69.3 | 100.0 | 75.7 | 95.0 |
| Rocky Mtn Nat'l Park Beaver Meadows | May 29, 1980: | | | | | |
| | 1981 | 33.401 | 84.6 | 100.0 | 81.0 | 90.8 |
| | 1982 | 36.793 | 84.9 | 100.0 | 94.2 | 95.1 |
| | 1983 | 45.344 | 94.2 | 100.0 | 92.7 | 93.3 |
| | 1984 | 43.143 | 78.6 | 98.1 | 88.1 | 86.3 |
| Mesa Verde Nat'l Park | April 28, 1981: | | | | | |
| | 1982 | 64.938 | 86.8 | 100.0 | 92.2 | 91.9 |
| | 1983 | 57.291 | 84.6 | 100.0 | 94.4 | 81.1 |
| | 1984 | 40.842 | 77.3 | 96.2 | 94.8 | 68.6 |
| Rocky Mtn Nat'l Park Loch Vale | August 16, 1983: | | | | | |
| | 1984 | 111.142 | 76.7 | 98.1 | 82.7 | 62.8 |
| Las Animas Fish Hatchery | October 4, 1983: | | | | | |
| | 1984 | 33.492 | 61.6 | 100.0 | 41.6 | 71.6 |
| Buffalo Pass | February 7, 1984: | | | No Annual Data Available | | |
| Niwot Saddle | June 5, 1984: | | | No Annual Data Available | | |

NATIONAL ATMOSPHERIC DEPOSITION PROGRAM/ NATIONAL TRENDS NETWORK
Station Quality Assurance Report: Site Representativeness

Printed: 8-AUG-1986
ALAMOSA Station Number: 60060
CAL Code: CO00

Alamosa County, CO
Began Network Operations: 800422

Data Available for For Determining Site Representativeness:

Longitude: 105 51 55 Latitude: 37 26 36 Elevation: 2298 meters
Ecoregion: M313
Site Visitation Results:

| Visit Date | Violations of Siting Criteria Noted: Regional | Local | Within 30m | Collector/ Rain Gage Options | | Rain Gage Calibration/ | Turnover |
|---|---|---|---|---|---|---|---|
| 821112 | , | 10, , , | 1,2, , ,5, , , ,9 | NO | YES | OK | OK |

Data Available for Determining Site Performance:

| Dates Analyzed | Sent | Measured | Standard | Difference | Audit Type | Commments |
|---|---|---|---|---|---|---|
| pH: | | | | | | |
| 0 | 811000 | 4.36 | 4.10 | 0.260 | intersite05 | |
| 0 | 820400 | 4.51 | 4.52 | -0.010 | intersite06 | |
| 0 | 821100 | 4.24 | 3.95 | 0.290 | intersite07 | |
| 0 | 830500 | 3.77 | 3.79 | -0.020 | intersite08 | |
| 0 | 831100 | 4.91 | 4.51 | 0.400 | intersite09 | |
| 0 | 840900 | 4.12 | 4.10 | 0.020 | intersite10 | |
| 0 | 860108 | 4.60 | 4.65 | -0.050 | intersite15 | |
| 860414 | 860407 | 4.80 | 4.99 | -0.190 | intersite16 | |

**Figure 6. NADP/NTN Station Quality Assurance Report: Alamosa**

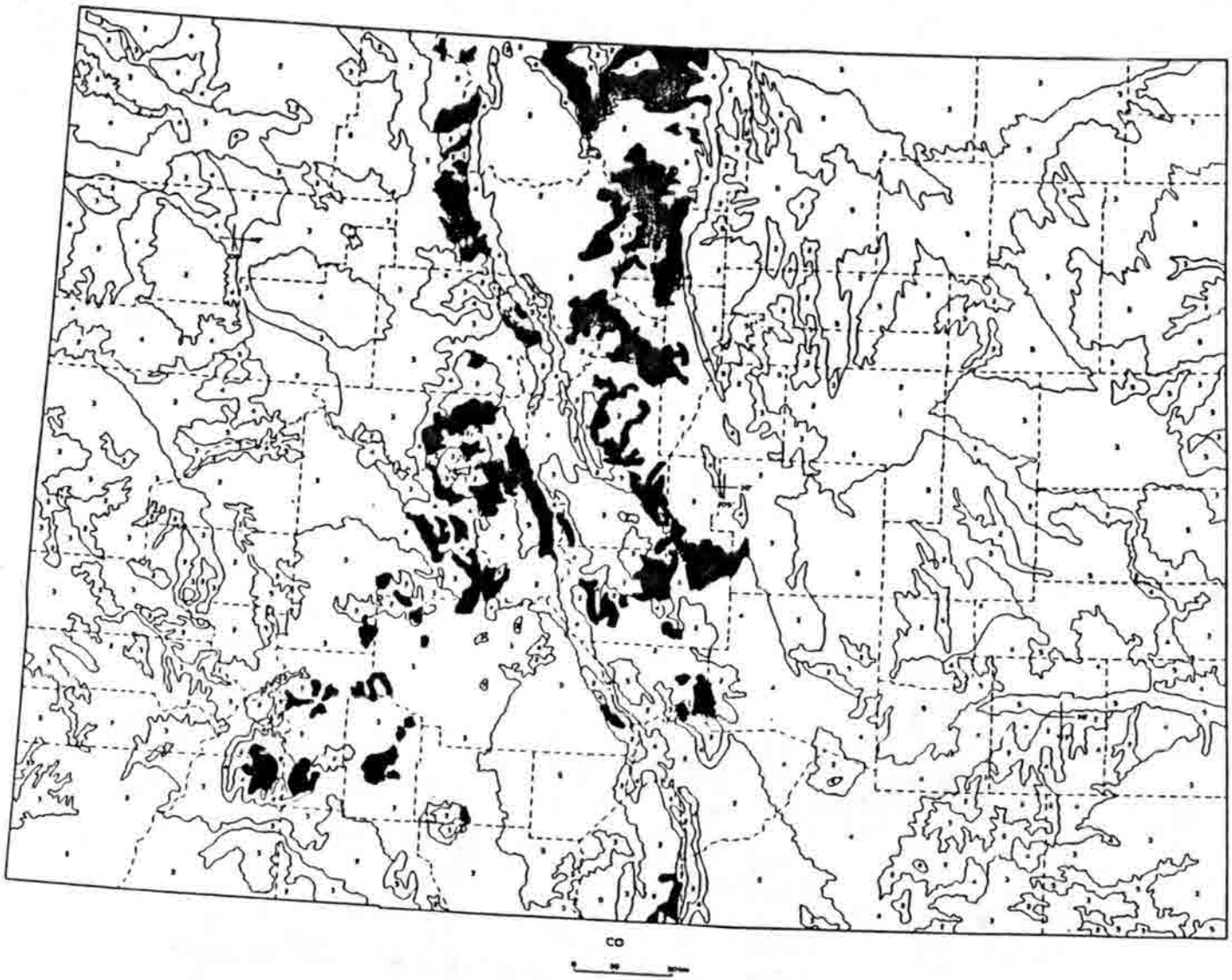


**Figure 7. Distribution Of Surface Waters Sensitive To Acid Deposition In Colorado** (From NADP, 1982. [Norton, ed])

Geological Survey, and S, a Bell Laboratories interactive software package for data analysis and graphics. Limited resources are available to apply these tools to specific NADP/NTN data requests.

## REFERENCES


1. Brooks, M.H., L.J. Schroder, and B.A. Malo, 1985. Interlaboratory comparability, bias, and precision for four laboratories measuring constituents in precipitation, November 1982–August 1983. Water-Resources Investigations Report 85-4313, U.S. Geological Survey, Lakewood, Colorado.

2. Bowersox, V.C., 1985. Data validation procedures for wet deposition samples at the Central Analytical Laboratory of the National Atmospheric Deposition Program. Transactions: Quality Assurance in Air Pollution Measurements. An APCA International Specialty Conference, Boulder, Colorado, October, 1984.

3. Dossett, S., 1984. Aerochem Metrics Precipitation Collector Maintenance Manual. Contract Report to the National Atmospheric Deposition Program, SWS, No. 343, Illinois State Water Survey, Champaign, Illinois. September, 1984, p. 28.

4. National Atmospheric Deposition Program, 1982. NADP Instruction Manual: Site Operations. Natural Resource Ecology Laboratory, Colorado State University, Fort Collins, Colorado.

5. National Atmospheric Deposition Program, 1982. Distribution of Surface Waters Sensitive to Acidic Precipitation: A State Level Atlas. Stephen A. Norton, ed., Department of Geological Sciences, University of Maine, Orono, Maine.

6. National Atmospheric Deposition Program, 1984. NADP Instruction Manual: Site Selection and Installation. Natural Resource Ecology Laboratory, Colorado State University, Fort Collins, Colorado.

7. National Atmospheric Deposition Program, 1985. NADP Annual Summary of Precipitation Chemistry for 1982. Natural Resource Ecology Laboratory, Colorado State University, Fort Collins, Colorado.

8. Schroder, L.J., and J.O. Brennan, 1985. Precision of the measurement of pH and specific conductance at National Atmospheric Deposition Program monitoring sites, October 1981–November 1983. Water-Resources Investigations Report 84-4325, U.S. Geological Survey, Lakewood, Colorado.

9. Schroder, L.J., A.W. Bricker, and T.C. Willoughby, 1985. Precision and bias of selected analyses reported by the National Atmospheric Deposition Program and National Trends Network–1983 and January 1980 through September 1984. Water-Resources Investigations Report 85-4275, U.S. Geological Survey, Lakewood, Colorado.

10. Trenberth, K.E., 1983. What are the seasons? *Bull. Amer. Meteor. Soc.*, **64**, 1276–1282.

## APPENDIX A : Site Description Questionnaire For The NADP/NTN Station At Alamosa

Last update:July 26 1985
Last reviewed:

SITE IDENTIFICATION
station: Alamosa
county: Alamosa
state: Colorado
saroad: 060060
CAL code: CO00
latitude: 37 26 36
longitude: 105 51 55
elevation: 2298m
USGS Map:
Ecoregion: M3113

ADMINISTRATION
operating agency: NOAA-National Weather Service
funding agency: NOAA-Air Resources Laboratory
site ownership: City and County of Alamosa

Site Operator: Harvey Teyler
address .. Weather Service Office
2490 South State Avenue
Alamosa, Colorado 81101
phone .. 303-589-3232

Operator's Supervisor:

address ..

phone ..

Preliminary Printout to:
Richard Artz
address .. DOC/NOAA/Air Resources Laboratory
Room 927, Gramax
8060 13th Street
Silver Spring, MD 20910
phone .. 301-427-7295

INSTRUMENTATION
collector: Aerochem Metrics model: 301
power: 110AC snow roof: no trickle charger: no
rain gage: Belfort model: 5-780
event recorder: yes alter shield: no
recording:yes weighing: yes opening: 20.3cm

distance: 6m direction: North
annual precipitation: 182mm 145mm 87.6cm
(total)(rain) (snow depth)
nearest alternate rain gage: 192m at weather yard years: 40
wind instrumentation located within 0.5 km:
manufacturer: model:
recording: speed only speed: yes direction: yes
distance: direction: height:

CO-LOCATED INSTRUMENTATION within 0.5 km
aerosol samplers:
gas measurements:
meteorological instruments:
1) psychrometer
2) Belfort 5-775-B rain gage
3) temperature
4) 8" dip NWS rain gage
5) evaporation pan
other:
turbidity

OTHER ASSOCIATED RESEARCH ACTIVITIES
(please describe...1....2...etc)

POTENTIAL LOCAL CONTRIBUTORS TO DEPOSITION at the Site
Within 30 m of the sampler.(all objects taller than sampler):
structures: none
trees: none
other: none

access is good in summer and winter
public access road is paved
collector is 200m from the road.
describe other than public road access to the site: none
special logistical problems include: none

Within 200 m of the sampler:
predominate land use is: 100% pasture
unpaved roads and parking areas: none

AGRICULTURAL OPERATIONS within 1 km of the sampler: none

TRANSPORTATION RELATED SOURCES within 10 km of the sampler:
main highways: none
other paved roads:
1) parking lot surface material: asphalt
distance: 300m direction: East traffic volume: light
2) route no. 160 traffic volume: light
distance: 2.8km direction: North
3) route no.: local road to airport traffic volume:

distance: 215m direction: E

lake/river/rail:
1) rail traffic:
distance: 2.8km direction: North

airports:
location: on site traffic: light to medium
distance: 500m direction: East

other transportation related:
1) type: fuel storage
distance: less than 400m direction: E and SE

STATIONARY SOURCES within 60 km of the sampler:
power plants: none
industry: none
other stationary sources: none

AREA SOURCES within 60 km of the sampler:
type: Alamosa pop.13,000
distance: 2.8km direction: West

GEOLOGY
Soil type within 1 km of the site is sandy.
A soils map has not been made available.

LABORATORY FACILITIES
Available laboratory facilities are good
These facilities are not shared.
Located: ~ 300m
The type of low conductivity water used is bottled.
EQUIPMENT:
pH meter:
manufacturer: Corning model: 125
pH probe:
manufacturer: Corning model: combination 476223
conductivity meter:
manufacturer: Barnstead model: PM-70CB
conductivity probe:
manufacturer: Yellow Springs Instrument Co. model: 3403
balance:
manufacturer: Ohaus model: 1119-D
Special problems?

DOCUMENTS furnished to the coordinator's office
map: type: date:
scale drawing: yes scale:1cm=10' date: October 18 1983
pictures: yes date: November 8 1982
October 18 1983

other: 1979 climatological summary
1982 climatological summary
1979 meteorological data
NOAA station location sheet: Position Information for weather service specialist which contains a four-page description of the area

OPERATIONAL HISTORY

| Date | Comment |
|---|---|
| April 22 1980 | Site startup. |
| June 15 1982 | Site discontinued by sponsor through Aug. 82. |
| August 24 1982 | Site restarted by sponsor. |
| October 8 1982 | Site visitation by Jerre Wilson and Dave Bigelow. |
| October 18 1982 | Site relocated 192m South of previous location to get away from influence of beacon tower. Previous site at weather yard. |

EQUIPMENT HISTORY

| Date | Comment |
|---|---|
| October 18 1983 | Rain gage replaced with Belfort 5-780. |
| October 18 1983 | Event pen added to rain gage. |

## APPENDIX B : NADP/NTN Siting Criteria

Listed below is the number key to the NADP/NTN siting criteria. Blanks indicate no siting criteria violations. Numbers between blanks correspond to the key below.

ON SITE On Site Requirements (within 30 meters)

1. Recommended Installation of the collector is on the standard 3 foot high aluminum base over undisturbed ground. In areas having an accumulation of over 2 feet of snow per year, the collector may be raised off the ground on a platform. This platform will be no higher than the maximum anticipated snowpack. In general, platforms are discouraged.
2. The collector should be oriented with the WET side bucket to the west and the sensor pointing north.
3. Naturally vegetated, level areas are preferred, but grassed areas and slopes up to $\pm$ 15% will be tolerated. If possible, such ground cover should surround the collector for a distance of approximately 20 meters. The slope should be within the prescribed value in the ground cover area. In farm areas a vegetated buffer strip must surround the collector for at least 20 meters.
4. The base of the collector will not be enclosed.
5. Objects with sufficient mass to deflect the wind (with the exception of an alter wind shields) over 1 meter high will not be located within 5 meters of the collector.
6. The rain gage should be located within 30 meters of the collector, but no closer than 5 meters. It's orifice should be located within 1 foot of the same level as the orifice of the collector.
7. Collectors located in areas which normally receive snow will only have a snow roof installed on the moving lid of the collector when problems with opening and closing are encountered. Such a lid will be left on year round.
8. Annual vegetation will be maintained at less than 2 feet.
9. No object or structure shall project onto the collector or rain gage with an angle greater than 45 degrees from the horizontal (30 degrees is considered optimal, but 45 degrees is the highest angle acceptable). Therefore the distance from the sampler to the object must be at least equal to the height of the object (preferably twice the height of the object). Pay particular attention to anemometer towers and overhead wires.

LOCAL Local Requirements (within 1 km)

10. No surface storage of agricultural products, fuels, vehicles, or other foreign materials within 100 meters of the collector will be allowed. Parking lots and maintenance yards with frequent use are a particular problem.
11. Grazing animals and pasture will not be closer than 20 meters to the collector. Feedlots, dairy barns, etc, in which large concentrations of animals are housed will be no closer than 500 meters to the collector.
12. Frequent moving sources of pollution, such as air, ground, or water traffic or the medium on which they traverse (e.g. runway, taxiway, road, or navigable river) within 100 meters of the collector. The local road net around the site is of particular concern.
13. Residential type buildings should not be within a 30 degree cone.

REGN Regional Requirements (within 50 km)

14. Continuous industrial-type operations such as factories, chemical plants, power plants, etc will not be within 10 km of the collector. Additionally if the emissions sources are located in the general upwind direction (i.e the mean annual west-to-east flow in most cases) of the collector, then they should be no closer than 20 km to the collector.

15. The collector should not be located within 10 km of a moderate-sized suburban or urban area. A general definition of this classification is one having 10,000 or more people. This distance should be increased to 20 km if the urban area is in the general upwind direction of the collector. For the larger cities (i.e. populations greater than 75,000) the collector should be no closer than 20 km if it is in the upwind direction, and 40 km if it is in the downwind direction.

# A 2-D Finite Element Simulation of Temperature Gradient Metamorphism

Mark Christon
Patrick Burns
Erik Thompson
Department of Mechanical Engineering
Colorado State University
Fort Collins, Colorado 80523

Richard Sommerfeld
Rocky Mountain Forest and
Range Experiment Station
240 West Prospect
Fort Collins, Colorado 80526

August 14, 1986

**Abstract**

In dry snow packs experiencing a temperature gradient, heat and mass transport are responsible for the metamorphism of ice crystals. The work presented herein investigates the influence of geometry, density, and temperature on the coupled, simultaneous heat and mass transport in idealized, two dimensional ice lattice cells. The results of the analysis show clearly that both the mass and heat transport are strongly dependent upon the ice lattice geometry. The effective diffusion coefficient is enhanced relative to the diffusion coefficient for water vapor in air for all of the two dimensional geometries studied. In addition, the preferential growth of branch grains has been verified using both static and dynamic, computer generated images of ice lattice cells undergoing temperature gradient metamorphism.

## INTRODUCTION

In recent years, environmental changes have focused attention on the problem of acid deposition and its effects on freshwater resources throughout the world. In the United States, the National Acid Precipitation Assessment Program has been implemented to improve the understanding of acid deposition and environmental processes. In Colorado, the deposition rates of ions such as sulfate and nitrate are low relative to the northeast portion of the United States and many parts of Western Europe. However, in remote areas where the hydrological systems are small, topsoils are thin, and the waters are dilute, even low deposition rates of pollutants can have a marked influence on the local environment.

Deposition of particles in both wet and dry forms occurs by several mechanisms. In general, particles reach the ground by fall-out, wash-out, rain-out or pump-out. These atmospheric processes constitute only a small part of the whole acid deposition problem. In addition to deposition, a clear

understanding of the complex events that occur once pollutants reach the ground is necessary. Acidic particles may be input directly to a water system by a rainfall event or stored in a snow pack and released in a spring melt. Ultimately, acid input to a freshwater stream or lake may cause both short and long term depressions in the pH and alkalinity levels. Water quality changes are believed to be due to the deposition of hydrogen, sulfate, nitrate and ammonium ions.

The problem of acid deposition involves many facets of the environment and encompasses a broad range of scientific areas. The seasonal snowcover plays an important role in the acid deposition chain because it can accumulate pollutants during the winter and release them in the spring in an acid pulse. The acid input to a snowcover can be significant because falling snow is an effective scavenger resulting in the wash-out of pollutants. Pollutants adsorbed on ice surfaces in a snowcover do not remain fixed to a single crystal. A snow pack evolves during a winter season with ice recrystallizing due to temperature gradient metamorphism. In some instances, a layer of snow can completely recrystallize in a time scale of 10 to 20 days when temperature gradient metamorphism is active. This recrystallization process ultimately results in the release of particles adsorbed on ice crystal surfaces. The liberated pollutants can take part in biological, chemical and mechanical processes in the snowcover. The preferential elution of ions such as sulfate and nitrate in the spring melt may be linked to the redistribution of pollutants in a snowcover when temperature gradient metamorphism occurs. Detailed knowledge of the heat and mass transport on a microscopic scale would provide a first step in the prediction of pollutant movement in a snowcover due to temperature gradient metamorphism.

The metamorphism of snow may be subdivided into two main categories. The first type of metamorphism is due to local variations in surface energy which cause differences in the water vapor concentration over the ice crystals that constitute the snow pack. These concentration differences drive a mass transport process known as equi-temperature metamorphism. This has also been referred to as "radius-of-curvature" metamorphism (Colbeck, 1980) because the local surface energy is a function of the ice crystal radius of curvature. It should be noted that surface energy variations may arise from other causes such as localized stresses in the ice crystals. "Radius-of-curvature" and temperature gradient metamorphism may occur simultaneously, however, the mass flow rates occurring during temperature gradient metamorphism exceed the flow rates observed during equi-temperature metamorphism by several orders of magnitude (Gray and Male, 1981; Perla, 1978; deQuervain, 1973; Yosida, 1955).

At the base of seasonal snow covers, the temperature usually remains about 0° during the winter months. When the ambient temperature is less than this base temperature, a temperature gradient results. The earth is a relatively constant heat source providing approximately 0.005 $W \cdot m^{-2}$ of energy on the average (Carslaw and Jaeger, 1959). The change in snow structure occurring due to an applied gradient is known as temperature gradient metamorphism and has been observed to occur for temperature gradients greater than $10°C \cdot m^{-1}$. In this case, the concentration differences which drive the mass transport across ice lattice pores are due to temperature differences. As in the equi-temperature process, temperature gradient metamorphism is actually a coupled, simultaneous heat and mass transport phenomenon. However, instead of surface energy determing the water vapor pressure, the impressed temperature gradient determines the local ice crystal temperature which in turn establishes the local water vapor concentration at the ice surfaces. The metamorphism process slows considerably when the snow density is greater than about 350 $kg \cdot m^{-3}$ (Marbouty, 1980). It has been demonstrated that the density of snow undergoing temperature gradient metamorphism is relatively constant when compaction is negligible (Sommerfeld, 1983; Marbouty, 1980; Giddings and LaChapelle, 1962; Yosida, 1955). This implies that the ice mass only undergoes a relocation on the scale of the ice crystals during temperature gradient metamorphism. This mass relocation has been

referred to by Yosida as the "hand-to-hand" process (Yosida, 1955). In the ice lattices of snow packs, preferential growth and decay sites exist which influence the mass relocation. These preferential sites have been characterized as branch grains which do nothing for the snow pack strength but directly influence the local crystal growth rates (Sommerfeld, 1983). Temperature gradient metamorphism is a semi-reversible process with respect to the direction of the impressed temperature gradient (Kuriowa, 1974).

Although there has been considerable work done in the area of temperature gradient metamorphism, most of the analyses have been one dimensional or addressed only the de-coupled vapor transport problem. On a microscale, multi-dimensional analyses have only been able to account for pairs of ice crystals or ice crystal clusters (Colbeck, 1983; Gubler, 1985). There has been very little detailed numerical analysis of the coupled heat and mass transport problem in two dimensions because of the extraordinary computing requirements to attain meaningful results. Supercomputers are making it possible to model processes such as temperature gradient metamorphism which were considered numerically intractable only a few years ago.

The goal of the research presented herein is to analyze idealized, two dimensional, vertical sections of a snow matrix to attain detailed information about mass transfer rates, mass flux distributions, water vapor concentration and temperature distributions, and effective diffusion coefficients and thermal conductivities for an impressed temperature gradient of $40°C \cdot m^{-1}$. Results are computed for variable temperature, density, and geometry for the initial conditions, while constant density is utilized for the transient analysis. The geometrical scope of the study includes a one dimensional test case and six different ice lattice pores with and without branch grains. A finite element model of the coupled, non-linear, simultaneous heat and mass transfer process is utilized to analyze the problem in 2-D. Deforming meshes are implemented to simulate the growth/decay process which occurs over time in an ice lattice pore. Use of the Cyber 205 supercomputer at Colorado State University makes it possible to study multiple geometries and perform sensitivity studies using highly refined meshes. Output from the transient analysis is post-processed using the Computer Aided Engineering Lab at Colorado State University to generate a color videotape of the simulated temperature gradient metamorphism process. By utilizing high resolution computer graphics to generate a movie of the simulation, direct comparison with Kuriowa's experimental film of temperature gradient metamorphism is achieved.

## ANALYSIS

Snow is a complex and interesting composition of ice crystals which form an intricate matrix of ice and air. The ice crystals which constitute a snow cover may be categorized as either branch, chain or link grains (Gubler, 1978). Figure 1 shows a two dimensional representation of the components of an ice lattice viewed on a microscopic scale. Dry snow is made of ice crystals existing at a temperature and pressure below the triple point of water. The various crystal components of a snow pack metamorphose over time with the chain and link grains being sacrificed for the growth of branch grains. From a stereological basis, the ratio of the area of ice to the area of water vapor in a two dimensional slice of snow may be considered representative of the snow density. In this analysis, the area ratio is used rather than density because of its relation to the fundamental pore geometries considered.

In order to arrive at governing equations for the problem, assumptions about the thermodynamics as well as the heat and mass transport are required. The analysis is limited to dry snow which requires that only the solid and vapor phases of water be present. Specifically, the snow is modeled as a single component, two phase substance. The air which exists in the ice lattice pores with the water vapor plays an insignificant part in the determination of the equilibrium vapor pressure.

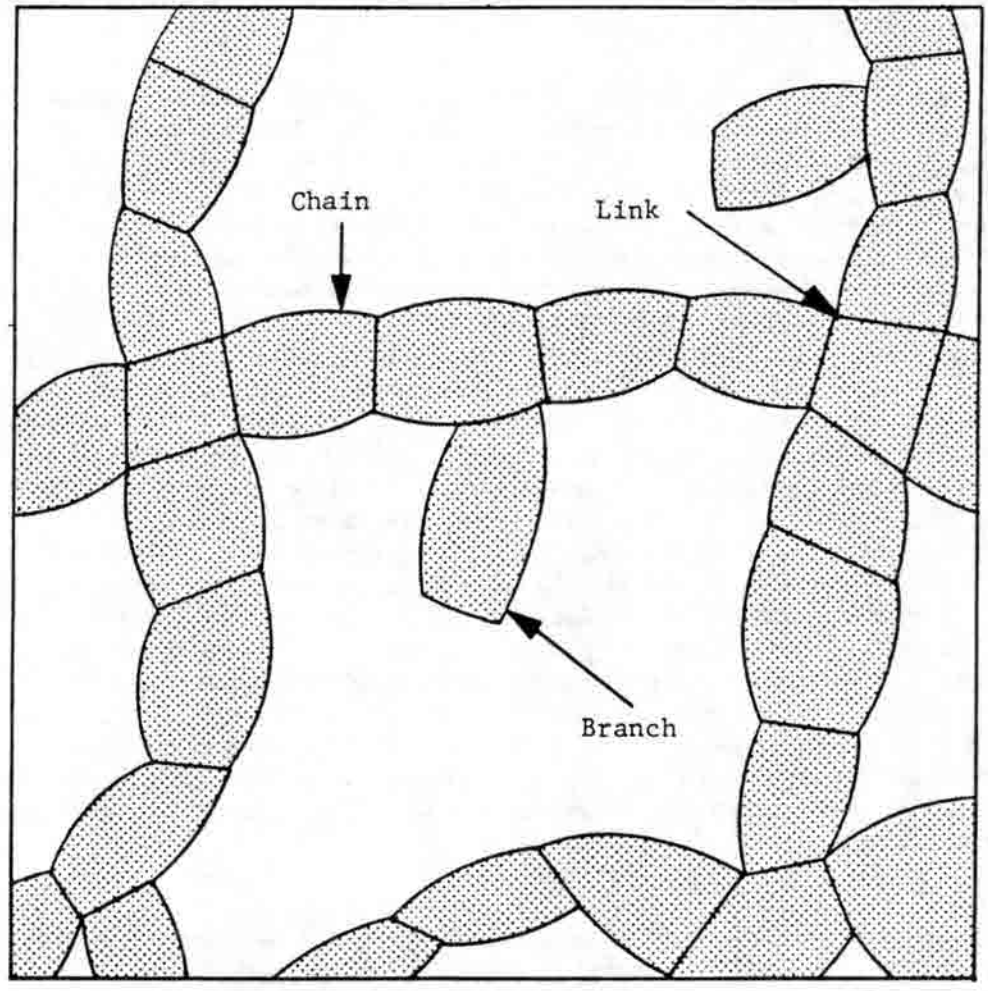


Figure 1. Microscopic View of Ice Lattice Constituents

Essentially, the air acts as a medium through which the water vapor diffuses. The concept of local thermodynamic equilibrium is applied at the interface between the solid and vapor phases. This is a good approximation when the mass flux rates across an interface are low (which is the case here). Additionally, the vapor phase is treated as an ideal gas. The effect of surface curvature on the equilibrium vapor pressure is neglected as surface energy effects are important only at points where the radius is less than about $10^{-8}$m. The question of natural convection can be considered on both the macroscale and the microscale. It has been demonstrated that free convection can occur only under extreme conditions (Christon, 1986; Palm and Tveitereid, 1979; Akitaya, 1974). For the mass conservation equation, the storage term is neglected. This has been supported by experimental evidence that the snow density remains constant during temperature gradient metamorphism when compaction is not significant (Sommerfeld, 1983; Marbouty, 1980; Giddings and LaChapelle, 1962; Yosida, 1955). From a dimensional analysis of the energy equation, two parameters arise which determine whether or not the storage term is significant. The diffusion coefficient arises in the non-dimensional parameters because the mass diffusion process is essentially the rate limiting process in temperature gradient metamorphism. Since both of these parameters are small, the storage effects can be neglected. The energy and mass conservation equations for the problem are given as:

Energy:

$$\frac{\partial}{\partial x}\left(k_x \frac{\partial T}{\partial x}\right) + \frac{\partial}{\partial y}\left(k_y \frac{\partial T}{\partial y}\right) = -Q \tag{1}$$

Mass Conservation:

$$\frac{\partial}{\partial x}\left(D_x \frac{\partial \rho_v}{\partial x}\right) + \frac{\partial}{\partial y}\left(D_y \frac{\partial \rho_v}{\partial y}\right) = 0 \tag{2}$$

For the thermal problem, temperatures along the upper and lower horizontal ice grains of the ice lattice pores are specified corresponding to an impressed temperature gradient of $40°\text{C}\cdot\text{m}^{-1}$. Symmetry between adjacent ice lattice pores is utilized. For the diffusion problem, the vapor concentration at the solid/vapor interface is based on the interface temperature distribution. It is important to note that the domains for the two governing equations are different, but overlap. The diffusion equation is valid only in the ice lattice pore where the vapor phase exists. The thermal domain includes the solid matrix, and the pore. Although both the mass and energy conservation equations are linear, partial differential equations, they are coupled in a non-linear fashion. The coupling term between the equations is:

$$Q = \left(-D\bar{A} \cdot \frac{\partial \rho_v}{\partial \bar{n}}\right) H_{sg} \tag{3}$$

The coupling term represents a spatial distribution of heat sources and sinks at the solid/vapor interface which depend upon the vapor concentration gradient which is a non-linear function of temperature.

Solving the coupled mass conservation and energy equations yields four of the six primary variables of interest. The primary variables are:

1. Mass Transfer Rates in the Ice Lattice Pores
2. Mass Flux Rate Distributions
3. Water Vapor Concentration Distributions

4. Temperature Distributions

5. Effective Diffusion Coefficients

6. Effective Thermal Conductivities

In order to evaluate the effective diffusion coefficient and the thermal conductivity, the following equations are required.

$$D_{eff} = -\frac{\overline{\dot{m}}}{A} \frac{\Delta y}{[\rho(T_c) - \rho(T_h)]} \tag{4}$$

$$k_{eff} = -\frac{Q}{A} \frac{\Delta y}{[T_c - T_h]} \tag{5}$$

The definition for the effective diffusion coefficient is consistent with the definition of the thermal conductivity and incorporates the thermal boundary conditions.

The form for the governing equations for the problem allows a finite element formulation using variational principles for both the energy and mass conservation equations. In this case the solution to the continuum problem is a temperature and water vapor concentration which makes the variational principle for each governing equation a stationary value (Zienkiewicz, 1983). In the model, six-node iso-parametric elements are implemented to allow for a parabolic variation in both temperature and concentration. The domain for the thermal field does not coincide with the domain for the diffusion problem This requires the use of a separate finite element mesh for each domain, the thermal mesh being larger than the diffusion mesh to include the ice crystals. Because the two governing equations are coupled in a non-linear way, Newton's method is utilized. By using the finite element method, a single computer code may be used to analyze a wide range of geometries. In addition, the formulation for this problem is relatively general. The computer code may be used for the simulation of coupled heat and mass transfer processes similar to temperature gradient metamorphism for substances other than water by accounting for differences in the thermal conductivity and diffusion coefficient for the vapor phase.

## RESULTS AND DISCUSSION

The finite element code used in the analysis was written to exploit the vector processing capabilities of the Cyber 205 supercomputer. The Cyber 205 at Colorado State University can perform mathematical operations on vectors up to 65,535 elements long. Utilizing the vector processing capabilities of the Cyber 205 provided an extremely fast, efficient computer program. Timing comparisons between the Cyber 205 and a CDC 170/830 showed a speed up by a factor of 13 on the Cyber 205 for problems using 400 nodes in the thermal finite element mesh. The problems considered in this research required from 1000 to 4000 nodes in the thermal mesh. The memory requirements for the runs reported here exceeded the storage capacity of the CDC 180/830. From convergence studies, it was found that accurate mass conservation requirements controlled the mesh refinement. For all of the geometries analyzed, the finite element meshes were refined until a mass conservation of about 2% was achieved. For the transient analysis, it was found that remeshing was required every two time steps to maintain accurate information about mass flow and mass flux rates.

The geometries used for the analysis included pores with and without branch grains for a range of area ratios from 0.1 to 0.5. Figure 2 shows the concentration field for four different pore geometries considered collectively. This was one of the geometrical configurations used in the transient analysis. Figure 3 shows the temperature field for this problem and serves to demonstrate that the symmetry

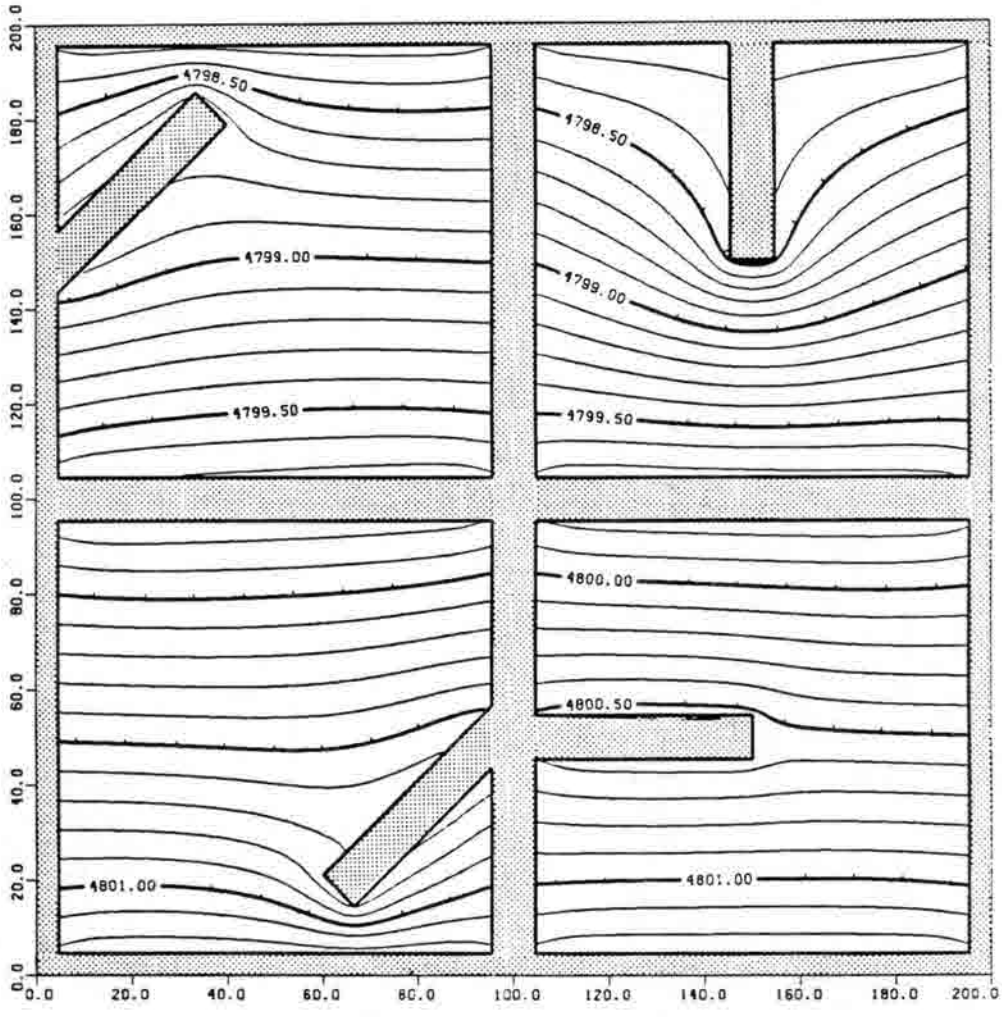


Figure 2. Lines of Constant Concentration at Time = 0.0 Seconds for the Ice Lattice Used in the Transient Analysis ($kg \cdot m^{-3}$ x 1.E-6).

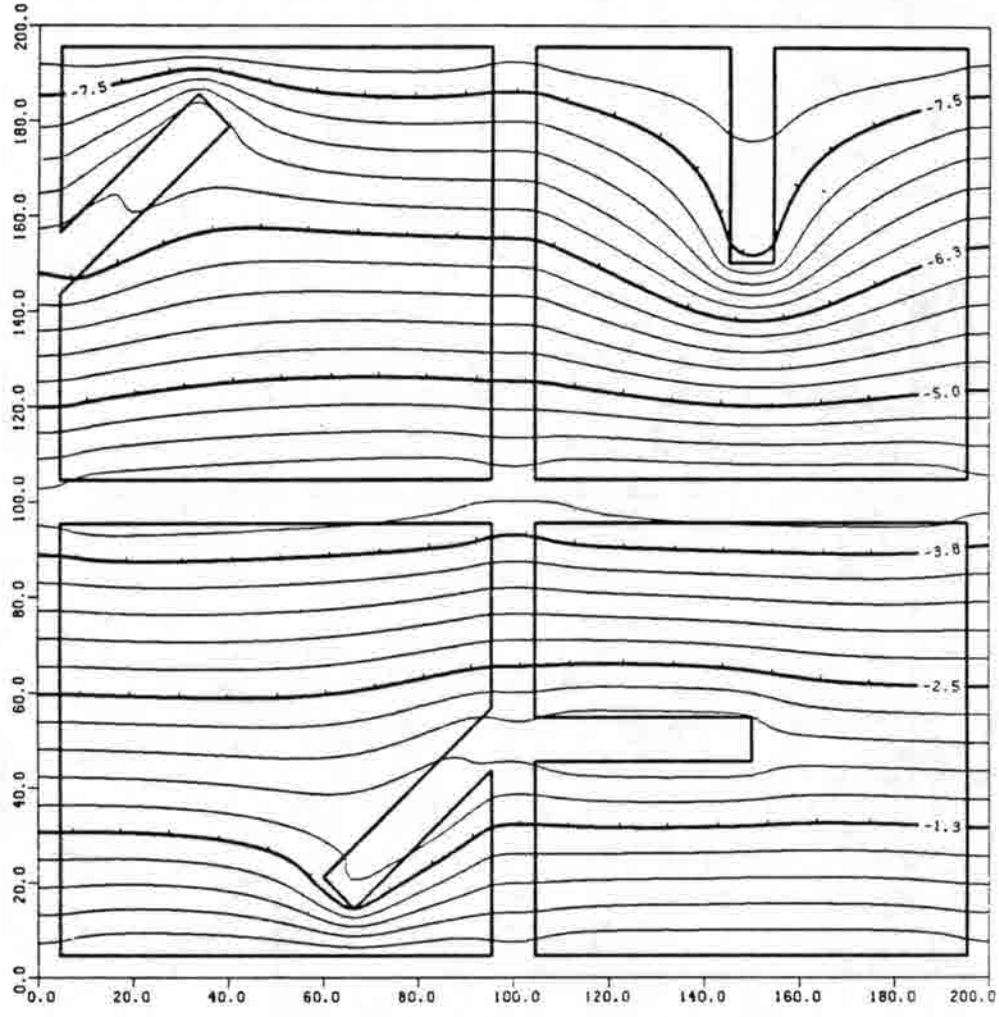


Figure 3. Lines of Constant Temperature at Time = 0.0 Seconds for the Ice Lattice Used in the Transient Analysis (°C x 1.E-3).

boundary condition along the centerline of the vertical ice crystals was a good approximation. The thermal gradients in the vertical ice crystals illustrate that considering all ice crystals to be isothermal at a temperature based on the mean impressed temperature gradient is not an acceptable approximation. From Figures 2 and 3 it is noted that pore interaction in the horizontal direction is unimportant. The analysis of the individual geometries yielded results almost identical to each of the pores presented in Figures 2 and 3.

The "hand-to-hand" transport of mass occurs inside ice lattice pores as shown by the flux plot in Figure 4. The relative vector lengths in this figure represent the magnitude of the mass flux rate at each point in the domain. The horizontal branch geometry is essentially a non-growth case. This plot also demonstrates that the "hand-to-hand" process occurs across the horizontal ice crystals which separate the ice lattice pores. A geometry suggested by de Quervain was also analyzed. The mass flux distribution in Figure 5 illustrates that the "hand-to-hand" transport of mass occurs across the pore spaces via the branch grains. It is clear that the redistribution of mass in the pore spaces is highly dependent upon the local pore space geometry.

The effective diffusion coefficient for the 45° branch grain geometry with an area ratio of 0.5 and base temperature of 263°K is 2.5 times greater than the diffusion coefficient for water vapor in air. For the geometry containing no branches, at an area ratio of 0.1 and a temperature of 273°K, the effective diffusion coefficient is 1.05 times the value for $D_{wv}$. The effective diffusion coefficient increases with the area ratio for all of the geometries considered here because a relatively constant temperature difference across smaller pore spaces for the higher area ratios results in larger temperature and concentration gradients across the vapor space. The maximum flow rates and effective diffusion coefficients are for an area ratio of 0.5 or a density of approximately 458 $kg \cdot m^{-3}$. This does not agree with the experimental observations that temperature gradient metamorphisms slows greatly for densities of around 350 $kg \cdot m^{-3}$. In this analysis, the ice lattice pores are changed in a uniform manner for increasing area ratios. Real snow is made up of ice lattices with a random distribution of geometries and area ratios. The observed decrease in the activity of temperature gradient metamorphism at a density of 350 $kg \cdot m^{-3}$ simply indicates that on the average there are more pore configurations which do not enhance the vapor transport rates.

The effective thermal conductivity for the geometry with no branch, area ratio of 0.5 and a base temperature of 0°C is 26.3% of the thermal conductivity of ice. The effective thermal conductivity decreases with both area ratio and temperature. In addition, branch grains in the ice lattice pores did not improve the thermal conductivity. The no-branch geometry yields the highest value of thermal conductivity because it has the largest percentage of the highly conducting ice oriented in the direction of the temperature gradient. Conduction alone is 68 to 95% of the total heat transfer rate for the geometries and area ratios considered here.

The transient analyses began with the geometries shown in Figures 4 and 5. The effective diffusion coefficient increases with time because the horizontal interfaces in the ice lattice pores move down toward the warmer base temperature as demonstrated by the videotape of the simulation. Since the interface temperatures become warmer with time, the driving potential for mass transport also increases with time. The effective thermal conductivity decreases with time. Mass from the highly conducting vertical ice crystals relocates on branch grains and on the upper horizontal ice crystals. The net effect being that the area for conduction in the ice crystals oriented in the direction of the temperature gradient is reduced with time.

The thermal boundary conditions control the heat and mass transport on the scale of the ice lattices. That is, the boundary conditions for the diffusion problem are a direct consequence of the thermal boundary conditions. Figure 3 shows that the symmetry or zero heat flux constraint is an acceptable boundary condition in the analysis, and that the individual ice lattice pores may be

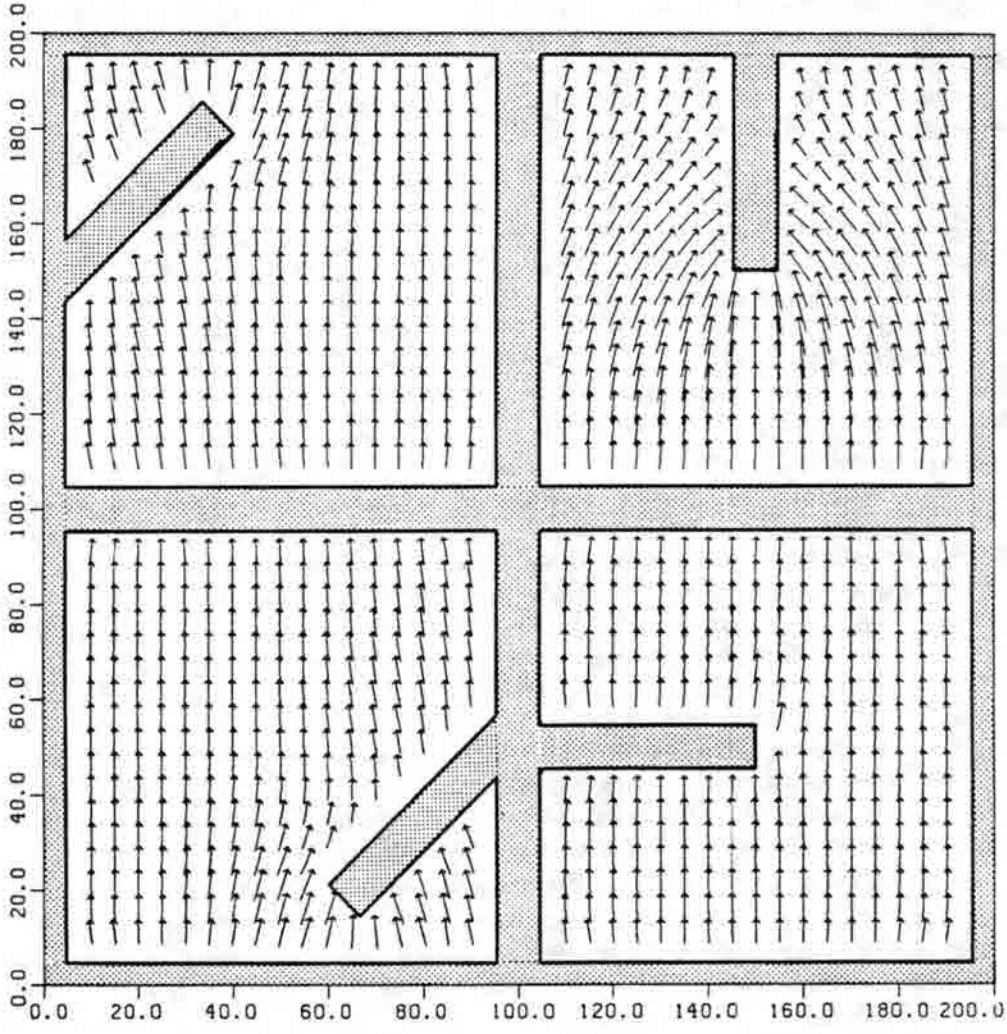


Figure 4. Mass Flux Plot at Time = 0.0 Seconds for the Multiple Pore Ice Lattice Used in the Transient Analysis.

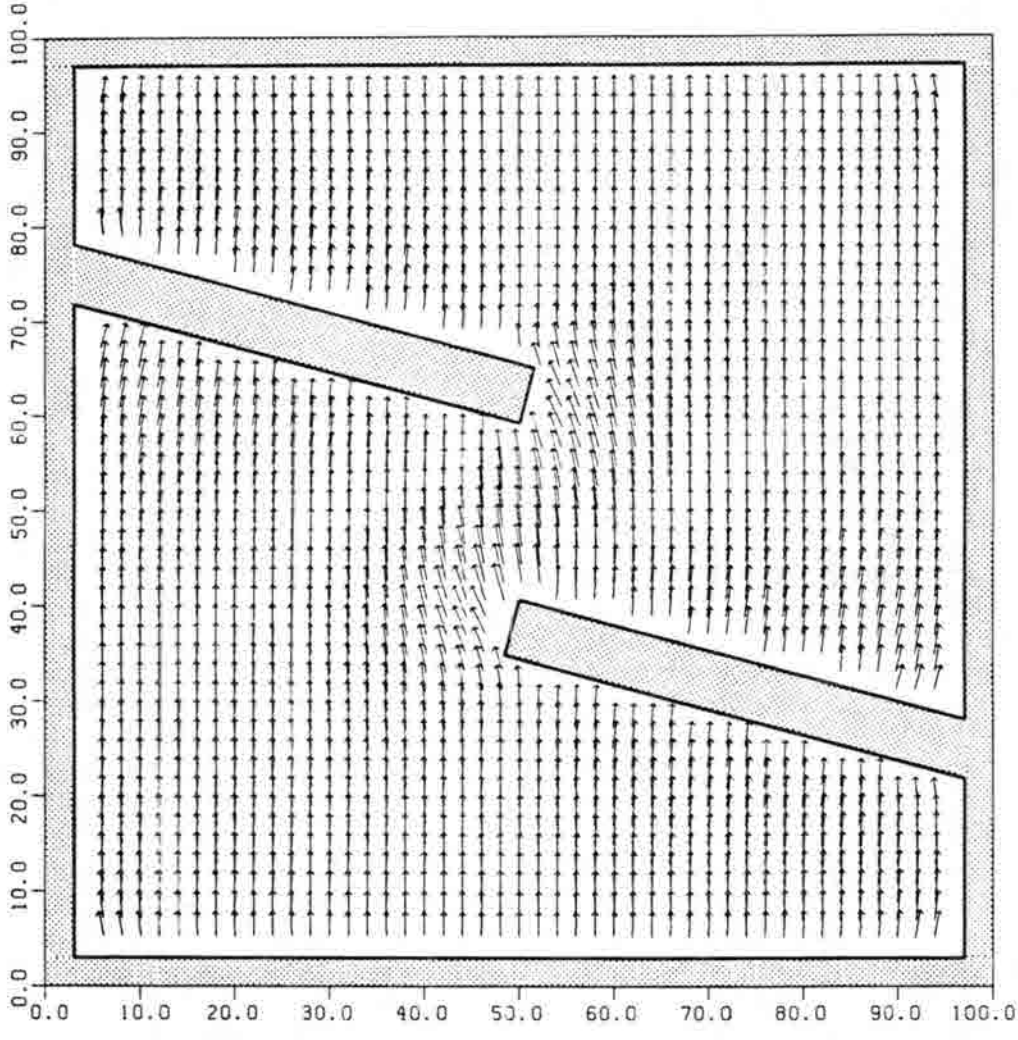


Figure 5. Mass Flux Plot at Time = 0.0 Seconds for the de Quervain Geometry Used in the Transient Analysis.

considered independently without sacrificing any vital information about the temperature gradient metamorphism process. The pore independence is true only in the case of the temperature and concentration fields.

The two dimensional model does not reveal the interaction between the ice lattice pores which would be evident in a three dimensional model. However, the research does show that the "hand-to-hand" transport of water vapor occurs both inside and across the ice lattice pores. It is clear from the analysis of multiple pores that growth, decay and non-growth situations can occur simultaneously in a single ice lattice pore. Branch grains oreinted normal to the impressed temperature gradient constitute a non-growth situation. The videotape of the transient simulation confirms the importance of branch grains in the "hand-to-hand" process, and demonstrates that branch grains act as preferential growth and decay sites.

## CONCLUSIONS AND RECOMMENDATIONS

Although the extent of numerical analysis of temperature gradient metamorphism has been limited, this study has demonstrated that modeling this process is well within the realm of supercomputing. The use of a supercomputer in this research permitted the analysis of the coupled heat and mass transport in snow on a microscale which has not been fully considered before.

One of the primary conclusions from this research was that the coupled heat and mass transport problem must be considered to accurately model temperature gradient metamorphism. There were significant thermal gradients in the vertically oriented ice grains of the lattice geometries which could not be detected by considering the diffusion problem alone. The use of electrostatic potential analogy neglects the coupling between the energy and mass conservation equations, and requires assumptions about the thermal field which are unrealistic. In addition, the electrostatic analogy is difficult to apply to relatively simple geometries involving more than two ice crystals unless the ice crystals are grouped together to form clusters of ice. Although it was evident that the "hand-to-hand" process did occur across ice lattice pores, this model does not indicate what a good communication length would be. The interaction between pores in a three dimensional sense is required to determine a reasonable communication length.

The current research has been brought to the point where the statistical nature of snow needs to be considered. The results for the effective diffusion coefficient and thermal conductivity could be implemented in a Monte Carlo sampling technique using measured data of pore length distributions. This approach would provide a link between the microscopic and macroscopic levels. This would mean that direct experimental data could be used to verify the accuracy of the results presented in this paper. This type of analysis would also provide the information necessary to make predictions of the redistribution of pollutants in a snowcover.

In order to attain a true picture of the coupled, simultaneous transport of heat and mass on the microscale, the current model needs to be extended to three dimensions. This would yield information about the effective diffusion coefficient and thermal conductivity which would be better suited to the Monte Carlo sampling technique described above. Additionally, the current numerical model could be revised to include the presence of a pollutant phase if information about the effect of the pollutant on the vapor pressure were available. By generating videotape of the transient simulation, the pollutant phase could be tracked through the ice lattices. This would provide a significant step forward in the problem of acid snow, acid shock, and the prediction of pollutant redistribution.

## ACKNOWLEDGEMENTS

This research was funded by the USDA on grant 28–K5–356. The supercomputer time was provided by the National Science Foundation on grant ESC–8515113. The authors are indebted to these agencies for this support. The graphics software for the movie generation was developed by Jeff Courtney.

## REFERENCES

Akitaya, Einzi, 1974. Contributions from the Institute on Low Temperature Science. Series A, No. 26, The Institute of Low Temperature Science, Hokkaido University, Sapporo, Japan, p. 1–67.

Carslaw, H.S., and J.C. Jaeger, 1959. Conduction of Heat in Solids. 2nd Edition, Clarendon Press, Oxford.

Christon, M., P. Burns, D. Sommerfeld, and E. Thompson, 1986. Water vapor transport in snow, a 2-D simulation of temperature gradient metamorphism. NATO–ASI Series, in edit, Les Arcs, France.

Colbeck, S.C., 1980. Thermodynamics of snow metamorphism due to variations in curvature. *J. Glaciology*, **26**, 291–301.

Colbeck, S.C., 1983. Theory of metamorphism of dry snow. *J. Geophys. Res.*, **88**, 5475–5482.

de Quervain, M.R., 1973. Snow structure, heat and mass flux through snow. Proceedings, International Symposium on the Role of Snow and Ice in Hydrology, Symposium on Properties and Processes. UNESCO-WMO-IAHS, Geneva.

Giddings, J.C., and E. LaChapelle, 1962. The formation rate of depth hoar. *J. Geophys. Res.*, **67, 6**.

Gray, D.M., and D.H. Male, 1981. Handbook of Snow. Pergamon Press, Ontario, Canada, Chapter 6.

Gubler, H., 1978. Determination of the mean number of bonds per snow grain and the dependence of the tensile strength of snow on stereological parameters. *J. Glaciology*, **20, 83**.

Gubler, H., 1985. Model for dry snow metamorphism by interparticle flux. *J. Glaciology*, **90**, 8081–8092.

Kuriowa, D., 1974. Metamorphism of snow and ice sintering observed by time lapse cinephotomicrography. Proceedings, Snow Mechanics Symposium, 82–88.

Marbouty, D., 1980. An experimental study of temperature gradient metamorphism. *J. Glaciology*, **26**, 303–311.

Palm, E., and M. Tveitereid, 1979. On heat and mass flux through dry snow. *J. Geophys. Res.*, **84**, 745–749.

Perla, R.I., 1978. Temperature gradient and equi-temperature metamorphism of dry snow. In Comptes Rendus, Deuxieme Recontre Internationale Sur la Neige et les Avalanches, Anena, Grenoble, France, p. 43–48.

Sommerfeld, R.A., 1983. A branch grain theory of temperature gradient metamorphism in snow. *J. Geophys. Res.*, **88**, 1484–1494.

Zienkiewcicz, O.C., 1983. The Finite Element Method. McGraw-Hill, London, UK.

Yosida, Z., et al., 1955. Physical studies on deposited snow. Contrib. Inst. Low Temp. Science. Hokkaido University, Sapporo, Japan. Series A, pp. 19–74.

# Acid Deposition in the Rocky Mountain Region: Research Plans and Priorities

Larry Svoboda
Acid Deposition Program
U.S. Environmental Protection Agency
Region VIII
Denver, Colorado

August 14, 1986

## INTRODUCTION

Acid deposition is an issue of growing concern in the Rocky Mountain area. Region VIII of the U.S. Environmental Protection Agency (EPA) believes that extensive research and monitoring is needed to support current decisions under the Clean Air Act Amendments of 1977 and to determine the need for additional acid deposition controls in the western United States. This paper presents the perspective of EPA Region VIII on the priority research and monitoring needed to respond to these policy and regulatory concerns.

## BACKGROUND

Many western ecosystems have a high potential sensitivity to acidic deposition. A large percentage of these sensitive ecosystems are located in areas designated as wilderness. These areas require special protection from air quality degradation under current provisions of the Clean Air Act. The Prevention of Significant Deterioration (PSD) Program requires the federal land manager, EPA, and the states to protect the air quality related values of most wilderness areas and national parks. The air quality related values of an area include any air pollution related change to an ecosystem including the potential acidification of lakes and streams. Therefore, the PSD program can be viewed as an "acid rain" control program for Class I areas. This is especially important in the western United States where relatively clean air and pristine ecosystems could be degraded by increasing population and future industrial growth. However, to assure the reasonable and adequate protection of sensitive resources, more research and monitoring is needed to support future regulatory decisions under the PSD program.

To date, no documented scientific evidence has been found to suggest that ecosystems in the Rocky Mountain region have been effected by acidic deposition. Unfortunately, however, the lack of evidence is insufficient reason to conclude that we have an existing or potential problem from acid deposition in the Rocky Mountain region. A research and monitoring program must be developed in the western United States to reduce the significant scientific uncertainties. This type of program is needed to assure that western air quality and ecosystems are adequately protected. The key research and monitoring priorities are discussed within the following four general areas: aquatic resources; terrestrial resources; mesoscale acid deposition model; and characterization of wet/dry deposition.

## 1. AQUATIC RESOURCES

High elevation lakes appear to be the resource at greatest risk from acid deposition in the Rocky Mountain region. Some lakes monitored in the San Juan Mountains of southwestern Colorado, for example, have shown that very little acid neutralizing capacity exists in many of these systems. Yet, acidic precipitation has been measured in the pH range of 4.7 to 5.0 suggesting the presence of anthropogenic contributions to deposition. Lake chemistry data from Phase I of the Western Lake Survey should provide valuable information on the geographical extent and distribution of sensitive lakes in the western United States. However, this information will be insufficient to determine the chemical and biological responses to continued atmospheric deposition. This is particularly true during periods of intense snowmelt and runoff when episodic acidification can adversely affect sensitive lakes. The potential occurrence and severity of episodic effects is poorly documented in the western United States. Some investigators have reported significant recruitment in some species caused by acidification of lakes from episodic events. While this work has not been documented, there appears to be much supporting evidence to suggest that springtime nitrate pulses may be of greater concern than summer sulfate levels in the western United States. Intensive work must be initiated to address this critical issue.

The biological resources at risk in the Rocky Mountain region are not well understood. Many of the high elevation lake systems are found in granitic formations with poor soil development. The biology of these systems must be characterized in sufficient detail to estimate the potential aquatic effects of acidic deposition.

Intensive research and monitoring needs to be performed on high elevation lakes to establish both baseline information and predictive abilities for potential chemical and biological changes from acid deposition.

## TERRESTRIAL RESOURCES

The potential effects of acidic deposition on western forests is also an issue of intense interest to the public and scientific and regulatory communities. The Western Conifers Research Cooperative (WCRC), funded by the EPA, is an important first step to a better understanding of the potential effects of deposition on western fronts. The plan for this program is to perform a region-wide assessment of the potential risk of forest damage from primary and transformed air pollutants. Ozone will also be examined as a possible contributing agent to forest decline. The WCRC is an important program which must continue to address the threat of air pollution to western forests.

## MESOSCALE ACID DEPOSITION MODEL

As discussed above, the EPA, states, and federal land managers (NPS and USFS) act in concert to protect air quality related values through the PSD program. Under requirements of the Act, these agencies must assure that new emission sources do not cause exceedances of PSD requirements or National Ambient Air Quality Standards (NAAQS). To meet these responsibilities, air regulatory agencies and federal land managers require validated atmospheric modeling methods that enable them to:

1) Assess the magnitude of potential adverse environmental impacts arising from different configurations of existing and new emission sources;

2) Determine the degree to which specific precursor pollutant sources contribute to environmental stress;

3) Assess the impacts of proposed local and distant emissions on Class I PSD increments, air quality related values, and NAAQS; and

4) Make specific recommendations for mitigating adverse impacts based on quantitative analyses of impacts and uncertainties.

The modeling of acid deposition and related air quality issues in the Rocky Mountain region is complicated by the complex topography, wind flow of the area, and the difficulty of predicting acid deposition. Development of a regional modeling methodology capable of addressing the specific air quality related concerns of the Rocky Mountain region requires an extensive review of available models and deposition modules.

Since no regulatory models currently exist for the purposes as defined above, the Rocky Mountain Acid Deposition Modeling Project was approved for funding by the EPA. This project requires an acid deposition model that can treat both local and mesoscale processes directly related to the formation, transport, and removal of acid materials in the Rocky Mountain Region. Currently available models are to be assessed because more advanced acid deposition models are still under development and are not expected to be available for regulatory use within the near future (3-5 years). Thus, the EPA, state air regulatory agencies, and the federal land managers need a mesoscale acid deposition model assembled from the best and/or most appropriate model components available today to evaluate a range of problems related to acid deposition in the complex terrain of the Rocky Mountain region. Some present day models already contain many of the features required of the model. Thus with minor adaptations, a modeling methodology can be developed that will meet the immediate needs of the regulatory community.

The Rocky Mountain Mesoscale modeling effort is now underway. Candidate models are being identified for use in complex terrain. Once a model(s) has been selected, it will be modified to include deposition prediction capabilities for use within the existing PSD regulatory process. It is not intended to be a model used for effects research or scientific application. The objective is to develop the best regulatory tool possible within existing constraints and an appropriate timeframe.

## CHARACTERIZATION OF WET/DRY DEPOSITION IN THE WEST

Current and future deposition patterns do not appear to be adequately characterized with the existing monitoring network. This is espcially true for high elevation sites where the most sensitive western ecosystems are found. In Colorado, for example, there were ten NADP/NTN collection sites in 1984. Two of these sites are located at relatively high elevation with the remainder located at lower elevation sites where alkaline material is believed to affect precipitation chemistry. There is a need to initiate an intensive research and monitoring program to quantify the variability of existing monitoring methods to accurately measure the chemistry and the volume of snow. Many of the most sensitive lakes in the Rocky Mountain region receive most of their annual hydrological input in the form of snow. There is a critical need to measure deposition in snow and to develop a better understanding of snowpack dynamics and snowpack meltwater. Consequently, additional high elevation wet collection sites are needed in the Rocky Mountain region as part of an overall effort to investigate the potential effects from episodic acidification of ecosystems.

Additionally, the likelihood of orographic and cloud impaction effects increase with elevation, yet, little work has been directed to this important subject. At least one mountain cloud chemistry site should be designated and supported in the Rocky Mountain area. This type of work would reveal the presence, absence, and/or magnitude of mountain cloud impacts in the west and would appear to provide a valuable comparison with mountain cloud studies being done in the eastern United States. Preliminary and unpublished reports suggest that significant differences exist between cloud chemistry and precipitation similar to observations made in the eastern United States. Consequently,

work needs to be initiated to investigate western cloud chemistry and evaluate the potential effects of cloud impaction on sensitive ecosystems.

The copper smelters in the United States and Mexico are one of the largest groups of sulfur dioxide emitters in the northern hemisphere. Once the new Mexican smelter (Nacazzari) starts up in 1986, there will be an additional 300,000 to 500,000 tons per year of sulfur dioxide emitted in the region. Recently, published reports have identified copper smelters as a major source of acidic deposition in the western United States. The actual correlation between smelter emissions and deposition in the west will remain a major uncertainty unless appropriate action is taken to monitor the emissions from this major group of sources. A monitoring network should be established and a field study performed to measure copper smelter emissions (both U.S. and Mexican). This network would provide the information necessary to evaluate the potential effects of smelter emissions on the western United States.

## SUMMARY

The Rocky Mountain region contains many ecosystems which are highly sensitive to acid deposition. Based on current knowledge, no acid deposition damage appears to have occurred in these sensitive areas. However, the sensitivity of lakes in the region is sufficient reason to be concerned about the potential for future environmental effects if emissions were to increase in the western United States. There is a critical need for knowledge regarding the natural variability of sensitive high elevation ecosystems and the ecological response of these systems to increasing levels of acid deposition. This information is needed to support current and future regulatory decisions to assure that air quality and ecosystems are adequately protected in the region.

# Preliminary Results of NADP Sampling on Niwot Ridge, Colorado

David Greenland
Department of Geography
University of Colorado
Boulder, Colorado 80309

August 14, 1986

An increasing number of studies have shown that the phenomenon of acid precipitation is not only a problem in the eastern U.S. but is also a potential threat to parts of the west. In particular, a number of groups of investigators have noted some form of acid deposition in the Colorado Front Range area.

This paper reviews some of the present knowledge of acidic deposition in the Front Range of Colorado and presents preliminary results from National Atmospheric Deposition Program sampling (NADP) in the Niwot Ridge/Green Lakes Valley area. The area is one of the sites of the NSF funded Long Term Ecological Research Program and includes both alpine tundra and alpine lakes. The sampler is located on an exposed ridge at 3520 m (11,550 ft) in the alpine tundra (Figure 1).

## THE NIWOT RIDGE/GREEN LAKES VALLEY AREA

The area of focus is selected partly because of the large amount of related work that has been performed here in the past and that is currently in progress. The area is covered by the climate observation sites of the Institute of Arctic and Alpine Research (INSTAAR) Front Range Transect, and occasionally by observations from the NOAA Prototype Regional Observation and Forecast Service (PROFS) network. The area is within the Roosevelt National Forest, part of which forms the Front Range Biosphere Reserve. Air quality work in the area up to 1982 has been reviewed by Greenland (1982) and besides the work of Lewis and Grant has included studies by NOAA's Aeronomy Laboratory and Global Monitoring for Climatic Change Program, the U.S.G.S., the University of Colorado Chemistry Department and the Cooperative Institute for Research into Environmental Sciences (CIRES), NCAR, Colorado College, the Ford Motor Company, and the University of Michigan.

A key instrument for the examination of atmospheric deposition in the Niwot Ridge area is the NADP sampler at the Saddle. Samples, taken once per week, are analyzed by the Illinois Water Survey for pH, conductivity, and concentrations of $Ca$, $Mg$, $K$, $Na$, $NH_4$ (ammonium), $NO_3$ (nitrate), $Cl$, $SO_4$ (sulfate), $PO_4$ (phosphate), $H+$, and cation/anion ratios. Field measurements of pH and conductance are made.

## PREVIOUS STUDIES

The studies by Lewis and Grant (1978, 1979a, 1979b, 1980a, 1980b) and Grant and Lewis (1982) have attracted much attention for their discovery of unexpectedly low pH values for bulk precipitation

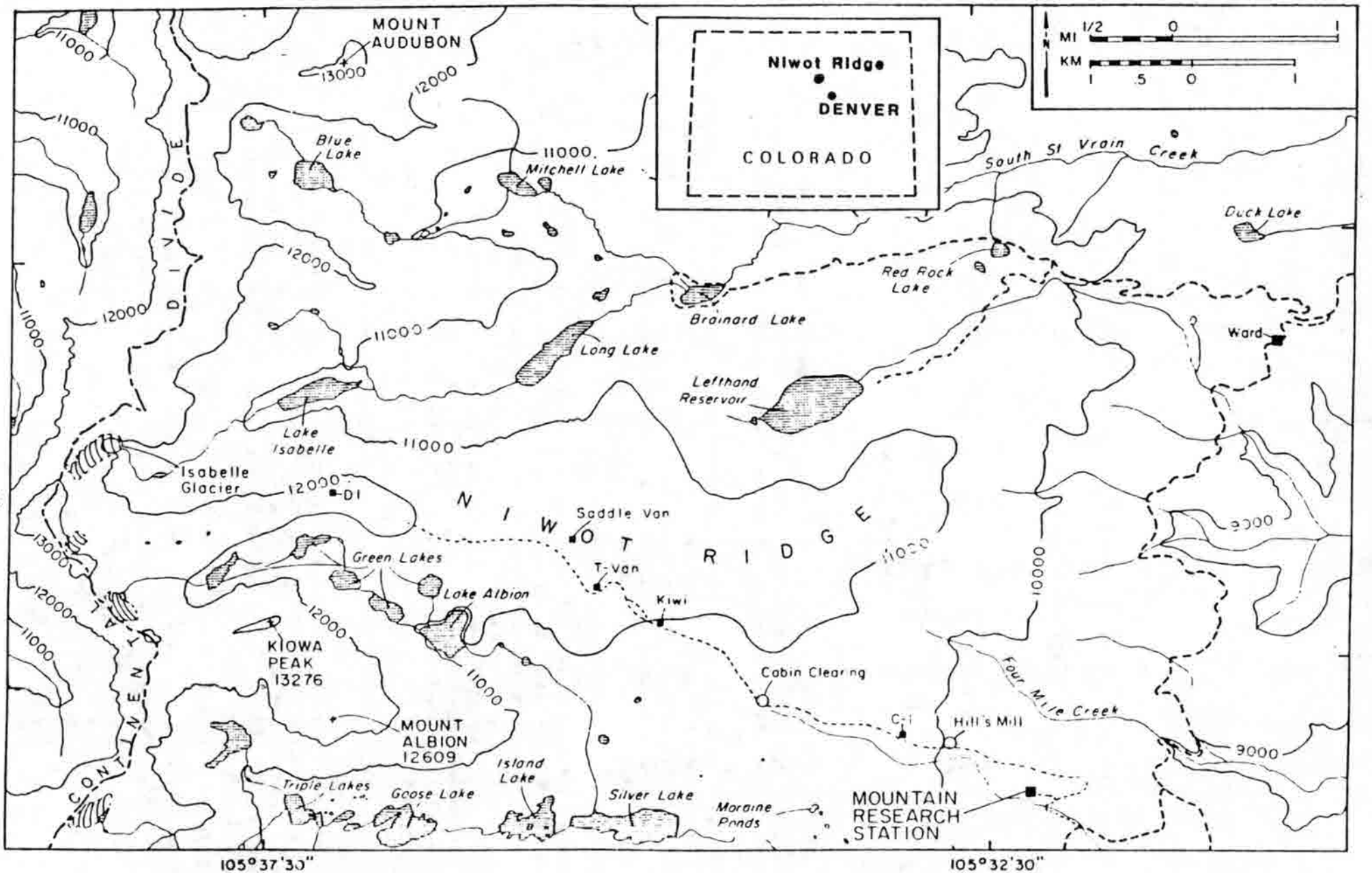


Fig. 1. Niwot Ridge and its location. The NADP sampler is near the Saddle van.

in the Colorado Front Range and a significant downward trend in this value in the late 1970s. They have also shown that this trend may be more widespread than the Front Range and may have been occurring since at least 1938 (Lewis, et al., 1984; Lewis, 1982). This was achieved by re-examining the pH and alkalinity content of Colorado lakes first investigated in 1938. Difficulties arise because of the different analytical methods used in this study.

An important study of precipitation chemistry at the Saddle on Niwot Ridge is being conducted by the U.S. Geological Survey who have monitored precipitation amount, temperature, pH, and specific conductance. Early results for summer precipitation indicate that 65 percent of the continuous pH measurements were between 3.40 and 4.10, with an average of 3.80 and a minimum of 2.59 (Reddy, et al., 1985). So far, these extraordinary pH values have remained unexplained but it is interesting to note that they are in a similar range to the values obtained within clouds over the eastern plains of Colorado by Nagamoto, et al. (1983).

Between 1975 and 1980, Lewis and Grant recorded at the Mountain Research Station site values of pH of wet deposition for the most number of weeks between 4.5 and 5.0 and for the second most number of weeks between 4.0 and 4.5. A map of pH values for the state from 1982–83 data shows the Niwot Ridge area in a location having pH values between 4.6 and 5.0 (Lewis, et al., 1984).

Grant and Lewis (1982) attribute increasing acidity to increasing amounts of nitric acid in the precipitation. While being markedly acidic, the precipitation shows comparatively low levels of sulfates ($SO_4^{2-}$). However, rather large amounts of calcium ($Ca_{2+}$) and sodium ($Na_{2+}$) in both wet and dry fallout suggest terrestrial sources are a major contributor to deposition. This work is continuing.

Nagamoto, et al. (1983) found precipitation in the form of snow in the eastern foothills of the Front Range to be much less acidic than rain. They suggest that this might be due to the fact that snow crystals have a greater scavenging efficiency than rain drops for capturing atmospheric soil particles which are alkaline in the area. The capturing of alkaline dust has also been noted as an important phenomenon in the mountains of northern Utah (Messer, 1983). Snow cores from the Wasatch mountains had low concentrations of ($NO_3^-$) and the higher concentrations of ($SO_4^{2-}$) which were thought to originate from the Salt Lake City/Provo metropolitan area. However, the associated acid was effectively titrated by alkaline dust, resulting in pHs of the snow ranging from 5.89 to 6.77. Both of these sets of results suggest the importance of examining ambient particulate matter for its alkalinity. The potential importance of "carbonate-containing dust" has also been alluded to by Kling and Grant (1984) who find that rain collected in open areas on Niwot Ridge is 20 times more acidic than precipitation collection under nearby aspen canopies. It should be remembered however, that not all forms of carbonate may act directly as buffers.

The question of the sources of pollutants entering the Front Range area has received some attention but it is now time to move to a greater level of detail than has been given in the past. Lewis and Grant originally believed that the source of the acidity lay far to the west. This may be true but the view has been questioned by Kelly and Stedman (1980), and NOAA measurements (Fehsenfeld, 1984) suggest that the urban corridor to the east is a major contributor. This is supported by the measurements of Huebert, et al. (1982) who found that both the gas phase concentrations of nitric acid, its precursors and nitrate aerosols markedly increased in value at a site at 3000 m on Niwot Ridge when the air came from the east. Furthermore, Bollinger, et al. (1984) found that clean air at the same site could be associated with times when air trajectories came from the relatively sparsely populated northwest and when Denver air was isolated by a ground based temperature inversion. A source of Front Range air pollutants in the east or southeast is further supported by the investigations of Nagamoto, et al. (1983) who found very low pH values in the clouds over eastern Colorado, and particularly near Denver. They believe that the most acidic rain or snow in winter

which arrives in Colorado is associated with low pressure centers tracking across or to the south of the state and bringing in marine surface air across the industrial areas of Texas and then into the state. Such a source might account for the lower pH found in the precipitation of the Front Range and the Rocky Mountain National Park, but does not necessarily explain parallel events occurring on the western slope.

Using samplers at 42 sites throughout the state for a one year period between 1982 and 1983, Lewis, et al. (1984) noted that the lowest pH values (average below 5.0) were found near the continental divide in the northern third and southern third of the state. Their studies suggest that emissions of $NO_x$ and $SO_2$ from power plants within or near the borders of the state are of a magnitude similar to that of the total deposition of $SO_4^=$ and $NO_3^{-N}$ within the state. They noted gradients of acidity which seemed to be largely explained by: 1) location of power plants and urban areas with respect to prevailing winds; 2) differential transport of strong acids and alkalis (they postulate a tendency for divalent cations and carbonates to sediment out as air travels upslope whereas strong acids remain in the air until they are scrubbed out by moisture); and 3) the direct relationship between strong acid deposition and the amount of wet precipitation. Oppenheimer, et al. (1985) in advocating a linearity concept note that on an annual basis over a four year period there is an association between wet deposition of sulfur at Colorado NADP stations and sulfur emissions from non-ferrous metal smelters in Arizona, Utah, Nevada, Idaho and New Mexico.

In summary, the potential areas for sources of high levels of potential acid producing substances on Niwot Ridge include metal smelters and power plants to the west and southwest, the Front Range urban corridor, urban-industrial areas of the west coast, and even industrial areas of Texas.

## DATA

The data used in the present study were collected for the periods 5 June, 1984 to 29 January, 1985 and 14 May, 1985 to 11 March, 1986. The latter is the last date for which analyses were available for consideration in this paper. Missing data were omitted from the seasonal sums and averages. Data were missing for the weeks January 8–15, 1985, June 4–11, 1985 and October 15–29, 1985.

## RESULTS

Preliminary examination of the seasonal averages of concentrations (Table 1, Figure 2) indicates: 1) in all seasons $NO_3$ and $SO_4$ are the dominant species to be deposited. Summer 1984 is the only exception to this when high concentrations of $NH_4$ and $PO_4$ were also found; 2) concentrations are highest in the summer and least in the fall, with winter having intermediate values.

A similar examination of the seasonal average weekly deposition values (Table 1, Figure 3) naturally indicates that the same species are dominant but further shows the summer season to be overwhelmingly important in being the season when the highest absolute values of the species are deposited. This season is followed in importance by fall and then by winter when, relative to the other seasons, very little deposition appears to occur. To the extent that $NO_3$ and $SO_4$ are precursors of nitric and sulfuric acid respectively, these results differ somewhat from the earlier ones of Lewis and Grant (1982) who found that, at an elevation about 1550 feet lower, nitric acid was more frequent than sulfuric acid. The summer of 1984 has far higher deposition values than that of 1985 or other seasons. Further studies have shown that the summer of 1984 had a higher value of precipitation than any other summer in the period 1951–1985 (Greenland, 1987).

The low values of deposition in winter may be due to: 1) the actual absence of the species in the deposition; 2) snow being an effective scavenger of alkaline particles which have then reacted with the major depositional species (see earlier comments of Nagamoto, et al., 1983); 3) the sampler

Table 1. Seasonal Values of Concentrations and Deposition.

AVERAGE CONCENTRATIONS mg/l

| | Ca | Mg | K | Na | NH4 | NO3 | Cl | SO4 | PO4 |
|---|---|---|---|---|---|---|---|---|---|
| Summer 84 | 0.299 | 0.069 | 0.769 | 0.213 | 1.946 | 1.655 | 0.215 | 1.902 | 1.420 |
| Fall 84 | 0.303 | 0.065 | 0.043 | 0.124 | 0.242 | 1.229 | 0.142 | 1.128 | 0.004 |
| Winter 84/85 | 0.463 | 0.269 | 0.596 | 0.643 | 0.108 | 1.724 | 0.846 | 1.776 | 0.009 |
| Summer 85 | 1.151 | 0.179 | 0.371 | 0.308 | 0.732 | 3.704 | 0.563 | 3.668 | 0.015 |
| Fall 85 | 0.259 | 0.059 | 0.029 | 0.061 | 0.060 | 0.573 | 0.087 | 1.263 | 0.004 |
| Winter 85/86 | 0.259 | 0.053 | 0.041 | 0.099 | 0.148 | 1.300 | 0.148 | 1.100 | 0.021 |

AVERAGE WEEKLY DEPOSITION mg/sq.m

| | Ca | Mg | K | Na | NH4 | NO3 | Cl | SO4 | PO4 | H |
|---|---|---|---|---|---|---|---|---|---|---|
| Summer 84 | 4.108 | 0.837 | 5.162 | 1.837 | 14.328 | 27.822 | 2.819 | 28.453 | 7.664 | 0.315 |
| Fall 84 | 2.166 | 0.425 | 0.401 | 0.706 | 1.598 | 8.705 | 1.059 | 8.318 | 0.035 | 0.088 |
| Winter 84/85 | 0.254 | 0.114 | 0.184 | 0.274 | 0.082 | 0.772 | 0.302 | 1.058 | 0.010 | 0.004 |
| Summer 85 | 2.326 | 0.421 | 1.393 | 0.808 | 1.214 | 8.255 | 1.860 | 9.231 | 0.056 | 0.086 |
| Fall 85 | 1.339 | 0.311 | 0.159 | 0.408 | 0.614 | 5.247 | 0.722 | 6.651 | 0.037 | 0.119 |
| Winter 85/86 | 0.421 | 0.082 | 0.082 | 0.177 | 0.178 | 2.656 | 0.251 | 1.950 | 0.062 | 0.055 |

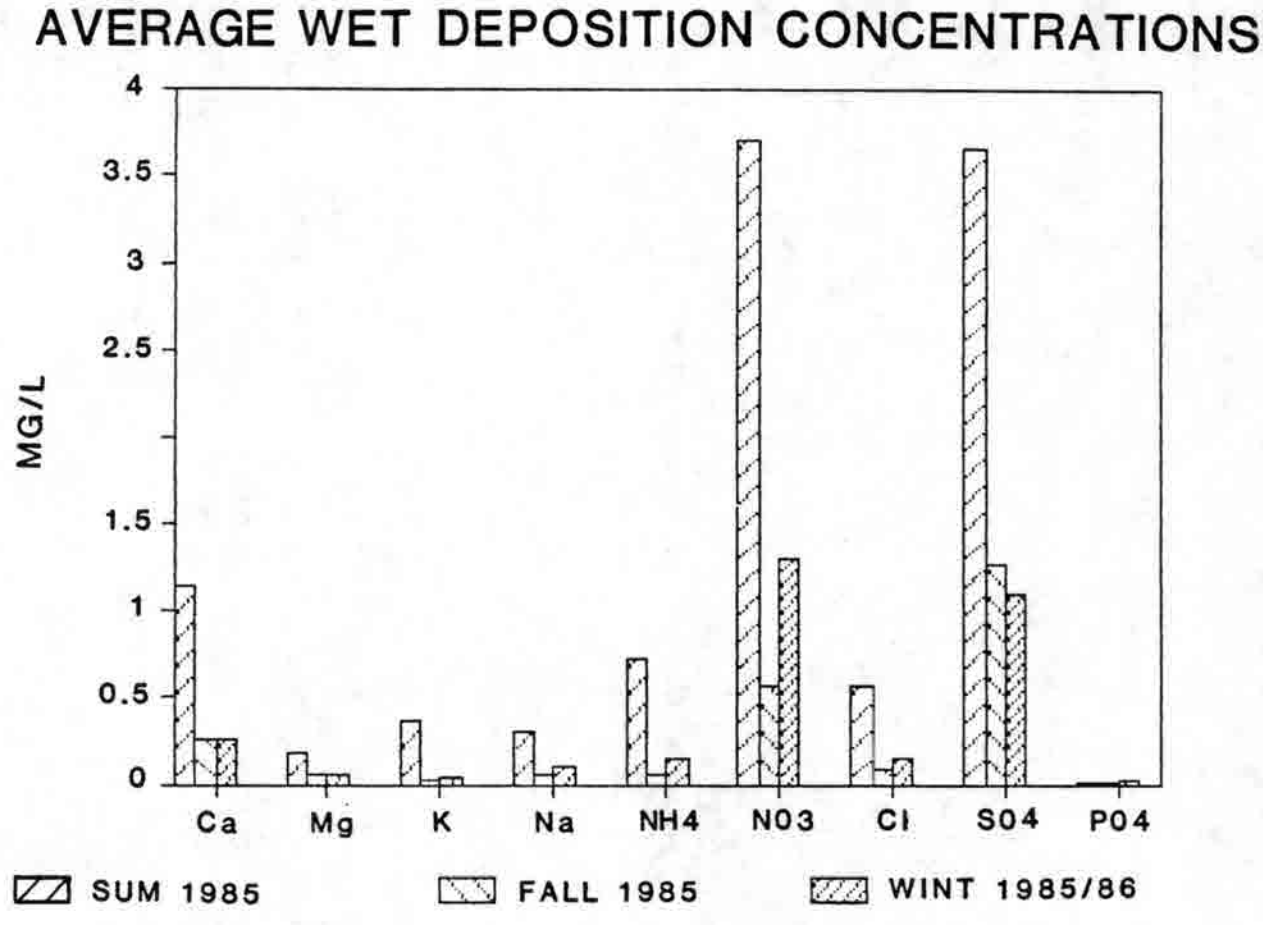


Fig. 2. Seasonal averages of wet deposition concentrations.

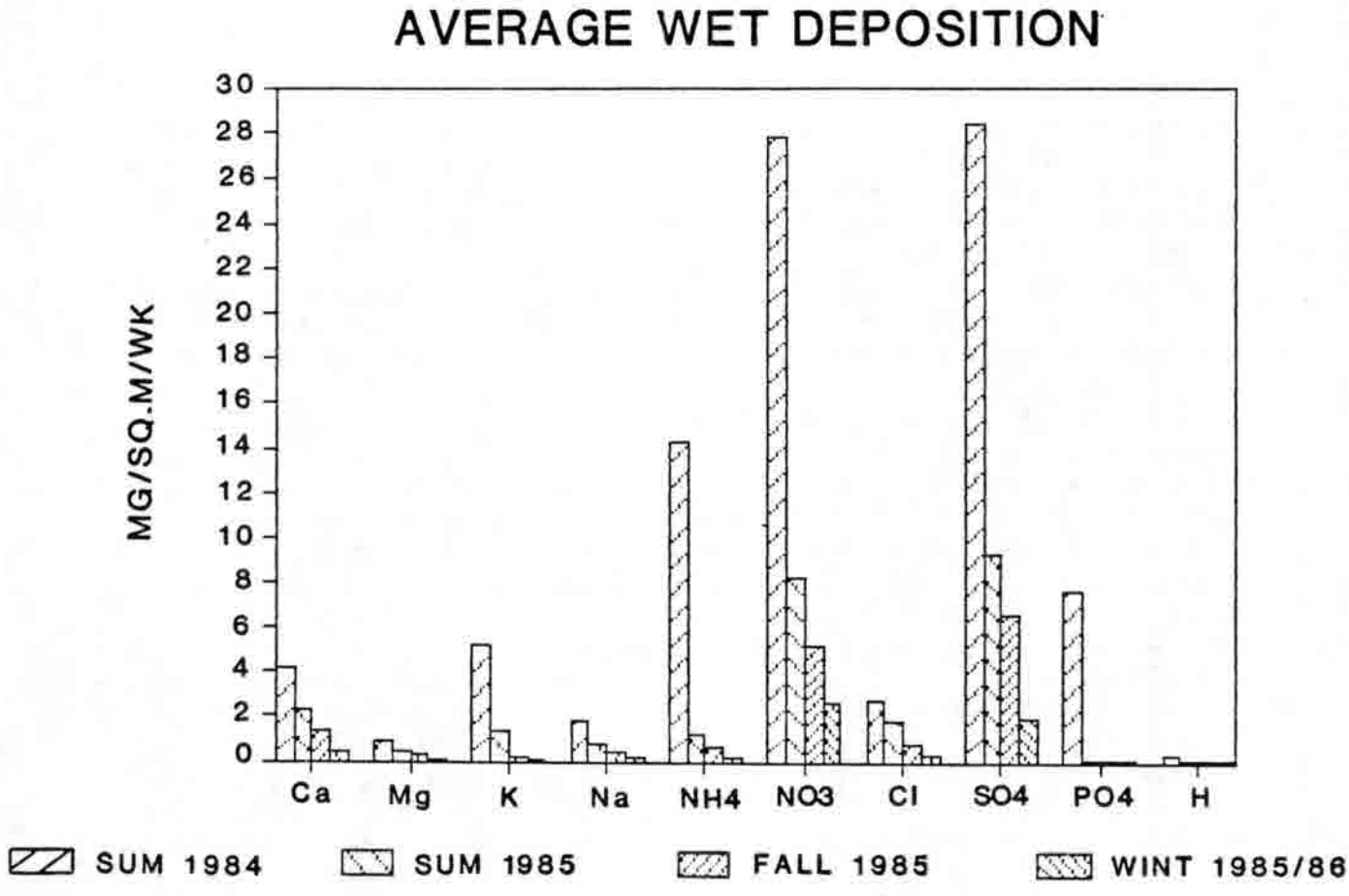


Fig. 3. Seasonal averages of wet depositions.

being an ineffective catcher of the deposition in the snow (for various reasons – shielding, failure of the cover to work properly). Judging, however, by the actual sample size, the sampler was an efficient collector in the second winter season. The sample size (Table 2) was low in the winter of 1984/5 suggesting inefficient collection but was reasonably high during the 1985/6 winter, by which time the sampler had been screened with a snow fence shelter.

Summary indices of the chemical data (Table 2, Figure 4) show that for most seasons sampled there is a fairly good balance between anions and cations (an exception being summer 1984) and that there has been decreasing average values of pH, although this is certainly not statistically significant given the small sample size.

Time series of the data immediately indicate some interesting periods. The analysis was performed in two parts because of missing data in the winter of 1985: part one was for the summer, fall, and early winter of 1984, while part two was for the summer of 1985 and into the winter of 1986. In both analyses $NO_3$, $SO_4$, averages and concentrations, pH, and sample volume were used as indicators since these items appeared to be important from the earlier analysis.

In the first part surprisingly high concentrations of $NO_3$ and $SO_4$ were found for week 10 (starting 8/7/84)(Figure 5) but high depositions of $NO_3$ and $SO_4$ appear on week 8 (starting 7/24/84)(Figure 6) associated with high precipitation values at the same time. The highest pH in the period (Figure 7) occurred at the same time as the high concentration values, while the lowest pH was measured for the week following the high concentration values (week 11). No explanation of this is offered.

In the second part of the record (Figure 8) nitrate and sulfate concentrations are high in weeks 7 and 12 (beginning respectively, 7/2/85 and 8/6/85) but $SO_4$ concentrations were also high on weeks 2 and 23 (beginning 5/21/85 and 10/29/85). Nitrate and sulfate deposition values (Figure 9) were irregular and not entirely in phase but showed a somewhat positive direct relation with the sample volume (Figure 10) as expected. pH was less variable in this period being highest in week 5 (beginning 6/18/85) and lowest in week 11 (beginning 7/30/85)(Figure 11).

A regression analysis was made using weekly values of $NO_3$ and $SO_4$ concentrations as dependent variables and wind speed and direction indices derived from daily synoptic charts as independent variables. The latter included weekly averages of surface isobaric gradient over Niwot Ridge and 500 kms upwind of Niwot Ridge and modal wind direction for the week at this location. In all cases the correlation coefficients were very low. A possible interpretation of this result is that deposition values are determined more by events happening on a daily time scale rather than a weekly time scale.

Some of the more interesting weeks were selected as case studies for further examination in terms of the synoptic meterological conditions that prevailed. Details of these are given in Appendix 1, but the more important points emerging from this investigation include:

1) A variety of different synoptic conditions are associated with periods of high deposition or low pH in the wet deposition records of Niwot Ridge.

2) In particular, some completely different synoptic patterns between summer and winter seasons can lead to high deposition rates.

3) Two typical situations appear to be:

a) In summer, when there is an upper southwesterly flow sometimes accompanied by the potential for a surface easterly flow. This often happens when a surface high pressure zone is located in the midsection of the continent and a 500 mb high pressure zone is centered south of Colorado (Figure A1).

Table 2. Chemical Data for Niwot Ridge Deposition

| | Lab Conduct | Lab pH |
|---|---|---|
| Summer 84 | 23.4 | 5.4 |
| Fall 84 | 9.7 | 5.2 |
| Winter 84/85 | 17.9 | 5.6 |
| Summer 85 | 30.1 | 5.3 |
| Fall 85 | 11.0 | 5.0 |
| Winter 85/86 | 13.3 | 4.9 |

| | Sample Vol ml | Anions meq/l | Cations meq/l |
|---|---|---|---|
| Summer 84 | 1418.3 | 117.2 | 170.6 |
| Fall 84 | 726.3 | 47.4 | 49.1 |
| Winter 84/85 | 39.5 | 88.9 | 98.6 |
| Summer 85 | 494.5 | 152.3 | 147.6 |
| Fall 85 | 732.2 | 37.9 | 36.3 |
| Winter 85/86 | 327.4 | 48.4 | 46.2 |

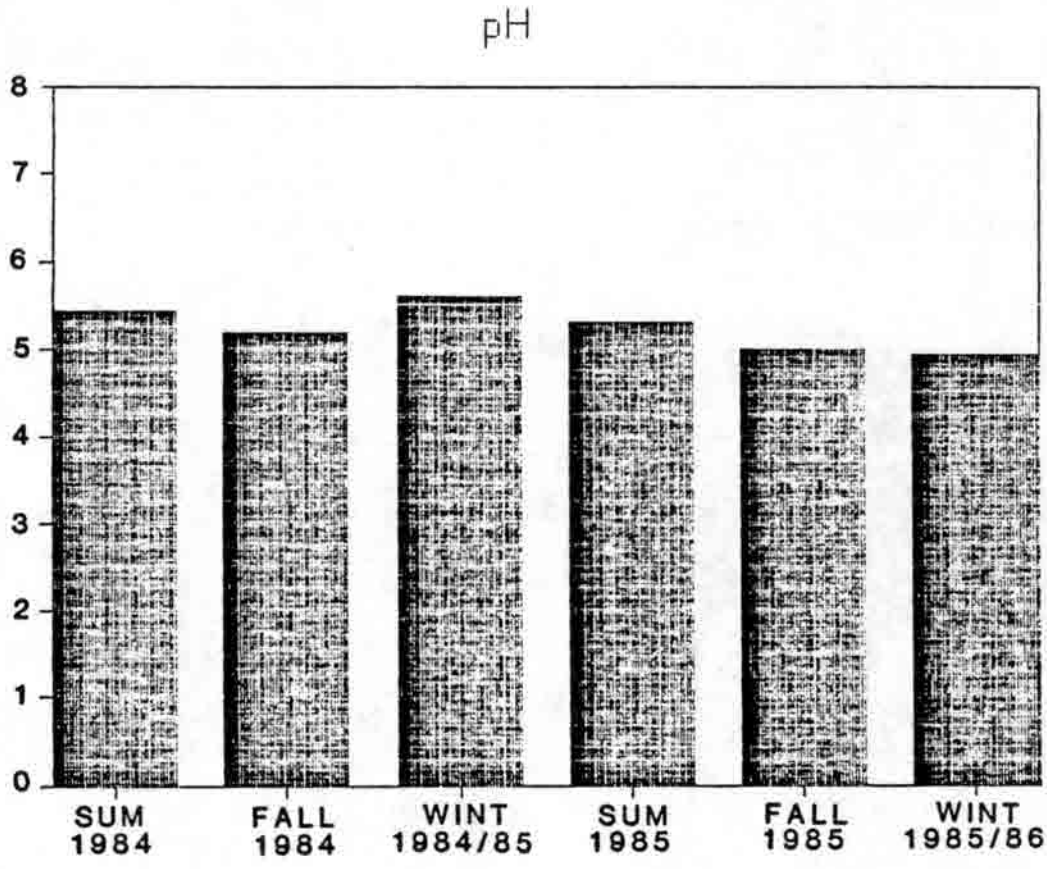


Fig. 4. Seasonal averages of pH.

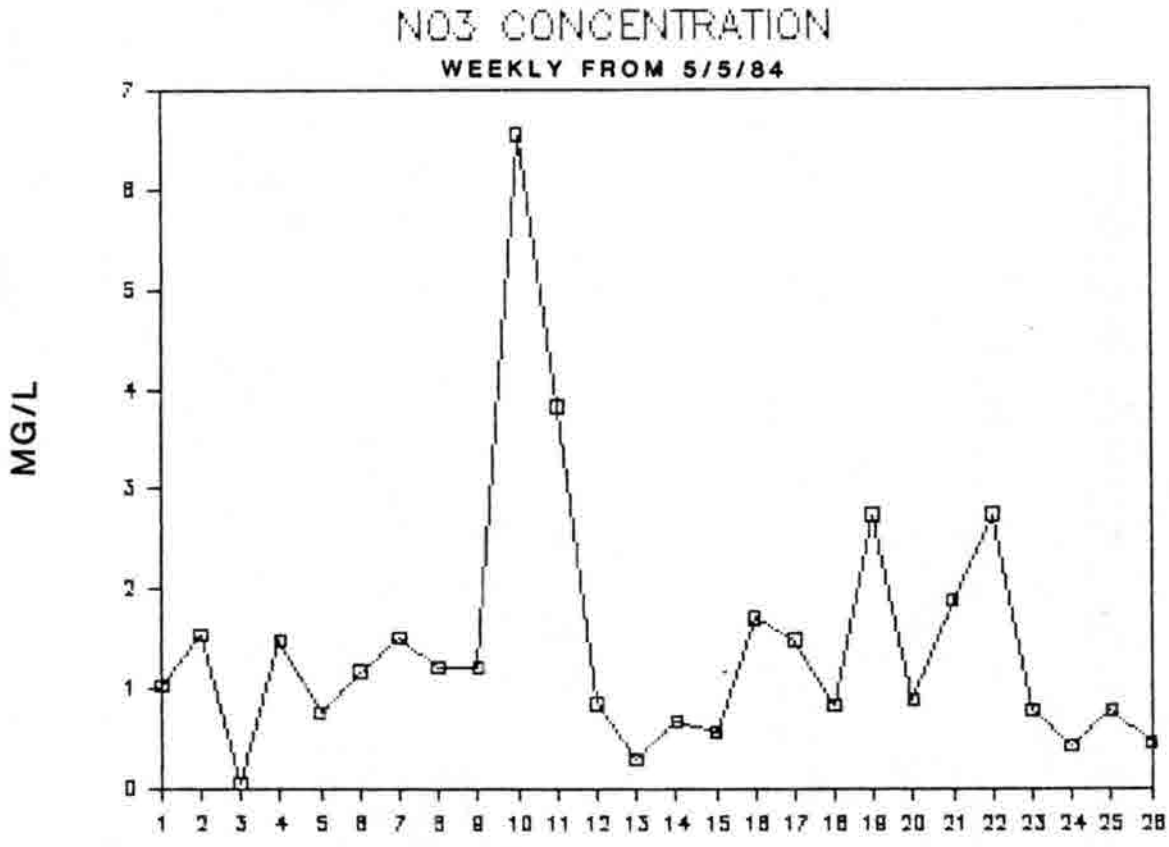


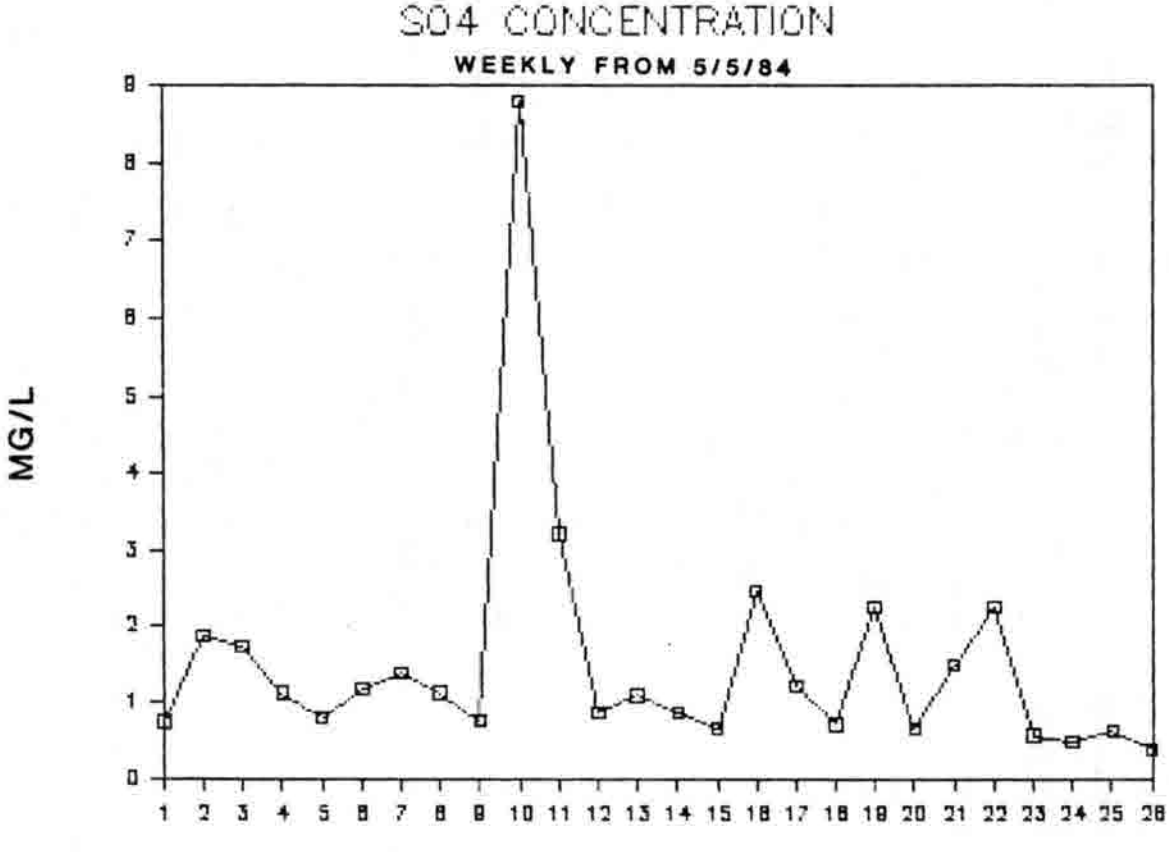


Fig. 5. Weekly values of concentration of NO3 and SO4 in 1984.

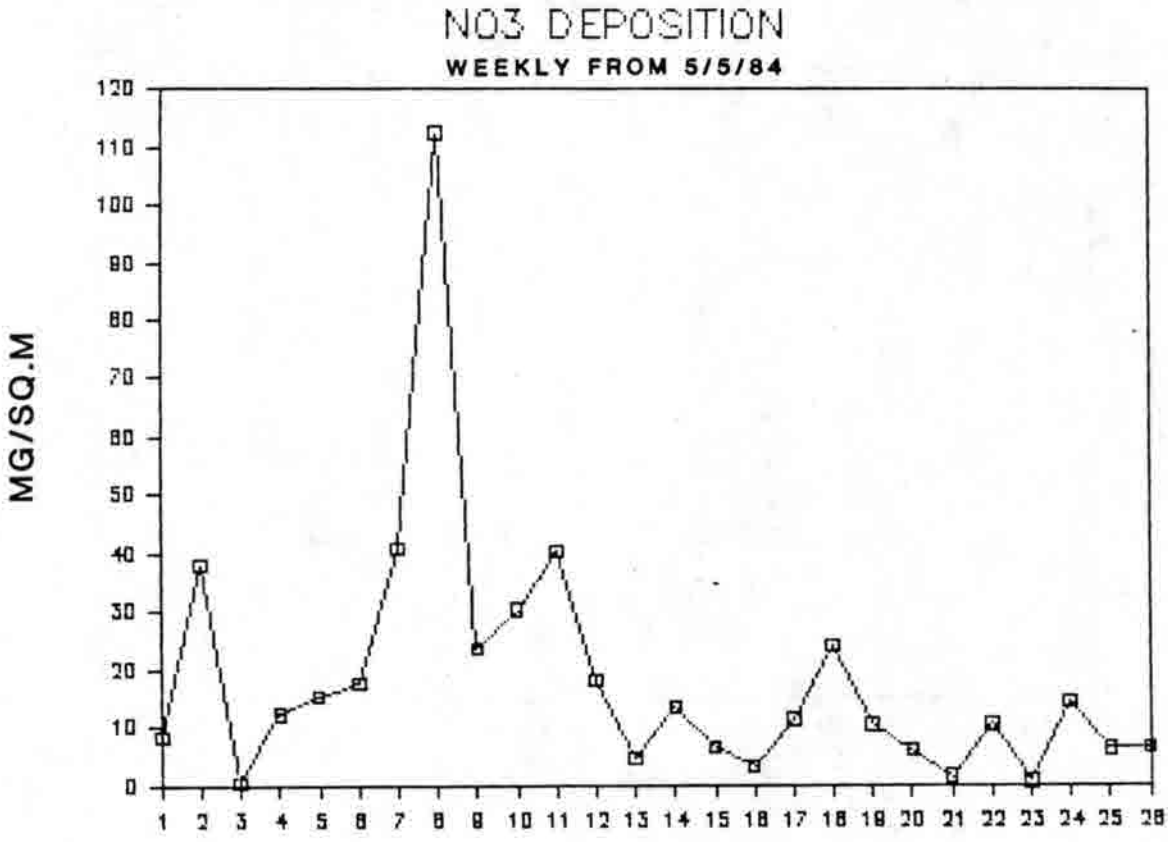


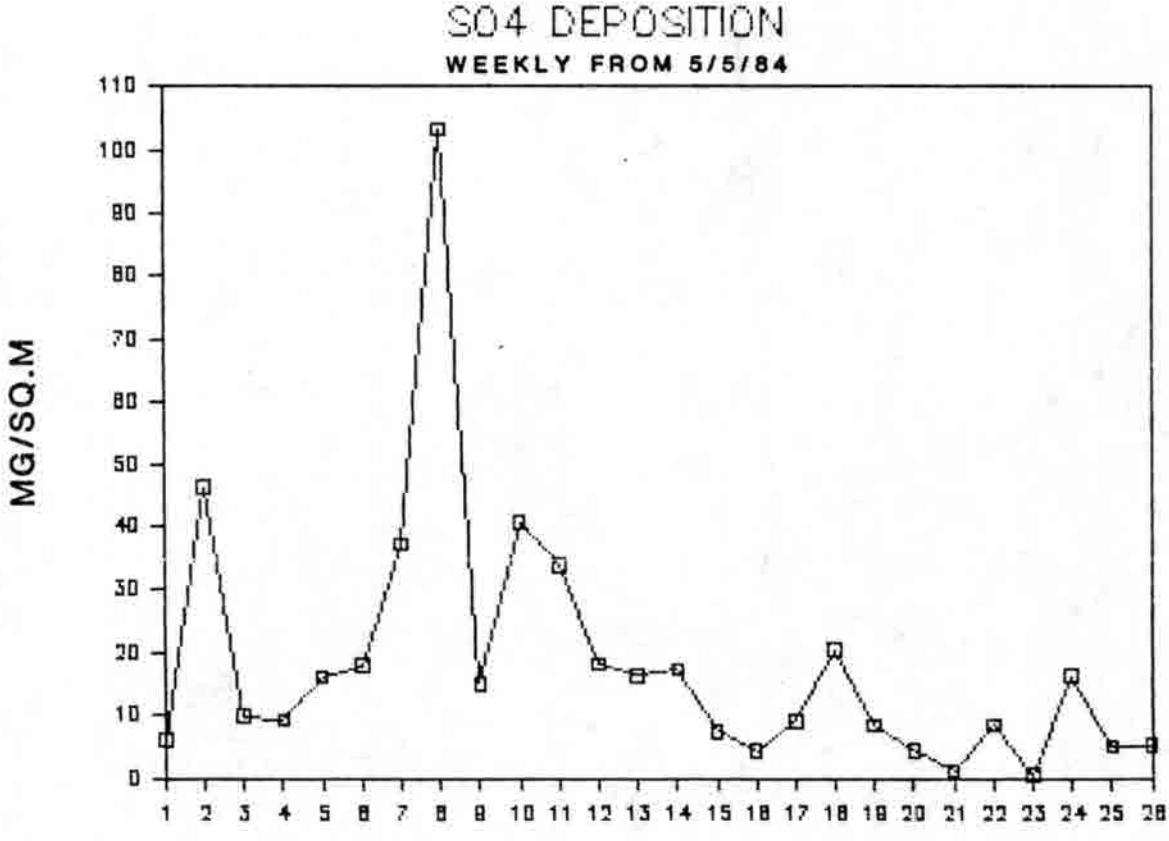


Fig. 6. Weekly values of deposition of NO3 and SO4 in 1984.

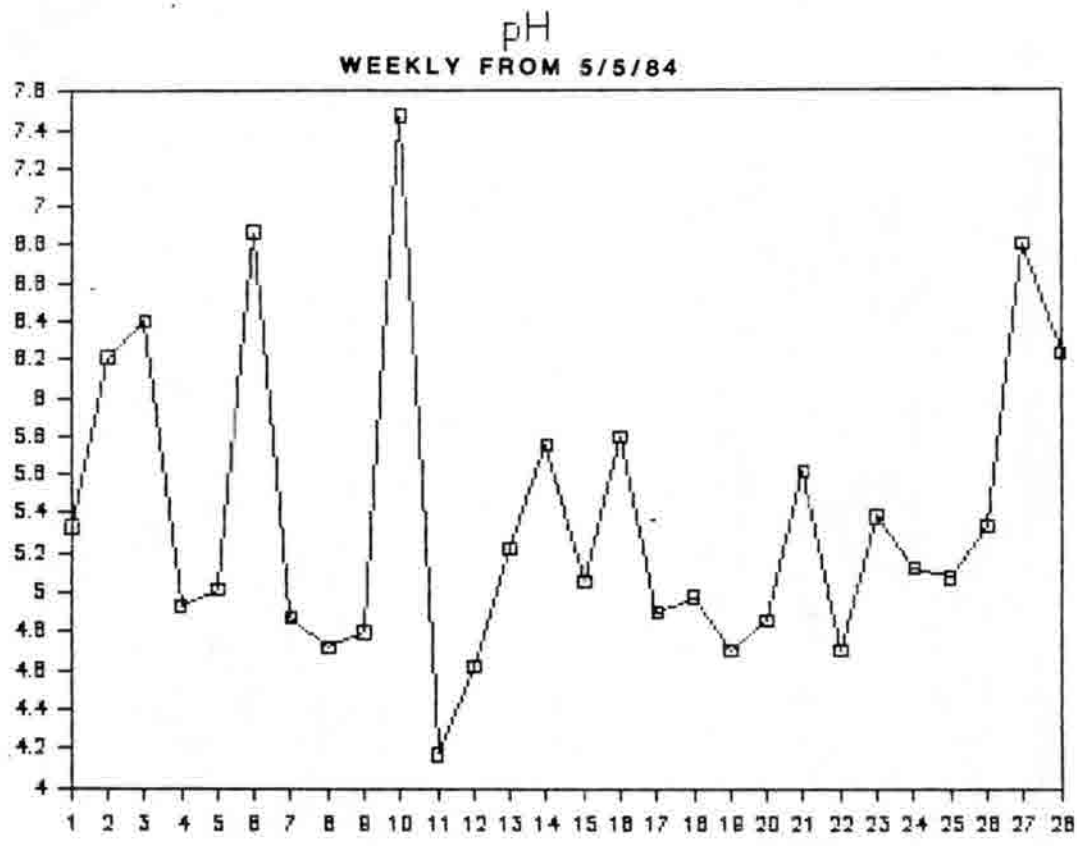


Fig. 7. Weekly values of pH in 1984.

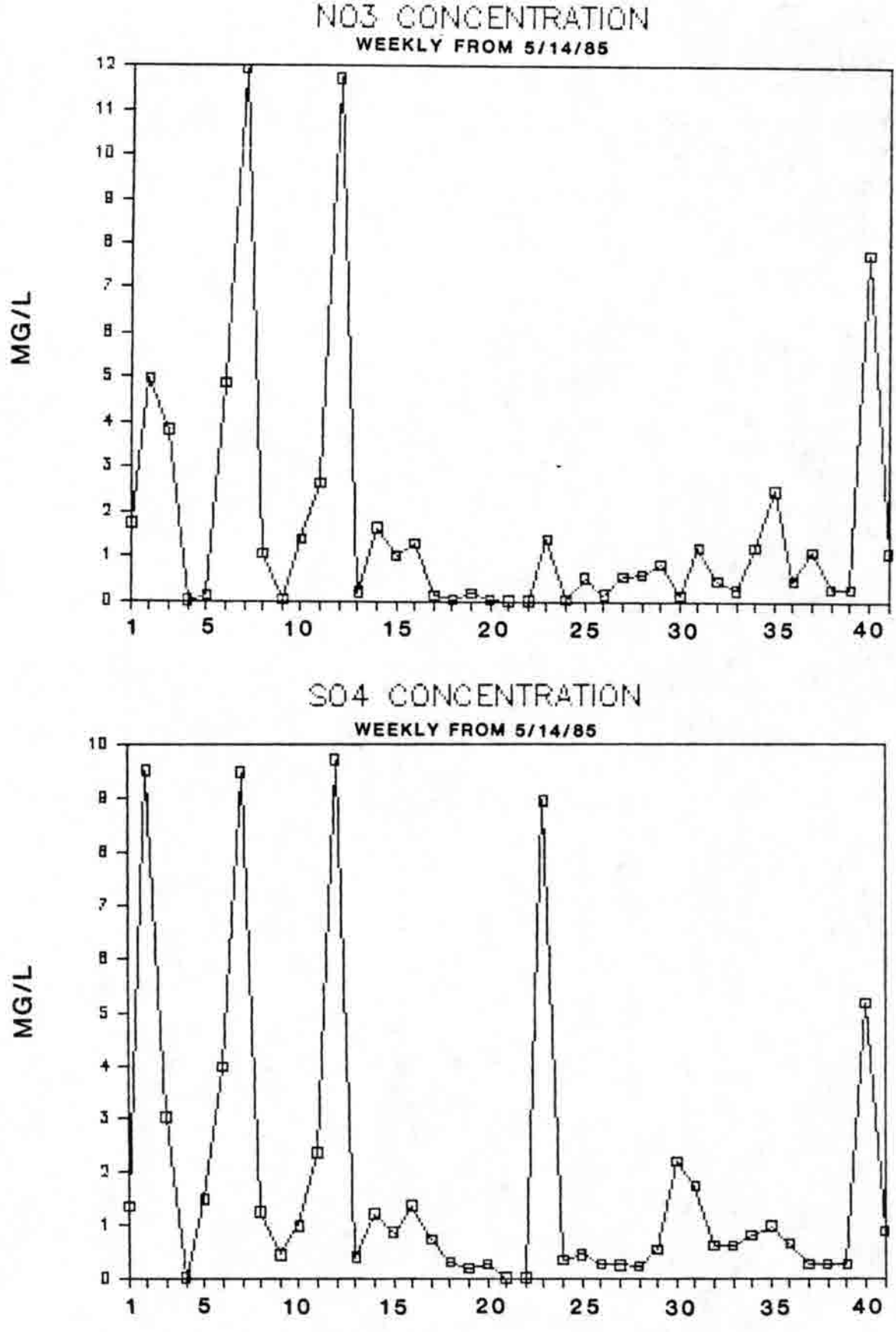


Fig. 8. Weekly values of concentration of NO3 and SO4 in 1985/6.

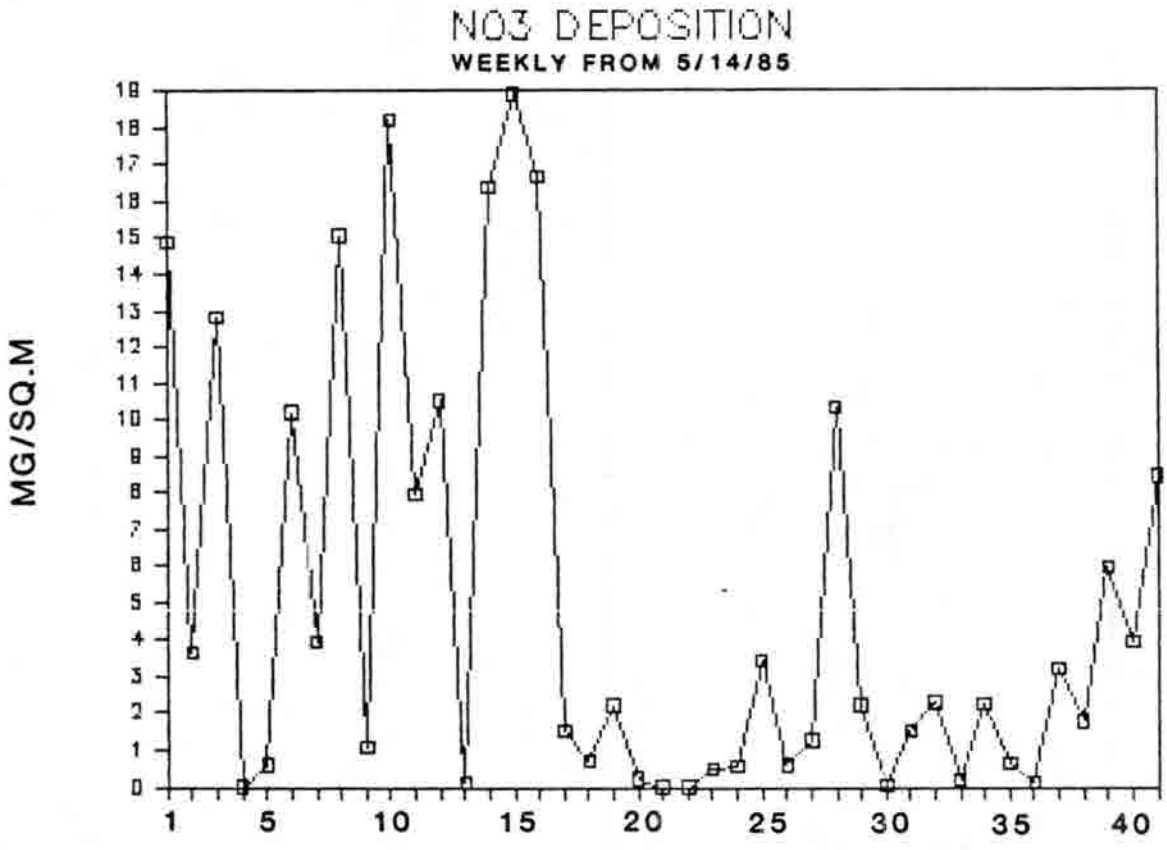


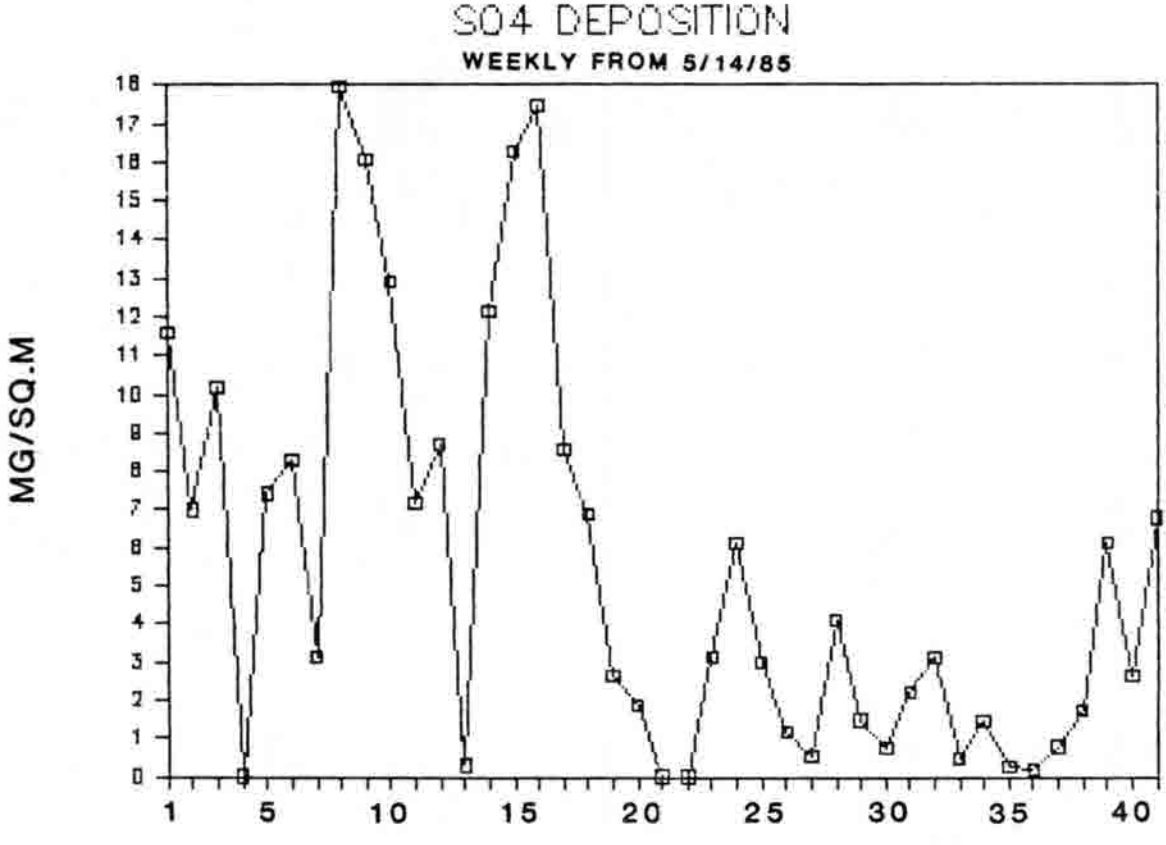


Fig. 9. Weekly values of deposition of NO3 and SO4 in 1985/6.

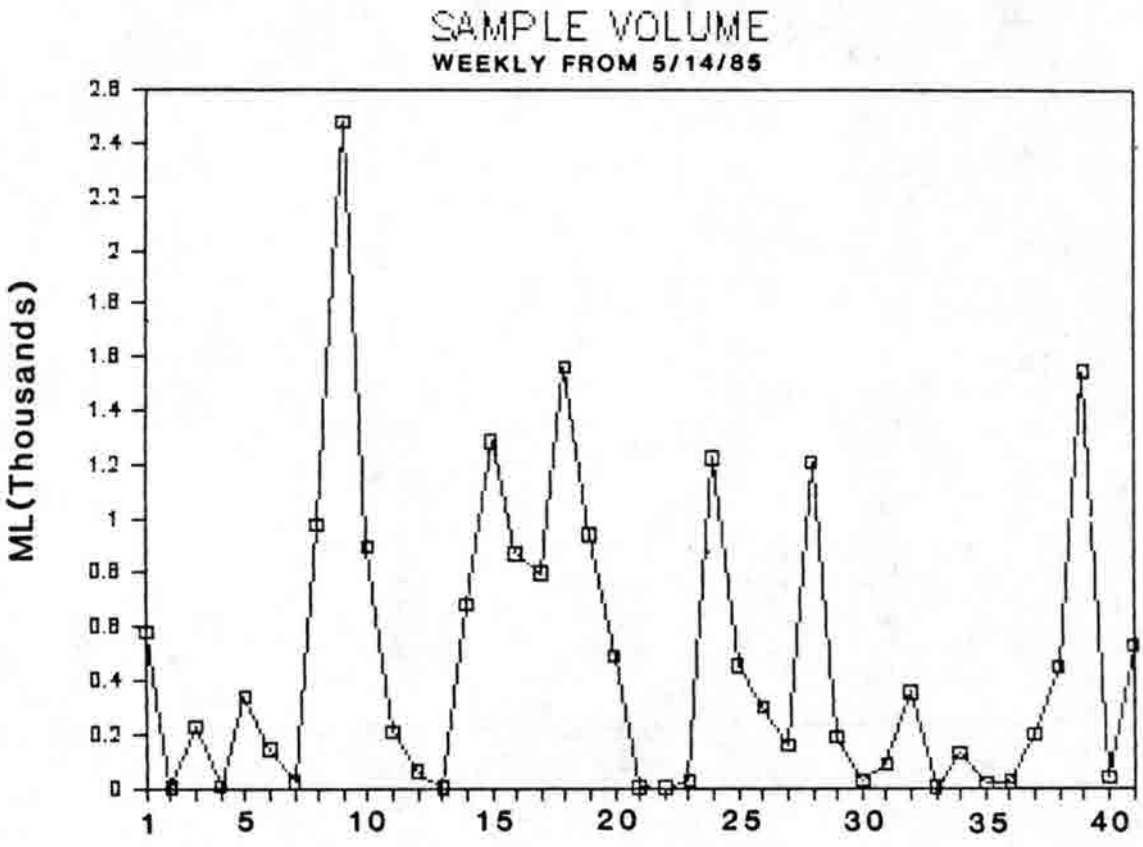


Fig. 10. Weekly values of sample volume in 1985/6.

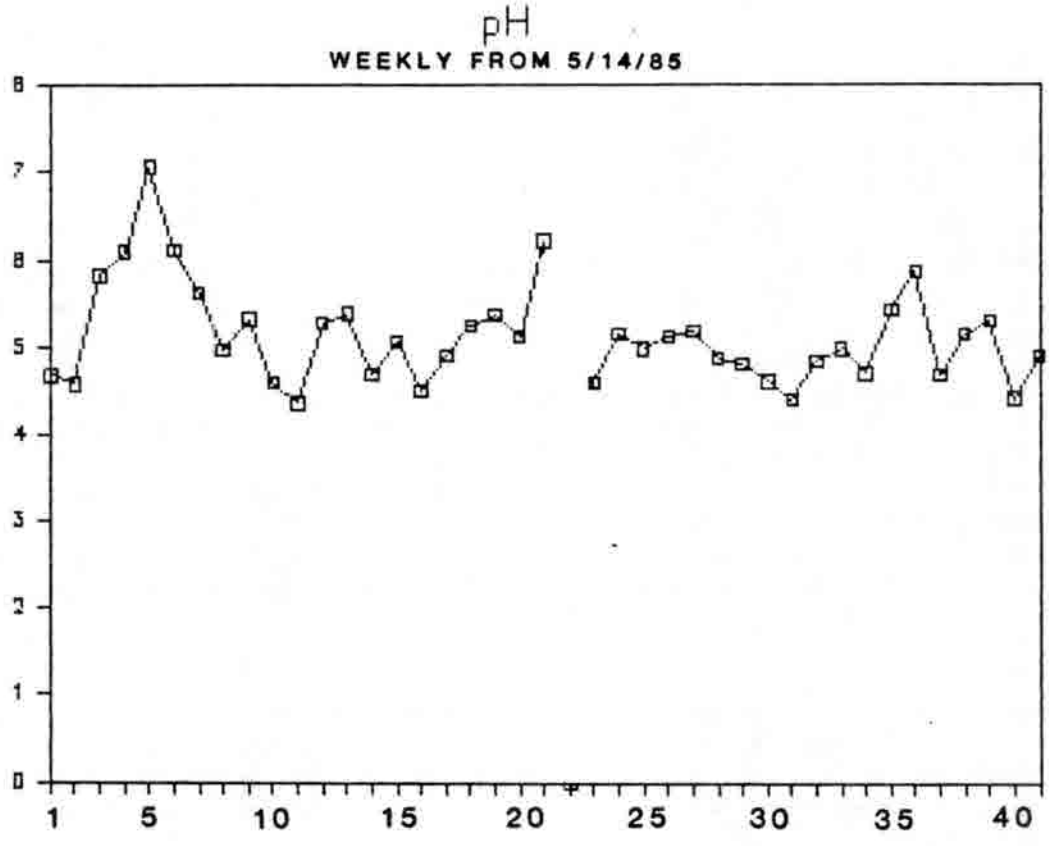


Fig. 11. Weekly values of pH in 1985/6.

b) In winter, when there is strong northwesterly flow in the upper air which might be turned anti-cyclonically in the vicinity of the Front Range by the presence of the Cheyenne Ridge consequently giving local upslope conditions (Figure A6).

There is clearly a need for a more detailed, systematic and comprehensive synoptic study of this kind, and one that would be ideally accompanied with an investigation of mesoscale wind conditions.

## CONCLUSIONS

Given the complexity of results so far obtained with respect to information on potential acid deposition in the Front Range of Colorado, preliminary results from the high altitude NADP sampling site of Niwot Ridge are interesting. The more important aspects of them include: 1) the identification of sulfates and nitrates as being of almost equal importance as being the most frequent species (of those that are sampled) deposited; 2) (assuming the validity of the winter deposition values of 1985/6) the importance of summer as a time when the bulk of wet deposition takes place at the site; and 3) the variable synoptic conditions under which noteworthy depositional events appear to occur.

## ACKNOWLEDGEMENTS

Preparation of this paper was funded in part by a grant from the National Science Foundation, Division of Biotic Systems and Resources, DEB 8012095. The same grant administered by the Institute of Arctic and Alpine Research at the University of Colorado supports the collection and analysis of the NADP data. I am grateful to Mr. Mark Losleben and Dr. P. J. Webber for making the data available.

## REFERENCES

Bollinger, J.M., C.J. Hahn, D.D. Parrish, P.C. Murphy, D.L. Albritton, and F.C. Fehsenfeld, 1984. $NO_x$ measurements in clean continental air and analysis of contributing meteorology. *J. Geophys. Res.*, **89**, 9623–9631.

Fehsenfeld, F.C., 1984. The study of atmospheric chemistry in the western United States. In Atmospheric Research Needs for the Western United States, Yamada, et al., eds. Los Alamos National Laboratory, New Mexico, LA–10109–C, UC–11, pp.28–31.

Grant, M.C., and W.M. Lewis, 1982. Chemical loading rates from precipitation in the Colorado Rockies. *Tellus*, **34**, 74–88.

Greenland, D., 1982. Air quality and surface energy budget. In Ecological Studies in the Colorado Alpine: A Festschrift for John W. Marr, J.C. Halfpenny, ed. Institute of Arctic and Alpine Research, University of Colorado, Boulder. Occasional Paper No. 37, pp.23–25.

Greenland, D., 1987. The climate of Niwot Ridge. Long Term Ecological Program Data Report. Institute of Arctic and Alpine Research, University of Colorado, Boulder. CULTER (in press).

Huebert, B.J., R.B. Norton, M.J. Bollinger, D.D. Parrish, C.J. Hahn, Y.A. Bush, P.C. Murphy, F.C. Fehsenfeld, and D.L. Albritton, 1982. Gas phase and precipitation acidities in the Colorado mountains. International Symposium of Hydrometeorology. American Water Resources Association, pp.17–23.

Kelly, T., and D. Stedman, 1980. Effect of urban sources on acid precipitation in the western United States. *Science*, **210**, 1043.

## APPENDIX 1. SYNOPTIC CASE STUDIES

Daily synoptic weather charts published by NOAA were examined for each day of the week for certain periods identified as being noteworthy in terms of depositional events at Niwot Ridge. Events that would trigger an examination included high deposition rates or concentrations of nitrates (NO3) and/or sulfates (S04) or low pH values. The surface and 500 mb pressure patterns were the prime informational sources used since these can give information on general wind patterns as opposed to wind observations at individual points. The isobaric patterns were subjectively interpreted to give information on the direction and velocity of the gradient wind that would affect the Niwot Ridge area of Colorado. Given below are the results of these studies. In some instances the qualifying word "potential" is used indicating that in an area of complex terrain there is no guarantee that the gradient wind implied by the synoptic chart will actually occur. This is particularly true with the surface conditions.

Week beginning: 7/24/84. Reason of interest: High deposition rates.

Characterized by rather stagnant airmasses dominated by surface and 500 mb high pressure areas over or near Colorado but with several days with the potential for surface easterly flow (Fig A1).

Week beginning: 8/7/84. Reason of interest: High concentration rates.

Typified by stagnating air at both the surface and the 500 mb level. There were at least three days when both surface and upper air flow probably came from the east at low velocity. Generally though, there was a weak 500 mb level flow from the west.

Three Weeks beginning: 8/14/84. Reason of interest: Low pH.

Much of the period was dominated by a surface high pressure zone over the mid section of the country while a weak west or south-westerly flow occurred over Colorado at the 500 mb level. There were ample occasions for the potential for easterly flow at the surface and weak upper air flow from the south west or west (Fig. A2).

Week beginning: 5/21/85. Reason of interest: High S04 concentration by itself and low pH.

The first four days of the period were typified by having a surface high pressure zone to the north east or over Colorado and having weak 500 mb level flow indicated also from the east. The last three days had surface flow from the north west and 500 mb level flow from the west.

Week beginning: 7/2/85. Reason of interest: Both NO3 and SO4 concentrations being high.

A period in which surface winds were generally weak and from the west to north quadrant (or indeterminable (Fig. A3)) but 500 mb level winds were strong from the north west. These upper level winds swung around an upper high in the south west and presumably brought air from parts of California (Fig. A3).

Week beginning: 7/30/85. Reason of interest: low pH.

This was a period in which the surface winds were weak and probably from almost any direction except the east. However there was a consistent 500 mb level flow all the week from the south west. This flow was usually weak but was strong on the first two days of the week.

Week beginning: 8/6/85. Reason of interest: Both NO3 and SO4 concentrations high.

This was another week in which the surface flow was probably weak and variable in direction but the dominant feature is consistent 500 mb flow from the south west or west. This upper south-westerly flow was strong on four days of the period and one of them contained a frontal passage (Fig A4).

Week beginning: 9/10/85. Reason of interest: low pH

During this week three days had the potential for light surface winds from an easterly quarter while on the other days it probably came from a westerly direction. Once more, however, the most characteristic synoptic feature of the week is the frequent, and often strong 500 mb level flow from the south west (Fig. A5).

Week beginning: 10/29/85. Reason of interest: Only SO4 concentration high.

There was no clear pattern to the flow for this week. Wind directions at the surface were either variable or indeterminable. Flow at the 500 mb level was more consistent coming generally from the west and, for the last three days, strongly from the north west.

Week beginning: 12/24/85. Reason of interest: low pH.

This week showed a completely different pattern to those examined so far. Virtually all of the week had surface winds from a northerly direction which were sometimes quite strong. The 500 mb level flow was characterized by persistent strong winds from the north west (Fig. A6). Under such circumstances Schlatter (1985) has pointed out that the existence of the Cheyenne Ridge can give rise to the formation of anticyclonic turning of winds in the Boulder area. These winds would potentially bring air to Niwot Ridge from the Front Range Urban Corridor.

Week beginning: 2/25/86. Reason of interest: low pH.

This was another period of surface winds generally from the north but with upper air winds, as exemplified by the 500 mb flow, coming strongly from the north or north west.

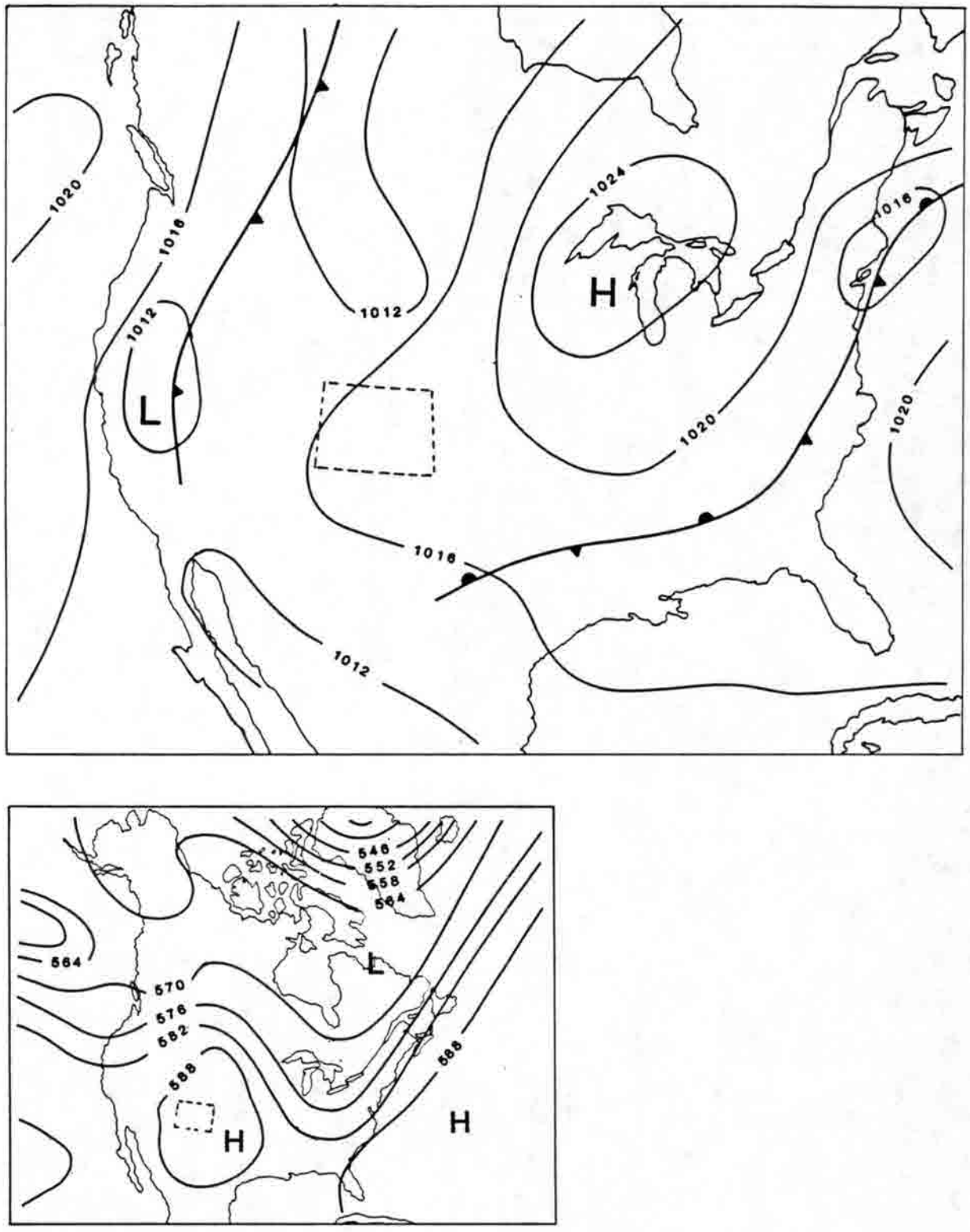


Fig. A1. Synoptic weather charts for the surface and 500 mb heights for July 28, 1984.

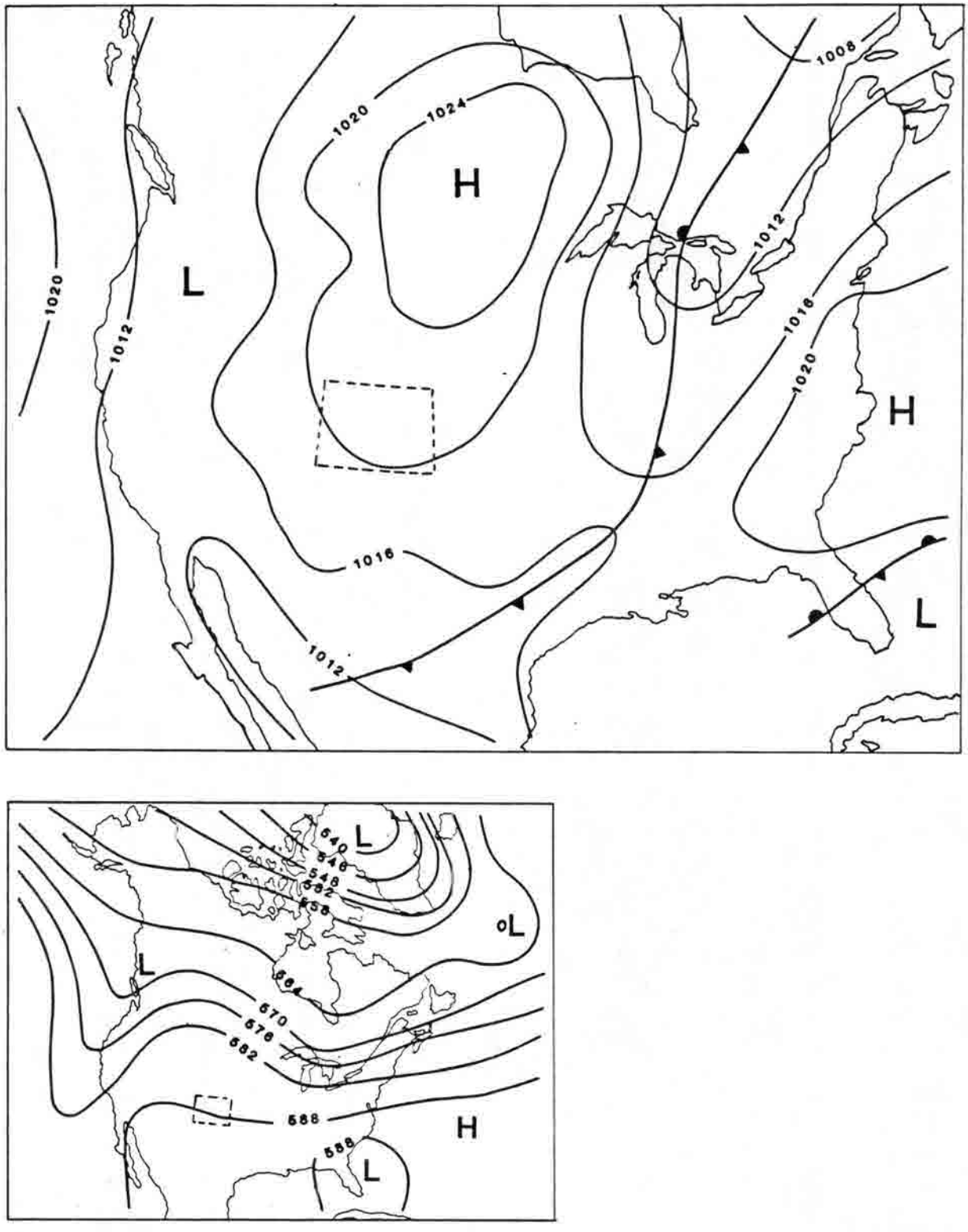


Fig. A2. Synoptic weather charts for the surface and 500 mb heights for August 22, 1984.

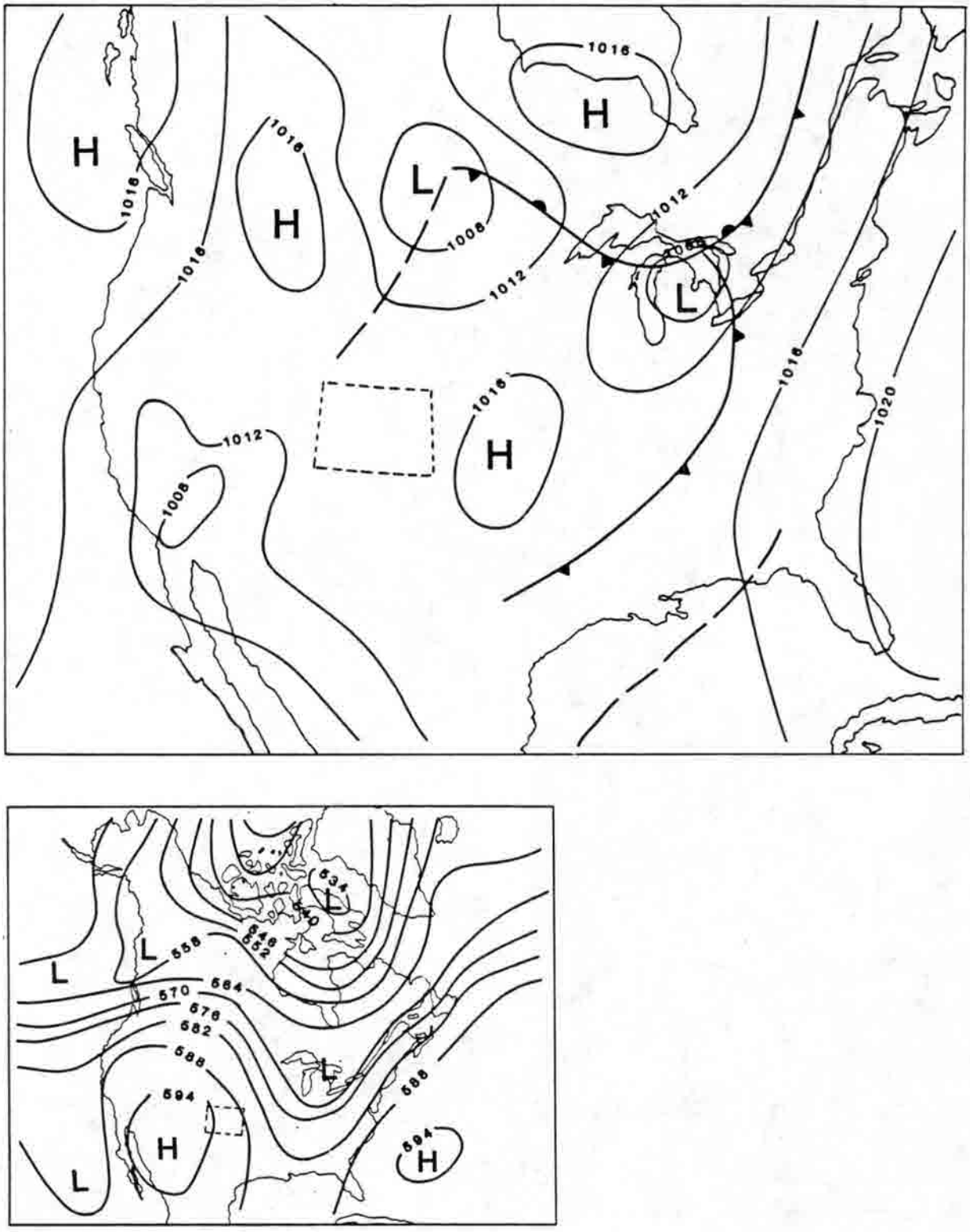


Fig. A3. Synoptic weather charts for the surface and 500 mb heights for July 6, 1985.

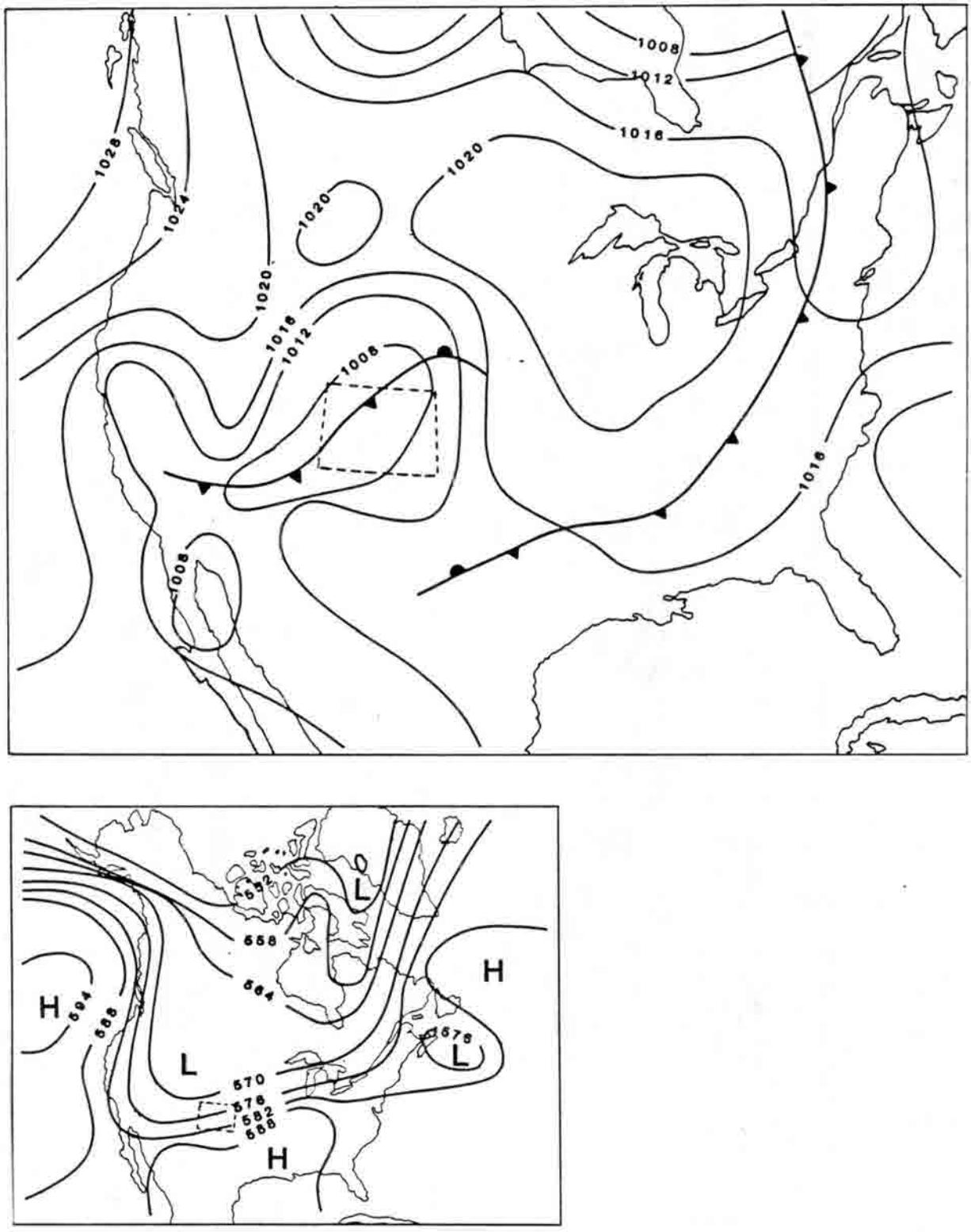


Fig. A4. Synoptic weather charts for the surface and 500 mb heights for August 11, 1985.

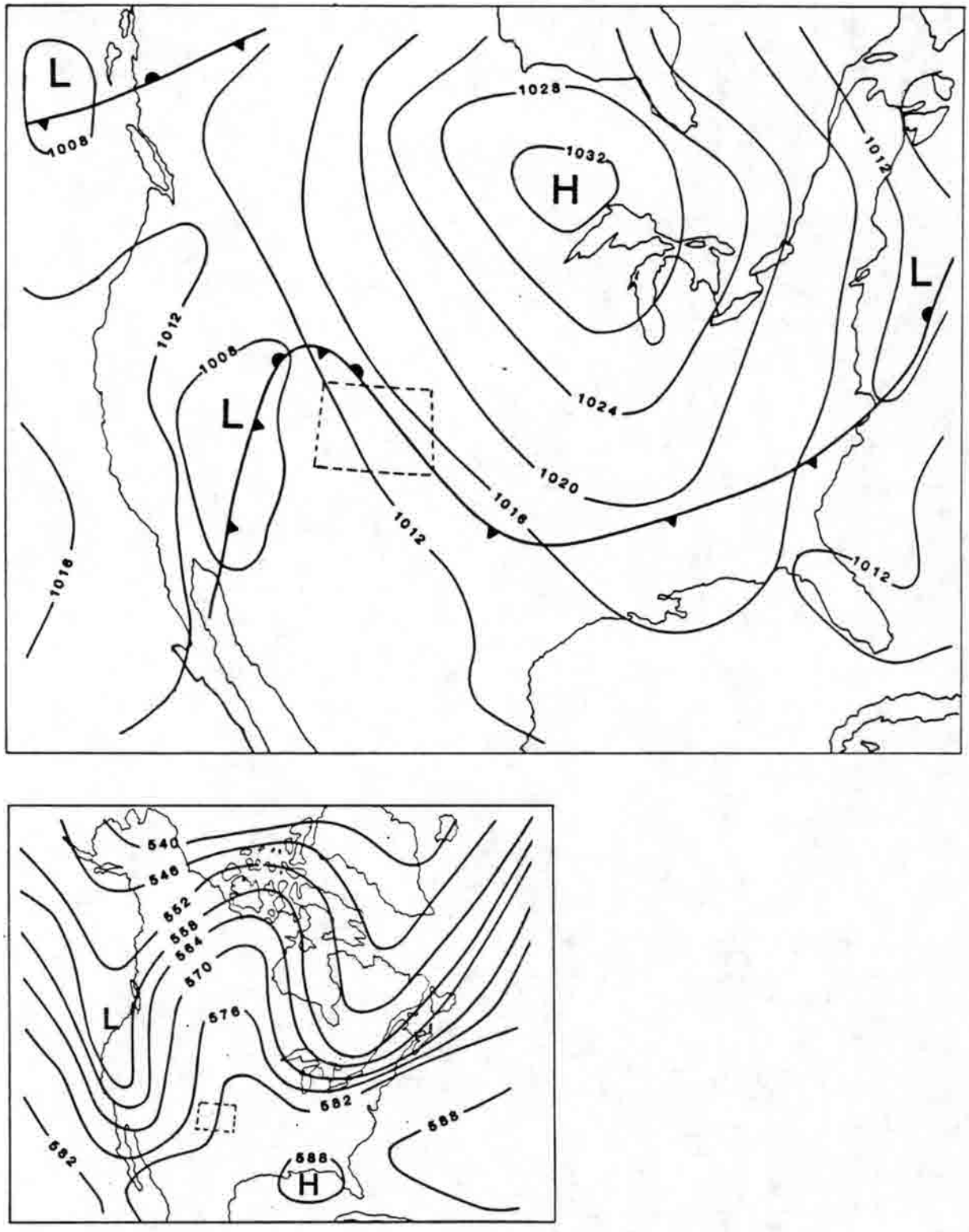


Fig. A5. Synoptic weather charts for the surface and 500 mb heights for September 11, 1985.

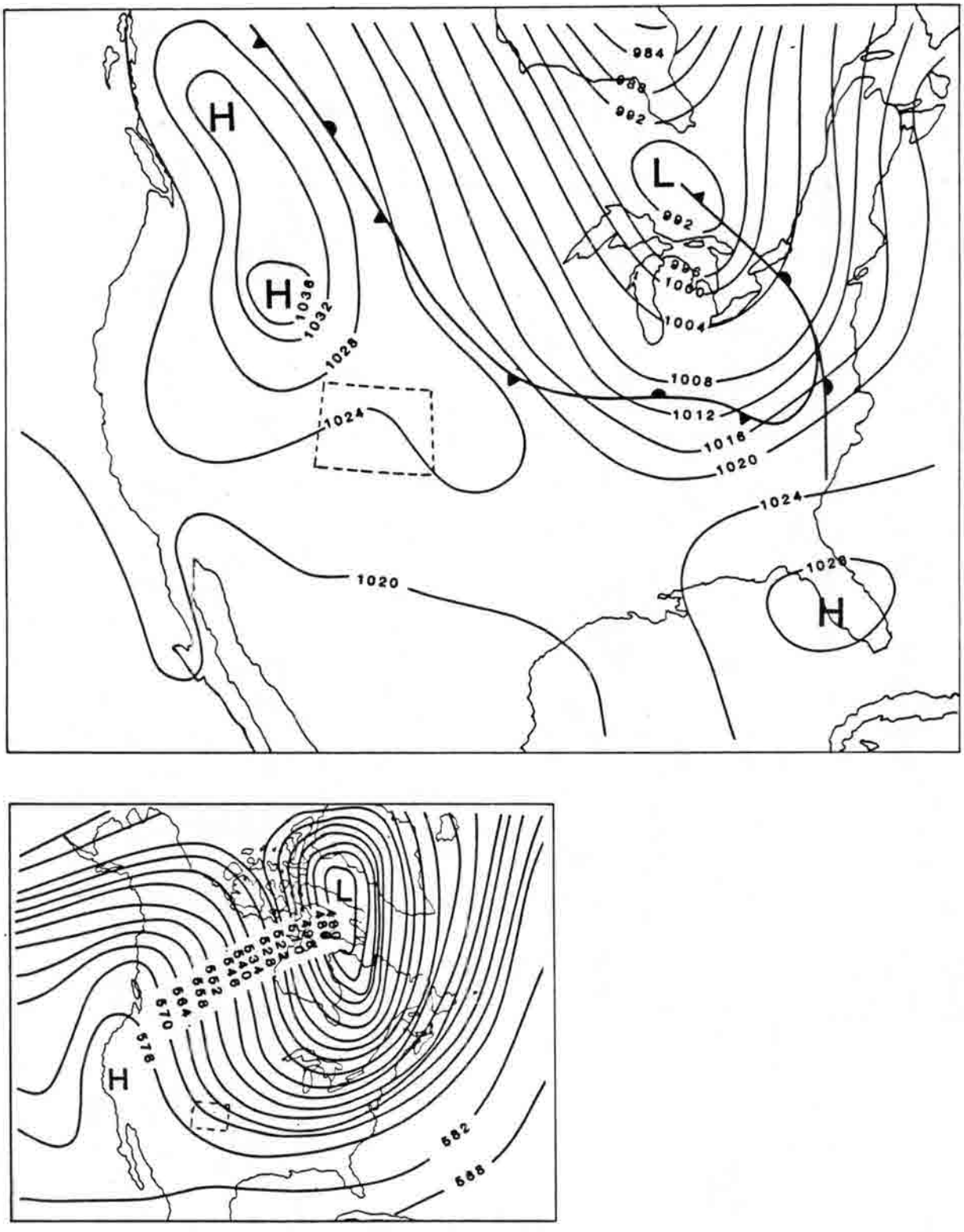


Fig. A6. Synoptic weather charts for the surface and 500 mb heights for December 27, 1985.

# The Rocky Mountain Acid Deposition Modeling Assessment Project – Goals and Current Status

Ralph E. Morris
Mei-Kao Liu
Systems Applications, Inc.

Larry Svoboda
U.S. Environmental Protection Agency
Region VIII

Alan Huber*
U.S. Environmental Protection Agency
Environmental Research Lab

August 14, 1986

## INTRODUCTION

Acid deposition has recently become an increasing concern in the western United States (World Resources Institute, 1985). Although this problem may not be as acute in the west as it is in the east, it has nevertheless become a concern of regulatory agencies because of the high sensitivity of western lakes at high altitudes and the rapid industrial growth expected to occur in certain areas of the west. An example of such an area is the region known as the Overthrust Belt in southwestern Wyoming. Several planned energy-related projects, including natural gas sweetening plants and coal-fired power plants, may considerably increase the emission of acid precursors in northeastern Utah and northwestern Colorado, and significantly affect ecosystems in the sensitive Rocky Mountain areas.

Under the 1977 Clean Air Act, the U.S. Environmental Protection Agency (EPA), along with other federal and state agencies, is required to preserve and protect air quality throughout the country. As part of the Prevention of Significant Deterioration (PSD) permitting processes, federal and state agencies are required to evaluate potential impacts of new emission sources. In particular, Section 165 of the Clean Air Act stipulates that, except in specially regulated instances, PSD increments shall not be exceeded and air quality related values (AQRVs) shall not be adversely affected. Air quality related concerns range from near-source plume blight to regional scale acid deposition problems. By law, the Federal Land Manager of Class I areas has a responsibility to protect air quality related values within those areas. New source permits cannot be issued by the EPA or the states when the Federal Manager concludes that adverse impacts on air quality or air

*On assignment from the National Oceanic and Atmospheric Administration, United States Department of Commerce

quality related values will occur. The locations of the 92 Class I areas in the western states are shown in Figure 1, while Table 1 identifies these areas.

Study Objectives

The objective of the Rocky Mountain Acid Deposition Modeling Assessment Project is to assemble an acid deposition model based on currently available air quality and meteorological models and modules that adequately describe the processes of acid deposition in the Rocky Mountain region. The model would be used by federal and state agencies in the western states. This effort differs from other acid deposition model development efforts, such as the NCAR/RADM, in that the model is to be designed specifically for use and application by western regulatory agencies to estimate acid deposition impacts from proposed new sources. The Western Acid Deposition Task Force provided the following guidelines on the design of the model.

> The anticipated use of this model is to analyze permit applications and evaluate urban development plans. The model is thus expected to simulate impacts of various air pollutants from both point and area sources.
>
> A typical modeling area will cover approximately 200 km to 300 km on a side to have the ability to calculate impacts from new sources within relatively short distances of Class I areas.
>
> The model should be able to handle events over long time periods, such as calculating seasonal and/or annual averages, in order to obtain cumulative impacts from both chronic and episodic events.
>
> The model should be able to simulate transport, diffusion, transformation, and deposition of pollutants over complex terrain in the Rocky Mountain region with relatively sparse NWS upper-air soundings.
>
> The model should be able to predict acid deposition fluxes of sulfur and nitrogen species.
>
> Treatment of both gas- and aqueous-phase chemistry is desirable.
>
> The model should treat orographic effects on precipitation, including enhanced precipitation rates, snowfall, and ice-phase processes.
>
> The modeling system should be simple enough to be used by a regulatory agency on a mid-sized computer.

Study Organization

The Rocky Mountain Acid Deposition Modeling Assessment Project is divided into three main tasks and three optional tasks as follows.

> Task 1
>
> Review and selection of candidate mesoscale meteorological models.
>
> Review and selection of candidate acid deposition models.
>
> Selection of first application scenarios.
>
> Task 2
>
> Acquisition, testing, and evaluation of model components.
>
> Assembly of hybrid modeling system.

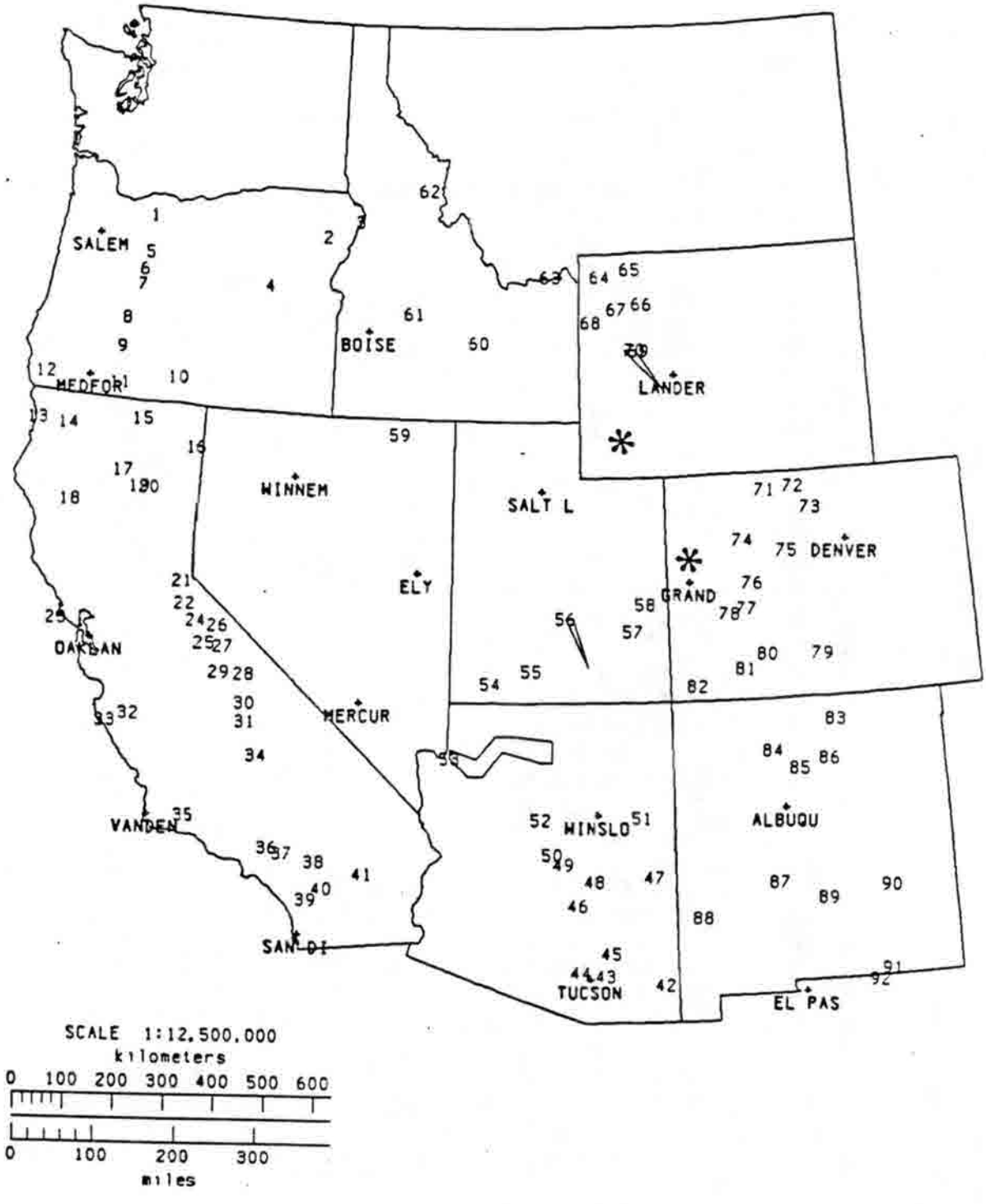


FIGURE 1. Class I areas and upper-air meteorological stations located in the West, exclusive of Washington and Montana. The locations of the first two application scenarios (in Wyoming and Colorado) are indicated by large asterisks. (Key to locations is in Table 1.)

TABLE 1. Key to Class I Areas located in the West.

| NO | NAME |
|---|---|
| 1 | Mount Hood Wilderness |
| 2 | Eagle Cap Wilderness |
| 3 | Hells Canyon Wilderness |
| 4 | Strawberry Mountain Wilderness |
| 5 | Mt. Jefferson Wilderness |
| 6 | Mt. Washington Wilderness |
| 7 | Three Sisters Wilderness |
| 8 | Diamond Peak Wilderness |
| 9 | Crater Lake National Park |
| 10 | Gearhart Mountain Wilderness |
| 11 | Mountain Lakes Wilderness |
| 12 | Kalmiopsis Wilderness |
| 13 | Redwood National Park |
| 14 | Marble Mountain Wilderness |
| 15 | Lava Beds Wilderness |
| 16 | South Warner Wilderness |
| 17 | Thousand Lakes Wilderness |
| 18 | Yolla-Bolly - Middle Eel Wilderness |
| 19 | Lassen Volcanic National Park |
| 20 | Caribou Wilderness |
| 21 | Desolation Wilderness |
| 22 | Mokelumne Wilderness |
| 23 | Point Reyes Wilderness |
| 24 | Emigrant Wilderness |
| 25 | Yosemite National Park |
| 26 | Boover Wilderness |
| 27 | Minarets Wilderness |
| 28 | John Muir Wilderness |
| 29 | Kaiser Wilderness |
| 30 | Kings Canyon National Park |
| 31 | Sequoia National Park |
| 32 | Pinnacles Wilderness |
| 33 | Ventana Wilderness |
| 34 | Dome Land Wilderness |
| 35 | San Rafael Wilderness |
| 36 | San Gabriel Wilderness |
| 37 | Cucamonga Wilderness |
| 38 | San Gorgonio Wilderness |
| 39 | Agua Tibia Wilderness |
| 40 | San Jacinto Wilderness |
| 41 | Joshua Tree Wilderness |
| 42 | Chiricahua Wilderness |
| 43 | Saguaro Wilderness - East |
| 44 | Saguaro Wilderness - West |
| 45 | Galiuro Wilderness |
| 46 | Superstition Wilderness |
| 47 | Mt. Baldy Wilderness |
| 48 | Sierra Ancha Wilderness |
| 49 | Mazatzal Wilderness |
| 50 | Pine Mountain Wilderness |



Continued

TABLE 1. Concluded.

| NO | NAME |
|---|---|
| 51 | Petrified Forest National Park |
| 52 | Sycamore Canyon Wilderness |
| 53 | Grand Canyon National Park |
| 54 | Zion National Park |
| 55 | Bryce Canyon National Park |
| 56 | Capitol Reef National Park |
| 57 | Canyonlands National Park |
| 58 | Arches National Park |
| 59 | Jarbridge Wilderness |
| 60 | Craters of the Moon Wilderness |
| 61 | Sawtooth Wilderness |
| 62 | Selway Bitterroot Wilderness |
| 63 | Red Rock Lakes Wilderness |
| 64 | Yellowstone National Park |
| 65 | North Absaroka Wilderness |
| 66 | Washakie Wilderness |
| 67 | Teton Wilderness |
| 68 | Grand Teton National Park |
| 69 | Fitzpatrick Wilderness |
| 70 | Bridger Wilderness |
| 71 | Mount Zirkel Wilderness |
| 72 | Rawah Wilderness |
| 73 | Rocky Mountain National Park |
| 74 | Flat Tops Wilderness |
| 75 | Eagles Nest Wilderness |
| 76 | Maroon-Bells Snowmass Wilderness |
| 77 | West Elk Wilderness |
| 78 | Black Canyon of the Gunnison Wilder. |
| 79 | Great Sand Dunes Wilderness |
| 80 | La Garita Wilderness |
| 81 | Weminuche Wilderness |
| 82 | Mesa Verde National Park |
| 83 | Wheeler Peak Wilderness |
| 84 | San Pedro Parks Wilderness |
| 85 | Bandelier Wilderness |
| 86 | Pecos Wilderness |
| 87 | Bosque del Apache Wilderness |
| 88 | Gila Wilderness |
| 89 | White Mountain Wilderness |
| 90 | Salt Creek Wilderness |
| 91 | Carlsbad Caverns National Parks |
| 92 | Guadalupe National Park |

Task 3

Delivery and installation of modeling system on the EPA's computer.

Optional Task 1

Assembly of an aerometric data base suitable for model operation and evaluation.

Optional Task 2

Detailed evaluation studies of the modeling system.

Optional Task 3

Refinement and adaptation of the modeling system.

At this time (August, 1986) Task 1 has been completed. The following draft documents were completed under this task: (1) a review of mesoscale meteorological models that can calculate wind fields in complex terrain (Morris, et al., 1986a); (2) a review of acid deposition models that could serve as the basis for a Rocky Mountain Model (Morris, et al., 1986b); and (3) a description of some typical application scenarios in the Rocky Mountain west (Morris, 1986). These draft documents also recommend models that would be most suitable for the development of a model for Rocky Mountain acid deposition issues. These three documents have been combined to form a final report entitled "Rocky Mountain Acid Deposition Modeling Assessment Review of Existing Mesoscale Models for Use in Complex Terrain" (Morris and Kessler, 1987) available through NTIS.

At meetings in Colorado on 28 and 29 July 1986, Systems Applications staff met with EPA staff and several members of the Western Atmospheric Deposition Task Force (WADTF) and its Atmospheric Processes Work Group (WADTF/AP) to review progress on the project and to collect comments before proceeding with the selection of meteorological and acid deposition models for testing (Task 2) and implementation and documentation (Task 3). Several issues were identified at that meeting that may help to focus the conceptual design of the modeling system. Before embarking on Task 2 of the project, written comments on the conceptual design of the model were requested from the regulatory agencies for whom the model is designed.

## TYPES OF APPLICATIONS FOR THE PROPOSED MODEL

The primary purpose of the Rocky Mountain Acid Deposition Model is to determine whether acid deposition from new sources and urban growth will adversely affect ecological systems in sensitive areas within complex terrain in the Rocky Mountains. To determine this, the model must predict the total cumulative deposition of sulfates and nitrates, as well as the contribution of the new source. Acid deposition modeling in the Rocky Mountains is further complicated by the complex terrain in the region, and the fact that many of the sensitive lakes are located at higher elevations, where orographic effects on precipitation increase wet deposition of pollutants.

The two application scenarios described here represent the types of new sources that have been proposed in the western Rockies. They include sufficiently diverse sources and emission characteristics to test the model's ability to predict cumulative and source-specific acid deposition at the sensitive areas.

One scenario includes a shale oil plant in western Colorado, the other includes three gas treatment plants in southwestern Wyoming. The relationship between the locations of these sources and the PSD Class I areas and acid-sensitive areas in the west is shown in Figures 1 and 2.

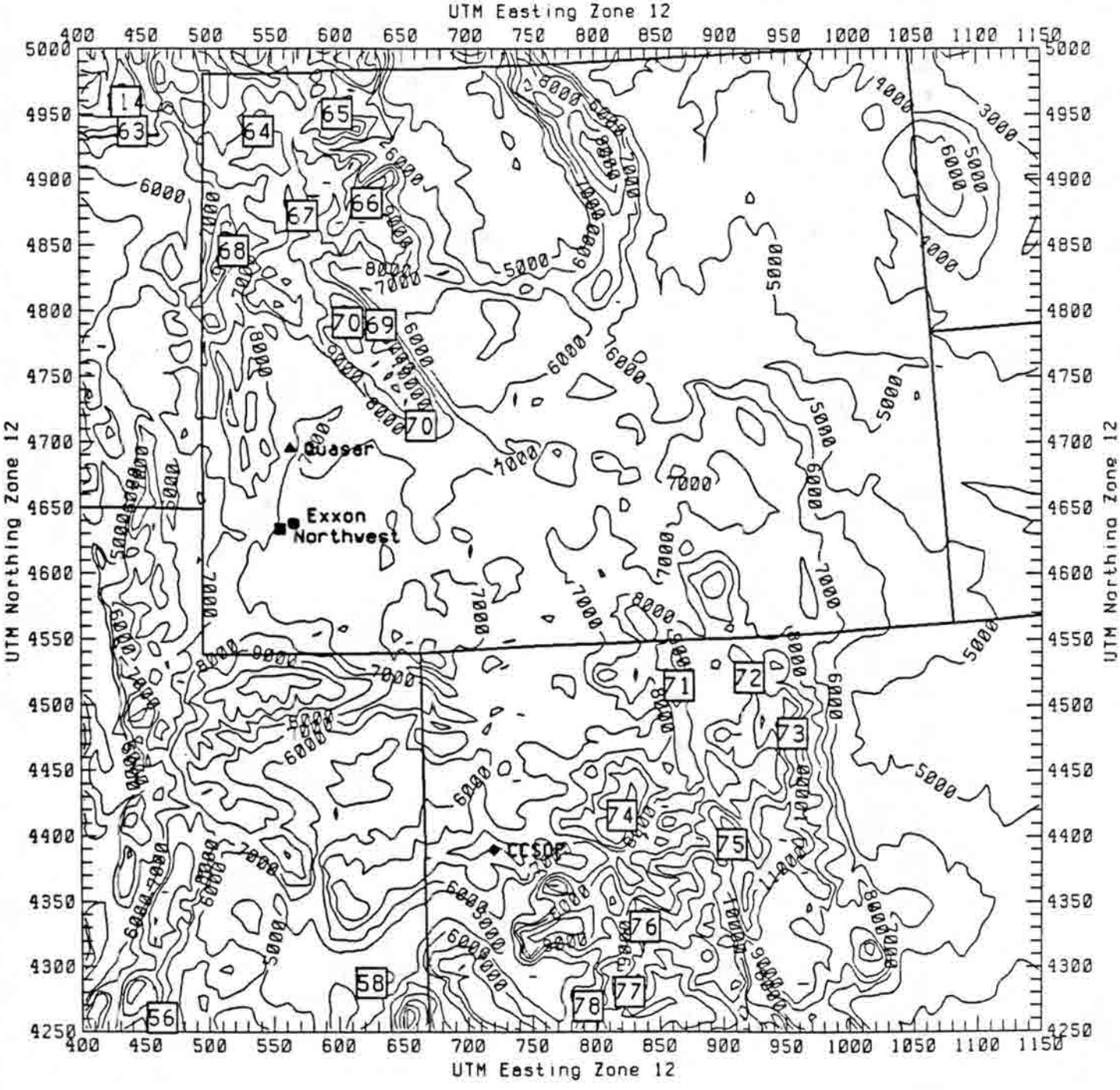


FIGURE 2. Relationship between application scenarios and PSD class I areas (see Table 1 for key). Terrain elevations are in feet above mean sea level.

Application Scenario No. 1 – Colorado Shale Oil Plant

The first application scenario is the Chevron Clear Creek Shale Oil Project (CCSOP), located in the south-central portion of the Piceance Basin in Garfield County, Colorado. This site is approximately 40 miles northeast of Grand Junction and 26 miles north of DeBeque. The closest PSD Class I area is the Flat Tops Wilderness Area, which lies approximately 50 to 55 miles to the northeast of the CCOSP site. Figure 2 shows the relationship between the CCSOP and Class I areas within a rather large (750 km x 750 km) region.

For this application scenario the Flat Tops and Maroon Bells Wilderness Areas will be the primary receptors of interest, however, estimates of cumulative and source-specific acid deposition would be calculated at all PSD Class I and sensitive areas.

The Flat Tops Wilderness Area includes several lakes that are susceptible to adverse effects from acid deposition because of law alkalinity (Turk and Adams, 1982). This area is one of the first major orographic barriers to air masses resulting from the predominantly southwest winds over the Piceance Basin. Thus, emissions from the CCSOP may be carried up to the Flat Tops Wilderness Area and precipitated out before they have been effectively dispersed.

Figures 3 and 4 show the terrain in a mesoscale region (250 km x 250 km) containing the CCSOP site and the Flat Tops and Maroon Bells Wilderness Area. This region is dominated by a series of ridges and valleys leading up to the Flat Tops Wilderness Area. Correct specification of the three-dimensional wind field and spatial variability of precipitation will be an important factor in modeling this scenario.

The extraction of oil from oil shale through combustion results primarily in emissions of $NO_x$ and $CO$. This application scenario will illustrate the model's ability to predict nitrogen deposition at source-receptor distances of about 80 km. Because of the low solubility of $NO$ and $NO_2$, wet deposition of nitrogen is usually in the form of nitrates or nitric acids. Thus it will be important to characterize the conversion of the emitted $NO_x$ to nitrates. The gas-phase conversion of $NO_x$ to nitrates is relatively rapid and depends on the availability of oxidizing precursors in the atmosphere. Nitrate formation in precipitation depends on a combination of gas-phase, gas-particle, and aqueous-phase reactions, with both reversible and irreversible conversions. Thus the correct specification of the background reactivity and precipitation patterns will be important for this application scenario.

Application Scenario No. 2 – Wyoming Gas Treatment Plants

The second application scenario includes three gas treatment plants located in the Riley Ridge area of southwestern Wyoming. These plants are the Exxon Shute Creek plant approximately five miles north of Opal, the Northwest/Mobil Craven Creek plant approximately 12 miles north-northeast of Opal, and the Quasar East Dry Basin plant approximately nine miles south-southwest of Big Piney. The closest PSD Class I areas are the Bridger and Fitzpatrick Wilderness Areas located in the Wind River Range (Figure 2). These wilderness areas are approximately 50 miles northeast of the Quasar East Dry Basin plant site, and approximately 80-85 miles north-northeast from the Exxon and Northwest/Mobil plant sites. Other nearby Class I areas include Grand Teton National Park and the Teton Wilderness Area, located due north from the plant sites (Figure 2).

Figures 5 and 6 show the terrain in a mesoscale region (250 km by 250 km) containing the gas plant sites and the Bridger and Fitzpatrick Wilderness Areas. The pollutants would be carried across a relatively flat area by southwest winds until they encounter the Wind River Range, where the air parcel would be forced upward, possibly resulting in orographic precipitation when the saturation level is achieved.

The main pollutant emitted from these sources is sulfur dioxide; some nitrogen oxides are also emitted. The scenario differs from the first because of the proximity of several major sources,

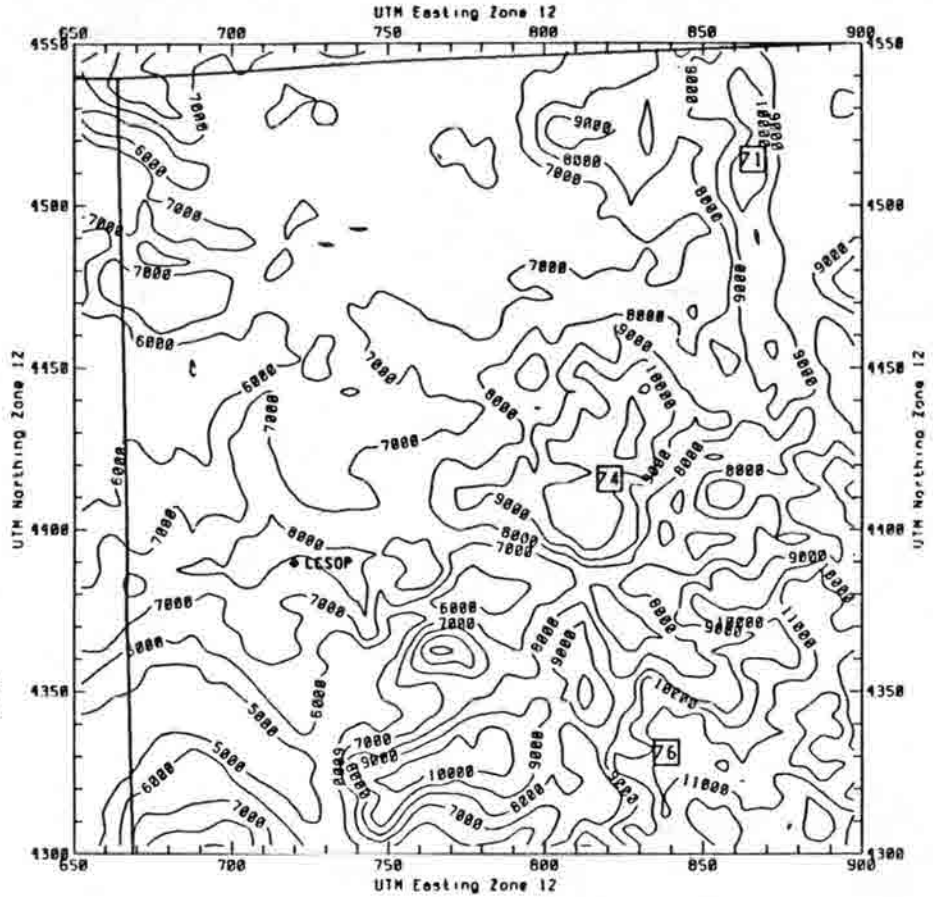


FIGURE 3. Application scenario #1 mesoscale region containing the Clear Creek shale oil plant (CCSOP) and two PSD class I areas--Flat Tops (74) and Maroon-Bells Snowmass Wilderness (76).

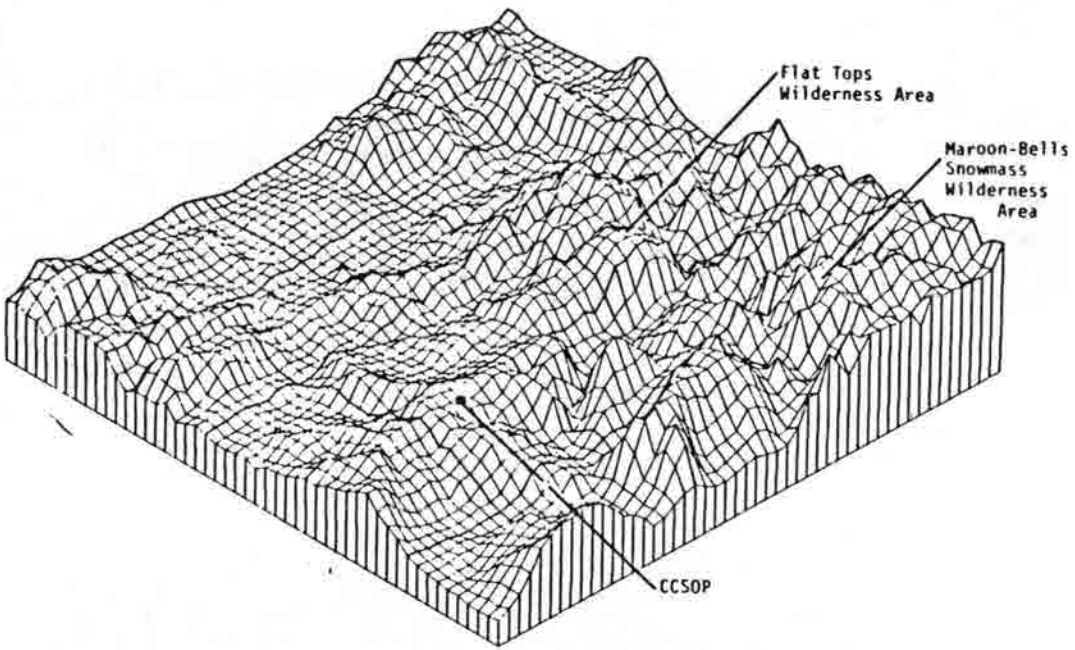


FIGURE 4. Three-dimensional perspective of terrain showing the first application scenario source and class I receptor areas.

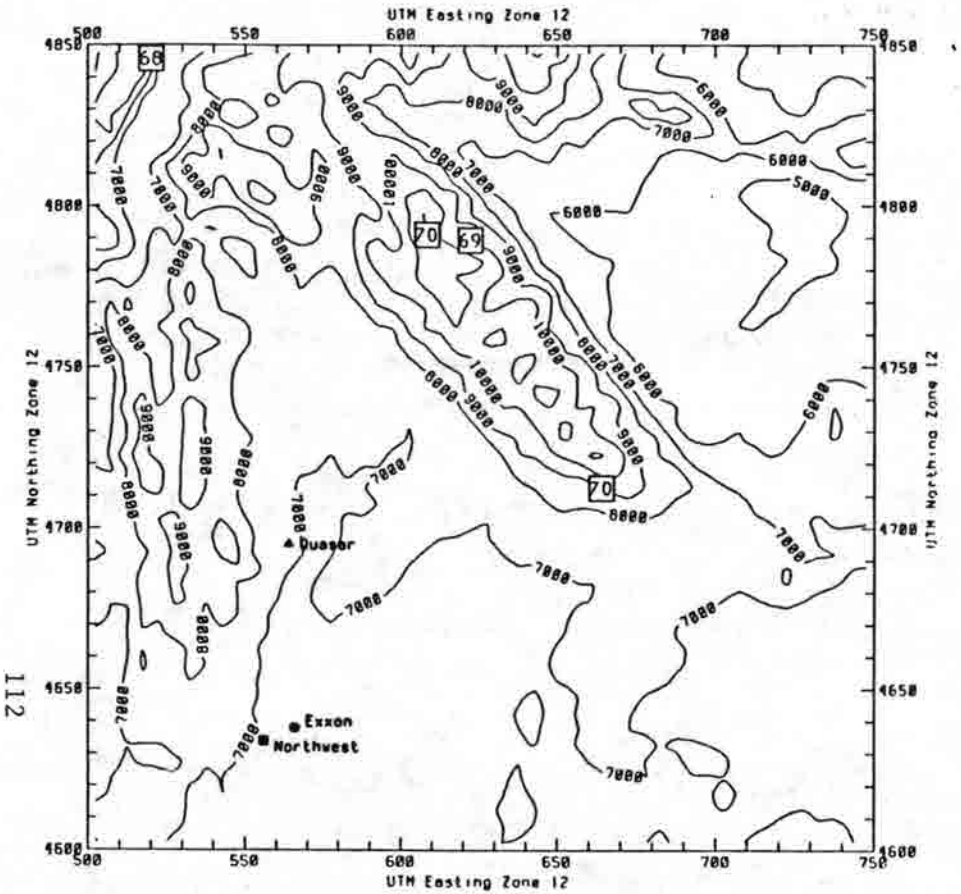


FIGURE 5. Application scenario #2 mesoscale region containing the three gas treatment plants and two PSD class I areas--Bridger Wilderness Area (area between the two boxes with number 70) and Fitzpatrick Wilderness Area (69), both in the Wind River Mountains.

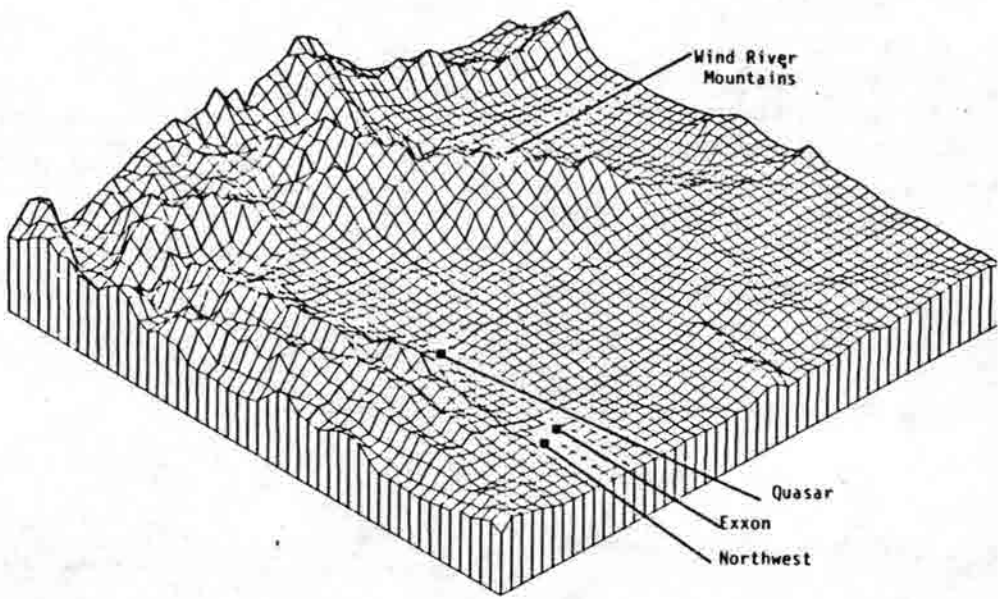


FIGURE 6. Three-dimensional perspective of terrain showing the sources in the second application scenario and the Wind River Mountains, which include the class I receptor areas.

including the Naughton and Jim Bridger Power Plants, the Opal Gas Plant, and other gas and chemical plants.

The gas-phase oxidation of $SO_2$ to sulfates is rather slow. However in the presence of hydrogen peroxide and other oxidizing agents, the aqueous-phase oxidation of $SO_2$ to sulfates is almost instantaneous. Thus, for this application scenario the transformation of the emitted $SO_2$ to sulfate will most likely be limited to the amount of hydrogen peroxide and other oxidizers available. It will be crucial to obtain an estimate of the oxidizing precursors and cloud amounts in order to properly estimate the proper $SO_2$ oxidation rate and resultant sulfate deposition.

## REVIEW AND SELECTION OF APPROPRIATE MESOSCALE METEOROLOGICAL MODELS

Over 60 mesoscale meteorological models were reviewed to select the most appropriate candidates for application to the Rocky Mountain region (Morris, et al., 1986a). This initial selection was based on a few critical factors: (1) the ablity of the model to simulate mesoscale meteorological processes over complex terrain; (2) flexibility and adaptability of the model; and (3) computational requirements.

These minimal requirements eliminated all but seven diagnostic (mass consistent) wind models and six prognostic (primitive equation) meteorological models. Table 2 shows the relative ranking of the diagnostic models and prognostic models as a result of the technical merit analysis.

## REVIEW AND SELECTION OF AN APPROPRIATE ACID DEPOSITION MODEL

Regional and mesoscale acid deposition models were surveyed and reviewed for potential candidates to apply to the Rocky Mountain region (Morris, et al., 1986b). The regional and mesoscale acid deposition models that have been developed in the past decade can be divided into four categories according to model framework: fixed-coordinate Eulerian models; moving-coordinate Lagrangian models; hybrid models that merge aspects of both the Lagrangian and Eulerian concepts; and statistical models that are used primarily for long-term averages. Because of the complex terrain in the Rocky Mountains and the importance of nonlinear chemical and deposition processes in acid deposition, the use of a statistical model may not be appropriate for this application.

The technical merits of the models under review were compared by assigning a relative score to the key components of each model (transport, dispersion, chemical transformation, wet- and dry-deposition). Based on this analysis, the Eulerian and Lagrangian acid deposition models were ranked as shown in Table 3.

## PROPOSED MODELING APPROACHES

The conceptual design for the Rocky Mountain Acid Deposition Model envisions a hybrid modeling system consisting of a meteorological model as a driver for an acid deposition model. Models will be developed to handle both mesoscale and regional issues.

Since cost considerations preclude the use of dynamic wind field models, we have recommended using an existing wind model, the Limited-Area Fine-Mesh (LFM) of the National Meteorological Center in Boulder, to characterize regional-scale wind fields, and a diagnostic (mass-conserving) wind model to characterize winds within a mesoscale modeling region. The LFM wind data is rather coarse (127 km) and can only characterize the regional upper level wind flow in the Rocky Mountains.

The wind fields will determine where pollutants are transported, while the acid deposition model will calculate the processes of dispersion, chemical transformation, dry deposition and wet deposition.

TABLE 2. Relative ranking of diagnostic and prognostic mesoscale meteorological models.

| Diagnostic Models | Prognostic Models |
|---|---|
| PNL/MELSAR-MET | NCAR/MM4 |
| SAI/CTWM | MESO/MASS |
| SAI/MVWM | CSU/MESOSCALE |
| LANL/ATMOS1 | NOAA/ERL |
| LLNL/MATHEW | LANL/HOTMAC |
| CIT/WIND | DREXEL/NCAR |
| SRI/DIAGNOSTIC | |

TABLE 3. Relative ranking of Eulerian and Lagrangian acid deposition models.

| Eulerian/Hybrid Models | Lagrangian Models |
|---|---|
| NCAR/RADM | SAI/CCADM |
| ERT/ADOM | ERT/MESOPUFF-II |
| UK/STEM-II | SAI/RIVAD |
| EPA/ROM | PNL/MELSAR-POLUT |
| SAI/RTM-III | |
| SAI/RTM-II | |
| UK/STEM | |

Two types of acid deposition models have been recommended: a Lagrangian (plume segment or puff) and an Eulerian (grid) model. We have proposed three conceptual designs, from which the regulatory agencies will have an opportunity to choose their preferred approach. The three proposed modeling approaches differ in whether Lagrangian or Eulerian models are used for both regional and mesoscale modeling. Several aspects of the approaches are compared in Table 4.

Alternative 1: Fully Lagrangian Approach

This approach is probably the least costly for all potential applications, including analyses of single sources, cumulative impacts (e.g., 20 sources in a mesoscale area and 80 sources in a larger region), and source attribution (i.e., determing relative source and source category contributions). The approach is particularly appropriate for analyses where it is important to keep track of the specific contributions of individual sources. Calculating the relative contributions of several sources to deposition may be an important use of the Rocky Mountain Deposition Model.

However, there are two technical problems with a Lagrangian approach that must be dealt with if it is to yield accurate predictions. First, the chemistry and deposition of plume parcels is calculated independently of other air parcels; this creates problems when plume parcels overlap and chemical and deposition mechanisms are nonlinear (which they are for aqueous-phase reactions and wet deposition). Second, each plume is divided into discrete puffs or segments, each of which is transported with winds appropriate for the centroid of that segment; this method does not account for plume dispersion caused by wind shear and divergence over the width of the segment, as is prevalent in complex terrain.

There may be ways to account for the uncertainties caused by these problems with the Lagrangian approach. This approach is similar to existing UNAMAP models used for PSD permitting work and has a low computational cost; it may be most acceptable to the end user. This approach also has advantages for analyzing the relative contributions of multiple sources.

Alternative 2: Lagrangain/Eulerian Combination

Most of the problems associated with an exclusively Lagrangian approach might be solved with a "hybrid" approach, using a Lagrangian model for the mesoscale area and an Eulerian model in the larger region. This approach is essentially the same as the first with the addition of having an Eulerian model calculate inputs for the Lagrangian model. The Eulerian model, with a complete chemical mechanism or a parameterized version, would be used to calculate boundary conditions for the mesoscale region and the background reactivity (i.e., concentrations of $O_3$, $H_2O_2$, and $OH$, important in sulfate and nitrate formation) of the smaller region. Since the Eulerian approach would properly account for the nonlinear chemistry of the emissions sources in the region, the uncertainties of the Lagrangian approach would be reduced. For example, if one were modeling only one source or group of sources in the smaller region, problems associated with plume overlap and long-distance dispersion would be less severe.

The regional (Eulerian) model would not necessarily have to be documented and delivered to the user; it could be applied every two or three years by a consultant who would supply the model output to the end user for input to the mesoscale Lagrangian model. Thus, costs for single-source evalulations would be kept relatively low while solving the problems associated with the fully Lagrangian approach. However, two models (Lagrangian and Eulerian) rather than one would need to be developed. Model evaluation of the Lagrangian component would be difficult. The regional Eulerian model could be evaluated by comparison with field measurements, then calculations of the mesoscale version of the Eulerian model could be compared with those of the Lagrangian mesoscale model. However, due to the lack of source-receptor data, no direct comparison of Lagrangian mesoscale model calculations with measurements could be made.

TABLE 4. Comparison of the attributes of the three alternatives for the Rocky Mountain Acid Deposition Model.

| Attribute | Alternative 1: Fully Lagrangian | Alternative 2: Lagrangian/Eulerian | Alternative 3: Nested Eulerian |
|---|---|---|---|
| TECHNICAL COMPLEXITY | Difficult or impossible to model nonlinear chemistry and dispersion at long distances accurately. | Nonlinear chemistry of regional sources can be modeled, but plume overlap in mesoscale region is still a problem. | Nonlinear chemistry and regional plume dispersion can be treated accurately. |
| NEAR-SOURCE RESOLUTION (PSD) | Accurate, depending on plume segement resolution. | Accurate, depending on plume segement resolution. | Limited to size of grid cell. |
| COMPUTATION COST | | | |
| Single Source | Approx. $100 per source-year | Approx. $100 per source-year plus approx. $5,000 for regional background | Approx. $5,000 per source-year plus approx. $5,000 for regional background |
| Multiple Sources (20 in mesoscale, 80 in large region) | Approx. $10,000 | Approx. $2,000 plus approx. $5,000 for regional background | Approx. $5,000 plus approx. $5,000 for regional background |
| Soure Attribution (evaluating relative source contributions) | Small cost | Larger cost | Probably economically infeasible |
| SIMILARITY TO OTHER MODELS | | | |
| UNAMAP | Most similar | Most similar | Least similar |
| RADM | Least similar | Least similar | Most similar |

Alternative 3: Nested Eulerian Approach

The two major technical problems associated with the first two alternatives – dealing with non-linear chemistry and large plume segments – would be eliminated with the third alternative. This approach uses the same grid model for both scales. The regional scale would be modeled with large grid squares, perhaps 100 km across, while the mesoscale region would be modeled with small grid squares, perhaps 2-5 km across, to provide higher resolution.

However, the technical advantages would cost considerably more. For an analysis of a single source, which is typical of PSD analyses, the nested model approach might cost $5,000 in computer resources, whereas a Lagrangian model could be exercised for $100. If the user could afford costs of approximately $5,000 per source-year (perhaps by passing on the costs to the applicant), this approach may be attractive for technical reasons. For large modeling analyses, involving perhaps 100 sources in a region, the Eulerian approach may be no more expensive than the Lagrangian approach. However, for source attribution studies (i.e., identifying the relative contributions of different sources in different states to deposition in a given sensitive area), the Eulerian approach is likely to be prohibitively expensive.

Although the model would most likely be acceptable to the scientific community, the model formulation would be quite different from other models with which the user is most familiar. However, the Eulerian model, like the Lagrangian model, could be applied as a "black box," without the need for detailed understanding of the inner workings of the "black box." The Eulerian approach would be most similar to NCAR's RADM and the engineering version of RADM.

## CONCLUSIONS

An acid deposition model for the Rocky Mountain region is to be designed for use by regulatory agencies in the western states. After reviewing and selecting mesoscale meteorological and acid deposition models appropriate to application in the Rocky Mountain region, three alternative modeling approaches were identified. The modeling approach taken will depend upon the recommendations of the regulatory agencies. The resulting modeling system should be operational by the end of summer 1987.

## REFERENCES

Morris, R.E., C-H. Yu, G.E. Moore, and D.A. Latimer, 1986a. Review and Selection of Appropriate Mesoscale Meteorological Models for Incorporation into a Rocky Mountain Acid Deposition Model. Systems Applications, Inc., San Rafael, California (SYSAPP–86/082).

Morris, R.E., C. Daly, D.A. Latimer, and M.K Liu, 1986b. Review and Selection of an Appropriate Acid Deposition Model for the Rocky Mountain Region. Systems Applications, Inc., San Rafael, California (SYSAPP–86/085).

Morris, R.E., 1986c. Selection of the First Application Scenarios for the Rocky Mountain Acid Deposition Model. Systems Applications, Inc., San Rafael, California (SYSAPP–86/107).

Morris, R.E., and R.C. Kessler, 1987. A Review of Existing Mesoscale Models for Use in Complex Terrain. Systems Applications, Inc., San Rafael, California (SYSAPP–87/044).

Roth, P., C. Blanchard, J. Harte, H. Michaels, and M. El-Ashry, 1985. The American West's Acid Rain Test. Energy and Resources Group, University of California at Berkeley.

Turk, J.T., and D.B. Adams, 1982. Sensitivity of Acidification of Lakes in the Flat Tops Wilderness Area, Colorado. Prepared for submission to Water Resources Research, U.S. Geological Survey, Lakewood, Colorado.

# Organic Acids and Other Organic Species in Colorado Atmospheric Aerosols

R.E. Sievers, P.R. Veltkamp, S.A. Beaton,
R.C. Greaves*, R.S. Hutte†, and R.M. Barkley
C.I.R.E.S. and
Dept. of Chemistry and Biochemistry
University of Colorado
Campus Box 215
Boulder, Colorado 80309

August 14, 1986

In an effort to gain a better understanding of acid deposition, much work has been carried out to determine the nature of the pollutant species and the extent of their involvement in pollution episodes. It is becoming increasingly recognized that ecosystem damage arises from the complex interplay of many atmospheric pollutants, not just from inorganic acids. Oxidants and organic compounds, both in the gas phase and in aerosol particles, are important determinants and indicators of atmospheric quality. The numerous organic compounds absorbed on the particles provide valuable information about the sources, transport, and chemical transformations of pollutants.

Two of the major processes for removal of organic compounds from the atmosphere are dry and wet deposition. Another important mechanism is chemical reaction, i.e., with OH radicals or ozone. These reactions are important in that the resulting products may be more water-soluble or less volatile, leading to aerosol formation, which may lead to subsequent removal by wet or dry deposition. Another removal mechanism of atmospheric organic species is absorption at the earth's surface by such materials as vegetation, soil and surface water.

Regardless of the removal mechanism, the net result is a cleansing of the atmosphere, but it is at the expense of deposition of pollutants on vegetation and in watersheds that feed surface and underground water resources. Because of this close interplay between the atmosphere and the earth's surface, it is important to conduct studies which attempt to identify the chemical species involved and trace them through the various pathways from sources to sinks. This is one objective of recent research in our laboratory which especially focused on organic species.

One of the studies undertaken has been to identify organic species present in atmospheric aerosols and precipitation from both rural (wilderness) and urban areas (1). The study consisted of measuring the concentrations of organic compounds in airborne particulate matter and in the vapor phase before, during, and after precipitation events and analysis of the organic compounds in these precipitation samples. The rain/snow samples were filtered to remove scavenged particulate matter, and

*Present Address: Environmental Science and Engineering, 7332 S. Alton Way, Suite H, Englwood, CO 80112.
†Present Address: Sievers Research, Inc., 2905 Center Green Ct., Boulder, CO 80301.

both the resulting filtrate and filtered material were extracted and analyzed for organic compounds by high resolution capillary chromatography coupled with mass spectrometric and other detectors.

Organic compounds representing many different classes of compounds have been found in aerosols and precipitation samples. These include aliphatic and aromatic hydrocarbons, acids, ketones, aldehydes, alcohols, ethers, and esters, as well as nitrogen and oxygen heterocycles. Table 1 lists representative compounds from various classes, as well as the ranges of their concentrations found in precipitation and aerosol particulate matter samples collected in Boulder, Colorado. Inspection of the data shows that the concentrations of carboxylic acids in the aerosol samples are roughly the same as those of the n-alkanes. It is important to keep in mind that, while most publicity has been devoted to "acid deposition", there are many non-acidic species which play important roles in atmospheric quality degradation and biosphere damage. Furthermore, various organic compounds can be oxidized by OH, NO, $HO_2$, and $O_2$ in a series of steps to form organic acids.

Total concentrations of various organic species were generally three to four times lower in concentration in precipitation samples collected at a rural location (Indian Peaks Wilderness Area) than in the urban samples. For example, the total concentrations of n-alkanes and fatty acids in 25 urban snow and rain samples collected over 10 precipitation events were 2–100 $\mu$g/L and 3–140 $\mu$g/L, respectively, while total concentrations in rural precipitation samples were 20–25 $\mu$g/L n-alkanes and 18–50 $\mu$g/L fatty acids.

Rain or melted snow samples from this study showed that most of the organic compounds were associated with the particulate matter. However, those with appreciable water solubilities, such as acids, aldehydes, and alcohols, were found in both the particulate and aqueous phases.

Carbon preference indices can be used as a measure of the general source of organic species in an aerosol or precipitation sample. These indices are a ratio of the total concentrations of odd-carbon-number hydrocarbons to even-carbon-number hydrocarbons and the ratio of even to odd for carboxylic acids. Biogenic sources produce hydrocarbons which are predominantly odd in carbon number, and acids which are predominantly even. Thus, aerosols arising from natural sources, such as trees and plants, have carbon preference indices (denoted $CPI_H$ or $CPI_A$) which are greater than 1.0. On the other hand, aerosols from most anthropogenic sources, such as fossil fuels, do not show a preference of one over the other, resulting in a CPI of 1.0.

The ranges, averages, and standard deviations for the $CPI_H$ and $CPI_A$ for urban and rural samples in this study are in Table 2, along with values for other samples from previous reports. The $CPI_H$ value for urban precipitation is the result from 20 samples, the same value for urban aerosol particulate matter was the mean observed in 10 precipitation events, and the rural precipitation $CPI_H$ value is for 3 precipitation events, all of which were under upslope meteorological conditions. Under these conditions, pollution from the Denver/Boulder metropolitan area is transported to this remote sampling site.

The $CPI_A$ for the rural precipitation is larger than $CPI_A$ values for either urban precipitation or urban airborne matter indicating primarily natural sources for these compounds. This is to be expected, since vegetation produces greater concentrations of the even-carbon-numbered acids, such as n-tetradecaonic, n-hexadecanoic and n-octadecanoic, rather than the odd-carbon-numbered acids.

However, the average $CPI_H$ for the rural precipitation is somewhat lower than for urban precipitation. This is probably due in part to the small number of samples represented, as well as the winds transporting pollutants upslope from the Denver metropolitan area, which has more nearly equal concentrations of the odd- and even-carbon-numbered hydrocarbons.

Two other measures of anthropogenic vs. natural sources appear in the table. The first is the ratio of unresolved hydrocarbons in the "hydrocarbon hump" to the n-alkanes. An example of a

**Table 1. Concentration of Organic Compounds in Boulder Precipitation and Airborne Matter**

| | Urban Precipitation ($\mu$g/L) of water | Airborne Particulate Matter (ng/m$^3$) of air |
|---|---|---|
| **Hydrocarbons** | | |
| n-Hexadecane | 0.03-3.1 | 0.09-1.4 |
| n-Heptadecane | 0.04-2.5 | 0.28-1.8 |
| n-Octadecane | 0.08-1.4 | 0.48-2.2 |
| n-Nonadecane | 0.20-3.9 | 1.1-4.6 |
| n-Eicosane | 0.05-0.72 | 1.8-7.5 |
| n-Pentacosane | 0.20-3.1 | 0.53-16.4 |
| n-Hexacosane | 0.11-1.7 | 0.66-13.2 |
| n-Heptacosane | 0.6-14.2 | 0.9-14.3 |
| n-Octacosane | 0.25-8.0 | 0.8-17.1 |
| n-Nonacosane | 1.2-23.9 | 2.6-30.9 |
| **Alcohols** | | |
| 1-Decanol | < 0.03-0.1 | < 0.006-0.6 |
| 1-Tetradecanol | 0.1-2.3 | 9.5-13.1 |
| 1-Pentadecanol | < 0.03-0.7 | 2.9-3.8 |
| 1-Hexadecanol | 0.04-12.6 | 4.2-4.7 |
| Benzyl alcohol | 0.1-3.6 | 8.0-50.0 |
| **Polycyclic Aromatic Hydrocarbons** | | |
| Naphthalene | < 0.01-0.3 | < 0.008 |
| Fluorene | < 0.01-0.1 | < 0.001-0.3 |
| Pyrene | 0.002-0.07 | 2.2-4.4 |
| Benzo[a]pyrene | < 0.05 | 0.4-0.6 |
| Benzo[g,h,i]perylene | < 0.07 | < 0.01-0.04 |
| **Aldehydes and Ketones** | | |
| Benzaldehyde | 0.05-8.9 | 1.0-19.4 |
| Benzophenone | NQ | NQ |
| **Aromatic Acids** | | |
| Benzoic acid | 0.08-11.9 | 1.0-19.4 |
| Phenol | < 0.05-0.5 | < 0.05-1.8 |
| **Carboxylic Acids** | | |
| n-Tetradecanoic acid | 0.7-10.1 | 1.2-8.4 |
| n-Pentadecanoic acid | 0.2-3.4 | 0.6-8.0 |
| n-Hexadecanoic acid | 0.3-21.9 | 0.5-23.4 |
| n-Heptadecanoic acid | < 0.04-6.7 | < 0.04-5.7 |
| n-Octadecanoic acid | 0.3-17.6 | 2.1-24.4 |
| cis-9-Hexadecenoic acid | 0.07-6.2 | 0.5-23.3 |
| cis-9-Octadecenoic acid | 0.2-17.6 | 0.7-22.0 |

NQ-not quantified, identified on basis of mass spectrum.

**Table 2**

**Comparison of Urban and Rural Precipitation and Possible Sources**

| | $CPI_H$ | UR | $CPI_A$ | RUS | Reference |
|---|---|---|---|---|---|
| Urban Precip. | 1.2-6.6<br>3.0± 1.7 | < 1-8<br>4± 3 | 2.4-14.2<br>9.4± 3.5 | 0.13-0.66<br>0.36± 0.21 | (1) |
| Airborne Part. Matter | 1.1-1.5<br>1.2± 0.1 | 5-9<br>6± 1 | 3.9-16.3<br>8.8± 3.5 | 0.14-0.67<br>0.32± 0.22 | (1) |
| Rural Precip. | 1.6-3.3<br>2.5± 0.8 | < 1 | 11.6-14.8<br>12.9± 1.7 | 0.33-0.62<br>0.47± 0.15 | (1) |
| Soil | 3.4 | 10 | 8.2 | 1.1 | (3) |
| Crude Oil | 0.85-1.15 | | | | (4) |
| Calif. Aerosols | 1.2-3.1 | 1.2-3.4 | | | (5) |
| Higher Plants | | | 5.0-40.8 | 1.24-14.94 | (6) |

$CPI_H$ -Carbon Preference Index of n-alkanes ($C_{15}$-$C_{34}$)

UR -Unresolved hydrocarbon mixture, n-alkane

$CPI_A$ -Carbon Preference Index of fatty acids ($C_{13}$-$C_{19}$)

RUS -Ratio of unsaturated to saturated n-$C_{16}$ + n-$C_{18}$ acids

"hydrocarbon hump" is shown in Figure 1, a chromatogram of the hydrocarbon fraction of an urban precipitation sample. This unresolved group of peaks is indicative of anthropogenic sources which contain many branched and cyclic hydrocarbons in addition to n-alkanes. In contrast, Figure 2 shows a chromatogram from a rural precipitation sample in which the hydrocarbon hump is not present. The ratio described above is always less than one for natural sources, while for anthropogenic sources it can be much larger than one.

Another measure of the relative contributions of natural and anthropogenic sources is the ratio of the concentrations of unsaturated to saturated $C_{16}$ and $C_{18}$ carboxylic acids. A large value for this ratio indicates these acids are of recent biogenic origin (3,6).

A second study has focused on the sources and fates of organic compounds in the atmosphere and resulted in the development of a rapid and simple method for the collection and analysis of aerosol organic compounds associated with particulate matter (2). This technique allows observation of hourly changes in the composition of atmospheric aerosols. A small sampling tube containing a quartz fiber filter is used to collect the particulate matter in approximately 300 L of air, with short sampling times of one hour. The samples are then analyzed by thermally desorbing the volatile absorbed organic compounds into a gas chromatograph for either flame ionization or mass spectrometric detection.

Most of the same organic compounds were found in the aerosol samples as in the earlier study which employed a lengthy hi-volume sampler technique coupled with solvent extraction, but the simplification of the collection and analysis methodology permits a larger number of samples to be collected and rapidly analyzed.

During this study, 138 aerosol particulate samples were collected at a site in Boulder between April 18, 1985 and June 20, 1985. The samples were collected hourly, with sampling sessions lasting from 3 to 24 hours. Of the many peaks present in the chromatogram, 44 were chosen for identification and quantification in the samples. These data, as well as meteorological data and ozone and carbon monoxide concentrations corresponding to each sample, were then subjected to statistical analysis.

One of these statistical techniques, factor analysis, was particularly useful in discerning possible sources and the effects of atmospheric processes. In factor analysis, the relative contribution of the variables (factors) to the variance of a data set is determined. These factors can then be interpreted by the chemical and meteorological elements they contain. The interpretation of the factors extracted by factor analysis was effective in discerning sources and atmospheric processes. In this case, the data base consisted of concentrations of 44 organic compounds, wind speed, wind direction, cloud cover, temperature, time, CO concentration, $O_3$ concentration, hydrocarbon preference index, and the total concentration of the 44 compounds, for all 138 samples (i.e., 7590 numbers).

Factor analysis showed that 75.1% of the total variance in the data set could be accounted for by 9 factors. 53.1% of the variance can be accounted for by the three most significant factors. The factors were then interpreted by the chemical and meteorological elements they contained. Table 3 gives a listing of the nine factors, along with the factor loadings of the components in those factors.

Factor 1 accounts for 31.3% of the variance in the data set and has been interpreted as a photochemical factor. As seen in Table 3, this factor is made up of particulate phase concentrations of oxygenated species, such as ketones, aldehydes, acids, and furans, as well as gas phase concentrations of ozone. The compounds in this factor may be primary or secondary in nature. Certain compounds, such as ozone, acetic acid, heptanoic acid and phthalide, are known to be products of photochemical activity.

Further evidence that this factor is photochemical in nature is shown in Figure 3. In this figure, Factor 1 scores are plotted against the time of day. It can be seen that low Factor 1 scores occurred

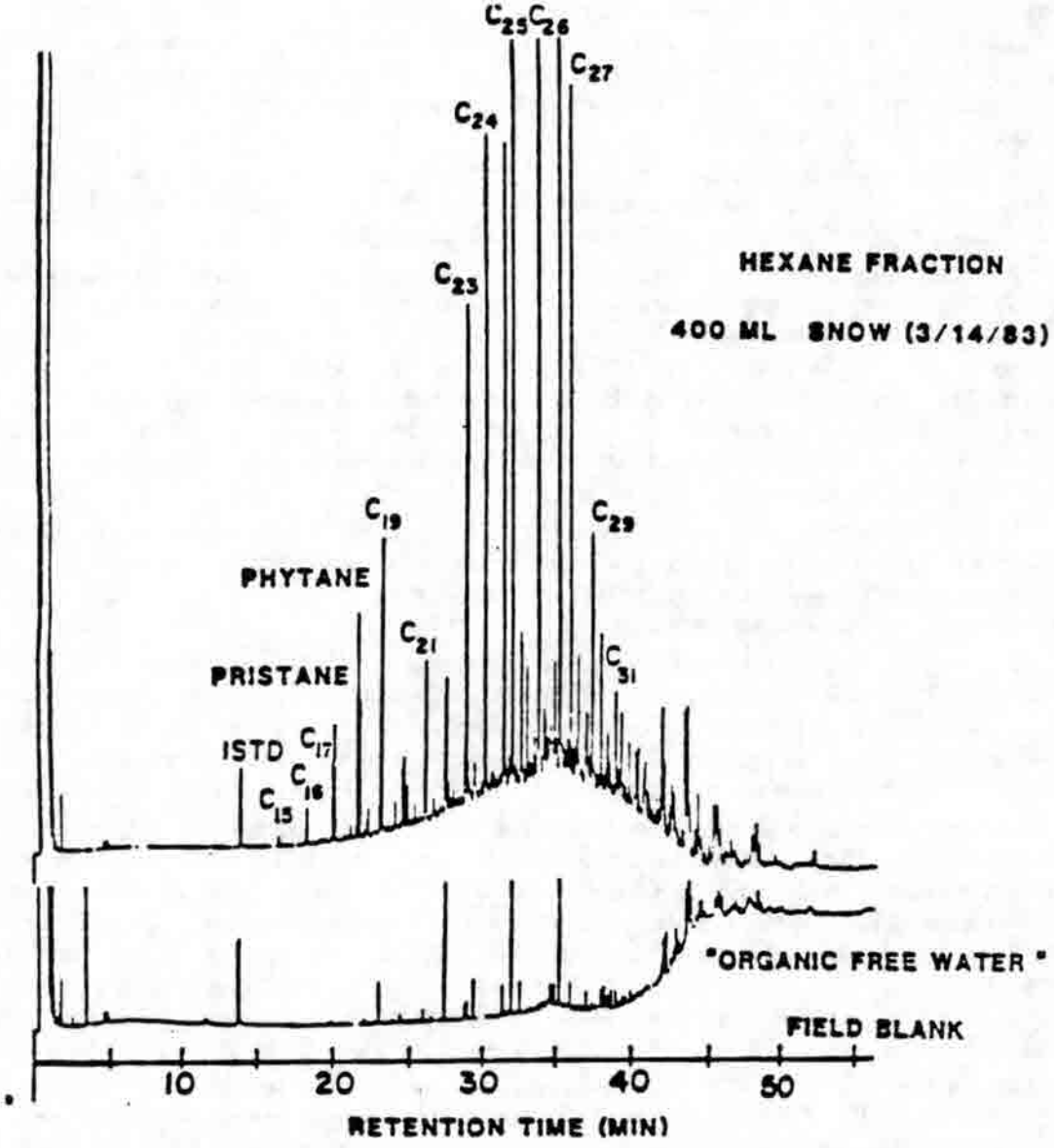


Figure 1. Hydrocarbon Fraction of Urban Precipitation.
GC conditions: 1$\mu$L on-column injection, 40°-325°C at 6°C/min
25 m x 0.31 mm ID ULTRA # 2, flame ionization detector (attenuation x4)

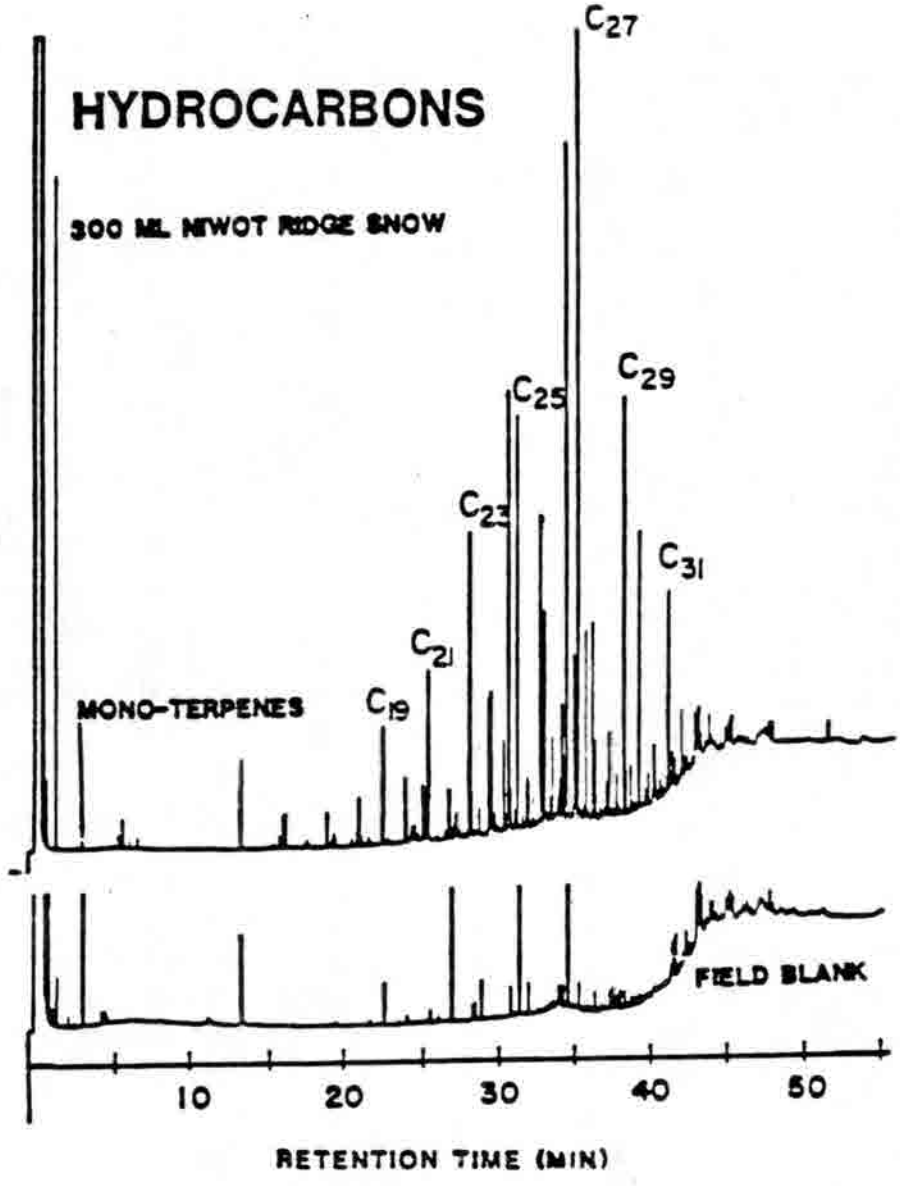


Figure 2. Hydrocarbon Fraction of Rural Precipitation.
GC conditions: 1$\mu$L on-column injection, 40°-325°C at 6°C/min
25 m x 0.31 mm ID ULTRA # 2, flame ionization detector (attenuation x4)

**Table 3. Concentrations of Volatile Compounds from the Thermal Desorption of Urban Airborne Particles**

| compound | min. conc.[h] ng/m$^3$ | max. conc. ng/m$^3$ | mean conc. ng/m$^3$ | standard dev.[i] | chrom. retention index[j] |
|---|---|---|---|---|---|
| **Factor 1** | | | | | |
| (1) 2,3,-dihydro-5/ -methyl furan[b] | < 15 | 160 | 43 | 29 | 709 |
| (2) acetic acid[b] | < 210 | 1200 | 420 | 220 | 723 |
| (3) 2,5-dimethyl furan[b] | < 6.4 | 17 | 8.7 | 2.1 | 768 |
| (4) 4-methyl-3/ -pentene-2-one[b] | < 18 | 48 | 24 | 5.5 | 805 |
| (5) $\alpha$-angelicalactone[b] | < 32 | 84 | 46 | 12 | 870 |
| (6) dihydro-4,4-dimethyl/ -2(3H)-furanone[b] | < 19 | 58 | 27 | 7.9 | 988 |
| (7) heptanoic acid[b] | < 30 | 170 | 59 | 32 | 1109 |
| (8) 1,3-indandione[b] | < 26 | 99 | 40 | 11 | 1342 |
| (9) 5,6,7,7a-tetrahydro-/ 4,4,7a-trimethyl-(S)/ -2(4H)-benzofuranone[c] | < 0.7 | 14 | 2.7 | 2.7 | 1541 |
| (10) ethenyl benzaldehyde[c] | < 19 | 50 | 26 | 7.1 | 1576 |
| (11) 1-phenyl- 1-penten-3-one[c] | < 19 | 64 | 26 | 10 | 1583 |
| **Factor 2** | | | | | |
| (12) terpenoid[d,f] | < 5.7 | 130 | 18 | 21 | 1123 |
| (13) camphor[b] | < 5.7 | 25 | 8.9 | 4.5 | 1165 |
| (14) terpenoid[d,e] | < 5.7 | 33 | 9.7 | 5.0 | 1182 |
| (15) 1-(1,4-dimethyl-3-cyclo/ hexen-1-yl)-ethanone[c] | < 5.7 | 110 | 16 | 17 | 1189 |
| (17) terpenoid[d,f] | < 5.7 | 150 | 29 | 28 | 1226 |
| (18) piperitone[b] | < 5.7 | 28 | 9.1 | 4.0 | 1253 |
| (19) n-nonanoic acid[b] | < 26 | 56 | 34 | 7.1 | 1287 |
| (20) branched acid[d] | < 0.3 | 26 | 3.9 | 4.2 | 1826 |
| **Factor 3** | | | | | |
| (21) n-octadecane[b] | < 0.3 | 19 | 2.0 | 1.8 | 1800 |
| (22) n-nonacosane[b] | < 0.3 | 75 | 5.0 | 8.1 | 1900 |
| (23) n-eicosane[b] | < 0.3 | 11 | 2.9 | 2.1 | 2000 |
| (24) n-heneicosane[b] | < 0.3 | 32 | 5.2 | 4.1 | 2100 |
| (25) n-docosane[b] | < 0.3 | 14 | 4.3 | 2.7 | 2200 |
| (26) n-tricosane[b] | < 0.3 | 20 | 5.5 | 4.2 | 2300 |
| (27) n-tetracosane[b] | < 0.3 | 6.3 | 2.1 | 1.1 | 2400 |
| (28) n-pentacosane[b] | < 0.3 | 16 | 5.0 | 3.1 | 2500 |

(see legend on following page)

[a]Numbers in parentheses refer to chromatographic peaks in Figure 4. GC/FID was used for compound quantitations using calibration curves derived by measuring responses from authentic standards. For compounds for which authentic standards were unavailable, quantitation was performed using calibration plots from analogous compounds, assuming a similar flame ionization response factor. Unknown terpenoids were estimated using the camphor calibration plot. [b]Compounds were identified by comparison of their mass spectra to literature mass spectra and by comparison of their mass spectra and retention times to those of authentic standards measured in our laboratory. [c]Compounds were tentatively identified by comparison of their mass spectra to literature mass spectra. [d]Compound type was identified by mass spectral interpretation and comparing the mass spectrum to the mass spectra of analogous compounds. [e]138 m/z was the highest mass in this mass spectra. [f]150 m/z was the highest mass in this mass spectra. [g]Values listed are the detection limits. [h]Values represent the standard deviation of the ambient compound concentrations in aerosols over time. Analytical precision of repetitive quantitations, as measured by percent relative standard deviation, ranges between 15 and 30%. [i]The programmed temperature chromatographic retention index is relative to n-alkanes.

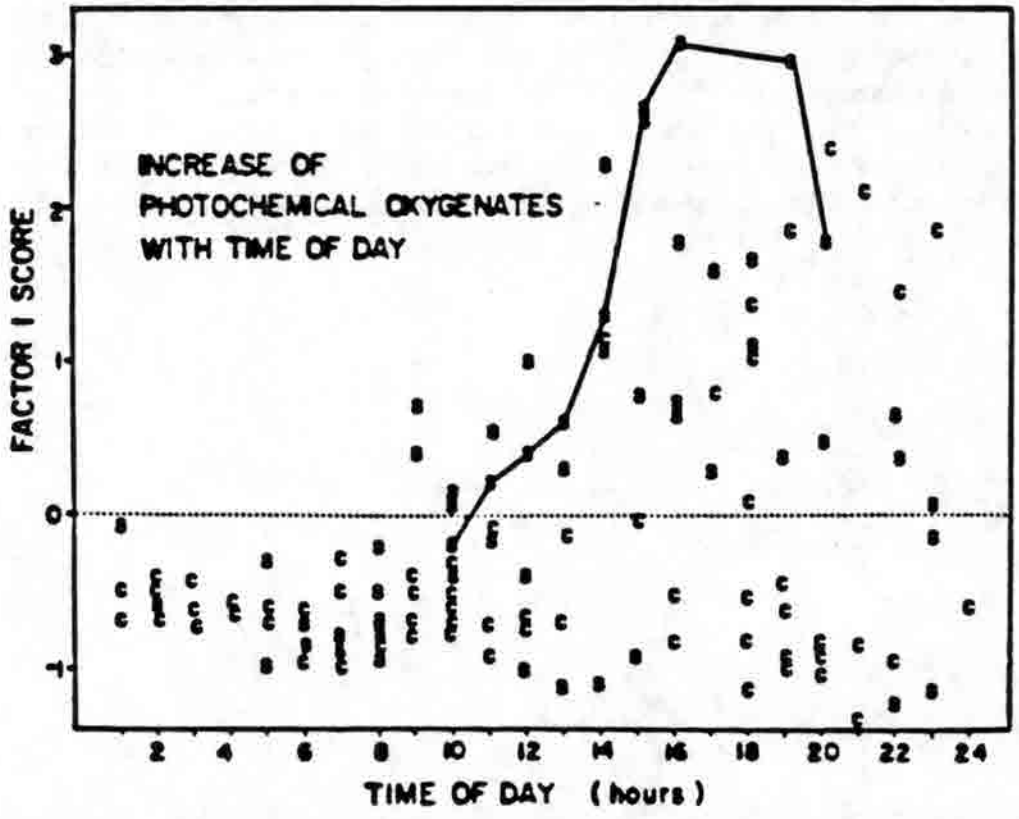


**Figure 8.** A large number of high Factor 1 scores during sunny days and low Factor 1 scores during the night and cloudy days (S=low cloud cover, C=high cloud cover). The line connects values during the course of one sunny day.

at night, while those with high scores occurred during the day. It is also seen that most of the high daytime Factor 1 scores occurred on sunny days, while low daytime scores are found on cloudy days. For those few samples that exhibit high scores on cloudy days, it was observed that often there had been extensive sunshine earlier that day.

In reviewing chromatograms obtained from the samples, one can find cases in which one factor has dominated, thereby forming a characteristic "signature". One such case is demonstrated in Figure 4a. This sample was taken on June 19, 1985 between 3:00 and 4:00 in the afternoon. The wind was southeast (i.e., from the Denver area) at 4 km/h. The temperature was 27°C with full sunlight. The ozone concentration was rather high at 90 ppb (it ranged from 2 ppb to 100 ppb with an average of 42 ppb during this study). The labeled peaks are compounds which make up Factor 1; these are mostly oxygenated organic compounds that are known or suspected to be products of photochemical oxidation. While these samples were taken in Boulder, meteorological conditions frequently transport these Front Range air masses to the Indian Peaks Wilderness Area, where many of these anthropogenic pollutants are often observed at significant levels.

Conversely, evidence of transport of terpenoid compounds in the aerosols from the conifer forests west of Boulder was observed when the wind was from the west. This is reflected in the components making up Factor 2. This factor contains the concentrations of bornyl acetate, piperitone and camphor, all of which have been identified in emissions from trees and plants common to this area. Most notably, this factor also contains the west to east wind direction. As an example, Figure 4b shows a chromatogram with a signature of Factor 2. The sample was taken May 22, 1985 between 4:00 and 5:00 a.m., when there was a westerly breeze of 2 km/h. As expected, the carbon monoxide and ozone concentrations were very low. The labeled peaks are terpenoids and other compounds found in trees and plants.

Factor 3 contains the concentrations of CO and 6 saturated hydrocarbons, from n-eicosane ($C_{20}H_{42}$) to n-pentacosane ($C_{25}H_{52}$). Since these are all well known constituents of automobile emissions, this factor has been interpreted as a vehicular factor. The chromatogram in Figure 4c shows the characteristic presence of n-alkanes. The elution period towards the end of the chromatogram, with its noticeable progression of n-alkanes, is similar to that in other chromatograms of samples taken in downtown Denver during rush hour traffic. The sample in Figure 4c was taken on June 19, 1985 between 7:00 and 8:00 a.m. The wind was southeast at 4 km/h, the CO concentration was 0.6 ppb (it ranged from 0.0 ppb to 3.4 ppb with an average of 0.8 ppb during the study), and the ozone concentration was 28 ppb.

This interpretation is further strengthened when one plots the Factor 3 scores against the time of day, as in Figure 5. Here it can be seen that the Factor 3 scores increase sharply with morning traffic between 6:00 and 9:00 a.m., especially if one follows the sequence of samples taken on one day, as shown by the solid line.

These studies have shown that the organic compounds associated with atmospheric particulate matter are found in precipitation samples, with the result that these aerosols contribute to acid deposition phenomena. The studies have also shown that the highly complex nature of the organic constituents of aerosols can be unraveled, providing a means for source apportionment, as well as for tracking air masses and observing changes in constitutents of the aerosol. Emissions of pollutants from urban areas along the Front Range of Colorado are being transported under upslope meteorological conditions to the wildnerness areas along the Continental Divide.

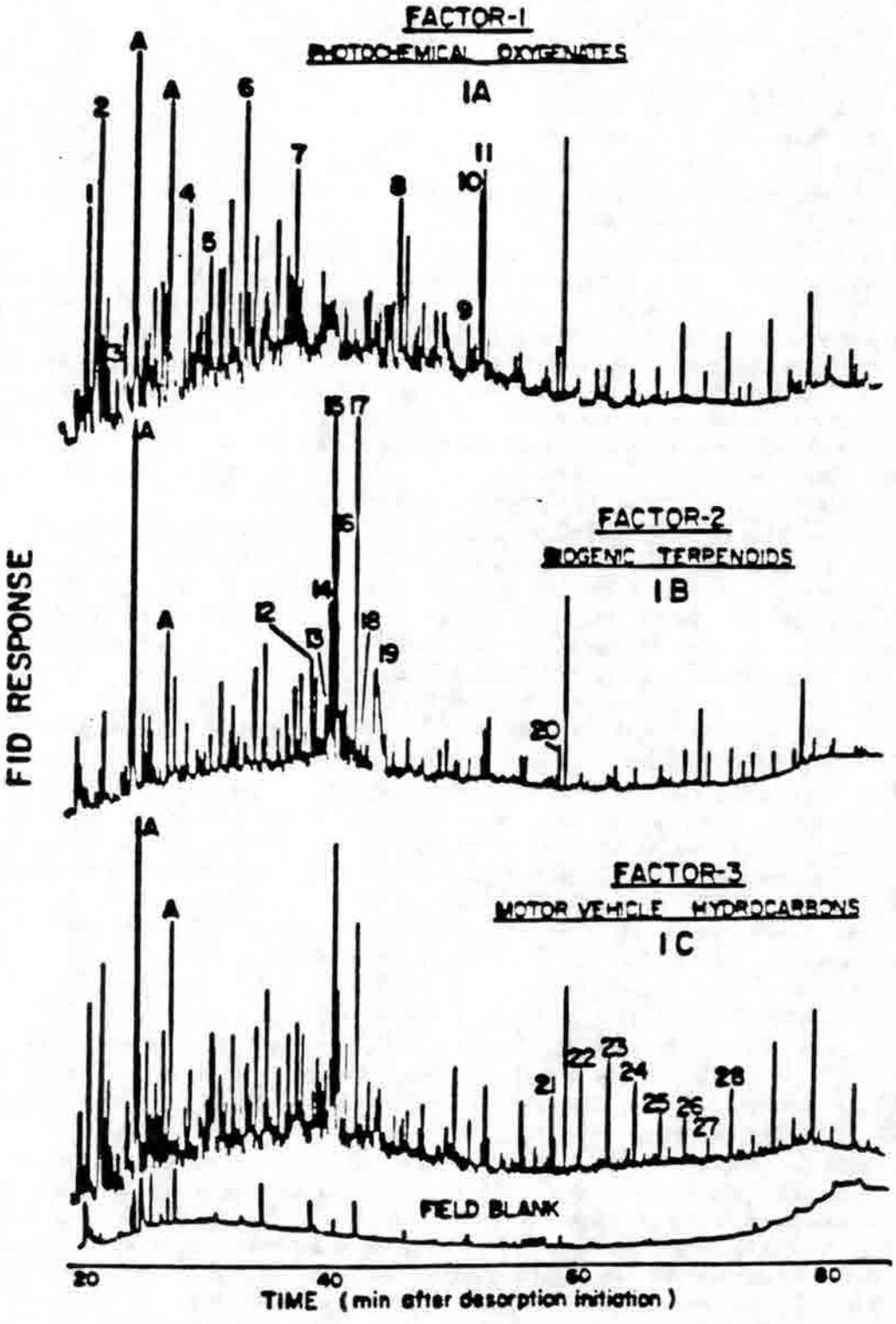


Figure 4. Chromatographic signatures of particles collected on different days dominated by organic compounds from aerosol sources dictated by: photochemistry (1A), wind direction (1B), and source strengths (1C). The numbers on this figure are identified in Table 3.

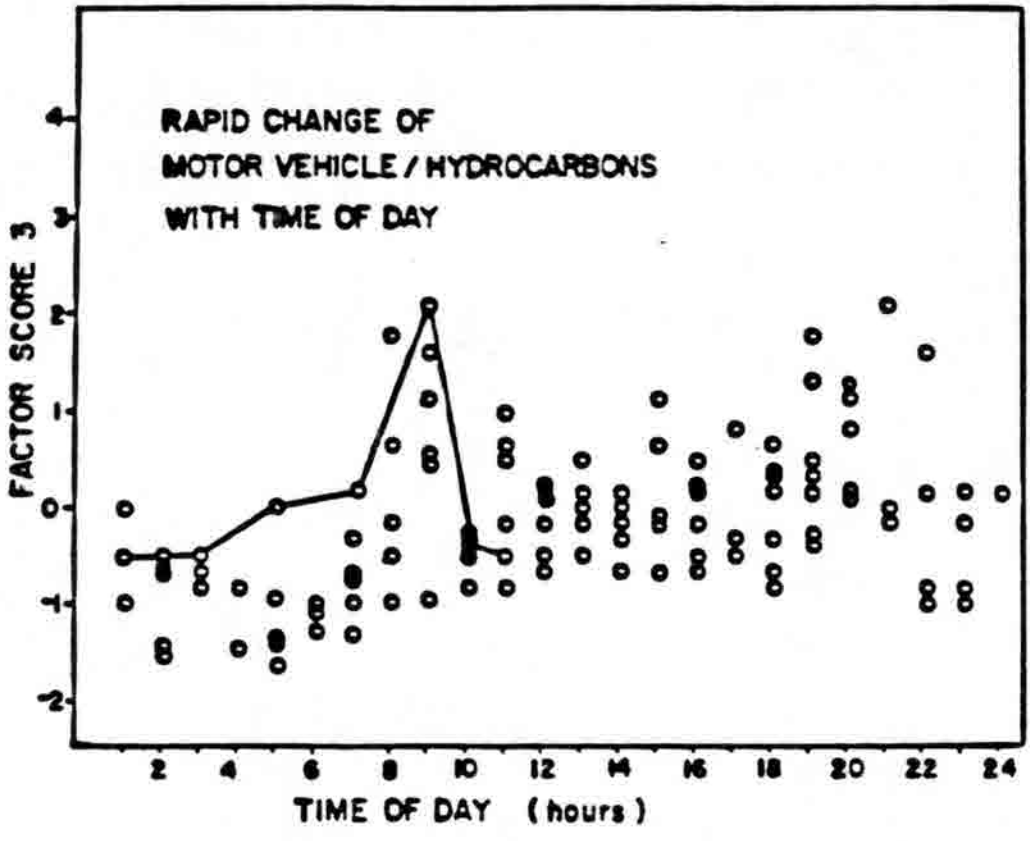


Figure 5. Rapid increase in Factor 3 scores during periods of heavy traffic volume (6:00 to 9:00 in the morning). The line connects values during the course of one day.

## REFERENCES

(1) Hutte, R.S., 1984. Ph.D. thesis, University of Colorado.

(2) Greaves, R.C., 1986. Ph.D. thesis, University of Colorado.

(3) Lodge, J.P., Jr., A.P. Waggoner, D.T. Klodt, and C.N. Crain, 1981. *Atmos. Environ.*, **15**, 431.

(4) Cooper, J.E., and E.E. Bray, 1963. *Geochim. Cosmochim. Acta*, **27**, 1113.

(5) Simoneit, B.R.T., M.A. Mazurek, and T.A. Cahill, 1980. *J. Air Poll. Control Assoc.*, **30**, 387.

(6) Eichmann, R., P. Neuling, G. Ketseridis, J. Hahn, R. Jaenick, and C. Junge, 1979. *Atmos. Environ.*, **13**, 587.

# Impurities on the Surface of Ice

Richard A. Sommerfeld
Rocky Mountain Forest and Range
Experiment Station
240 W. Prospect Street
Fort Collins, Colorado 80526

August 14, 1986

## INTRODUCTION

Interest in ice chemistry is currently being generated because of the lively interest in acid deposition. Snow represents a considerable fraction of precipitation volume and water storage in many climates. A mountain may hold more than $10^5$ cubic meters of snow throughout the winter. A feeling for the amount of water stored in snow can be gained by remembering that major dams can be forced to cause flooding simply becaue of the timing of the snow melt.

Snow is a network of water vapor saturated air and finely divided ice and the amount of ice surface can be very large. A cubic meter of snow may contain $10^4$ square meters of ice surface. Thus there are about $10^{10}$ square meters of ice surface in the snow on a moderate sized mountain. Pollutants associated with this surface could be present in fairly large quantities, especially considering the fact that a mountainside often feeds a few small lakes.

In most climates, the ice phase is involved in the formation of precipitation. It may fall as snow or hail, or melt to fall as rain. A moderate sized storm may contain $10^{10}$ square meters of ice surface. Thus the interaction of ice with airborne pollutants is important in all phases of precipitation borne pollution.

Research in acid deposition shares qualities with most types of geophysical research. The progress of relatively simple physical and chemic processes becomes extremely complicated as they interact under the physical conditions that force them in conflicting directions. In the snowpack, processes are generally driven by varying weather conditions. To ask and answer the appropriate questions, three different levels of research are necessary: the naturalist-observational level, the intermediate level, and the fundamental level. Most of the pollutant related work in snow has been at the naturalist or intermediate level. This work has raised some fundamental questions that must be answered before quantitative predictions are possible. In some cases answers are available from the literature. In most cases fundamental measurements are necessary to complete our knowledge.

An early assumption in assessing pollutant storage in snow appears to be that snow and any pollutants its contains are quiescent during the below freezing periods. A contributor to this assumption may be the fact that most snow hydrologists are quiescent during the below freezing period. The historical importance of runoff predicition in snow hydrology research tied much of the work to the start of the melt season.

The changes that occur in snowpacks during the cold season have been studied in detail, because of their importance in avalanche research (Seligman, 1936; Eugster, 1952; Sommerfeld and

LaChapelle, 1970; Akitaya, 1974; de Quervain, 1974). Those studies are a part of a body of literature that has shown that the snowpack is far from quiescent at below freezing temperatures but that the crystal forms constantly change. The results also indicate that pollutants can move in the snowpack under the influence of the same metamorphic processes because volatile substances must obey the same laws as water vapor. Although a qualitative understanding of these processes has been developed, a quantitative understanding has not been developed to the point that these movements can be predicted. It is not possible, with the present state of knowledge, to predict even the direction of movement of pollutant species in many cases. More quantitative data on the physical chemistry of ice phase systems are necessary to quantification of the storage and transport of pollutants in snow.

I would like to discuss briefly some of the field observations as they pertain to snow, to give an example of intermediate level processes and show how they raise some very fundamental questions about the physical chemistry of ice. I would also like to show that these questions are beginning to be answered.

## OBSERVATIONS

Because of a phenomenon called acid flush, the pollutants associated with the ice surfaces that constitute snow can be released in a fairly short time. That phenomenon can cause high pollutant concentrations for periods of time that are important to developing organisms in a mountain environment. There is evidence that the first 10% of the melt water from the beginning of the melt season may contain 50% of the pollutants contained in the snow. The circumstances favoring acid flush are not well known and it is not known whether it is common or rare. If it is common, it could have serious environmental effects (Johannessen and Henriksen, 1978). The physical fact behind "acid flush" is that most substances are insoluble in ice. Therefore any impurity in the snow is likely to be associated with some type of ice surface. Melting, of course, starts at the surfaces of the ice grains that make up snowpacks. Thus pollutants are immediately available to the first melt water and those that are water soluble will move with that water.

There is some evidence that rime particles contain a larger concentration of pollutants than other types of solid precipitation (Borys, et al., 1982). Rime particles are supercooled water droplets that freeze from the outside when they contact a freezing nucleus. While most pollutants are excluded from the ice, in rime they may be trapped as inclusions by the rapidly freezing ice matrix (Lamb and Blumenstien, 1986). Vapor grown snow crystals are much less likely to trap inclusions of impurities and any impurities apart from the freezing nucleus are probably associated with exterior surfaces. These observations hint that different types of snow crystals may acquire and transport pollutants in different ways and that the changes in crystal form that occur in the cold snowpack may rearrange the pollutants.

## SNOW METAMORPHISM

As an example of the intermediate type of research, I want to look at types of snow metamorphism that occur on the ground. Snow falls as complex shapes with very small radii of curvature and a very high specific surface area. The resultant surface free energy drives changes of shape to decrease the surface area. This process is termed equitemperature metamorphism because it is only important in the absence of temperature gradients larger than about 10°C $m^{-}1$ (Sommerfeld and LaChapelle, 1970). Once the radii of curvature of the ice particles are large than 100 $\mu$m, the process slows to insignificance (Perla, 1978) in the seasonal snowpack. The mean radius of curvature of 100 year old snow in Greenland is about 1 mm (reference from Sommerfeld and LaChapelle).

Because of heat stored in the ground, the bottoms of most snowpacks are at about the freezing point. During the winter the upper surface may be a much lower temperatures, resulting in a thermal

gradient across the snow layer. The thermal gradient forces a vapor pressure gradient and water vapor diffuses up through the snowpack. The water vapor is transferred from ice particle to ice particle. Each particle is simultaneously a source and a sink of water vapor in a transport process termed "hand to hand" by Yosida and colleagues (1955). Temperature gradient metamorphism (Sommerfeld and LaChapelle, 1970) can cause the complete recrystallization of the snow in a few days (Sommerfeld, 1983).

Qualitatively, temperature gradient metamorphism is well understood, but the process has proved difficult to quantify. The mass flux, $J$, through a snow layer is given by,

$$J = -D_{eff} dm/dz$$

$D_{eff}$ is the effective diffusion coefficient and $dm/dz$ is the mass concentration gradient. The value of $D_{eff}$ is currently the subject of controversy. Estimates range from a value slightly less than the diffusion coefficient of water vapor in air to more than three times that value, depending on the assumptions made (Giddings and LaChapelle, 1962; Sommerfeld, 1983; Colbeck, 1983; Gubler, 1985). Recently, a finite element analysis showed that it may range between 1.1 to 2.5 times that of water vapor, depending on the geometry (Christen, et al., in press). Preliminary measurements with stable isotope fractionation indicate a value of two times that of water vapor in air (Sommerfeld, et al., in preparation).

The final process in the life of a seasonal snowpack is melt metamorphism. Once this process starts, the snowpack is no longer dry. However, it is during this process that acid flush occurs. When the fundamental processes in melt metamorphism are identified, it is necessary to quantify them to explain and predict observational level phenomena.

## FUNDAMENTAL PROCESSES

In dry snow, two processes are fundamental to the storage and transport of pollutants. One, the solid solubility of substances in ice, is well enough understood at for the first stage of intermediate level quantification. With the other, ice surface chemistry, research has been spotty with contradictory results.

The solubility of substances in ice is, in general, very low. Most substances that are very soluble in water have very low solubilities in ice. The exceptions are compounds of $HF$ and some substances that are known to form solid clathrates. $CO_2$ is a probably example (Adamson, 1982). In general, however, the solid solubilities of pollutants in ice are either known or their determination is fairly straightforward using well known techniques. Further research concerning this process will probably occur at the intermediate level investigating such questions as: How are insoluble impurities segregated during the formation of different types of snow crystals (Lamb and Blumenstein, 1986)?

In the case of ice surface chemistry our understanding is not nearly so well developed. What is known is that a mobile layer with some liquid-like properties exists on the surface of ice and greatly complicates ice surface chemistry. Several observations show the existence of such a layer but disagree on such fundamental quantities as its thickness and the temperature range in which it exists. At normal earth surface temperatures ice is within 85% of its absolute melting point. Solids often exhibit special properties in this temperature range. Some, like ice, are suspected of having a mobile, disordered, liquid-like layer on their surfaces.

Theoretical calculations indicate that such a layer exists on the surface of ice and that its thickness is about 50 A (Fletcher, 1970). Some research has shown that at temperatures above -35°C, immediate adhesion occurs on ice to ice contact (Gubler, 1982). Calculations from these experiments indicate a surface layer thickness of about 1 $\mu$m. At about -20°C ice spheres adhere strongly to glass

after a few days (personal observation). The adhesion of two different solids generally indicates that the surface of one of the solids is mobile enough to conform in some way to the other surface.

Measurements of the temperatures of wires cutting through ice blocks indicate that some process in addition to pressure melting is important. The presence of a liquid-like surface is a qualitative explanation of the data (Telford and Turner, 1963).

The electrical conductivity of solid ice is very low, except under very special conditions. The surface conductivity of ice is higher in the temperature range we are considering. Measurements indicate a surface layer thickness of about 10 $\mu$m (Jaccard, 1967; Golecki and Jaccard, 1978). Although the assumptions in that work have recently been challenged, there is still clear evidence of a surface layer (Turner and Stoe, 1986).

Nuclear magnetic resonance measurements generally give broad band signals for solids and narrow spikes for liquids. As the temperature of ice increases past -10°C, the resonance spectrum changes from a broad band to a broad band plus a spike (Ushikova and Troshkina, 1975). Measurements indicate a layer thickness of 0 at -10° to about 60 A at 0°C.

A small amount of data exists on the surface absorption of a few substances on ice. These data indicate anomalous effects wherein the ice does not act as a passive absorbent, as is the case with most solids, but is greatly modified by the absorption. Two different effects are indicated by the limited data. At liquid nitrogen temperatures argon, nitrogen, hexane and propane appear to absorb physically in a straightforward way. Ethane and $CO_2$ exhibit very slow equilibration rates and very high absorption (Adamson, 1982). The explanation put forward is that these compounds form clathrates in the solid body of the ice. The rate data, however, are not consistent with a simple diffusion model. Also, the effect has not been investigated in the temperate range of interest in earth surface processes. $CO$, n-pentane, and n-hexane exhibit anomalous behavior at temperatures above -35°C (Adamson, 1982). The interpretation is that the absorbate interacts with the surface to form a "surface half clathrate". This interpretation is consistent with the data. However, no definitive experiments have been conducted to test the idea and measurements were not conducted above about -30°C. Recently Sommerfeld and Lamb (1986) showed that $SO_2$ absorbed on ice shows anomalous behavior in the temperature range -3° to -35°C. Unlike most substances, the amount absorbed on ice decreased with decreasing temperature (Figure 1). Although preliminary, these measurements also indicate an anomalous surface on ice down to -35°C.

## IMPLICATIONS

I would like to conclude by giving some of the implications that can be drawn from our limited understanding of intermediate and fundamental observations. This will help to highlight where future research is needed. Both equitemperature and temperature gradient metamorphism cause a decrease of surface area that would directly affect any material that was absorbed on the surface. Because the change in the amount of surface area is probably limited, it may only be important in the early changes of new snow.

More important is the fact that temperature gradient metamorphism forces all the water molecules through the vapor phase. Thus any pollutants associated with the ice can be remobilized. This is true of both gaseous and aerosol pollutants. Remobilization could mean a redistribution of the pollutants within the snowpack or their removal. Snow is mainly air and the surface layers are fairly permeable. The influx of clean air when pollutants are remobilized would mean that pollutants could be flushed out. Aerosols might be released into the interstitial air. On the other hand, they may stay attached to small ice particles that become detached from the ice matrix. In this way, aerosols may physically work their way lower in the snowpack. Gaseous absorbates would be remobilized into the air locally as their particular crystals lost surface area.

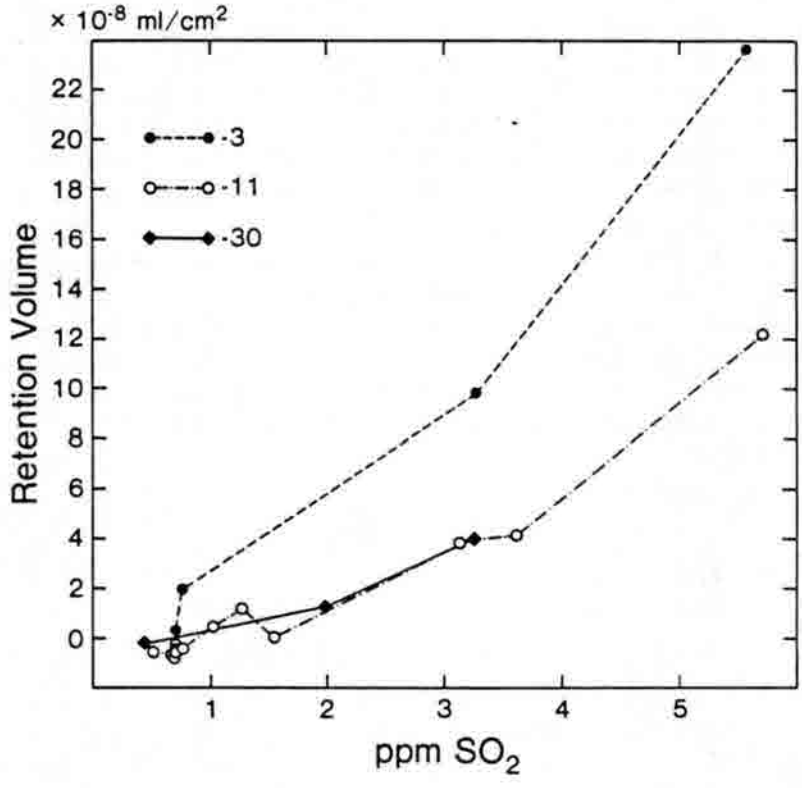


Figure 1. Retention Volume of $SO_2$ STP on ice -3°, -11°, and -30° C.

In the case of a layer of rimed snow, the original rime particles would sublimate away, freeing pollutant inclusions. The pollutants would then be free to interact with ice surfaces and with the interstitial air.

Besides being released by recrystallization, absorbed gases would diffuse under the thermal gradient. Depending on the physical chemistry of the absorption process the diffusion might occur in either direction. Taking $SO_2$ as an example (Figure 1), the vapor pressure of $SO_2$ at any given surface concentration is higher at -35° than at -3°C. A snow layer with an originally uniform concentration of $SO_2$ may have a thermal gradient imposed on it by weather conditions. In that case the equilibrium vapor pressure of $SO_2$ at the warmer (usually lower) boundary would be lower than at the colder boundary. $SO_2$ would diffuse and concentrate at the warmer boundary until the vapor pressure gradient became zero. Such a process could move pollutants toward the ground and enhance the acid flush at the beginning of the melt season. On the other hand, it could move pollutants out of the snowpack under conditions that cause a reversal of the usual thermal gradient. The rate of diffusion depends on the vapor pressure gradient and the diffusion coefficient of $SO_2$. Since the vapor pressure gradient depends on the temperature gradient, this process would also be subject to the geometrical enhancement of the diffusion coefficient discussed above for water vapor.

Melt-freeze metamorphism could act similarly to temperature gradient metamorphism in that it causes the recrystallization of the entire snowpack. If several episodes occur during the season, this process could suppress the acid flush by releasing the pollutants in smaller amounts and at different times. In a different climate, the onset of melting in a pack that was dry throughout the winter would give rise to an acid flush. The insolubility of substances in ice is the fundamental property that drives the phenomenon of acid flush. The complex surface of ice can cause complexities in the behavior of pollutant gases absorbed on the snow particles. This, in turn, could affect the timing and severity of the acid flush.

## REFERENCES


Akitaya, E., 1974. Studies on depth hoar. Contributions from the Institute of Low Temperature Science, Series A, no. 26, Hokkaido University, Sapporo, Japan, p. 1-67.

Adamson, A.W., 1982. Physical Chemistry of Surfaces. Interscience Publishers, Inc., New York, 629 pp.

Borys, R.D., P.J. DeMott, E.E. Hindman, and D. Feng, 1982. The significance of snow crystal and mountain-surface riming to the removal of atmospheric trace constituents from cold clouds. Presented at the 4th International Conference on Precipitation Scavenging, Dry Deposition and Resuspension.

Christen, M., P. Burns, and R.A. Sommerfeld, 1986. The modeling of temperature gradient metamorphism. In The Chemistry of Seasonal Snowpacks, Proceedings of the NATO-ASI, July 13-23, Les Arcs, France.

Colbeck, S.C., 1983. Theory of metamorphism of dry snow. *J. Geophys. Res.*, **88**, 5472-5482.

Eugster, H.P., 1952. Beitrag zu einer Gefugeanalysi des schnees. Beitrag zur Geologie der Schweiz-Geotechnische, Serie-Hydrologie 5. Leiferung, 64 p.

Fletcher, N.H., 1970. The Chemical Physics of Ice. Cambridge University Press, Cambridge, England.

Giddings, C.J., and E.R. LaChapelle, 1962. The formation rate of depth hoar. *J. Geophys. Res.*, **67**, 2377-2383.

Golecki, I., and C. Jaccard, 1978. Intrinsic surface disorder in ice near the melting point. *J. Physics and Solid State Physics*, **11**.

Gubler, H., 1985. Model for dry snow metamorphism by interparticle vapor flux. *J. Geophys. Res.*, **90**, 8081-8092.

Gubler, H., 1982. Strength of bonds between ice grains after short contact times. *J. Glaciology*, **28**, 82.

Jaccard, C., 1967. Electrical conductivity of the surface layer of ice. In Physics of Snow and Ice (H. Oura, ed.), Proceedings of the International Conference on Low Temperature Science, August 14-19, Sapporo, Japan. The Institute of Low Temperature Science, Hokkaido University.

Johannessen, M., and A. Henriksen, 1978. Chemistry of snow meltwater: Changes in concentration during melting. *Water Resources Research*, **14**, 615-619.

Perla, R.I, 1978. Temperature gradient and equi-temperature metamorphism of dry snow. In Comtes Rendus. Deuxieme recontre internationale sur la neige les avalanches, April 12-13, Grenoble, France, p. 43-48.

Quervain, M.R., de, 1973. Snow structure, heat and mass flux through snow. International Symposium on the Role of Snow and Ice in Hydrology, Symposium on Properties and Processes, 1972, Banff, Alberta, Canada.

Seligman, G., 1936. Snow structure and ski fields. McMillian & Co., London, England.

Sommerfeld, R.A., 1983. A branch grain theory of temperature gradient metamorphism in snow. *J. Geophys. Res.*, **88**, 1484-1494.

Sommerfeld, R.A., and E.R. LaChapelle, 1970. The classification of snow metamorphism. *J. Glaciology*, **9**, 3-17.

Sommerfeld, R.A., and D. Lamb, 1986. Preliminary measurements of $SO_2$ absorbed on ice. *Geophys. Res. Letters*, **13**, 349-351.

Sommerfeld, R.A., I. Friedman, and M. Nilles, 1986. The fractionation of stable isotopes in snow during temperature gradient metamorphism. In The Chemistry of Seasonal Snowpacks, Proceedings of the NATO-ASI, July 13-23, Les Arcs, France.

Telford, J.W., and J.S. Turner, 1963. The motion of a wire through ice. *Philosophical Magazine*, **8:87**, 527-531.

Turner, G.J., and C.D. Stoe, 1986. D. C. conductivity of the ice surface. *Solid State Communications*, **58**, 403-405.

Yosida, Z., and colleagues [sic], 1955. Physical studies on deposited snow. 1. Thermal properties. Contributions from the Institute of Low Temperature Science, Hokkaido University, Sapporo, 74 pp.

# Atmospheric Free Radicals and Dry Deposition in Bennett, Colorado

D. Stedman, X. Liu, B. Evilsizor,
D. Stocker, and J. Ray
Department of Chemistry
University of Denver
Denver, Colorado 80208

August 14, 1986

The hydroxyl and hydroperoxy radicals are of paramount importance in any discussion or investigation involving atmospheric chemistry. They are involved in virtually every reaction pertaining to the oxidation of reduced atmospheric species. Consequently a great deal of effort has been expended developing measurement techniques (Ortgies, et al., 1980; Davis, et al., 1981b; Wang, et al., 1981; Hard, et al., 1984; and Mihelcic, et al., 1982).

Our technique of measuring peroxy radicals by chemical amplification (Cantrell, et al., 1984), uses the oxidizing chain reaction in which $HO^{\cdot}$ and $HO_2\cdot$ participate directly. Some $RO_2\cdot$ become $HO_2\cdot$ after a few reaction steps. The yield of $NO$ oxidized to $NO_2$ by ambient radicals is measured, and an ambient total peroxy radical concentration (which in clean air is expected to be mostly $HO_2\cdot$) is inferred. Presented here are the results of laboratory calibrations of the detector and some ambient measurements.

A major sink for atmospheric pollutants is loss to the surface via dry deposition. Determination of dry deposition by means of eddy correlation has also been carried out at the Rybicka farm site near Bennett, Colorado, and the results are shown herein.

Apparatus. The chemical amplifier and eddy correlation equipment are subject to continuous updating, but are fundamentally similar to those described elsewhere (Cantrell, et al., 1984; Wendel, et al., 1983).

## RESULTS AND DISCUSSION

Calibration. To circumvent the problem of producing a known amount of radicals, the second order decay of a high steady state concentration (~ 150 pptv) of hydroperoxyl radicals in a 1000 L Teflon gas bag is measured. The radicals are produced by photolysis of air mixtures containing a few ppm of $Cl_2$ with 2% $H_2$ using near UV fluorescent lights.

The radicals decay in the dark at a known rate and the following relationship results

$$Chain\ length = 2k_{recombination}/slope$$

where $k_{recombination}$ is given as $2.6 * 10^{12} cm^{-3} s^{-1}$ and the slope is that measured after plotting the inverse $NO_2$ mixing ratio versus time. Figure 1 is the chart tracing of an achieved steady state

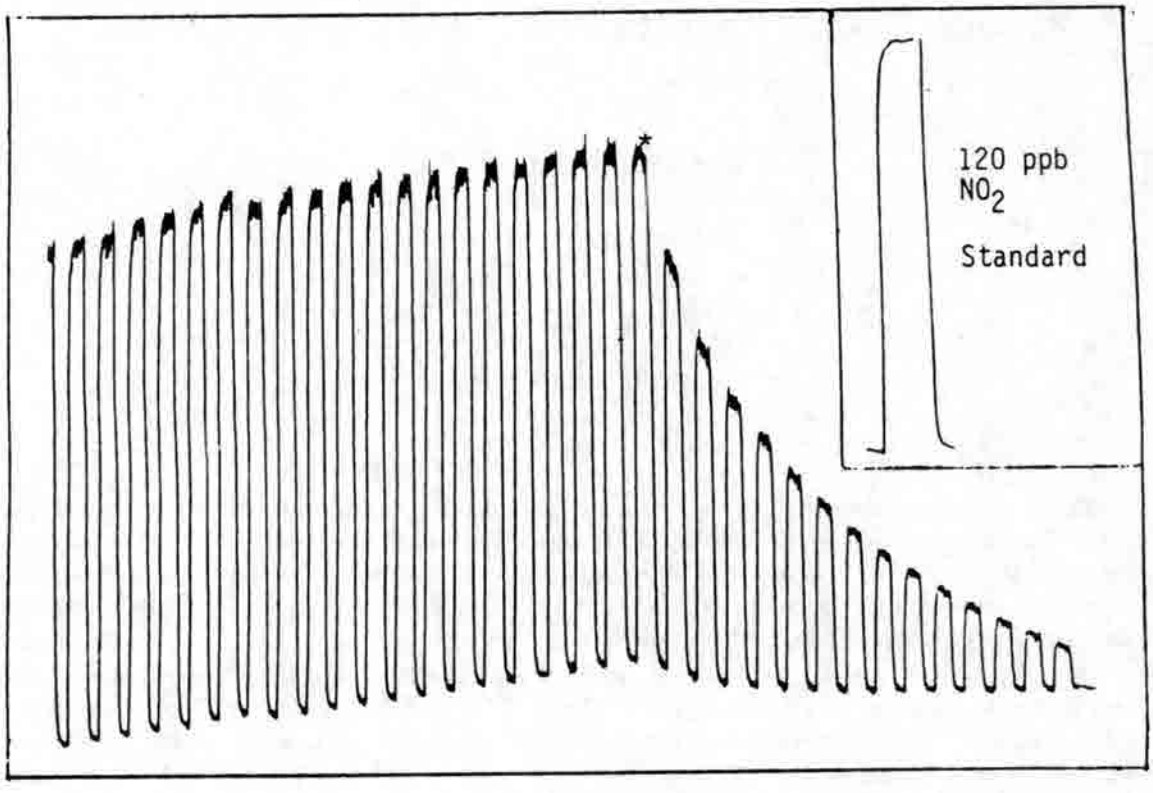


Figure 1. Actual chart tracing of a steady state radical signal and subsequent dark decay (*). Radicals were generated with a $Cl_2/H_2$/Air mixture in a Teflon gas bag.

followed by dark decay starting at the star. This method of calibration is reproducible, yielding chain lengths from 400 to 600. The lower than predicted chain lengths may be caused by unoptimized reagent gas flows or unaccounted for loss factors such as surface removal or radicals.

Field Measurements. Clean air ambient radical concentrations were measured in a collabrative effort with the National Center for Atmospheric Research at a field site 12 miles northeast of Bennett, Colorado. Data was acquired for selected days in the months of June and July. The radical reactor was positioned 2.5 meters off of the ground on the roof of a trailer parked in a wheat field. The eddy correlation detectors had their intakes at 6m above the ground on a tower upwind of the trailer.

Calculations of radical concentrations were made using a chain length of 350, resulting from calibrations made for the instrumental conditions maintained. Data obtained in the month of June are shown in Figure 2, along with corresponding $j(O_3)$ values and background measurements given as ppbv of $NO_2$. The background may be attributed mainly to ozone because of the consistently low (<10 ppbv) mixing ratios measured for $NO_2$. This assumption was carried through and the calculated values were used to check instrumental $NO_2$ response and subsequently in the radical signal quantitation.

Figure 3 shows typical data for the eddy correlation $NO_x$ flux showing diurnal variation with flux to the ground at night and flux up from the crop during the day, with a net flux close to zero for that site.

## CONCLUSIONS

Using our technique of chemical amplification for the measurement of atmospheric free radicals we have built a field instrument, calibrated it in the laboratory, and carried out field measurements. Values of $[HO_2.]$ in clean air reached consistent noon-peaking values of approximately 3-5 * $10^8$ molecules $cm^{-3}$. The $NO_x$ flux data are the first flux data from a site such as this, therefore comparison can only be made with other ecosystems.

## ACKNOWLEDGMENTS

We would like to thank Dr. A. C. Delany of NCAR for his help, facilities, and cooperation in our field efforts, and the National Science Foundation and Coordinating Research Council for their support of our research.

## REFERENCES

Cantrell, C.A., D.H. Stedman, and G.J. Wendel, 1984. *Anal. Chem.*, **54**, 1496-1502.

Davis, D.D., M.O. Rodgers, S.D. Fischer, and K. Asai, 1981. *Geophys. Res. Lett.*, **8**, 73-76.

Hard, T.M., R.J. O'Brien, and C.Y. Chan, 1984. *Environmental Sci. and Tech.*, **18**, 768-777.

Trainer, M., D. Kempa, and D.H. Ehhalt, 1982. 2nd AMS Symposium on the Composition of the Nonurban Troposphere, 327-329.

Ortgies, G., K.H. Gericke, and F.J. Comes, 1980. *Geosphys. Res. Lett.*, **7**, 905-908.

Perner, D., D.H. Ehhalt, H.W. Patz, U. Platt, E.P. Roth, and A. Volz, 1976. *Geophys. Res. Lett.*, **3**, 466-468.

Wang, C.C., L. Davis, P.M. Selzer, and R. Munoz, 1981. *J. Geophys. Res.*, **86**, 1181-1186.

Wendel, G.J., D.H. Stedman, C.A. Cantrell, and L.D. Damrauer, 1983. *Anal. Chem.*, **55**, 937-940.

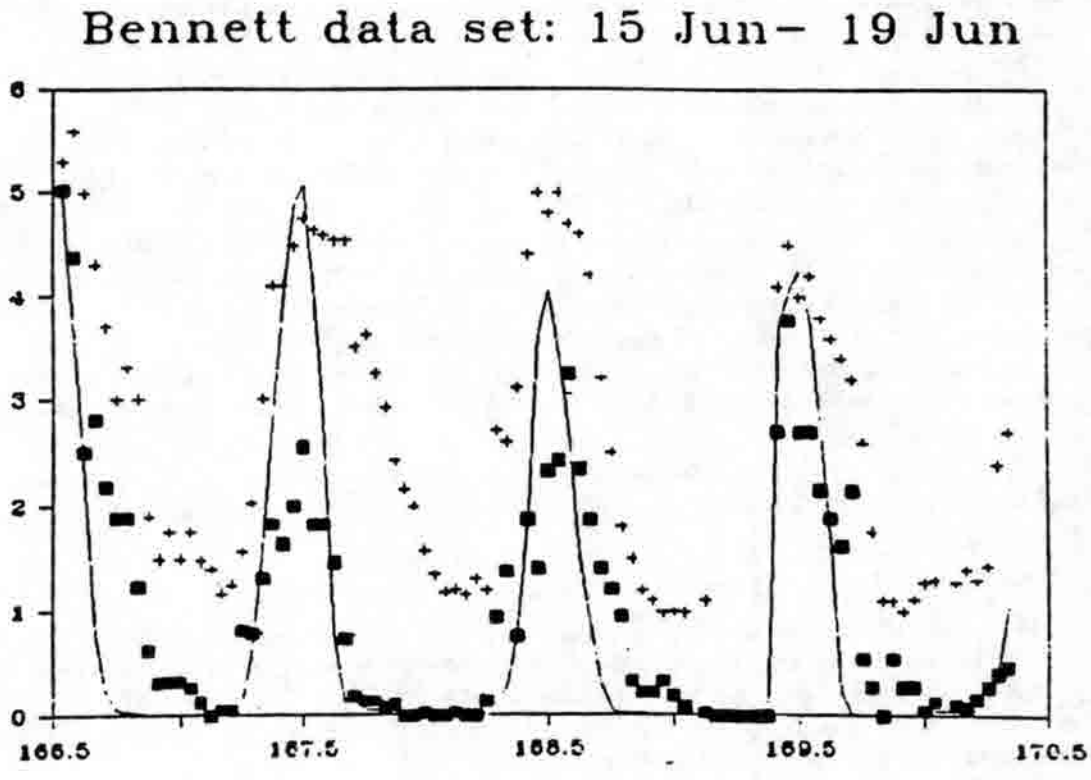


Figure 2. Free Radical, background, and $j(O_3$ data from the Bennett field site during June 1985. Noon-peaking values on the order of 3-5 x $10^8$ molecules/$cm^3$ are in good agreement with the predicted value calculated for the observed conditions. Free Radical data are shown by the squares backgrounded by the +s and $j(O_3)$ by the solid lines.

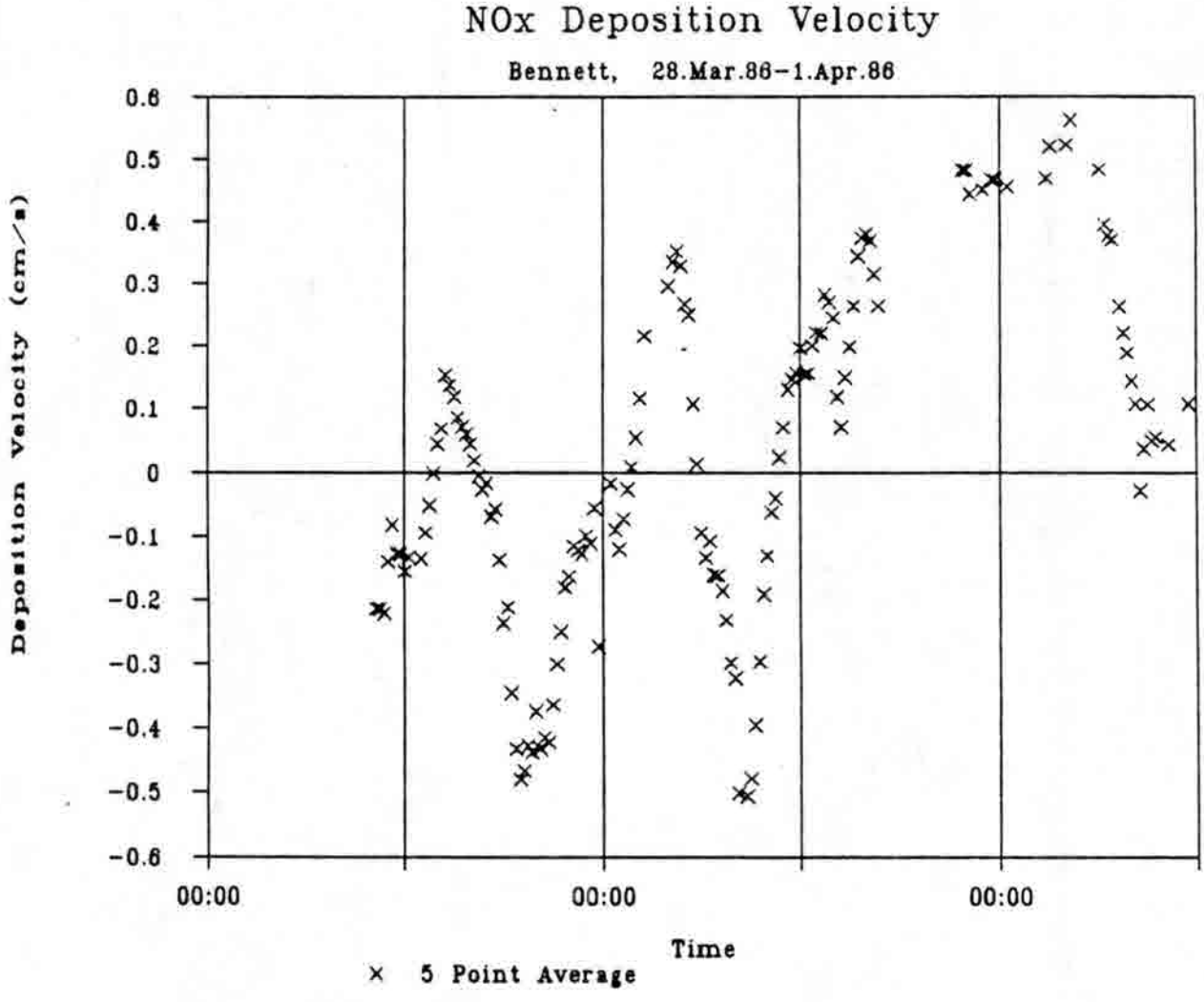
NOx Deposition Velocity
Bennett, 28.Mar.86-1.Apr.86
Deposition Velocity (cm/s)
0.6
0.5
0.4
0.3
0.2
0.1
0
-0.1
-0.2
-0.3
-0.4
-0.5
-0.6
00:00
00:00
00:00
Time
× 5 Point Average

Figure 3.

# Session IV

# Transport and Dispersion of Pollution in Colorado

# Divergence and Vorticity in the Rocky Mountain Plateau Circulation

Sumner Barr
Los Alamos National Laboratory
Los Alamos, New Mexico 87544

August 14, 1986

## I. INTRODUCTION

Mountainous regions of major areal extent have the potential to produce systematic regional circulations with day to night reversals. During the day the elevated land mass absorbs solar energy and serves as a warm spot relative to the surrounding air at the same altitude. This creates a general low level convergence into the area of elevated topography. At night, cooling at ground level reverses the thermal circulation to outflow from the high ground. The pattern of convective cloudiness that forms during the day over mountainous areas in summertime serves to enhance the effect. Release of latent heat in the cloud-forming condensation processes during the day warms the atmosphere above the mountains. Similarly, evaporative cooling occurs in this area at night. Tang and Reiter (1984) found evidence of this diurnally varying plateau circulation over the massive and high Tibetan Plateau. Reiter and Tang (1984) report a similar pattern over the Rocky Mountains in the summer season. In the other seasons of the year the effect is swamped by migratory synoptic scale circulation features. Reiter and Tang develop the 850 mb geopotential height pattern by upward hydrostatic adjustment of surface pressures from 44 stations in the mountain west. They performed the analysis on a record of seven July periods between 1975 and 1982. They present the 850 mb height fields for 3-hourly intervals throughout the diurnal period.

Figure 1 shows streamlines estimated from Reiter and Tang's Figure 2 by simply adopting a 45° cross-isobar wind. Figure 1a represents the time of maximum outflow and 1b the time of maximum convergence. The reversing wind patterns decribed in Figure 1 have helped explain some otherwise mysterious wind soundings. For example, Barr and Clements (1981) present data on a 1.5 km deep layer of vigorous easterly wind over the Piceance Basin of Western Colorado during two nights when conventional analyses all suggested weak southwesterly flow. Figure 2 shows the temporal trend of low level wind directions at the Piceance Basin site compared with winds derived from Reiter and Tang's pressure analyses. Both reflect a fairly rapid evening transition from westerly to easterly. Differences in timing aren't too important considering that the Reiter-Tang pressure fields are based on an ensemble while the Piceance Basin observations are for particular nights.

Based on evidence similar to that described above and the enormous practical implications of a systematic plateau circulation in the Rocky Mountain regions of Colorado, Wyoming, New Mexico and Utah, collaborators from Colorado State University and Los Alamos National Laboratory designed an experimental program to observe evidence of the plateau circulation directly in the wind field. An array of 13 wind and temperature sensors were deployed at exposed locations on mountain peaks from Steamboat Springs, CO south to Santa Fe, NM and west to Grand Mesa, CO. The

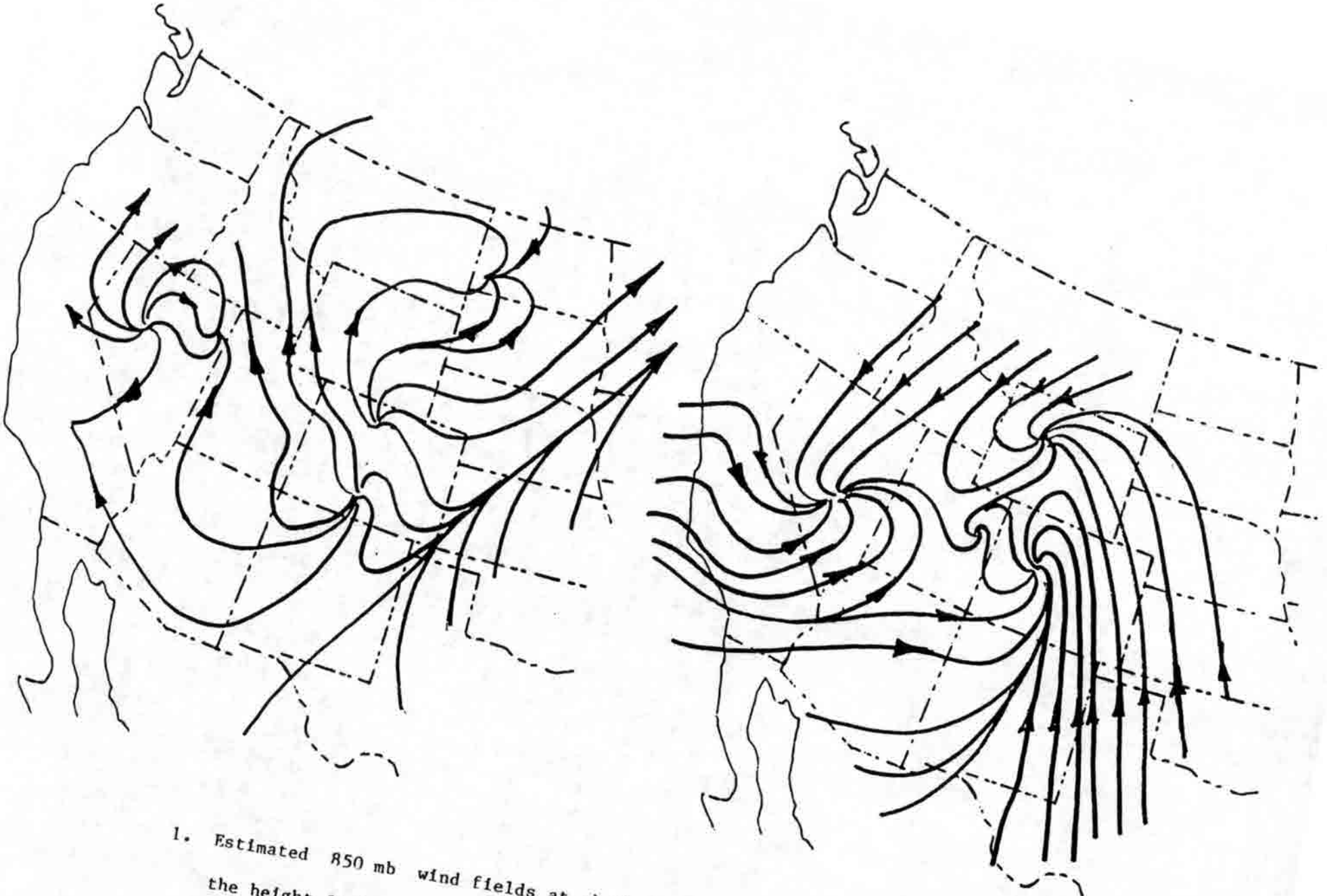

1. Estimated 850 mb wind fields at a) 0500 MST and b) 1700 MST derived from the height fields described by Reiter and Tang (1984).

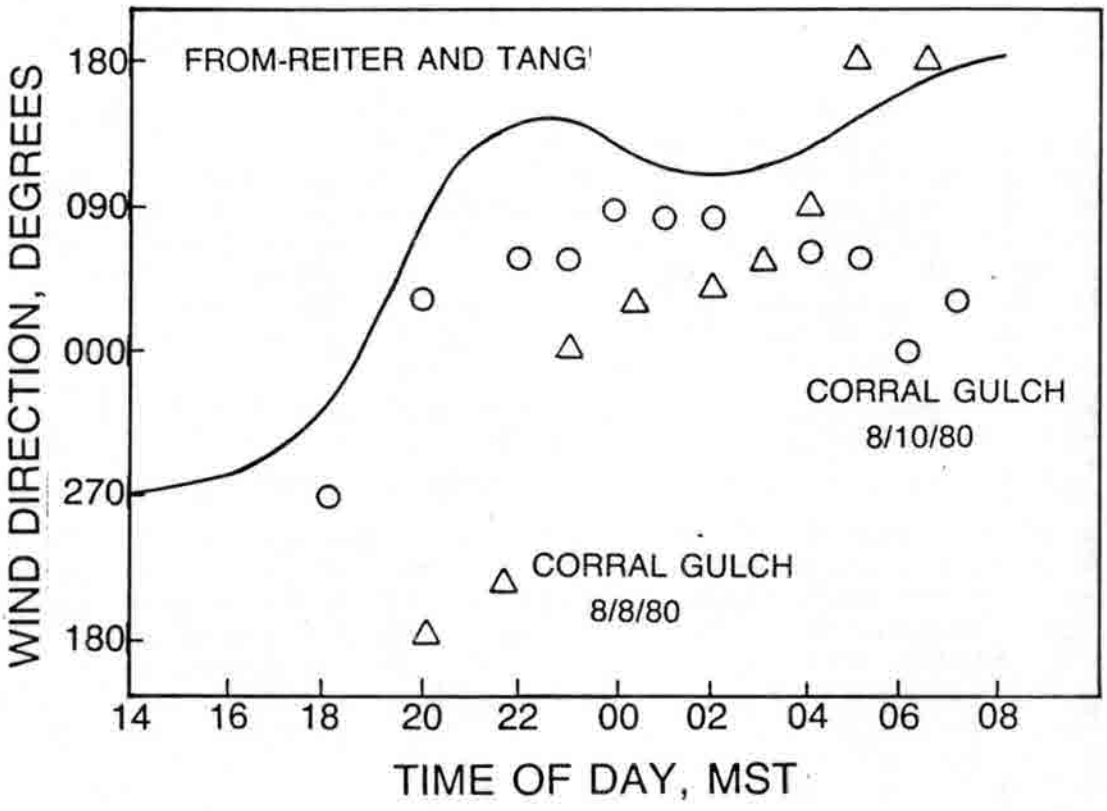


2. Comparison of observed low level wind directions at a Piceance Basin site with directions estimated from Rieter and Tang for the appropriate location.

object of the study was to place the sensors at exposed locations out of local drainage winds, and hopefully free of local aerodynamic recirculations so that they would respond to the larger scale plateau circulation winds. The mountain peaks were used as very tall proxy towers. In this way some hypotheses on the existence and properties of the Rocky Mountain plateau circulation could be tested continuously during a two month period of expected maximum influence. The cost for this depolyment was a small fraction of the cost to maintain an array of upper air soundings. Positive results from this relatively inexpensive experiment can be used to justify a more elaborate array of soundings. Details of the Rocky Mountain Peak Experiment (ROMPEX) are described by Sheaffer (1986).

This paper describes an effort at empirical analysis of the available ROMPEX wind data with emphasis on the divergence and vorticity magnitudes and, in a few cases, patterns.

## II. ESTIMATES OF THE MAGNITUDE OF THE PLATEAU CIRCULATION

It is instructive to estimate the magnitudes of the pressure gradient forces and the resulting wind fields in order to look for consistencies with the Reiter and Tang analyses and to see how the plateau circulation compares with synoptic influences on the wind and pressure fields. Whiteman and McKee (1978) and Whiteman (1981, 1982) report the results of three-hourly temperature soundings up to 6 km MSL over several locations in the Colorado Rockies. They show a deep convective boundary layer in the summer from 2 to 4 km above the main Rocky Mountain "plateau" (2 km MSL). At night a deep stable layer develops to altitudes as high as 2 km above the plateau. Based on a summary of warm season soundings, we have constructed a crude conceptual model of the relative heating and cooling above the plateau relative to the atmosphere above the surrounding plains. Figure 3 shows schematically the evolution of temperature profiles during the day and the subsequent night. An ambient tropospheric potential temperature profile of +3°C per km is imposed. This compares with the standard atmosphere and is reflected in many of the observed profiles. If the boundary layer over the plains does not exceed the 2 km height of the plateau, then we may examine perturbations to the ambient profile created in the boundary layer over the plateau. The convective boundary layer creates a shallow superadiabatic layer beneath a zone of constant potential temperature, the top of which is determined by the intersection of the ambient profile with the selected isentrope. Typical daytime warming leads to an average increase in potential temperature of 2 to 3°C over a layer 2 to 3 km in depth. Hydrostatic estimates of pressure at the height of the plateau surface are on the order of a few mb lower over the warm plateau than over the plains at the same height, assuming no pressure differential at 6 km MSL. Nighttime cooling over the plateau creates a similar plateau-plain pressure differential of about 2 mb. This pattern agrees very well with the contours of the 850 mb surface analyzed by Reiter and Tang.

We are further interested in the wind speed that results from a 2 mb pressure difference over the approximately 500 km radius of the Rocky Mountain plateau. Recognizing that even though we are dealing with a temporally evolving boundary layer flow on a relatively small scale, the simplicity of the geostrophic approximation is irresistable and the approximation will produce the expected order of magnitude of the winds. Substituting into $u_g = \frac{\partial P/\partial n}{\rho f}$ the values 210 Pa over $5 \times 10^5 m$, $\rho \cong 1 kg/m^3$ and $f = .94 \times 10^{-4} s^{-1}$ yields $u_g = 4.5 m/s$. Accounting for Ekman layer reduction in speed as well as the fact that throughout most of the day the driving force is evolving and has a magnitude less than the maximum, we can suggest that the plateau circulation has speeds of a few meters per second.

We can go one step further and estimate the expected vorticity and divergence from the wind field estimated in this section. Assuming a cross-isobar flow angle of 45°, a reasonable value for the lower boundary layer over rough terrain, and a net velocity of 3 m/s, we can evaluate equations

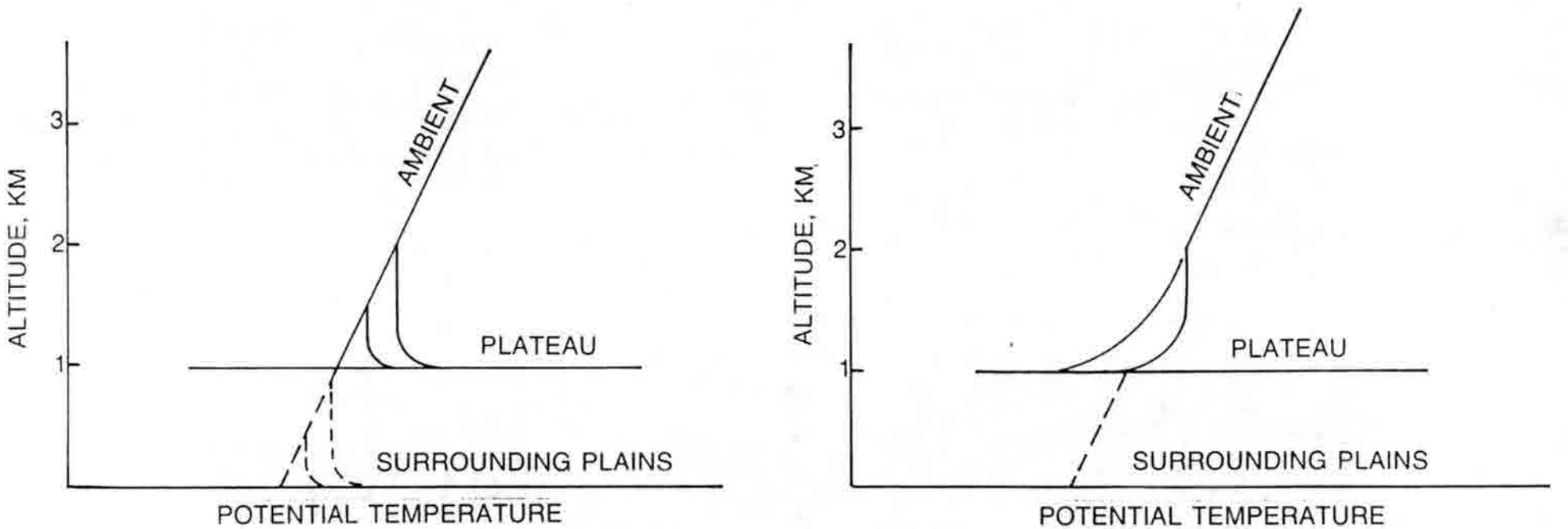


3. Schematic diagram of the thermal inequalities that drive the plateau circulation.

(1) and (2) over a circle of 500 km diameter. This yields values for both divergence and vorticity of $1.7 \times 10^{-5} s^{-1}$. This agrees within a factor of 2 with the values for the purest cases of plateau circulation in the ROMPEX data described in Section III.

The estimates are admittedly quite rough and not intended to represent any simulation effort. Instead, they are presented to show as directly as possible that the typical heating and cooling of the plateau boundary layer gives rise to the observed magnitude of pressure and wind which, in turn, reflect the correct magnitude of vorticity and divergence. More detailed modeling efforts are described by Sang and Reiter (1982).

The difficulty in diagnosing the plateau circulation can be seen by comparing the pressure gradient driving force for this system with synoptic pressure gradients. Above we have estimated a gradient of 2 mb over a 500 km lateral distance. This is equivalent to the weakest of synoptic pressure gradients in summer. In the presence of a front or cyclonic disturbance, summertime pressure gradients are more typically 10 mb over the same distance while a storm in winter will be double the value. Hence the local forcing can range from one half the total forcing down to a 10% perturbation. In the presence of the strong mixing, advection and alteration of the diurnal heating/cooling by clouds and widespread precipitation that occur in migratory synoptic systems, it is likely that the local forcing would be further diminished. Thus, it appears that the plateau circulation can be expected to be a major factor in Rocky Mountain transport wind fields only in favorable periods in the summer.

## III. ANALYSIS OF DATA

### A. Calculation of Divergence and Vorticity

A line integral method for estimating divergence and vorticity was introduced by Ceselski and Sapp (1975) and applied by Schaefer and Doswell (1979) and, more recently, by Shapiro and Zamora (1984). In this method the integrals:

$$D = \frac{\partial u}{\partial x} + \frac{dv}{dy} = \frac{1}{A} \int_c v_n ds \tag{1}$$

$$\zeta = \frac{\partial u}{\partial y} - \frac{\partial v}{\partial x} = \frac{1}{A} \int_c v_p ds \tag{2}$$

are evaluated around the minimum geometry for a closed curve, a triangle. In (1) and (2), A is the area enclosed by the path $c$, $v_n$, and $v_p$ are the velocity components normal to and parallel to the path, and $ds$ is an increment of the curve $c$. Figure 4 shows the array of triangles created from the available wind stations for the August 1985 period from the ROMPEX data set. Since each triangle yields an estimate of $D$ and $\zeta$ the calculation produces a field of divergence and vorticity for each time period. In most of the analysis described below the spatial averages of $D$ and $\zeta$ are used. Two periods were selected for analysis based on the completeness of the data records: July 10-20 and August 8 - September 7. Hourly values of divergence and vorticity were calculated.

One of our objectives is to look for diurnal variation in the area-averaged divergence and vorticity. In the absence of disturbance by migratory synoptic scale conditions, the expected pattern of the plateau circulation is inflow or convergence during the day and outflow or divergence at night. The time and space scale of the convergence-divergence cycle is large enough to expect an influence of the Coriolis force; so we would also expect cyclonic circulation in the daytime and anticyclonic circulation at night.

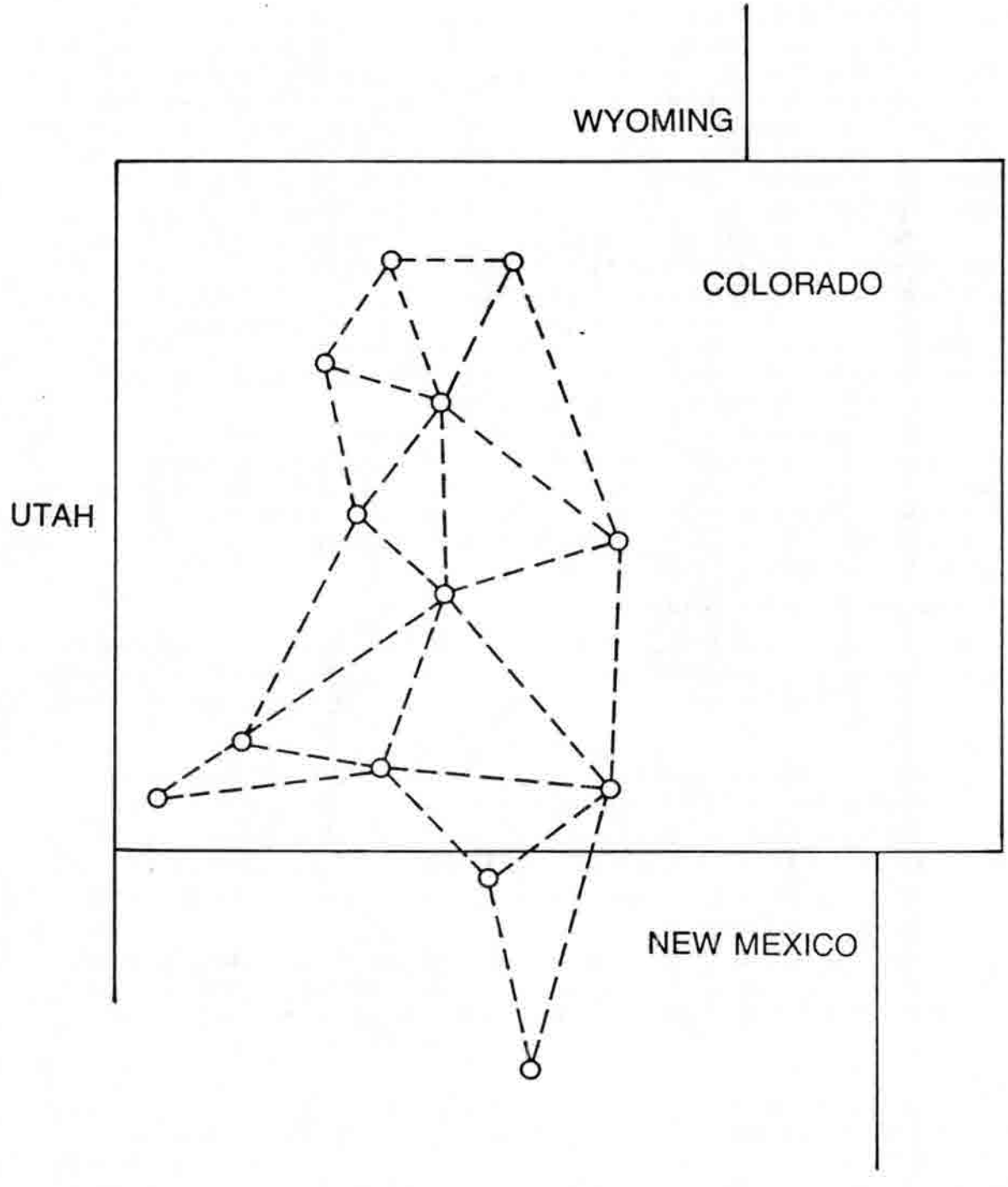


4. Diagram of the network of ROMPEX stations in Colorado and New Mexico and the triangles selected for estimating divergence and vorticity.

### B. Interpretation of the Time Series

Figure 5 presents time series plots of the spatial mean convergence and vorticity patterns. Although there appear to be diurnal variations it is clear that there is variability on other time scales. July 12, 15, 16 and 20, August 26, 27 and 30, and September 2 appear to offer the clearest cases of a diurnal pattern in both dynamical parameters. The other days are all strongly influenced by other circulations. There also appears to be a phase shift in which the vorticity lags the divergence by about three hours. We must keep in mind that Figure 4 refers to the mean properties over the entire observational array. There are many cases where the plateau circulation is dominant over the southern portion of the array while synoptic winds predominate in the north.

In order to look more specifically for the diurnal cycle in the somewhat noisy time series of Figure 4, we used a Fast Fourier transform calculation to produce the power spectra of Figures 6 and 7. Figure 6 displays the spectra for divergence (6a) and vorticity (6b) for the 10-day July period while Figures 7a and 7b show the same quantities for a thirty-day August-September period. The dominant feature of each of the spectra is the peak at the diurnal frequency of $1.16 \times 10^{-5}$ Hz. An apparent secondary peak at $2.5 \times 10^{-5}$ Hz is most likely the result of the nonsinusoidal shape of the dominant diurnal cycle being expressed in sinusoidal basis functions.

The August record shows a broad secondary maximum at a period of 4-5 days that doesn't appear in the July record. We suspect that this is the synoptic scale variation. The August record is barely long enough to suggest this spectral feature and the July record clearly is too short. Reiterating, the major features that appear in the power spectra of divergence and vorticity time series are distinct peaks at the diurnal frequency. These dynamical parameters are exhibiting the day to night reversals suggested by the plateau circulation hypothesis.

### C. Time and Space Dependence

Figures 8 and 9 present patterns of divergence and vorticity, respectively, for a 27-hour period identified as a case of good plateau circulation on July 19-20, 1985. Anticyclonic and divergent circulations are denoted as light stippled areas. There are several points to make regarding the patterns.

1. There are no pure region-wide patterns of all one sense. There are pockets of divergence in predominantly converging flow and vice-versa. The same holds for vorticity.

2. The area coverage for divergence (anticyclonic vorticity) includes most of the area at night and shrinks to a minor coverage during the day.

3. There is a measure of continuity in the evolution of the patterns with time although there are exceptions.

4. This case is dominated by strong nocturnal divergence in the northeast corner of the grid. This is not true of other cases. This area received heavy rainfall during the afternoon thunderstorms and could be a source of strong evaporative cooling at night.

## IV. CONCLUSIONS

Early results from analysis of the ROMPEX data set suggest that plateau circulation with characteristic dimensions of 500 km is a factor in the summertime wind fields over Colorado, Wyoming and New Mexico. Also, the deployment of sensors in exposed locations on mountain peaks appears to yield a representative sample of the regional scale circulation reflected in reasonable temporal and spatial patterns of derived quantities. The kinematic flow properties of divergence and vorticity are excellent diagnostics for interpreting the plateau circulation in the ROMPEX data set. Both

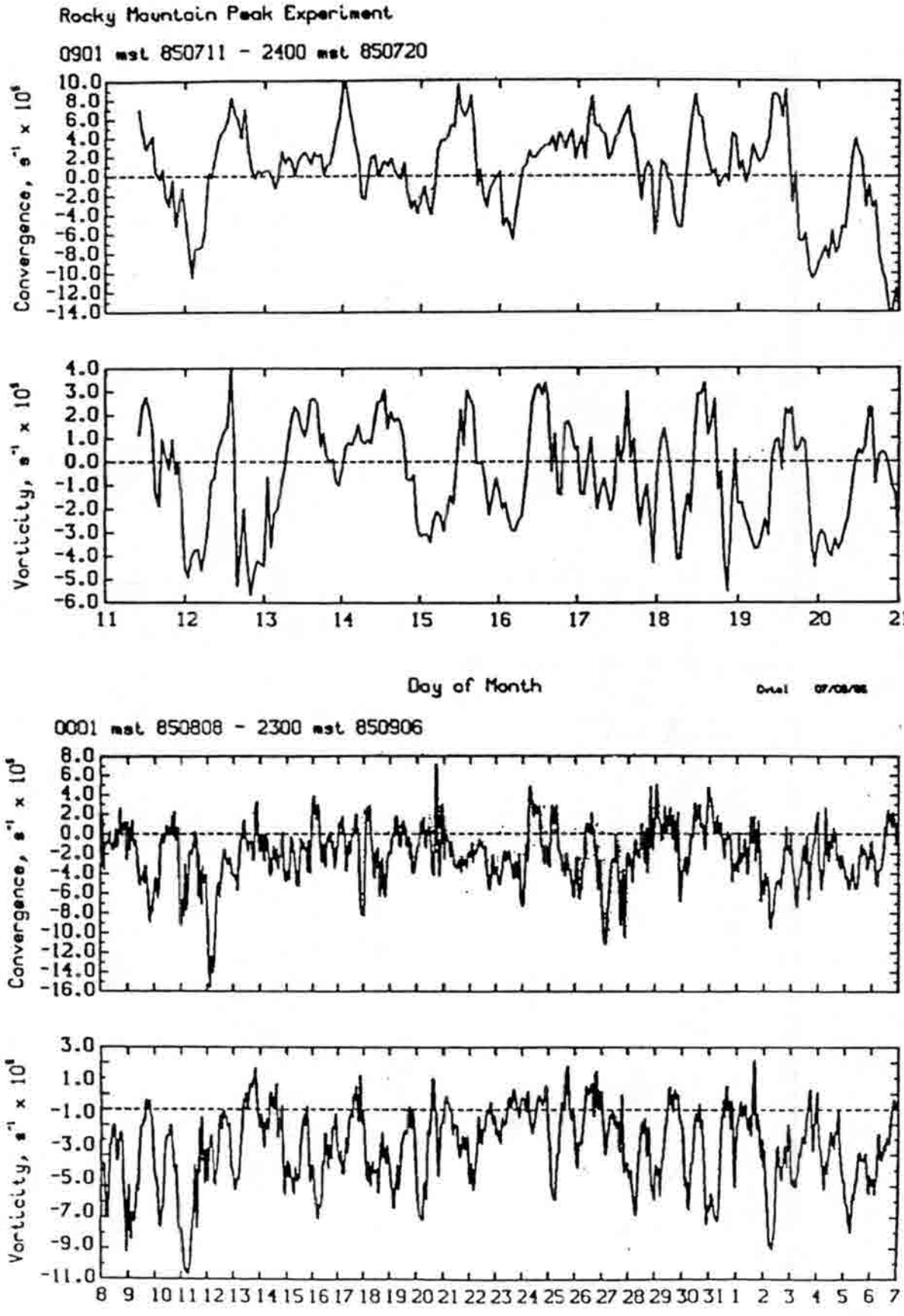


5. Time series of space-averaged divergence and vorticity from the ROMPEX network.

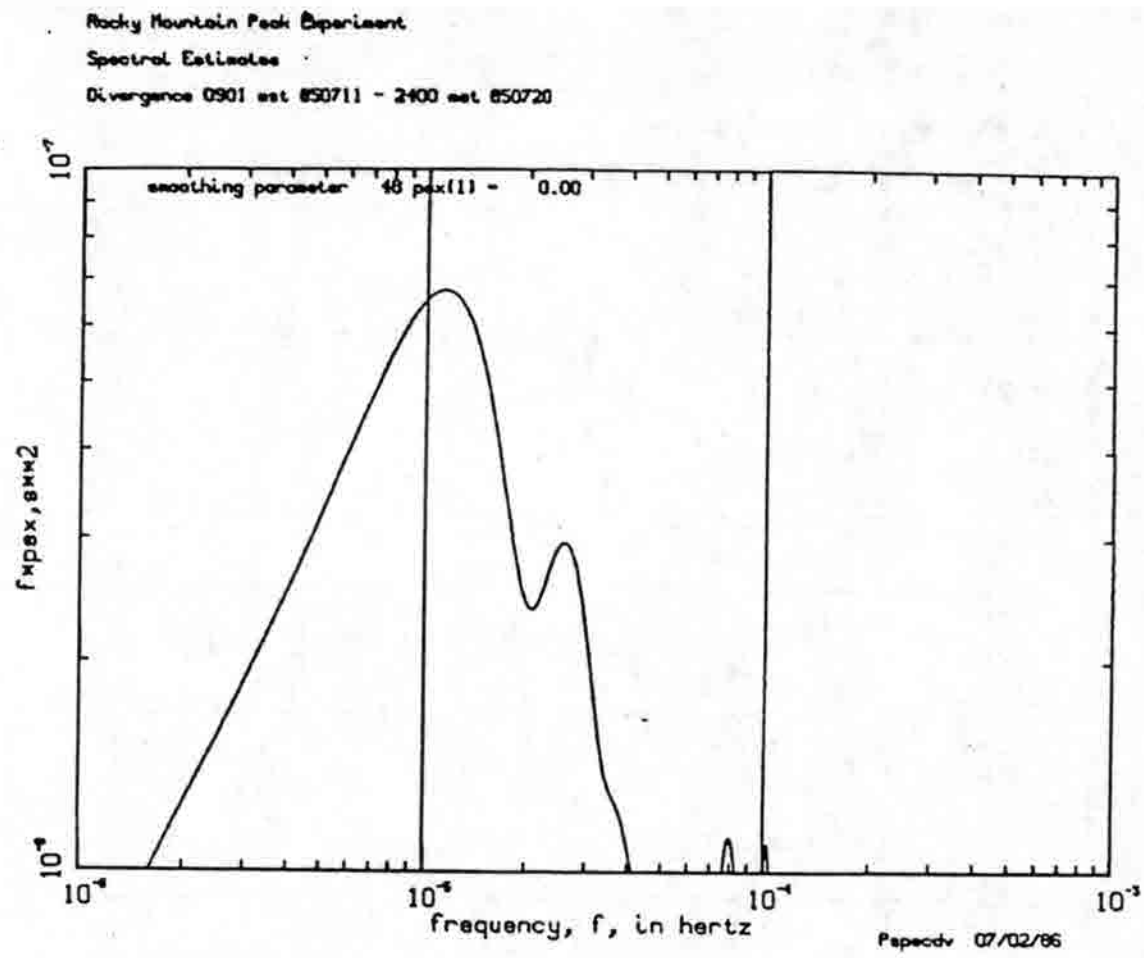


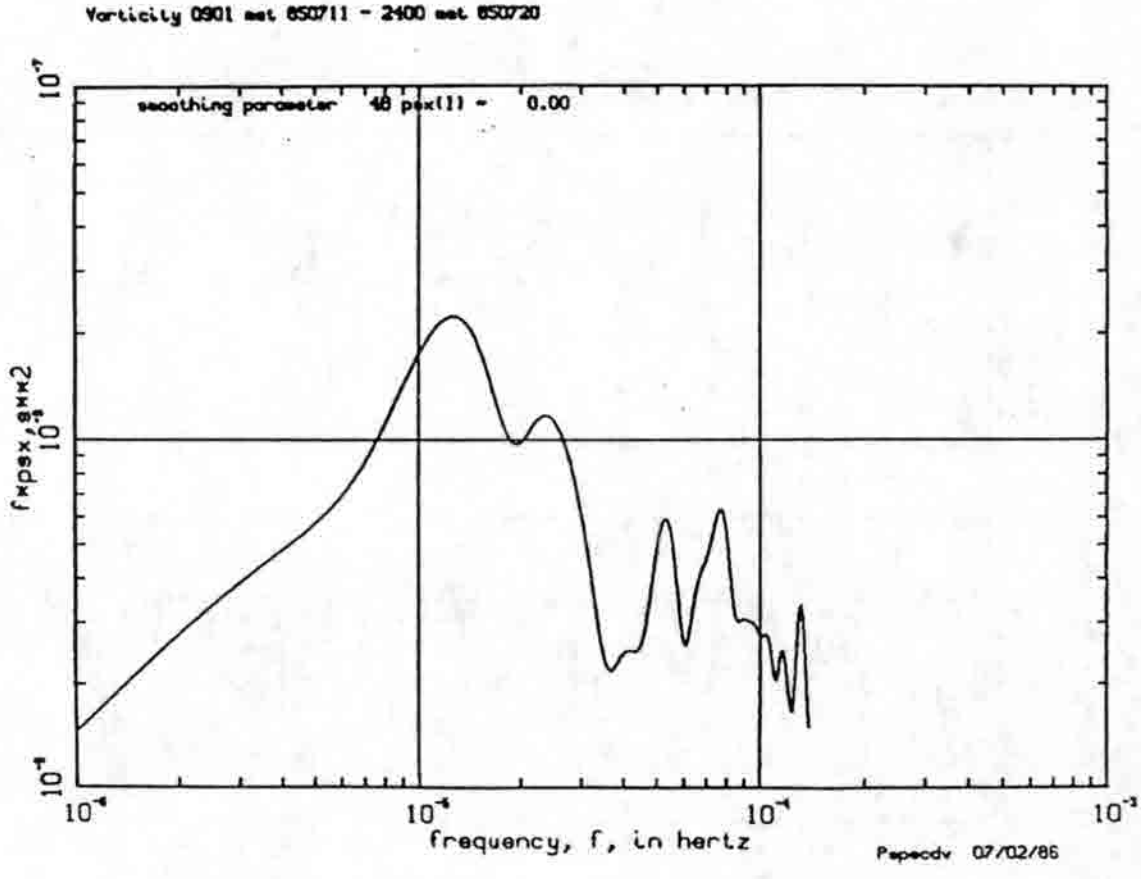


6. Spectra of a) Divergence and b) vorticity for a 10-day July 1985 period.

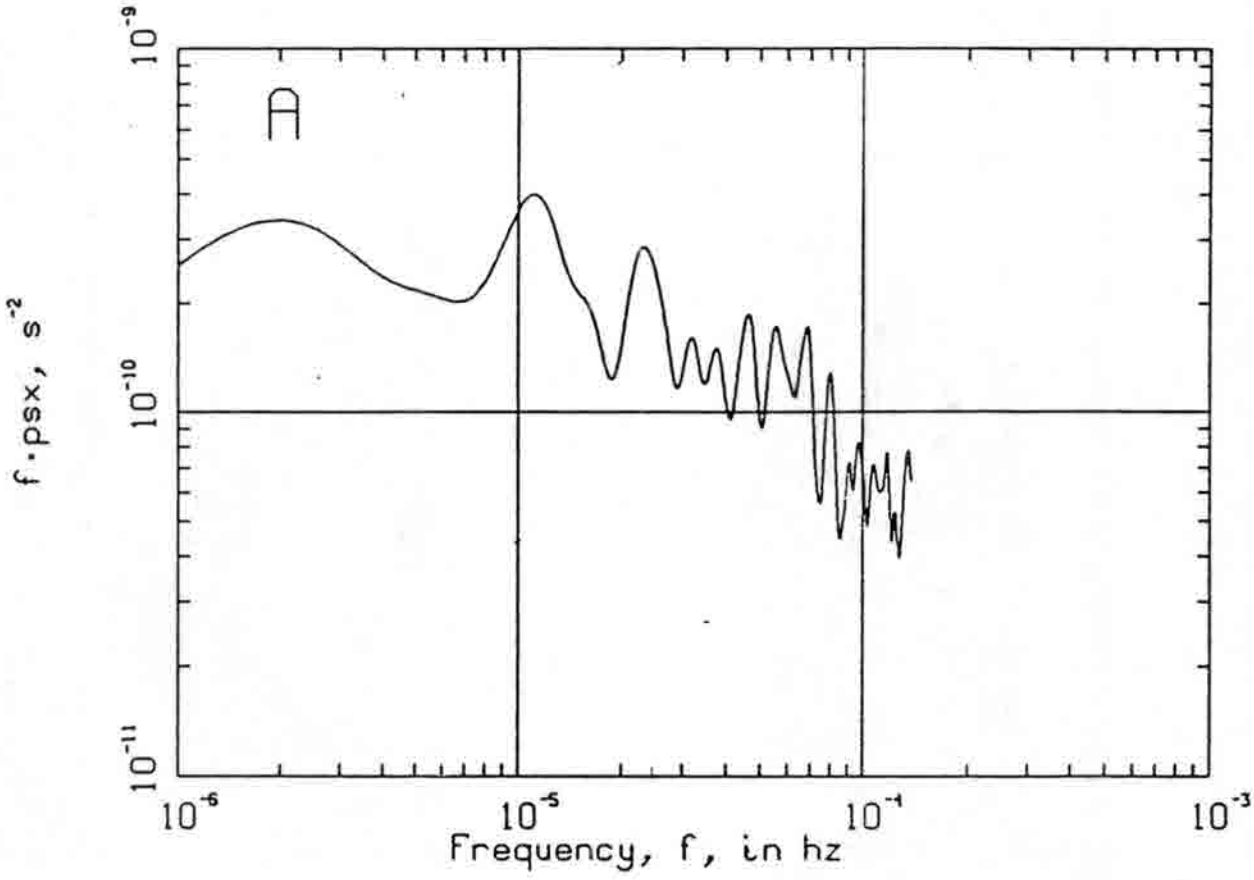


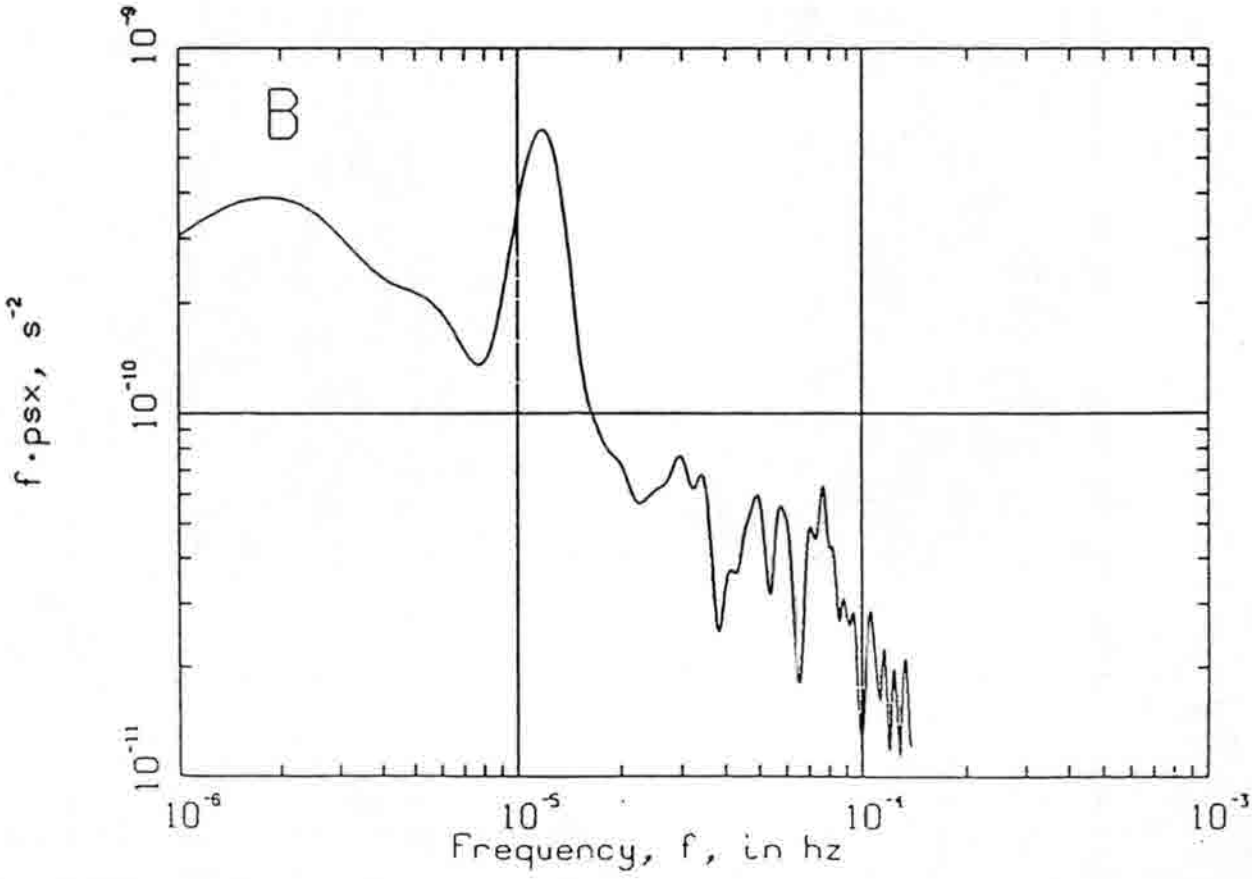


7. Spectra of a) Divergence and b) vorticity for a 30-day August-September, 1985 period.

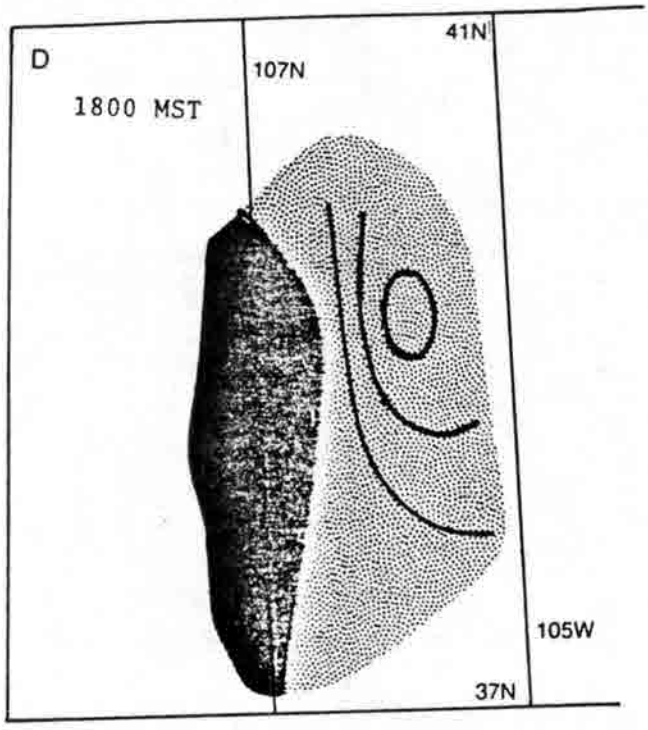


8a

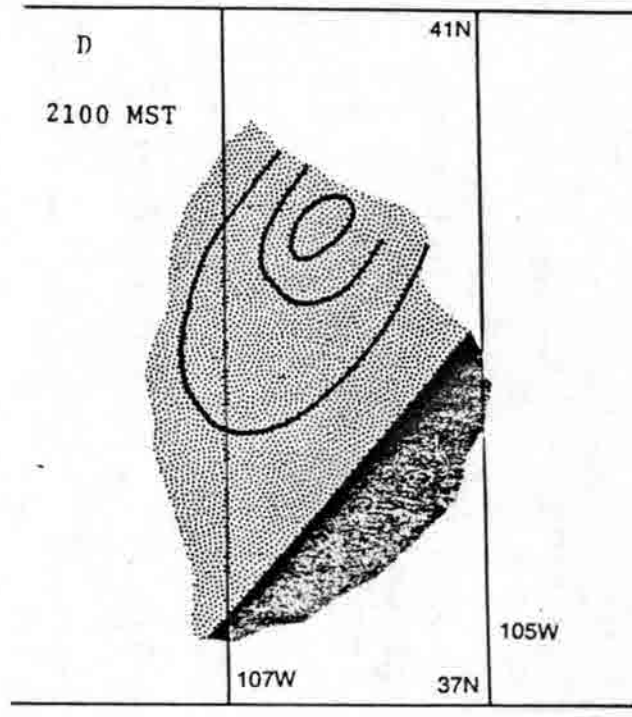


8b

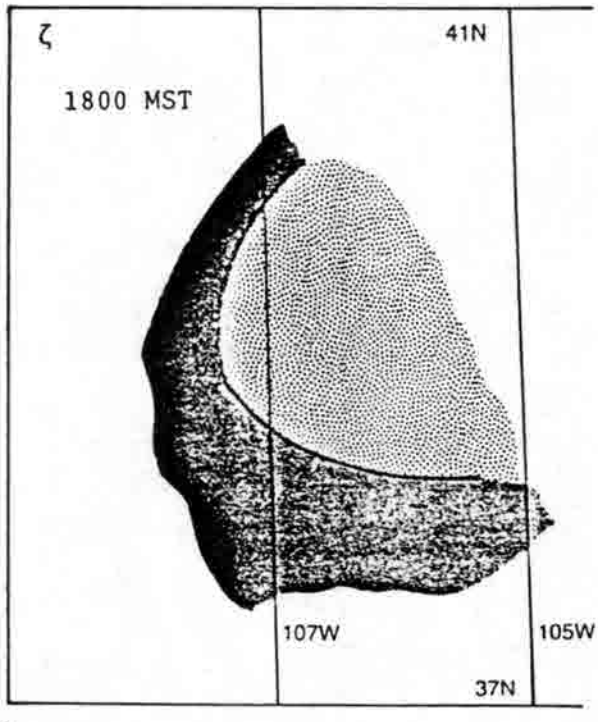


9a

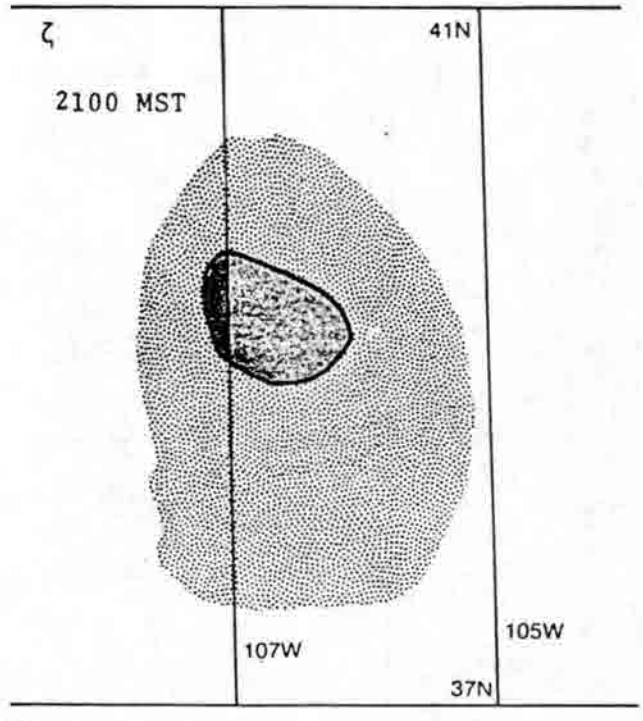


9b

8a-8j. (top) Divergence patterns at three-hour intervals for a 27-hour case during strong diurnal influence. Light stippled areas are divergent while dark shading is convergence. Contours are at values of $1 \times 10^{-4}$ $s^{-1}$.

9a-9j. (bottom) Vorticity patterns corresponding to Fig. 8. Light stippling represents anticyclonic vorticity. Contours are at values of $1 \times 10^{-4}$ $s^{-1}$.

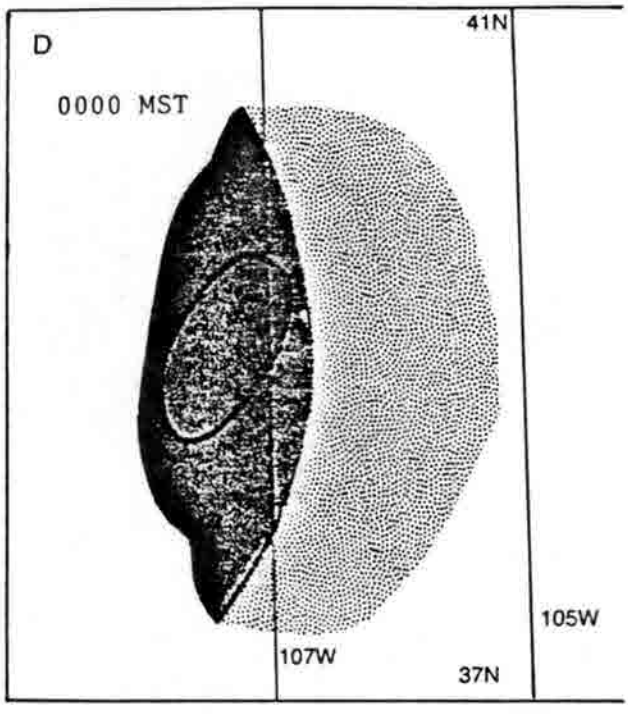
D
0000 MST
41N
105W
107W
37N

8c

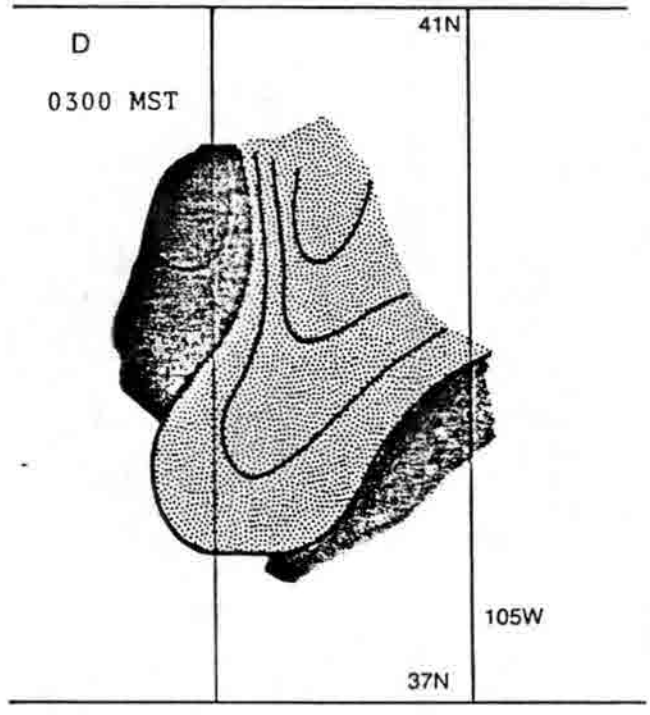
D
0300 MST
41N
105W
37N

8d

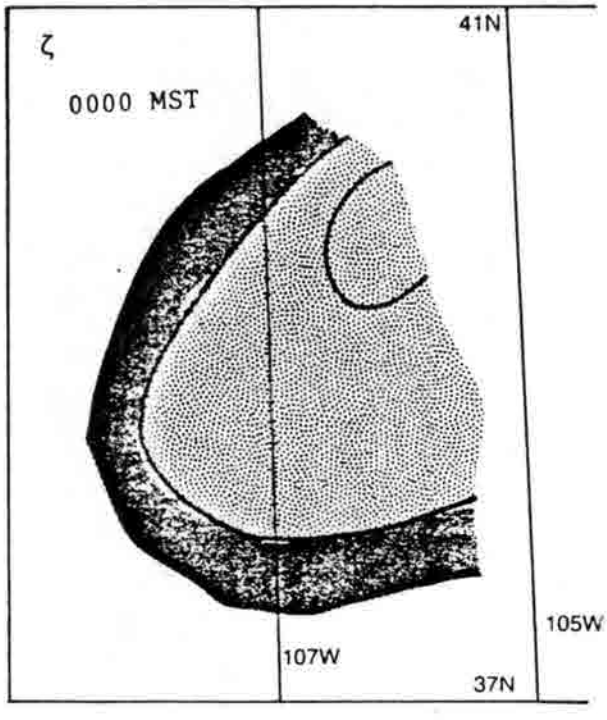
ζ
0000 MST
41N
105W
107W
37N

9c

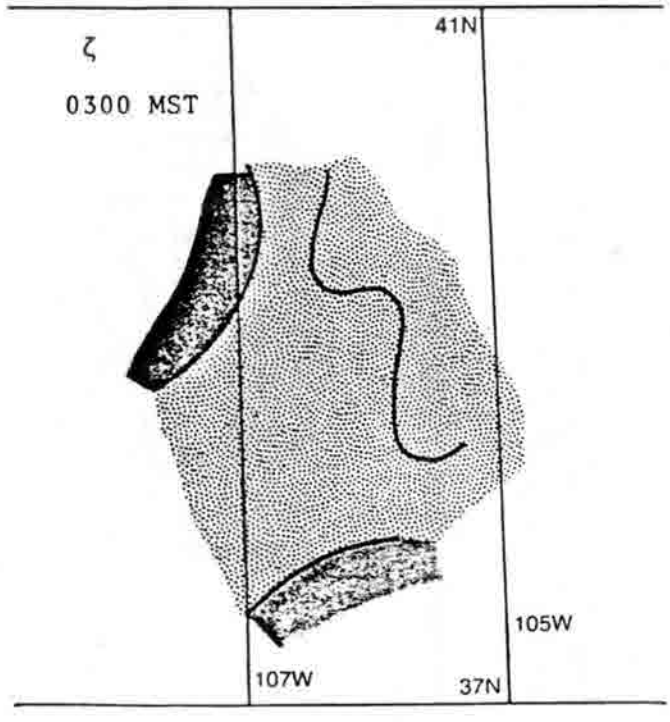
ζ
0300 MST
41N
105W
107W
37N

9d

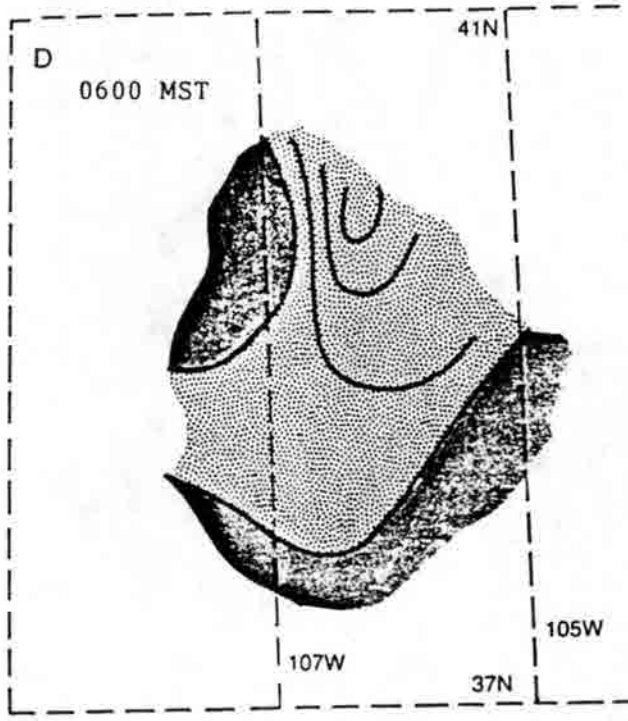
D
0600 MST
41N
105W
107W
37N

8e

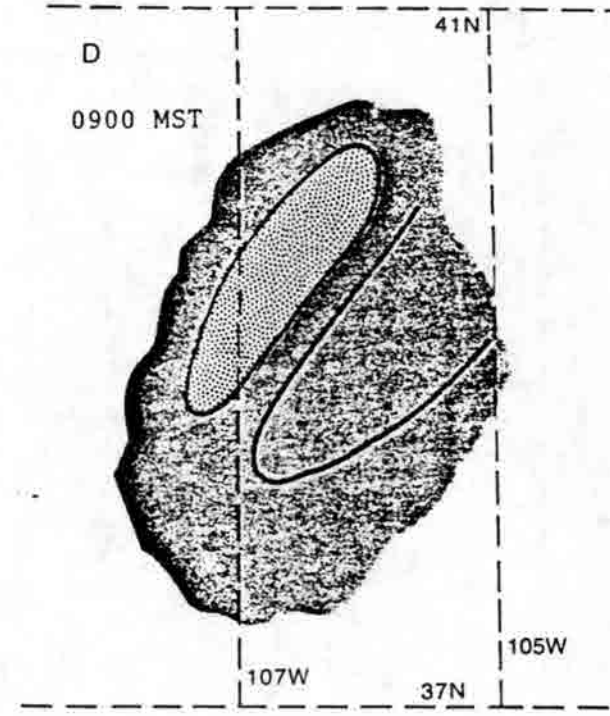
D
0900 MST
41N
105W
107W
37N

8f

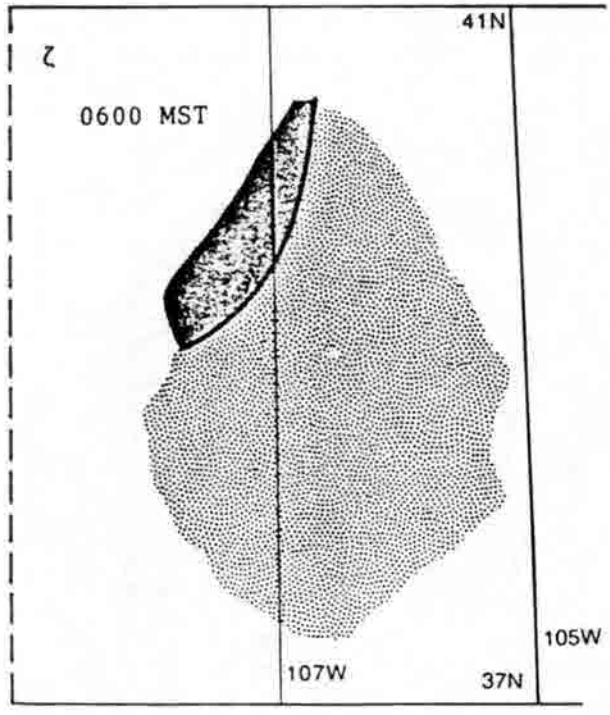
ζ
0600 MST
41N
105W
107W
37N

9e

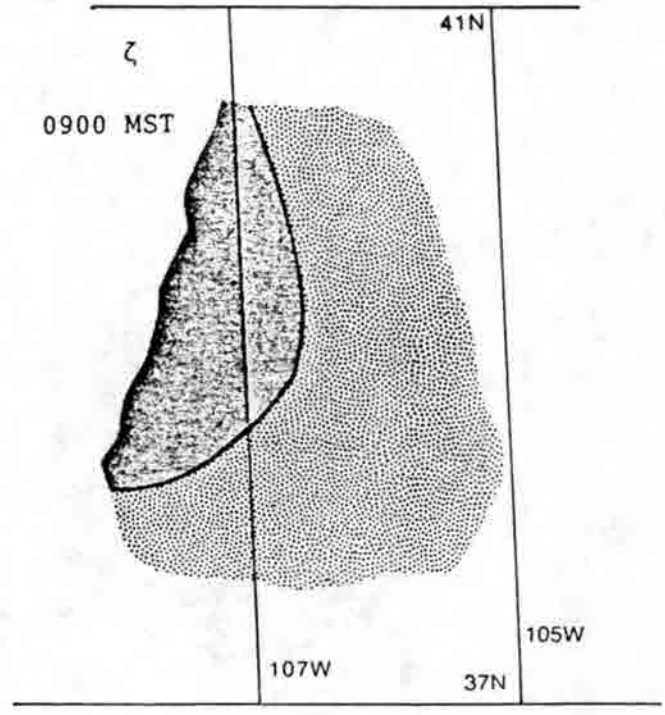
ζ
0900 MST
41N
105W
107W
37N

9f

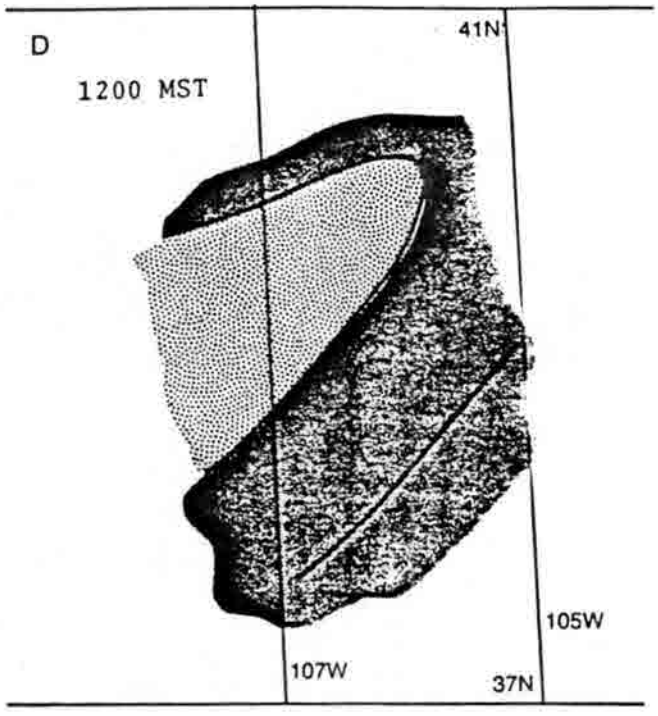
D
1200 MST
41N
105W
107W
37N

8g

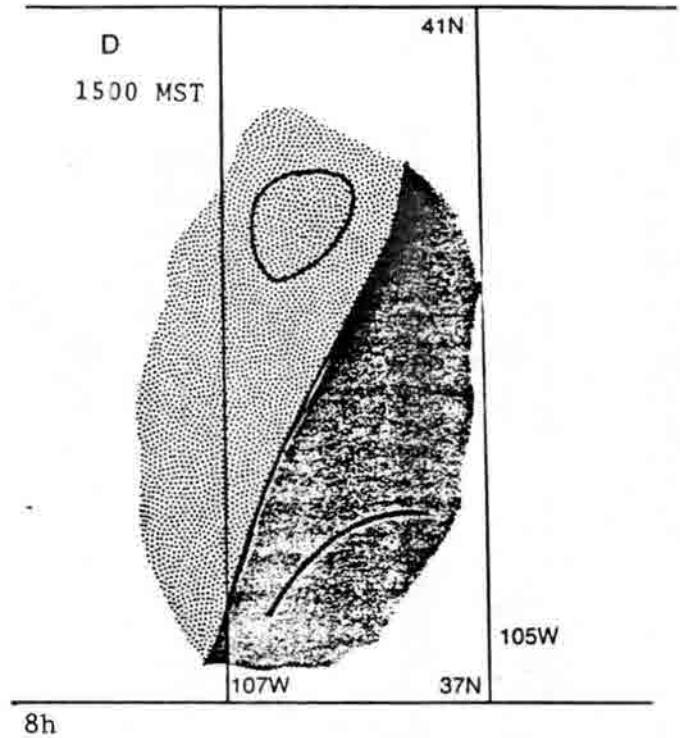
D
1500 MST
41N
105W
107W
37N

8h

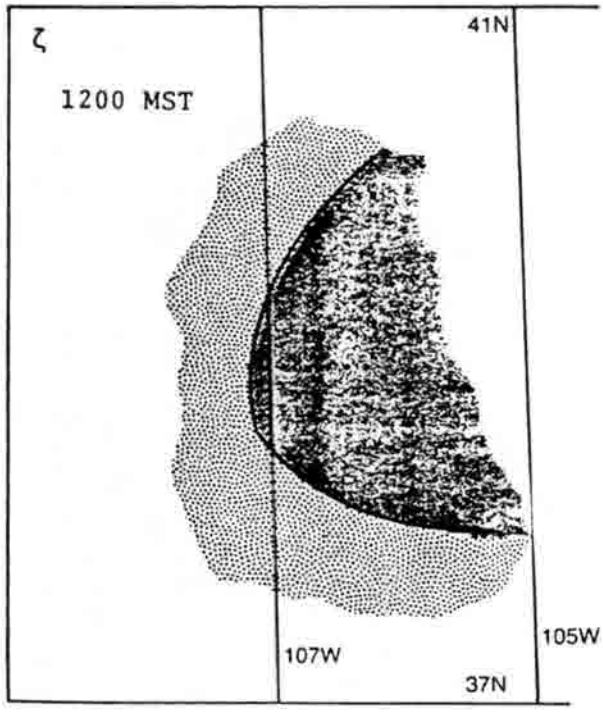
ζ
1200 MST
41N
105W
107W
37N

9g

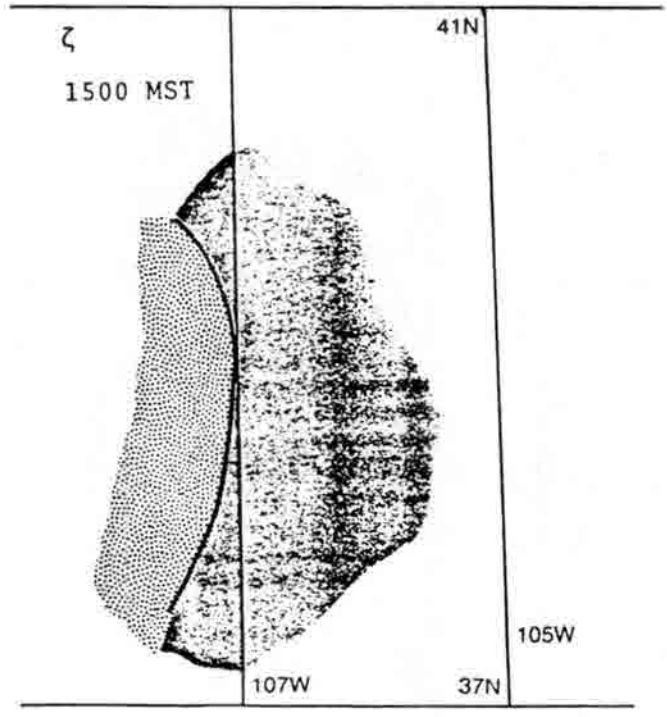
ζ
1500 MST
41N
105W
107W
37N

9h

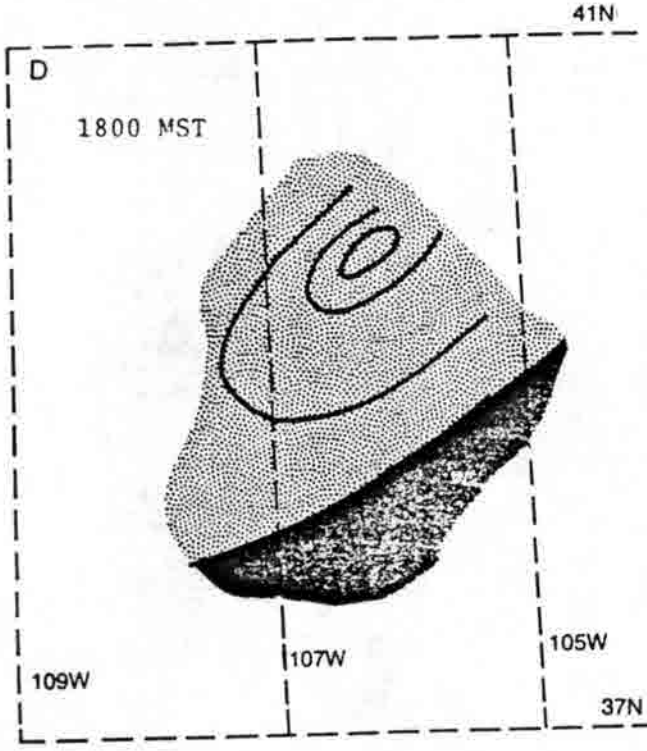
D
1800 MST
41N
109W
107W
105W
37N

8i

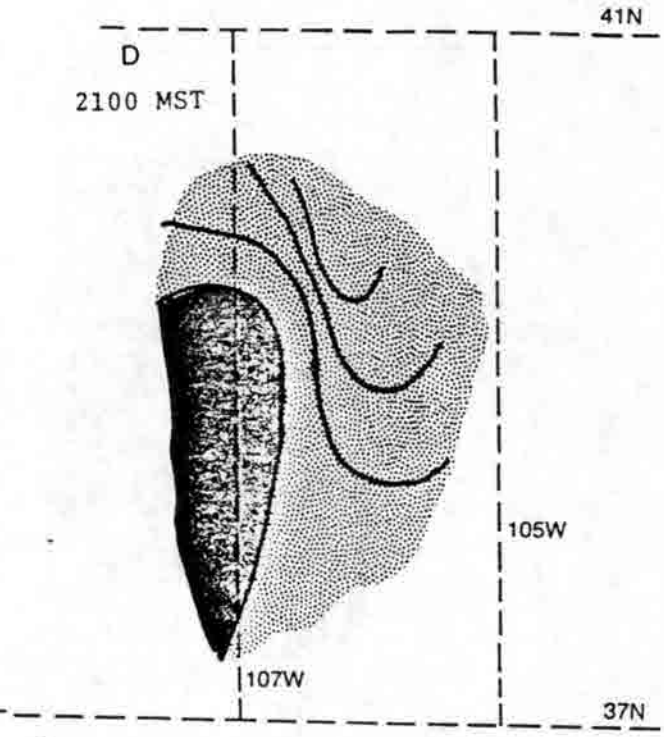
D
2100 MST
41N
107W
105W
37N

8j

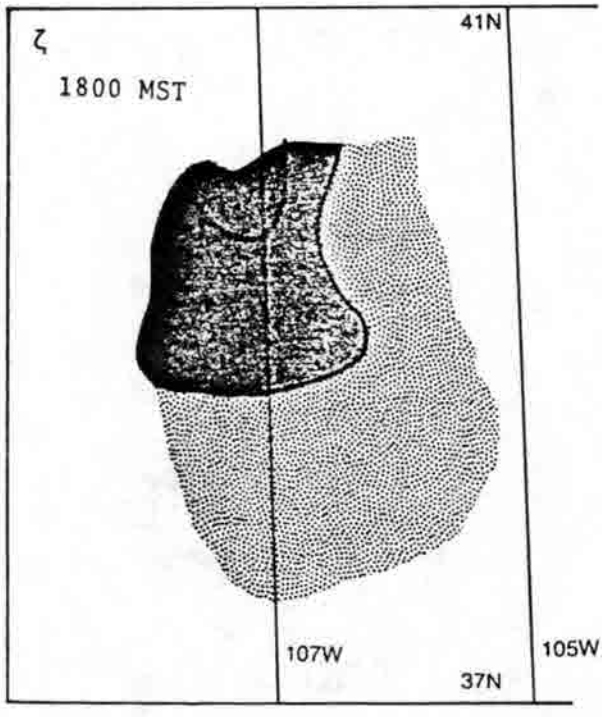
ζ
1800 MST
41N
107W
105W
37N

9i

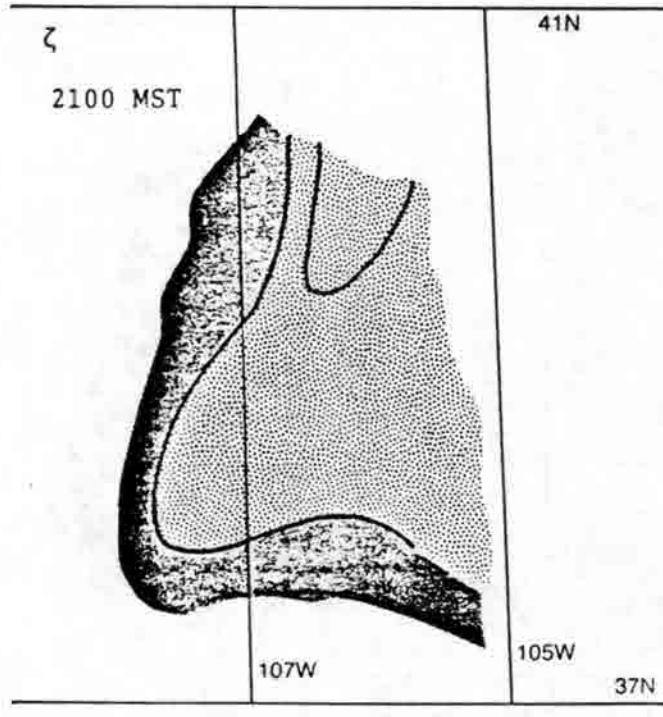
ζ
2100 MST
41N
107W
105W
37N

9j

parameters exhibit a clear diurnal variability as well as a suggested synoptic scale variability. The phase of the variations as well as the amplitudes are consistent with estimates based on the thermal forcing and resulting pressure fields. A comparison of forces suggests that the plateau circulation can represent everything from a dominance of the observed wind (when synoptic gradients are very weak) to an insignificant perturbation under vigorous synoptic flow.

The practical implications of the circulation are significant. As in the case of the Piceance Basin observations described in Section I, transport winds can be in the opposite direction to those indicated by synoptic analysis exclusive of the circulation domain. The diurnal reversal characteristic suggests that pollutant plumes may pass a particular location more than once.

The majority of cases exhibit spatial structure in the convergence field. Although the mean value for a particular day may represent convergence, for example, there are persistent and sometimes migratory pockets of divergence in the observation array. It is tempting to speculate on the relationship of such space-time variations to the vigor of mountain thundershowers. Those of us who live in the mountains often observe quite abrupt changes in the character of the local thunderstorm environment as if an extensive field of deep convection were squelched by a somewhat sudden subsidence. I will suggest that some important variations in the precipitation patterns and subsequent deposition patterns in summer depend on the plateau circulation.

The results from ROMPEX are demonstrating quite clear evidence of a component of the wind field that exhibits properties of the plateau circulation postulated by Reiter and Tang. It is appropriate to devise more elaborate experiments that may rely on vertical soundings of wind and temperature, and perhaps tracer releases. I encourage the continued effort in modeling the system that is currently under way at Colorado State University.

## REFERENCES


Barr, S., and W.E. Clements, 1981. Nocturnal wind characteristics in high terrain of the Piceance Basin, Colorado. Proceedings, 2nd Conf. on Mountain Meteorology, Steamboat Springs, CO, Amer. Meteor. Soc., 6 pp.

Ceselski, B.F., and L.L. Sapp, 1975. Objective wind field analysis using line integrals. *Mon. Wea. Rev.*, **103**, 89–100.

Reiter, E.R., and M. Tang, 1984. Plateau effects on diurnal circulation patterns. *Mon. Wea. Rev.*, **112**, 638–651.

Sang, J.-G., and E.R. Reiter, 1982. Model-derived effects of large-scale diurnal thermal forcing on meteorological fields. *Arch. Met. Geoph. Biokl.*, **A31**, 185–203.

Schaefer, J.T., and C.A. Doswell, III, 1979. On the interpolation of a vector field. *Mon. Wea. Rev.*, **107**, 458–476.

Schaefer, J., 1986. Draft report on ROMPEX. Colorado State University.

Shapiro, M., and R. Zamora, 1984. Diagnostic divergence and vorticity calculations using a network of mesoscale wind profilers. Proceedings, 10th Conf. Weather Forecasting and Analysis, June 25–29, Clearwater Beach, FL. Amer. Meteor. Soc., 386–391.

Tang, M., and E.R. Reiter, 1984. Plateau monsoons of the Northern Hemisphere: A comparison between North America and Tibet. *Mon. Wea. Rev.*, **112**, 617–736.

Whiteman, C.D., and T.B. McKee, 1978. Air pollution implications of inversion descent in mountain valleys. *Atmos. Env.*, 2151–2158.

# Contributions of Smelters and Other Sources to Pollution Sulfate at a Mountaintop Site in Northwestern Colorado

Randolph D. Borys*
Cloud and Aerosol Simulation Laboratory
Department of Atmospheric Science
Colorado State University
Fort Collins, Colorado 80523

Douglas H. Lowenthal and Kenneth A. Rahn
Center for Atmospheric Chemistry Studies
Graduate School of Oceanography
University of Rhode Island
Narragansett, Rhode Island 02882-1197

August 14, 1986

**Abstract**

Sulfate aerosol at a mountaintop site in northwestern Colorado during winter 1984-85 has been apportioned with an elemental tracer technique to three major types of source regions in the West: coal-based, oil-based, and nonferrous smelting. When combined with meteorological analysis, the chemical results suggest that 62±10% of the sulfate came from coal-based regions east and west of the continental divide, 21±4% came from nonferrous smelters in Arizona and New Mexico, and 16±4% came from regional southern California.

The mix of local vs. distant sources for pollution aerosol and acidic deposition in the West has received considerable attention recently, including the potential effect of nonferrous smelters in Arizona and New Mexico on receptors as far away as the Colorado Rockies (1). These concerns are quite legitimate, for the dryness of the West promotes long-range transport of aerosol and its gaseous precursors. The relatively weak pollution emissions in much of the West, when coupled with this efficient transport, render western air quality unusually susceptible to distant influences.

As part of a study of cloud physics and chemistry at the Storm Peak Laboratory (2) near Steamboat Springs, Colorado, we collected a series of high-volume aerosol samples during winter 1984-1985. In light of the recent discussion of the role of nonferrous smelters on sulfate in air and precipitation, stimulated largely by the report of Oppenheimer et al., 1985 (3) have detected a linear signal from the smelters throughout much of the Intermountain West, we decided to combine chemical and meteorological techniques to search for a smelter signal in these filters. Meteorological analysis alone is especially difficult in the West because of its irregular terrain.

*Current Affiliation: Atmospheric Sciences Center, Desert Research Institute, University of Nevada System, P.O. Box 60220, Reno, NV 89506

Consequently, we analyzed the filter samples for trace elements and sulfate. The overwhelming majority of the sulfate appeared to be pollution-derived, because marine Na accounted for less than 1% of the observed sulfate, and because gypsum from western soils could account for only about 10% of the sulfate even if all the Ca in the aerosol were assumed to be present as $CaSO_4$. Thus, we applied the seven-element regional tracer technique for pollution aerosol developed by Rahn and Lowenthal (4,5). A distinct smelter signal from the southwest was found, and accounted for 21±4% of the sulfate. In addition, three other regions contributed significantly to sulfate: the nearby Intermountain West, with a coal-based signal; parts of California, with an oil-like signal; and a region east of the Rockies, also with a coal-based signal.

From 19 November 1984 - 7 April 1985, 61 high-volume aerosol samples with a 10-$\mu$m cutoff diameter (defined as interstitial aerosol) were collected on acid-washed Whatman No. 41 cellulose filters at Storm Peak Laboratory and ranged in length from a few hours (when snow and/or cloud was present) to more than two weeks (when the laboratory was unoccupied). Portions of each sample were analyzed for 30-40 elements by instrumental neutron activation and for sulfate by ion chromatography (after leaching overnight in distilled-demineralized water). Snow or cloud was present at some time during 70% of the samples. The presence of cloud seemed not to influence the character of the interstitial aerosol measurably, however, for sulfate concentrations did not differ significantly between in-cloud and clear-sky samples. Figure 1 shows the concentrations of sulfate with time.

Because no regional signatures for potential sources in the West had been determined, three were adapted from earlier studies and are shown in Table 1. To represent nonferrous smelters, the SMELT signature was derived from eight daily samples at Underhill, Vermont during winter 1983-84 that were influenced strongly by nonferrous smelters in southern Ontario and Quebec, but with noncrustal V reduced to levels corresponding to the West instead of to the Northeast. SMELT thus strongly resembled the earlier SONT (4,5) by having elevated In and As. To represent emissions from the Intermountain West, which are dominated by coal combustion, the Lower Midwest signature LMW (5), which is also dominated by coal combustion, was used and renamed COAL. COAL is characterized by high Se and low noncrustal V. To reflect the major features of aerosol from Southern California, a signature called OIL was generated from earlier data from the San Francisco Bay area (7), but the noncrustal V reduced to values comparable to earlier data from the Los Angeles area (8) and As and In given values typical of eastern U.S. aerosol (5). OIL is characterized by high Zn and noncrustal V. OIL may differ from true Southern California aerosol for at least two reasons: its data are more than ten years old and it contains only minimal information from the Los Angeles area. At this time, howevever, OIL is the best estimate of the Southern California regional structure.

It is important to understand that these signatures are objective, i. e., they were created before they were used, they were not based on data from Storm Peak Laboratory, and they were not modified in any way to improve the fits to the samples. The fits reported are thus the originals. Even though we believe that these signatures are substantially correct, they should all be updated by direct measurements in the source regions.

Using the signatures of Table 1 and the least-squares (chemical element balance) procedures described earlier (5), the regional contributions to sulfate and the tracer elements in the aerosol samples from Storm Peak Laboratory were determined. Of the 61 samples, only the 27 with concentrations of five or more of the seven tracer elements and sulfate above the detection limit were apportioned; the volume-weighted average apportionments are shown in Table 2. Several of the main features of these results are analogues of those observed in the eastern United States (5): 1) the nearest region (COAL) tends to contribute much or most of the mass of elements emitted comparably in different areas (25-50% of the Sb, Zn, and noncr. Mn in this case); 2) the nearest region contributes the great

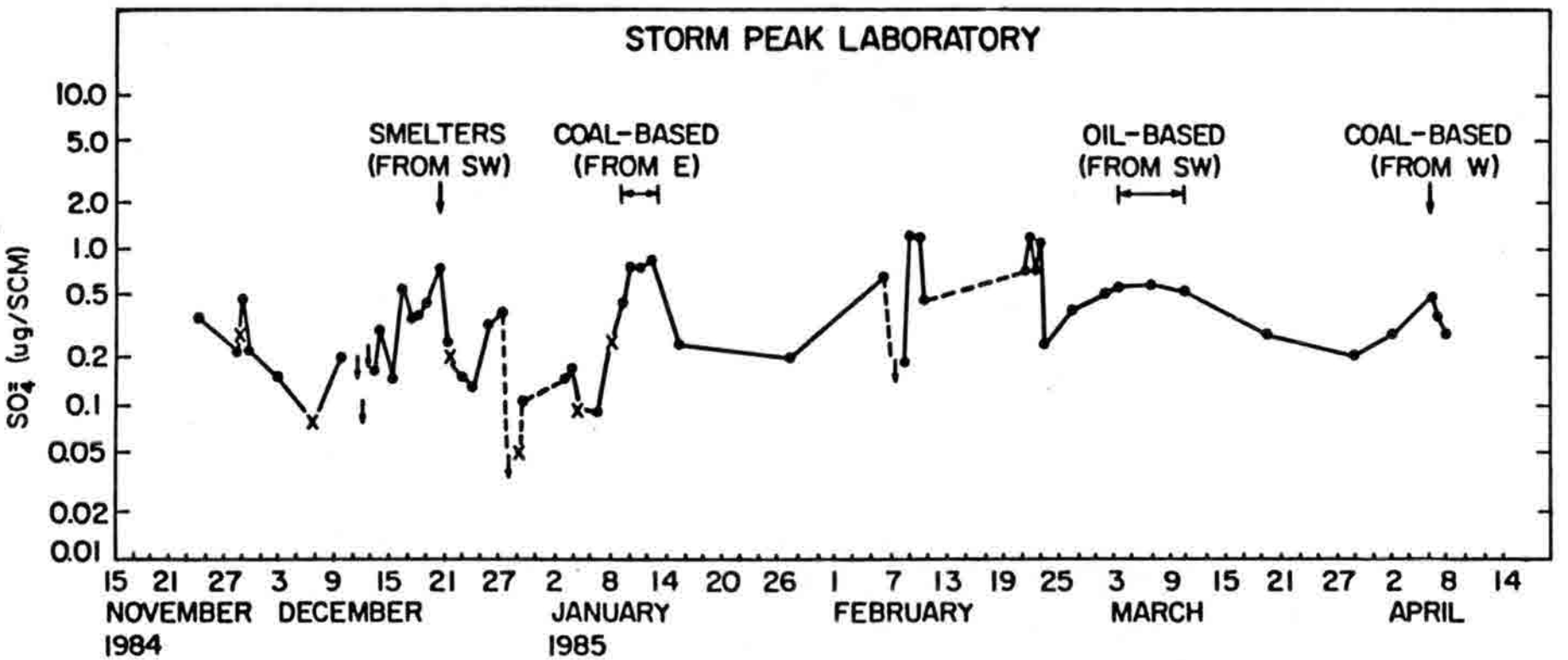


Figure 1. Time series of sulfate concentrations measured at Storm Peak Laboratory during winter 1984-85. Solid dots indicate samples with uncertainties below 25%, x's indicate uncertainties of 30-60%, and arrows indicate samples whose sulfate was below the detection limit. The serrated line shows the duration of each sample. Labelled samples refer to episodes discussed in the text.

Table 1. Regional elemental signatures used to apportion aerosol at Storm Peak Laboratory. Values given as ng $m^{-3}$, scaled to unit Se.

| | SMELT[1] | COAL[2] | OIL[3] |
|---|---|---|---|
| As | 3.6±1.4 | 0.23±0.05 | 0.70±0.30 |
| Sb | 0.30±0.11 | 0.148±0.038 | 1.50±0.60 |
| Se | 1.00±0.43 | 1.00±0.30 | 1.00±0.40 |
| Noncr. V | 0.50±0.20 | 0.160±0.064 | 7.0±3.0 |
| Zn | 26±11 | 5.3±0.9 | 97±39 |
| Noncr. Mn | 2.8±1.1 | 1.10±0.69 | 5.0±2.0 |
| In($x10^3$) | 47±23 | 1.0±1.0 | 4.0±2.0 |

[1] Smelter signal at Underhill, Vt. during winter 1983-84, with reduced vanadium.
[2] Same as Lower Midwest signature (ref. 5).
[3] Data from San Francisco Bay Area (ref. 7), with updated As, V, and In.

Table 2. Volume-weighted average regional apportionments* of sulfate and tracer elements in aerosol at Storm Peak Laboratory, winter 1984-85 (N = 27)

| | COAL | SMELT | OIL | Avg. pred. ng $m^{-3}$ | Avg. obs. ng $m^{-3}$ | Avg. obs./pred. |
|---|---|---|---|---|---|---|
| $SO_4^=$ | 62±10 | 21±4 | 16±4 | 414±39 | 336 | 0.82±0.40 |
| As | 17±4 | 78±18 | 4±1 | 0.087±0.013 | 0.110 | 1.01±0.20 |
| Sb | 41±8 | 24±5 | 35±10 | 0.024±0.003 | 0.024 | 1.12±0.29 |
| Se | 73±15 | 21±5 | 6±2 | 0.090±0.011 | 0.087 | 0.95±0.18 |
| Noncr.V | 18±5 | 16±4 | 66±21 | 0.058±0.010 | 0.059 | 0.94±0.26 |
| Zn | 25±5 | 36±8 | 39±11 | 1.37±0.17 | 1.41 | 1.08±0.26 |
| Noncr.Mn | 47±14 | 35±8 | 18±5 | 0.152±0.022 | 0.181 | 1.07±0.84 |
| In | 7±3 | 91±26 | 2±1 | 0.00098±0.00019 | 0.00050 | 0.55±0.54 |

* Uncertainties of apportionments will be higher than those listed here if the true signatures differ appreciably from those of Table 1.

majority of the mass of elements enriched in its own emissions (75±15% of the Se and 62±10% of the sulfate from COAL because of the coal burned there); 3) elements enriched in distant sources often come predominantly from those sources (63±21% of the noncrustal $V$ from OIL and 78±18% of the As and 91±26% of the In from SMELT).

From the standpoint of sulfate from the southwestern smelters, two results are of interest: a distinct component (21±4%) was found to come from the smelters, but not nearly as high a percentage as for As or In. Similar enrichments of As and In relative to sulfate were also noted for Canadian smelter aerosol sensed in New England (5).

These results for sulfate agree qualitatively with those reported by Oppenheimer et al. (2). They claimed to find a clear smelter signal in sulfate deposited as far north as Wyoming; we find a clear signal in the aerosol of northwestern Colorado. Their figures indicated that the smelters emitted as much as 74% of the $SO_2$ of the Intermountain West during the peak year 1981; we attribute 21±4% of the sulfate to the smelters during 1984-85, when smelter emissions were approximately one-third the 1981 levels. More recent results reported by Epstein and Oppenheimer (8) using the same data reduced to monthly, rather than yearly, means indicated 57% of the sulfate in Colorado precipitation could be attributed to smelter emissions during 1981.

The sulfate apportionments were a useful first step in determining the relative contributions of local and distant sources to the sulfate episodes. To complete the apportionment, the atmospheric transport associated with each episode was determined. Comparing meteorology with chemistry showed clearly that air and pollutants come to Colorado from an unusually large range of directions and distances.

The key to understanding this active transport is Colorado's unique geographical setting. The Colorado Rockies and the continental divide act both passively and actively to promote flow from the east in addition to the normal flow from the west. Passively, they hinder low-level air from the Pacific and western states from crossing Colorado, and thereby limit the influence of these regions largely to the western slope. Actively, the Rockies initiate lee-through development, which in combination with moisture from the Gulf of Mexico promotes the development of Colorado lows throughout the winter. In concert with shallow, cold polar air masses, these pressure systems lead to persistent large-scale easterly (retrograde) flow near the surface which can bring air to Colorado from distant sources to the east, perhaps as far away as the Northern Plains, the Midwest, or the Southeast. Storm Peak Laboratory is influenced by all these air masses because it is situated near the continental divide.

The combined meteorology and chemistry of episodes of enhanced sulfate at Storm Peak Laboratory offers additional insight into their most important source areas. Figure 2 shows meteorological maps for four such episodes. The first, for 5 April 1985, was the synoptic condition immediately after large-scale stagnation in the Intermountain West which resulted in the highest sulfate of the sampling period. Aerosol in this sample (5-6 April) was apportioned almost completely to the COAL signature, and represents local (Intermountain) sources. The heavy dashed line is the 700-mb back-trajectory, initiated from Storm Peak Laboratory (9). This trajectory is typical of post-frontal flushing of stagnant boundary layer in this kind of synoptic situation. The second map, for 18 December 1984, was associated with a smelter episode during the sample of 19-20 December, which showed the maximum smelter-aerosol coefficient of the winter. Note how the back-trajectory passed over the smelters of Arizona. The third map, for 6 March 1985, was associated with a pulse of aerosol from the direction of Southern California during 3-6 March, and had the highest OIL coefficient of the period. The back-trajectories passed over Southern California. The fourth map, for 9 January 1985, represents an unexpected but apparently common source of aerosol from the east. It was associated with persistent easterly winds observed at Storm Peak Laboratory and a sulfate

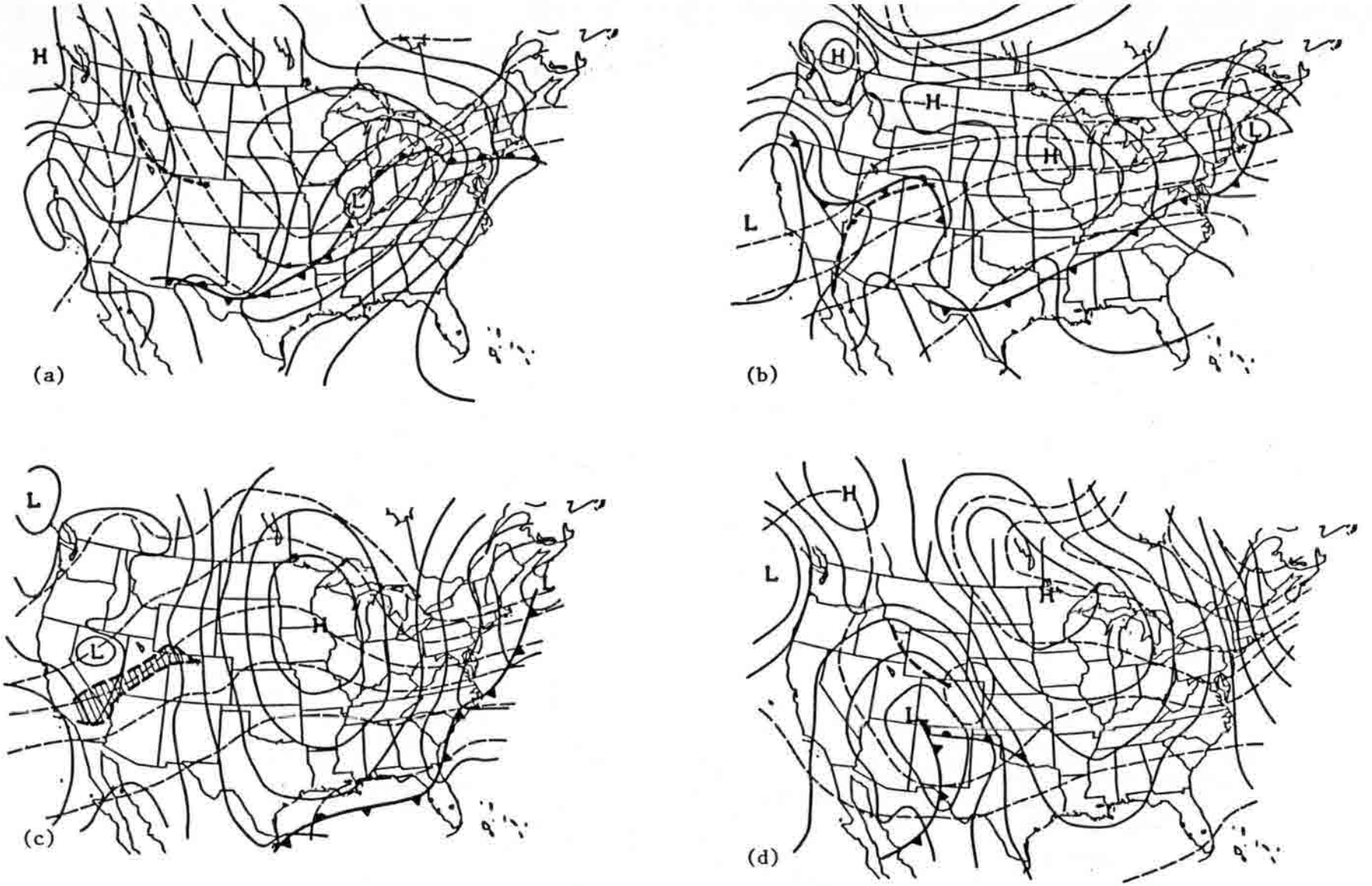


Figure 2. Surface and 700-mb meteorological maps (solid and dashed lines, respectively) associated with four types of sulfate episodes at Storm Peak Laboratory: (a) 4 April 1985 - from local (Intermountain) coal-based sources, (b) 18 December 1984 - from southwestern smelters, (c) 6 March 1985 - from southern California oil-based sources, and (d) 9 January 1985 - from coal-based sources east of the Rockies. Heavy dashed lines are the 36-hr back-trajectories at 700 mb associated with each event.

maximum from 9-12 January. Note how the 700-mb trajectory fails to depict this flow correctly, whereas the surface isobars better represent the observations.

In conclusion, atmospheric sulfate of winter 1984-85 at Storm Peak Laboratory in northwestern Colorado came from a variety of local and distant source regions. Approximately two-thirds originated in coal-based sources to the west and east. It is not possible to ascertain what fraction of this coal-based source originated within Colorado. The remaining one-third came from the southwestern smelters and southern California. In response to the low smelter emissions of winter 1984-85, the smelters appeared to contribute only 21±4% of the sulfate at Storm Peak Laboratory. To apportion local versus distant sources of western aerosol more accurately than this, signatures of relevant sources within Colorado and beyond will have to be determined separately.

## REFERENCES AND NOTES


1. W.M. Lewis and M.C. Grant, *Science*, **207**, 176 (1980); W.M. Lewis Jr. and M.C. Grant, *Tellus*, **34**, 74 (1982); R.A. Eldred, L.L. Ashbaugh, T.A. Cahill, R.G. Flocchini and M.L. Pitchford, *J. Air Pollut. Control Assoc.* , **33**, 1100 (1983); L.L. Ashbaugh, L.O. Myrup and R.G. Flocchini, *Atmos. Environ.* , **18**, 783 (1984); C.J. Popp, D.C. Brandvold, R.W. Ohline and L.A. Brandvold, in Deposition, Both Wet and Dry, Ann Arbor Science Press, Ann Arbor, Michigan (1984).

2. Storm Peak Laboratory is located at the ridge crest of the Park Range in northwestern Colorado (3200 m above mean sea level) between the Mt. Zirkel and Flattops Wilderness areas. This location provides unobstructed air flow for studying aerosol, clouds, and precipitation.

3. M. Oppenheimer, C.B. Epstein, R.E. Yuhnke, *Science*, **229**, 859 (1985).

4. K.A. Rahn and D.H. Lowenthal, *Science*, **223**, 132 (1984).

5. K.A. Rahn and D.H. Lowenthal, *Science*, **228**, 275 (1985).

6. W. John, R. Kaifer, K. Rahn, J.J. Wesolowski, *Atmos. Environ.*, **7**, 107 (1973).

7. G.L. Hoffman, Ph.D. Thesis, University of Hawaii, Honolulu (1971).

8. C.B. Epstein, and M. Oppenheimer, *Nature*, **323**, 245 (1986).

9. Trajectories were calculated by R. Artz of NOAA/ERL, Silver Spring, MD, with the ARL/ATAD model of J. Heffter, NOAA Tech. Memo. ERL/ARL-81, 17 pp., 1980. The layer chosen for the constant level trajectories 1700-1800m over smoothed terrain. This resulted in a trajectory which arrived at the elevation of Storm Peak Laboratory (3200m MSL). Trajectories were also run (not presented here) using the multilayer transport model incorporating wind shear and diurnal changes in the depth of the mixed layer described by J.F. Bresch, T. Henmi, E.R. Reiter and L.L. Ashbaugh, Pres. at the 77th Ann. Meeting of the A.P.C.A., June, 1984. The results of this model were the same.



10. We thank the Steamboat Ski Corporation and the U.S. Forest Service for their continued support of Storm Peak Laboratory. Samples were analyzed for trace elements at the Rhode Island Nuclear Science Center, Narragansett and for sulfate by D. Creager at Colorado State University, Fort Collins. Figures were drafted by L. McCall of Colorado State University. This work was supported in part by NSF Grants ATM-8318846 and ATM-8407543 and ONR Contract N00014-84-C-0035.

# Modeling the Interstate Transport of Acidic Pollutants into Colorado

Douglas A. Latimer
Systems Applications, Inc.
101 Lucas Valley Road
San Rafael, CA 94903

August 15, 1986

## INTRODUCTION

This paper discusses the calculated impacts of regional emissions on air quality and acid deposition in Colorado, focussing on long-range, interstate transport. The calculations involved preliminary regional air quality modeling that was performed to assist the Environmental Protection Agency (EPA) and several other federal agencies which are evaluating alternative policies for regulating regional visibility in the Southwest (1).

## DESCRIPTION OF THE MODELING APPROACH

The modeling approach used in this study included application of the regional transport model RIVAD (Regional Impacts on Visibility and Acid Deposition) which was used to track plume transport, dispersion, deposition, and atmospheric chemical reactions for each of the urban areas and point sources evaluated.

RIVAD is a Lagrangian regional model specifically developed to cost-effectively evaluate source-specific and cumulative regional effects on air quality, wet and dry deposition, and visibility. Emissions in the model are treated as discrete plume segments, which are transported, dispersed, depleted by wet and dry deposition, and chemically converted to sulfates ($SO_4^=$)and nitrates ($NO_3^-$). Upper air and surface meteorological data from National Weather Service (NWS) stations throughout the region are spatially and temporally interpolated to determine transport winds, stability, temperature, relative humidity, and precipitation rates. In the RIVAD model emissions are released from each source every three hours in a year (about 2920 time steps) and are tracked until they are transported out of the region. The effect (diurnally and seasonally) of time-varying sun angles on UV flux and $SO_2 - SO_4^=$ conversion rates is included. The chemical module involves eight reactions among $NO$, $NO_2$, $O_3$, $O_2$, $SO_2$, $OH\cdot$, $H_2O$, and $O('D)$, so that nonlinear $NO$-to-$NO_2$, $NO_2$-to-$NO_3$, and $SO_2$-to-$SO_4^=$ chemical conversion can be computed as a function of time and plume concentration. This chemical module is similar to the one employed in the EPA plume visibility model PLUVUE (2).

For this study, relatively rapid $SO_2$ oxidation in urban areas and in clouds and fog was parameterized to achieve agreement with annual-average sulfate measurements in California. Nighttime nitric acid formation via the reaction with $N_2O_5$ was also parameterized. Organic aerosol formation from anthropogenic hydrocarbon emissions was treated using an approach suggested by smog

chamber studies (3). An aerosol equilibrium submodule was used to calculate the fraction of nitric acid in the aerosol phase and the amount of liquid water associated with sulfate and nitrate.

RIVAD's treatment of atmospheric dispersion considers buoyancy-induced turbulence during plume rise, turbulence as a function of atmospheric stability (parameterized using the Pasquill-Turner classification scheme), horizontal dispersion at large transport times and long distances caused by plume meandering and vertical wind shear, and vertical limits on dispersion imposed by the height of the spatially and temporally varying mixed layer.

In this study, the RIVAD model calculated seasonal and annual average concentrations of $SO_2$, $NO$, $NO_2$, and $HNO_3$, particulate matter (PM-2.5 and PM-10) and $SO_4$ aerosol, light extinction coefficients, visual range (or visibility), and wet and dry deposition rates for sulfur and nitrogen.

The model has been evaluated in detail by comparing model calculations with available measurements of sulfate concentrations in ambient air and in precipitation and light extinction and scattering (4). The model appears to perform well, predicting patterns of seasonal and annual averages with small biases and correlations approaching 0.8.

## REGIONAL EMISSIONS

For this study, emission inventories were developed by E. H. Pechan & Associates (5) for both the 1980 base year and the 1995 projection for the six-state modeling region (California, Nevada, Utah, Arizona, Colorado, and New Mexico). The 1980 base year emission inventory was developed from the National Acid Precipitation Assessment Program (NAPAP) inventory and was modified using specific information available for large point sources in the region (including the copper smelters in Mexico). The future (1995) scenario was based on growth and control factors for urban areas and development and control plans for large point sources.

In the Southwest, the principal sources of $SO_2$ include copper smelters, fossil-fueled power plants, and the petroleum industry (i.e., refineries and oil-field operations). Copper smelters in 1980 were estimated to contribute 54 percent of southwestern U.S. $SO_2$ emissions. $NO_x$ emissions originate principally from motor vehicles and power plants.

## EMISSIONS SOURCE CONTRIBUTIONS

The complete study (1) evaluated emission source category contributions to visibility impairment and trends in air quality, visibility, and acid deposition over the period 1980–1995. This paper uses unpublished results of this study to estimate the states and emission source categories that contribute to atmospheric concentrations of sulfate and nitrate, two species that can cause acid deposition. Calculations were performed for two potentially acid sensitive areas in Colorado—Flat Tops Wilderness in northwestern Colorado and Mesa Verde National Park in the southwestern corner of the state. The percent contributions of various states and source categories to annual average sulfate and nitrate concentrations in the atmosphere were calculated for the modeled year, 1981. Table 1 summarizes the results of these calculations.

Note for Flat Tops (Table 1a) Colorado sources are estimated to contribute only a small fraction of the annual atmospheric concentrations of sulfate and nitrate (i.e., 1.3 percent of the sulfate and 10.9 percent of the nitrate). Nearly half of the sulfate and nitrate is calculated to originate from outside the modeled six-state Southwest: Texas contributes a significant fraction of sulfate and Wyoming a significant fraction of nitrate. California contributes a significant fraction of the wilderness area's sulfate but a small amount of its nitrate, which is deposited more rapidly during transport. Besides California $SO_2$ sources, copper smelters in Arizona, Nevada and Utah are estimated to contribute heavily to annual sulfate levels in Flat Tops. According to these model calculations, urban areas in

TABLE 1. Percent contributions of various source regions and categories to annual average (1981) sulfate and nitrate concentrations

(a) In Flat Tops Wilderness Area

| Source Region/Category | Percent Contribution Sulfate | Nitrate |
|---|---|---|
| California | | |
| Urban Areas | 25.5 | 2.8 |
| Arizona | | |
| Urban Areas | 0.2 | 2.9 |
| Smelters | 7.0 | 0 |
| Power Plants | 1.8 | 9.9 |
| New Mexico | | |
| Urban Areas | 0.1 | 0 |
| Smelters | 0.3 | 0 |
| Power Plants | 1.0 | 9.9 |
| Nevada | | |
| Urban Areas | 0.1 | 1.4 |
| Smelters | 6.4 | 0 |
| Power Plants | 1.8 | 2.6 |
| Utah | | |
| Urban Areas | 1.0 | 20.5 |
| Smelters | 3.1 | 0 |
| Power Plants | 0.8 | 6.3 |
| Other States | 49.0 | 41.8 |
| Mexico | | |
| Smelters | 0.5 | 0 |
| Subtotal | 98.7 | 89.1 |
| Colorado | | |
| Urban Areas | 0.4 | 1.7 |
| Power Plants | 0.9 | 9.2 |
| Total | 100.0 | 100.0 |

TABLE 1. (Continued).

(b) In Mesa Verde

| Source Region/Category | Percent Contribution Sulfate | Nitrate |
|---|---|---|
| California | | |
| Urban Areas | 28.7 | 1.6 |
| Arizona | | |
| Urban Areas | 0.4 | 6.6 |
| Smelters | 15.7 | 0 |
| Power Plants | 4.0 | 37.7 |
| New Mexico | | |
| Urban Areas | 0.2 | 0.2 |
| Smelters | 0.7 | 0 |
| Power Plants | 3.9 | 24.7 |
| Nevada | | |
| Urban Areas | 0.2 | 0.9 |
| Smelters | 6.4 | 0 |
| Power Plants | 2.9 | 3.9 |
| Utah | | |
| Urban Areas | 0.8 | 5.6 |
| Smelters | 1.7 | 0 |
| Power Plants | 0.7 | 8.8 |
| Other States | 31.0 | 6.8 |
| Mexico | | |
| Smelters | 2.2 | 0 |
| Subtotal | 99.9 | 96.6 |
| Colorado | | |
| Urban Areas | 0.3 | 0.8 |
| Power Plants | 0.7 | 2.6 |
| Total | 100.0 | 100.0 |

Utah–principally the Salt Lake City area located upwind of Flat Tops–contribute a sizeable fraction of the annual atmospheric nitrate.

For Mesa Verde National Park, the contributing sources are somewhat different (see Table 1b). Only a small fraction of the sulfate and nitrate was attributed to sources within Colorado; 1.0 and 3.4 percent, respectively. Sources located in California and other states outside the modeled six-state Southwest contribute a large fraction of the annual average atmospheric concentration of sulfate. However, smelters in Arizona and New Mexico contribute relatively more to sulfate in Mesa Verde than in Flat Tops, presumably due to the fact that Mesa Verde is closer to these sources than Flat Tops. Due to the relative proximity of Mesa Verde to large power plants in neighboring states, power plants in Arizona, New Mexico and Utah are estimated to contribute 38, 25 and 9 percent, respectively, of the annual nitrate concentrations.

The above contributions are appropriate only for airborne concentrations and possible for dry deposition fluxes (which are roughly proportional to annual average atmospheric concentrations). Percentage source contributions for wet deposition would likely be considerably different since most sulfate and nitrate is deposited in the summer months.

Figure 1 shows the calculated emission source contributions to annual wet sulfur deposition (in 1981) in western Colorado. Note that copper smelters are estimated to be larger contributors to wet sulfur deposition (i.e., 36 percent) than they are to annual atmospheric sulfate concentrations (i.e., 17.3 percent in Flat Tops and 26.7 percent in Mesa Verde). This can be explained by the fact that in summer, when most wet deposition occurs, winds are predominantly southerly which would cause smelter emissions to be transported directly to Colorado.

## REFERENCES


1. Systems Applications, Inc., 1985. Modeling regional haze in the Southwest: A preliminary assesssment of source contributions. Draft report, SYSAPP/85-038, San Rafael, California.

2. Johnson, C.D., D.A. Latimer, R.W. Bergstrom, and H. Hogo, 1980. User's manual for the plume visibility model (PLUVUE). EPA-450/4-80-032, U.S. Environmental Protection Agency, Research Triangle Park, North Carolina.

3. Miller, D.F., and D.W. Joseph, 1976. Smog chamber studies on photochemical aerosol precursor relationships. U.S. Environmental Protection Agency, Research Triangle Park, North Carolina.

4. Latimer, D.A., L.R. Chinkin, M.C. Dudik, H. Hogo, and R.G. Ireson, 1985. Uncertainties associated with modeling regional haze in the Southwest. API Publication No. 4403, American Petroleum Institute, Washington, D.C.

5. E.H. Pechan and Associates, 1984. PSD and visibility analyses, 1980 emission inventory and 1995 projections. E.H. Pechan and Associates, Inc., Springfield, Virginia.

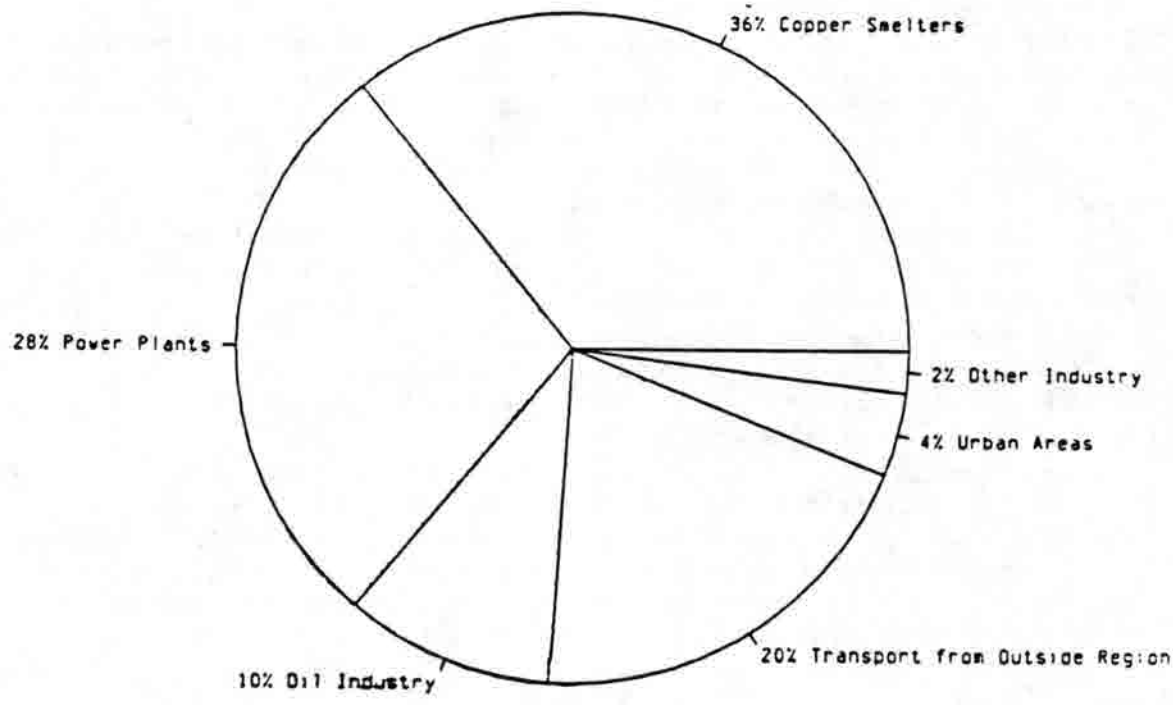


FIGURE 1. Estimated percent contributions of emission source categories to wet sulfur deposition in Colorado Rockies.

# Cloud Venting and Acid Deposition in Colorado

William R. Cotton
Department of Atmospheric Science
Colorado State University
and
Aster, Inc.
Fort Collins, Colorado

August 15, 1986

## INTRODUCTION

The term "cloud venting" refers to the process of transport of aerosol and gaseous matter including pollutants out of the boundary layer and into the cloud layer or middle and upper troposphere (Ching, 1982). Aerosol particles are readily scavenged by cloud droplets and precipitation elements, thereby being subjected to liquid-phase chemical reactions. Moreover, gases such as $SO_2$ undergo both gas-phase and liquid-phase transformations to sulfates and other aerosols. The ultimate fate of these species and their potential for becoming involved in acid wet depositions depends not only upon the chemical composition of the species but also on the extent to which the scavenged substances become involved in a precipitation process. We will show that the acid deposition of a particular species depends both on the precipitation efficiency of a cloud system and upon the actual nature of the precipitation process (i.e., an accretion-dominated process or a vapor deposition process).

In subsequent sections the processes involved in the scavenging of aerosols and gaseous matter will be reviewed. Cloud transport processes and precipitation processes will then be discussed for a variety of convective cloud types. Implications of these findings to Colorado acid deposition will then be made by considering the types of convective clouds which typically prevail over different portions of Colorado in the summertime.

## CLOUD SCAVENGING PROCESSES

Before we can consider the transport and wet deposition of acidic species, we must first recognize the various paths by which a gas such as $SO_2$ can be transformed into, say, sulfites and sulfates and thus contribute to the acid rain problem. One route is for gaseous matter such as $SO_2$ to be absorbed into liquid drops or ice particles. It can then dissolve in the hydrometeors where it will be subject to aqueous phase chemical reactions. The second route is for gas phase reactions to take place in the atmosphere; the resultant sulfate or nitrate aerosol particles will then become subject to being scavenged by the various hydrometeor species in a cloud. We shall see that the ultimate acid deposition at the surface by rainfall depends on the detailed precipitation processes in the cloud system, particularly when the ice phase is involved.

First let us consider an all-liquid cloud system. In this case the absorption or gaseous $SO_2$, for example, being a surface deposition process, is dominated by deposition onto small cloud droplets

as opposed to large raindrops. This is because ten-micron-sized cloud droplets have concentrations some 5 to 6 orders of magnitude greater than millimeter-sized raindrops. Moreover, because the surface-to-volume ratio is greater for small cloud droplets than for raindrops, the net surface area (summed over all drops) exposed by cloud droplets for surface absorption is orders of magnitude greater than it is for raindrops.

In the case of aerosol particles, the primary processes by which these particles are scavenged by a cloud system are:

1. Activation of the aerosol as cloud condensation nuclei or nucleation scavenging;
2. Brownian diffusion of the aerosol onto cloud droplets;
3. Thermophoretic and diffusiophoretic scavenging of aerosol;
4. Hydrodynamic capture of aerosol;
5. Electrical scavenging of particles.

Hydrodynamic capture is only important to the removal of the few aerosol particles that are quite large (i.e., greater than a few micrometers). Electrical scavenging appears to be only important in the intensely electrified regions of thunderstorms. By far the most important scavenging processes are (1), (2), and (3) with nucleation scavenging being the dominant process in the removal of sulfates and nitrates. Because thermophoresis dominates diffusiophoresis (Slinn and Hales, 1971), phoretic scavenging only enhances scavenging of submicron aerosol for evaporating droplets or ice crystals. Once embodied on cloud droplets and eligible for aqueous-phase reactions, the ultimate deposition of a chemical species on the ground depends on its involvement in a precipitation process. Cloud droplets are far too small to directly precipitate. Instead they contribute to rainfall by being collected by the larger cloud droplet and raindrop species. Thus the intensity of acid deposition by a non-ice-phase cloud is directly proportional to the precipitation efficiency (PE) of the cloud system. The PE of a cloud can be defined as the ratio of the precipitation rate to the flux of water vapor into the base of the cloud. We shall see that PE ranges from 10% or so to the order of 100%. Thus for a pure warm cloud the rate of acid deposition can vary widely. Those aerosol particles embodied in cloud droplets that have not become involved in rainfall will eventually be returned to the cloud-free atmosphere as the cloud droplets evaporate. They, of course, may have changed chemically or in size due to agglomeration and may have been transported vertically, perhaps to great heights.

In an ice-phase cloud the process of scavenging is even more complicated. In a mixed-phase cloud, nucleation scavenging of sulfates and nitrates still remains the principle scavenging process. Thus the aerosol particles become imbedded in cloud droplets. In an ice-phase cloud, however, the precipitation process can follow several different paths. One process is similar to an all-liquid cloud in which the cloud droplets are collected by larger precipitation elements (what we call a riming process). If this process is the prevalent precipitation process, then acid deposition will be proportional to the PE of the cloud as in an all-water cloud. However, as vapor deposition growth of ice crystals becomes more dominant as the major precipitation-forming process, the processes involved in the removal of acidic components that have become incorporated in cloud droplets become more complex. It is well known that as ice crystals grow in a water-saturated cloud, they do so at the expense of cloud droplets. That is, as the ice crystals grow by vapor deposition, they lower the supersaturation with respect to water causing the evaporation of cloud droplets. The evaporating droplets then release the dissolved gases and aerosol back to the atmosphere where they may migrate away from the cloud or be captured by other hydrometeors. Recapture of the released particles would be enhanced if the released particles are large enough for hydrodynamic capture or

if they encounter a large evaporating droplet or ice crystal and thereby become subject to phoretic scavenging. If recapture of released species is of secondary importance, then we would expect the wet deposition of trace substances to become less significant as vapor-grown crystals become the predominant contributor to snowfall. This is consistent with the findings of Scott (1981) and Borys, et al. (1983) who found that the pH of bulk snow collections decreased as the observed degree of crystal riming increased. This all makes sense until we examine the data reported by Lamb, et al. (1986). They designed a ground-based precipitation sampler which segregated the ice-phase precipitation elements according to fall velocity. The highest-fallspeed particles would generally be the more heavily rimed particles while the more vapor-grown crystals would be collected in the low fall velocity bin. They found in general that the highest ionic concentrations resided in the lowest fallspeed bin. This result seems quite inconsistent with Borys, et al.'s bulk measurements. The reason for the differences is not immediately obvious. Lamb, et al. interpret their results to imply that the vapor-grown crystals have the highest cross-sectional area and therefore when falling through a given depth will collect the greatest amount of particulates. They ignore the fact, however, that the collection efficiencies for such slowly falling crystals is generally quite small. It is for this reason that such crystals accrete few cloud droplets.

Borys (personal communication) has suggested that the difference may be due to the fact that Borys, et al.'s observations were taken in-cloud at a mountain observation site in the Park Range while Lamb, et al.'s were taken below cloud base. As the ice crystals settle through a dry subcloud layer, they evaporate concentrating any acids that may have accumulated. Furthermore, as the crystals sublime in the dry subcloud layer, phoretic scavenging of aerosol is enhanced, increasing the opportunity for increasing the concentrations of acidic material. Whatever the answer to this puzzle may be, we see that ice-phase precipitation processes greatly complicate our ability to understand acid deposition processes.

Nonetheless, while the particular form of precipitation particle is important to acid deposition, the major factor regulating acid deposition is the precipitation efficiency of the storm system. This is particularly true with regard to the more heavily precipitating summer convective storms. We shall now examine some of the cloud dynamic factors regulating storm PE and convective transport.

## CLOUD TRANSPORT PROCESSES AND PRECIPITATION EFFICIENCIES

In this section we will review the various types of convective clouds and examine their role in cloud venting and acid deposition. Our discussion will range from shallow boundary-layer-confined cumuli to ordinary thunderstorms to severe convective storms and finally to mesoscale convective systems.

### Boundary-layer-confined Cumuli

By boundary-layer-confined cumuli, we mean convective clouds whose tops are capped by an inversion at the top of the mixed layer. Such clouds may be considered as extensions of the dry boundary layer. In some cases they take the form of near solid stratocumulus cloud decks (see Fig. 1) or of more isolated cumulus elements (see Fig. 2). By providing an additional energy source to the boundary layer these contribute to a deepening of the boundary layer and in some cases to clouds greatly enhanced entrainment at the top of the mixed layer. If we consider cloud venting as an exhaustion of pollutants out of the boundary layer, then boundary-layer-confined cumuli are not in the strictest sense "cloud venters." They simply contribute to an intensification of the vertical mixing process. Nonetheless they do provide an aqueous-phase environment for chemical reactions to take place. In the more maritime, warm-based cumuli, they can also produce drizzle which, in turn, can result in acid deposition. In the summer in Colorado, boundary-layer-confined cumuli are typically so cold-based and continental in structure that they do not produce precipitation. In the

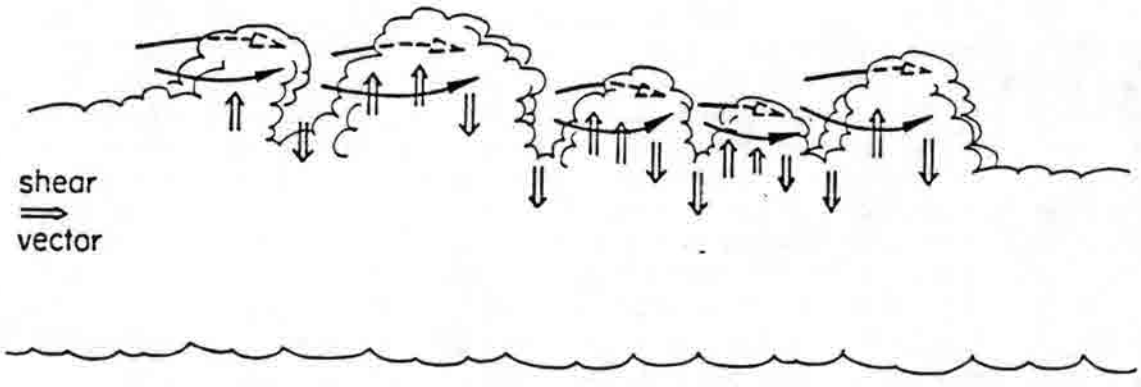


Figure 1. Illustration of the interaction of updrafts and vertical shear of the horizontal wind forming penetrative downdrafts downshear. (From Cotton and Anthes, 1987.)

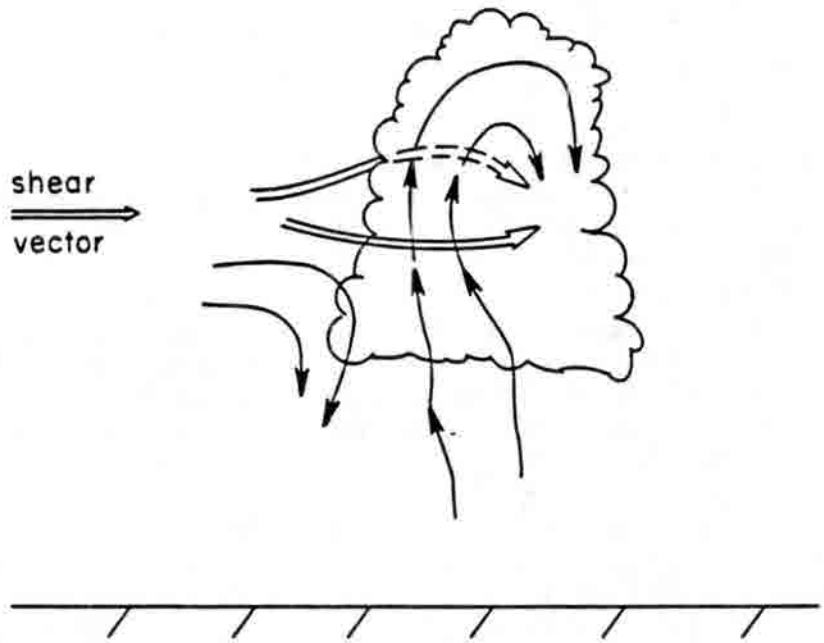


Figure 2. Illustration of circulations in boundary-layer-confined cumuli affecting vertical transport processes and entrainment. (From Cotton and Anthes, 1987.)

winter time orographic cloud environment, however, ice-phase vapor deposition growth and riming can contribute to significant precipitation from such shallow cumuli. Thus they have the potential for contributing to acid deposition without actually venting material out of the boundary layer.

### Towering Cumuli

Towering cumulus clouds or cumulus congestus are convective clouds which penetrate to heights in the troposphere much greater than the depth of the mixed layer or planetary boundary layer. In some cases, towering cumuli may penetrate through the entire depth of the troposphere. Towering cumuli may be found as relatively isolated clouds or in small clusters as shown in Figure 3a. Towering cumuli are also frequently found as a line of flanking clouds associated with multicellular thunderstorms.

Towering cumulus clouds are characterized by updrafts which extend through much of their depth. Downdrafts with vertical extent of the order of 1 to 2 km are also frequently found. Entrainment appears to occur principally laterally on the downshear side of the updraft, and by mixing through the tops of the rising towers. Updrafts in the rising towers can be quite vigorous, sometimes exceeding 20-25 m/s although more typically being of the order of 10 m/s. The term cloud venting is certainly appropriate for towering cumuli.

Precipitation from towering cumulus clouds normally occurs in an early formative stage since the lifetime of the cumulus elements is quite short, being of the order of 15-20 min. In cold-based, continental clouds, such as occur in Colorado, precipitation from these clouds is normally light to moderate in intensity. Some warm-based, maritime towering cumuli such as exist in the tropics can produce short-lived, intense showers. In general towering cumulus clouds are characterized by relatively low precipitation efficiencies owing to the diluting effects of entrainment and to their short lifetimes. As a consequence, towering cumulus clouds, in general, are not major contributors to acid precipitation except in locations such as mountaintop regions where they occur over a given site with a high frequency.

As we shall see, the towering cumulus stage is just one of several stages in the life cycle of ordinary multicellular thunderstorms. Many towering cumuli, however, never participate in the formation of cumulonimbi.

### Ordinary Single-cell Thunderstorms

The ordinary, single-cell thunderstorm is just one of many forms of cumulonimbi (thunderstorm). It is, however, the most common form of thunderstorm. This is the storm system type that Byers and Braham (1947) referred to as airmass thunderstorms. Figures 3a,b,c illustrate the three stages in the life cycle of an ordinary, single-cell thunderstorm as characterized by Byers and Braham (1947). The first stage was referred by Byers and Braham as the growth stage. It could also be called the towering cumulus stage. As with isolated towering cumuli, this stage is characterized principally by updrafts extending through much of the depth of the cloud towers. Quite frequently the towers are forced by a common region of subcloud convergence driven by a variety of mesoscale or larger-scale circulations.

The transition to the mature stage illustrated in Fig. 3b, is frequently characterized by the merger of neighboring convective towers. Precipitation formed during the growth stage in the towering cumuli settles into the subcloud layer where it evaporates, contributing to the formation of a cloud outflow pool. A gust front forms at the boundary of the outflow pool which contributes to the flow of warm, moist air into the updraft by lifting the low-level air. During the mature stage, updrafts may extend through much of the vertical extent of the cloud system. Downdrafts may simultaneously coexist with the updrafts. Typically the downdrafts extend from the middle troposphere to the surface. Downdrafts of lesser vertical extent may exist at any level in the cloud system.

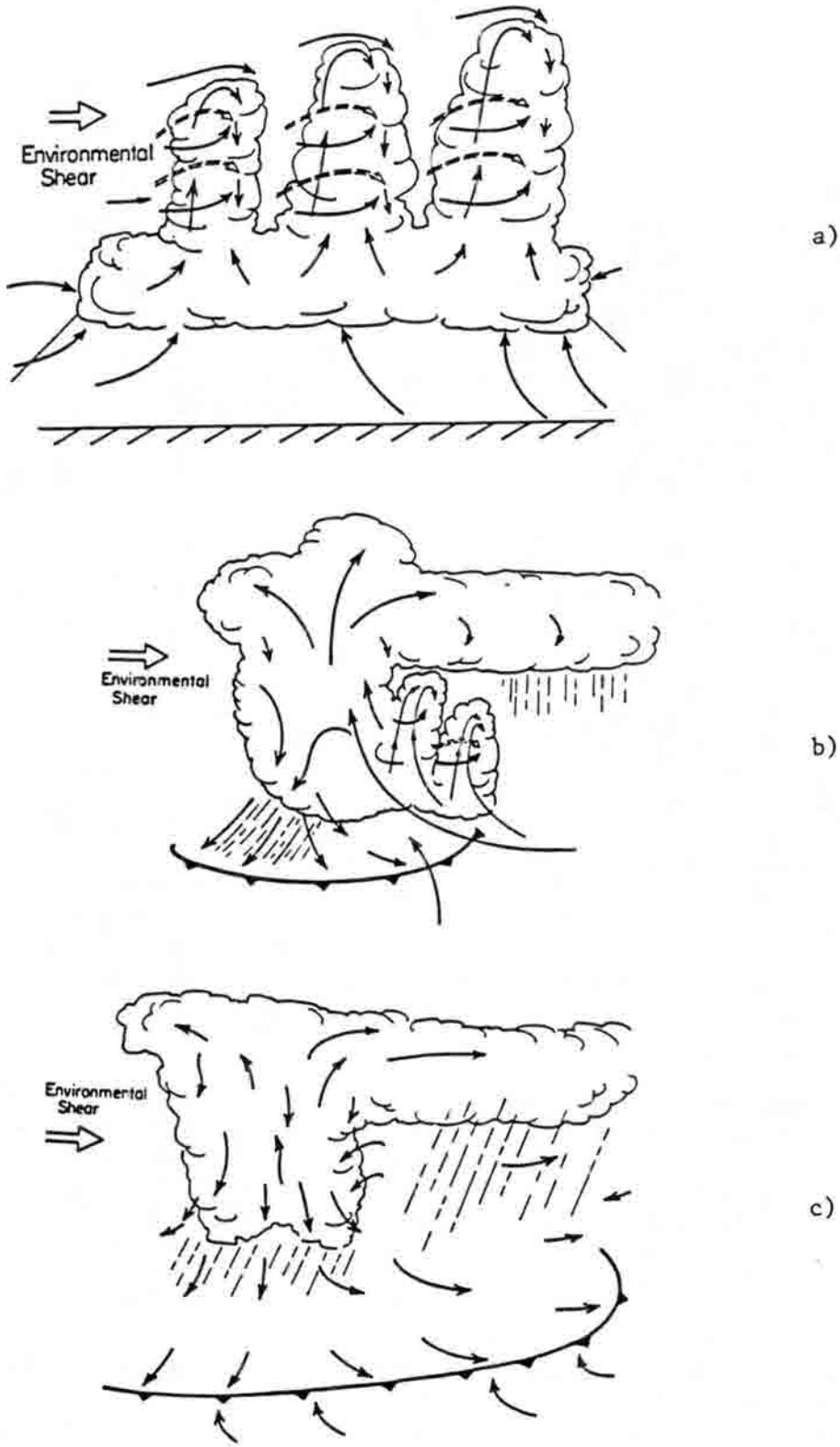


Figure 3. Schematic model of the lifecycle of an ordinary thunderstorm. (a) growth or cumulus stage, (b) mature stage, and (c) dissipating stage. (From Cotton and Anthes, 1987.)

Some of the updraft air is deposited in the upper troposphere in the stratiform anvil cloud. Some of it is mixed with the dry environmental air in the lower-level troposphere. Another portion of the updraft air achieves negative buoyancy as a consequence of water loading from precipitation falling into it, melting, and evaporative cooling as a result of mixing and downdraft air. This portion of the updraft air forms what Knupp (1985) called the 'up-down' downdraft component.

Eventually the gust front at the fringe of the diverging, cool, low-level outflow, outruns the updraft such that the air lifted by it can no longer fuel the updraft. The storm then enters its dissipating stage as shown in Fig. 3c. At this stage the storm is characterized primarily by downdrafts. Rainfall rates diminish with time.

The typical lifetime of an ordinary, single-cell thunderstorm from growth to dissipation stage is 45-60 min.

**Supercell Thunderstorm**

A constrasting storm type to the ordinary thunderstorm is the supercell storm. Following the growth stage and possibly storm-splitting (Klemp and Wilhelmson, 1978a,b), a long-lived, single cell thunderstorm occurs on occasion. The supercell storm, also referred to as a severe right-moving storm, is illustrated in Fig. 4. Such storms normally form in strong wind shears and are characterized by intense updrafts of order of magnitude of 3-35 m/s. Also present is a systematic inflow at middle levels which wraps around the updraft and descends to the surface in vigorous downdrafts. These storms are frequently, if not always, characterized as rotating storms. Rotation gives the storm inertial stability which contributes to its longevity. Another consequence of rotation is that updraft air is drawn into the convective storm by lower pressure aloft rather than by mechanically lifting by the gust front alone. Supercell storms also exhibit a distinctive radar echo feature. As a consequence of the strength of updrafts and/or their rotation, precipitation is unable to form at low to mid-levels in the updraft core. As a result an echo-free vault or bounded weak echo region forms. Precipitation forms at the fringe of the updrafts or in downdraft regions, often in the form of large hailstones.

Typical lifetimes of supercell storms ranges from 2-2.5 hours. During their lifetime supercells may spawn tornadoes, large hailstones, and severe wind gusts.

**Multicell Thunderstorms**

Ordinary, single-cell thunderstorms and supercell thunderstorms represent two ends of the spectrum of thunderstorm types. Between these two extremes lie a variety of multicell thunderstorm types which are more or less organized in terms of mesoscale circulations. As the name implies, the multicell storm is typically composed of two to four cells at a given time. At any time some cells may be in the cumulus stage, others in the mature stage, and others in the dissipating stage of a cumulonimbus cell. Horizontal and vertical radar depictions of a multicell storm at various times in the life cycle of a cumulonimbus cell are shown in Fig. 5. New cells form on the right flank of the complex and as they evolve through their lifecycle they either grow rapidly to become the new parent cell or move into the parent cell's circulation and merge with the parent cell.

The lifetime of individual cells is similar to that for ordinary thunderstorm cells, while the lifetime of the entire storm system may be several hours. Some multicell storms can be quite severe with updraft/downdraft strengths similar to those in supercells and comparable severe weather occurrences. Generally, however, multicell storms are less severe than the supercell storm. Some multicell storms, called organized multicellular storms by Foote and Wade (1982), exhibit a flow structure similar to supercell storms. Fig. 6 illustrates several branches of convective updrafts which penetrate through the depth of the troposphere. Likewise several downdraft components are illustrated, one of which wraps around the updraft as in the supercell model depicted in Fig. 4.

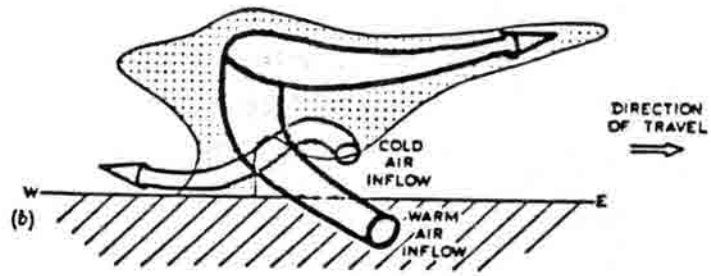


Figure 4. Model showing the airflow within a 3-dimensional SR storm travelling to the right of the tropospheric winds. The extent of precipitation is lightly stippled and the up and downdraught circulations are shown more heavily stippled. Air is shown entering and leaving the updraught with a component into the plane of the diagram. However, the principal difference of this organization is that cold air inflow, entering from outside the plane of the vertical section, produces a downdraught ahead of the updraught rather than behind it. (From Browning, 1965.)

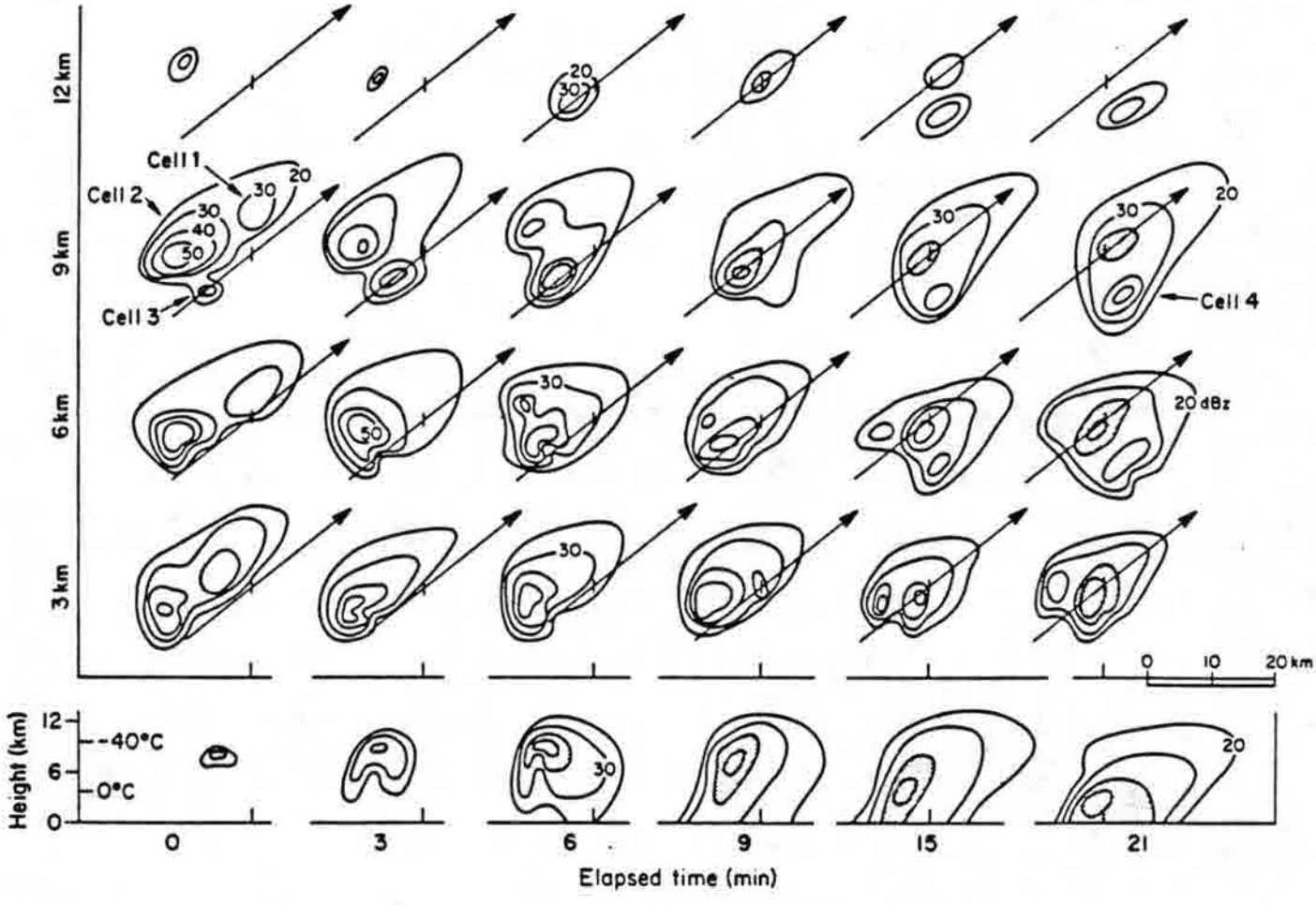


Figure 5. Schematic horizontal and vertical radar sections for an ordinary multicell storm at various stages during its evolution showing reflectivity contours at 10 dBZ intervals. Horizontal sections are illustrated for four altitudes (3, 6, 9 and 12 km AGL) at six different times. The arrow superimposed on each section depicts the direction of cell motion and is also a geographical reference line for the vertical sections at the bottom of the figure. Cell 3 is shaded to emphasize the history of an individual cell. [From Chisholm and Renick, 1972.]

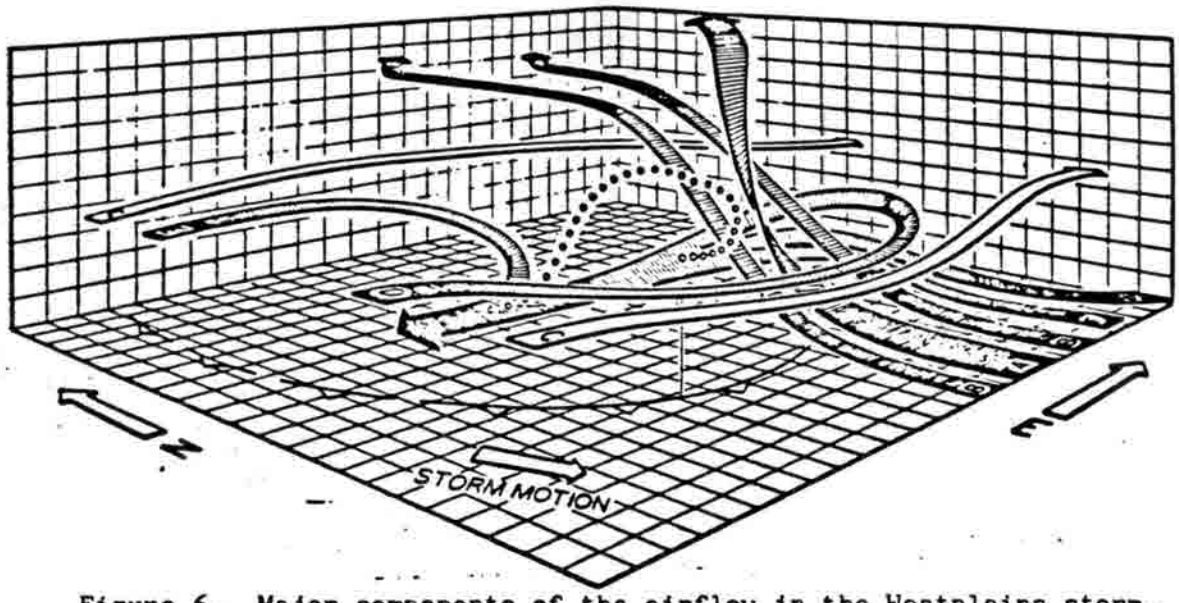


Figure 6. Major components of the airflow in the Westplains storm. The strong updraft is depicted by the ribbon labeled A, which starts in the low levels to the south-southeast of the storm, rises sharply in the storm interior, and leaves the storm toward the northeast to form the anvil outflow. On the flanks of the strong updraft the air rises more slowly and penetrates farther to the rear of the storm before also turning to the northeast. In the middle levels there is a tendency for the westerly environmental flow to be diverted around the sides of the storm (streamlines labeled C) but some air also enters the storm (streamlines D and E) and contributes to the downdraft. A contribution to the downdraft flux is also made by air originally in the low levels to th southeast and east of the storm (streamlines F and G), which then rises several kilometers before turning downward in the vicinity of the echo core. The various streamlines are depicted relative to the storm, which is moving toward the south-southeast as shown, rather than relative to the ground. The small circles indicate the possible trajectory of a hailstone. (From Foote and Frank, 1983).

There is some evidence that the entire storm system may be rotating on the mesoscale similar to a supercell (Schmidt, 1985).

It is obvious that thunderstorms, regardless of type, result in a large vertical exchange of upper and lower tropospheric air.

**Squall Line Thunderstorms**

Up to this point we have described thunderstorm systems whose horizontal dimensions may be on the order of 30-60 km. Occasionally thunderstorms organize into what we call mesoscale convective systems whose maximum horizontal dimension may exceed several hundred kilometers. One form of mesoscale convective system (MCS) is the squall line thunderstorm. As its name implies, the squall line storm is organized in a linear structure. The long axis of the storm may range from 70-200 km and in the case of pre-frontal squall lines it may be as large as 1200 km. The cross-line axis may range from 30 to over 100 km. Like a multicell thunderstorm, the squall line is composed of a number of thunderstorm cells. New cells typically form on the southern flank of the line and progress northward relative to the line during their lifetime. The cells may actually be supercell storms in the case of severe pre-frontal squall lines. Naturally the transport processes or cloud venting is determined by the particular characteristics of the individual cellular units. Fig. 7 illustrates a particularly intense pre-frontal squall line storm.

Squall lines generally form in strongly-sheared environments and as such they are relatively fast moving system ($\sim$ 25–30 m/s). While the rainfall rates in squall line storms may be quite intense, owing to their fast movement, the rainfall they deposit on the ground is typically no greater than 5–10 cm.

**Mesoscale Convective Complexes**

Perhaps the ultimate in thunderstorm systems affecting the Colorado area is the mesoscale convective complex (MCC). The horizontal dimensions of MCCs frequently exceed several hundred kilometers. Their lifetimes typically range from 6 to 18 hrs with some surviving for several days. During the growth stage of the MCC the cell structure varies from rather randomly organized multicellular units to smaller squall line units. Fig. 8 illustrates a particular thunderstorm organization and the extent of the stratiform region. As can be seen from Fig. 9, the MCC is characterized by intense convective rainfall early in its lifecycle which transforms into light stratiform rainfall as it evolves into its dissipating stage. Because MCCs develop in relatively weakly-sheared environments and survive for 18–24 hrs, they can dump in excess of 25 cm of rainfall over a given area.

As shown by Lyons, et al. (1986) an MCC can cleanse an area in excess of 500,000 $km^2$, transporting the air aloft in convective-scale and mesoscale downdrafts and replacing it with middle tropospheric air. Pollutants transported aloft, of course, can be scavenged by the cloud system thus contributing to acid deposition. Some of the pollutants will be transported into the upper tropospheric stratiform cloud where they may be deposited some distance away from the convective system in stratiform rainfall.

**Precipitation Efficiencies**

There have been only a few estimates of the precipitation efficiency of ordinary, single-cell thunderstorms. Braham (1952) estimated the water budget of Florida and Ohio ordinary, single-cell thunderstorms. Based on his data, the precipitation efficiency for such storms was slightly less than 20%. Since ordinary thunderstorms generally form in weak-wind-shear environments, one would expect that Braham's estimates should be comparable to Marwitz' (1972) estimates of precipitation efficiencies for High Plains thunderstorms (see Fig. 10). However, Fig. 10 suggests that in

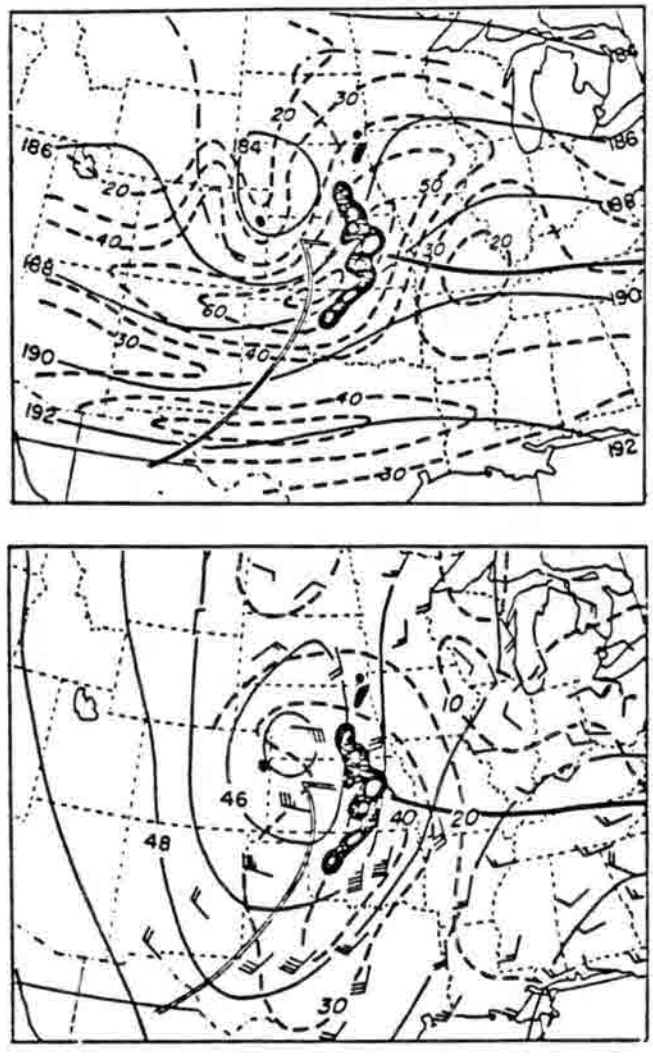


Figure 7. (a) 500-mb and (b) 850-mb charts, 2100 CST 20 May 1949. Solid lines, contours (hundreds of ft); dashed lines, isotachs (kn); thin double lines, surface fronts. Blacked-in areas, rainfall in excess of 0.20 in per hour; inner light areas, 0.50 in or more. [From Newton and Newton, 1959].

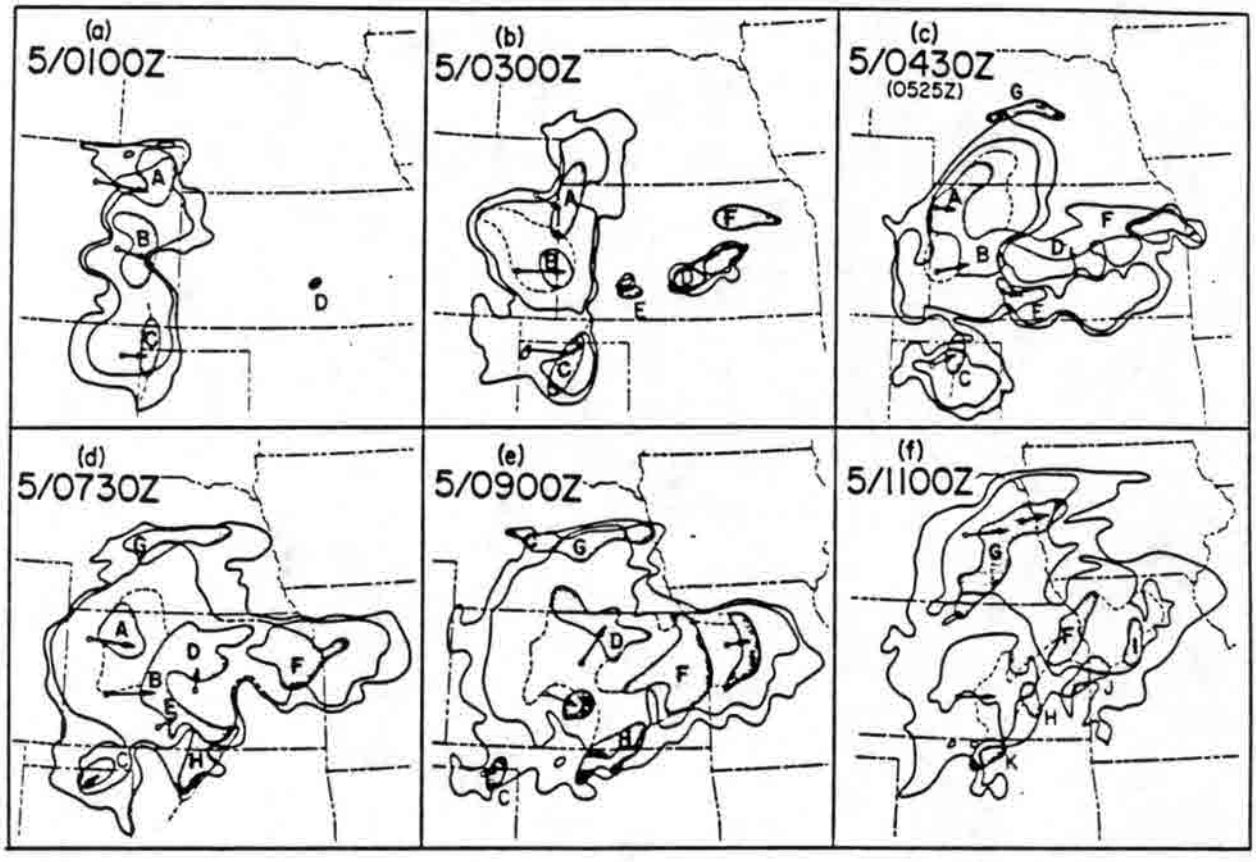


Figure 8. Schematic IR satellite and radar analysis, from 01 to 11 GMT 5 Aug 1977, for the western MCC #2, similar to Fig. 6. Dashed portions of IR contours [as in northeast Kansas in (d)] are estimated positions when the contours are ill-defined in the imagery. The second time label in (c), 0525 GMT, denotes a radar analysis time differing from the hour of the IR image, 0430 GMT. [From McAnelly and Cotton, 1986.]

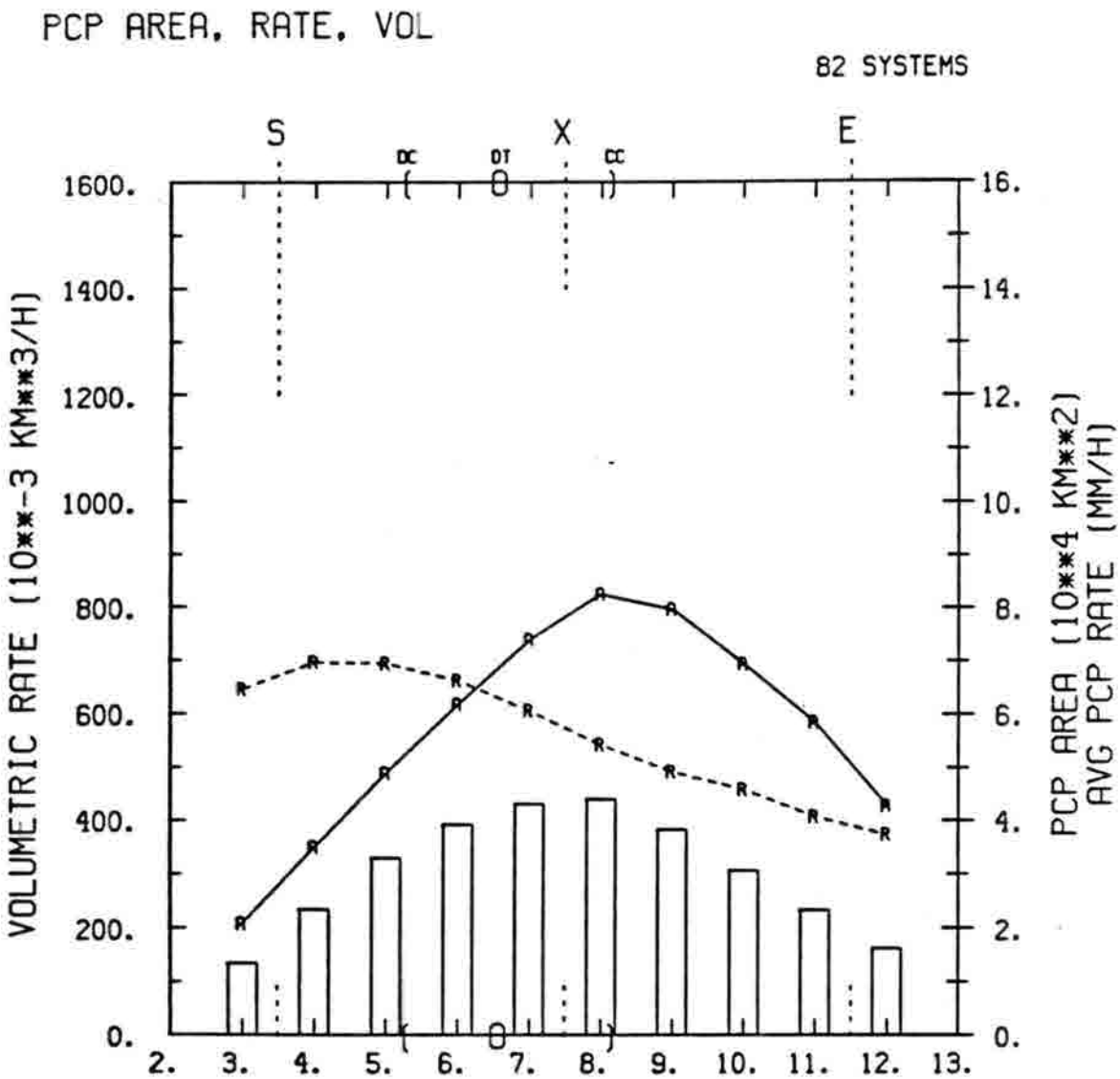


**Figure 9.** Time evolution of MCC precipitation characteristics, averaged over 82 systems. The time scale represents a normalized life-cycle (based on satellite-observed cloud shield size), where the MCC is defined to start, maximize, and end at times 3.5, 7.5 and 11.5, respectively. Solid curve shows area of active precipitation, and dashed curve shows average rainfall rate within that area. Their product gives the volumetric rainfall rate of the MCC, depicted by the bars. (From Cotton and Anthes, 1987.)

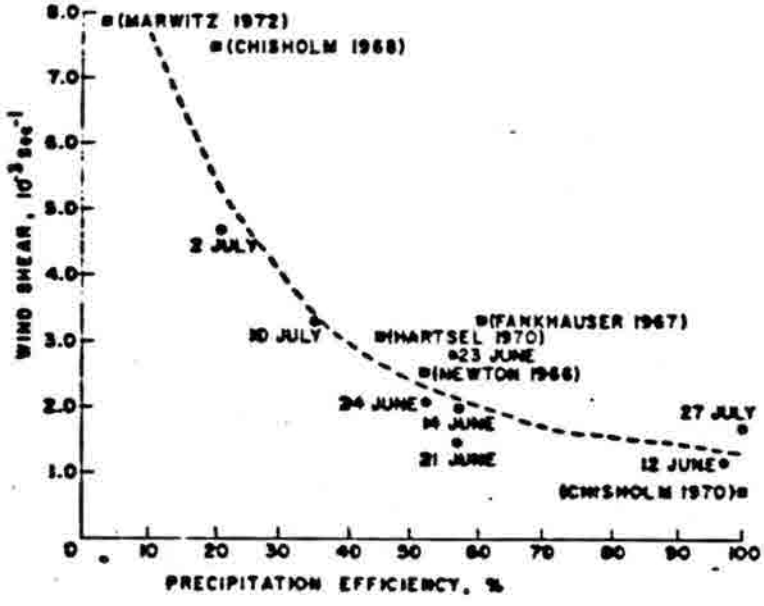


Figure 10. Scatter diagram of wind shear versus precipitation efficiency for 14 thunderstorms which occurred on the High Plains of North America. Data points from Auer and Marwitz are indicated by dots. Dashed line was free-hand fitted to data (From Marwitz, 1972d).

weakly-sheared environments, the precipitation efficiency should be 90% or greater. The discrepancy probably lies with the fact that the High Plains storms compiled by Marwitz are not ordinary thunderstorms but better organized multicellular storms.

Fig. 10 also illustrates that in the more strongly-sheared environment the precipitation efficiency may be as low as 10%. This reflects the preference for supercell storm occurrence in highly sheared environments. Apparently as a result of their intense updrafts, a large fraction of the water entering the base of such storms is detrained in large anvil clouds or evaporated in their intense downdrafts.

We have learned in recent years that wind shear is not the best index of storm type in a given environment. Weisman and Klemp (1984) proposed that the bulk Richardson number $R_i$, defined as $R_i = Buoyancy/0.5\Delta\bar{u}^{-2}$ where $\Delta\bar{u}$ is the difference between environmental wind speeds at low and mid-levels. The Richardson number is a better discriminator of storm stype than the wind shear. Under conditions of low values of $R_i$ supercells prevail whereas multicells prevail for larger values of $R_i$. Clearly one should evaluate the variation of precipitation efficiency with $R_i$.

Only a few estimates have been made of the precipitation efficiencies of mesoscale convective systems. Newton (1966) estimated the precipitation efficiency of a severe pre-frontal squall line to be 45–53%. Recently Lin (1986) estimated the PE of MCCs to be of similar magnitude during their developmental stages. He found, however, that the PE exceeded 100% during the MCC mature stage due to water stored in the stratiform region during its growth stages.

## CLOUD VENTING AND ACID DEPOSITION IN COLORADO

Our discussion thus far has been relatively general in its focus. We will now direct our attention to Colorado convective storms and to the process of cloud venting and acid deposition in Colorado. The emphasis in our discussion will be on summer convective storms. On occasion, deep convective clouds occur in the mountains in winter, the frequency of such events, however, is quite low. Therefore the contributions of deep convective clouds to cloud venting and acid deposition in the wintertime is probably small in a climatological sense. The occurrence of shallow cumuli in the wintertime in Colorado is quite high. We have noted that such clouds cannot be considered cloud venters because they simply mix the boundary-layer airmass or a middle-level airmass exhibiting potential instability. That is not to say that such shallow cumuli are not important contributors to wintertime acid deposition. Indeed, the wintertime orographic cumuli over the Rockies can be efficient producers of precipitation, especially the more heavily rimed forms of ice-phase precipitation. They can therefore be considered important contributors of acid wet deposition. Overall, wintertime orographic precipitation accounts for 70% of the annual precipitation in the high mountainous terrain.

It is in the summertime that the deep convective clouds which we can truly call cloud venters prevail. The size distribution, intensity and type of deep convective cloud in Colorado varies with the time of day, location, and season. While convective precipitation predominates in the summer months over the mountainous terrain, it contributes only 30% to annual amounts. Over the eastern Colorado plains and lower-lying terrain over western Colorado convective precipitation accounts for 65 to 50%, respectively. The late spring months of April, May and June are noted for the formation of the severe forms of convection, particularly over the eastern plains. During periods of frontal passage severe squall line thunderstorms, supercells, and severe multicellular storms may occur anywhere over the Colorado plains. Precipitation can be intense from these systems but it is also likely to be accompanied by large hailstones. The thunderstorms which occur under severe weather conditions are often those that occur during high wind shear conditions or small convective Richardson numbers. As a result those storms generally exhibit low precipitation efficiencies. They are the storms that exemplify the cloud venting process. Much of the gaseous and aerosol pollutants

that have built up along the Front Range will be exhausted from the lower layers and deposited in the mid to upper troposphere. The polluted boundary-layer air will in turn be replaced with the cleaner middle and lower tropospheric air which resides above the boundary layer. Thus in general, these storms will cleanse the low-level airmass. The pollutants deposited in the middle and upper troposphere will for the most part be transported out of Colorado to an unknown destination. Perhaps some of the material will be washed out in more stratiform precipitation over the High Plains to the east.

As the season progresses into July, a characteristic flow pattern becomes established. By mid-July the southwest monsoon normally develops which imports moist air from the southwest into the Colorado mountains. This flow is characterized by generally weak southwesterly flow from mountain-top levels through most of the troposphere. Less frequently, a well developed southeasterly flow develops around the western branch of the sub-tropical high which imports warm, moist air from the Gulf of Mexico over the High Plains and occasionally along the Front Range. On the more regional scale, heating of the mountainous terrain during the daytime and cooling at night drives a diurnally-varying slope circulation. This slope circulation and its interaction with the prevailing synoptic flow has a major influence on the distribution and intensity of moist, deep convection. It also determines to a large extent the characteristics of the air masses which feed the convective storms. To illustrate this phenomenon, we display illustrations of a conceptual model developed by Triopoli (1986).

Figures 11–15 illustrate the flow fields, temperature fields, and pressure fields which Tripoli derived from two- and three-dimensional numerical simulations of the evolution of convection over Colorado. Depicted is an east-west cross section from the Utah border over the divide west of Leadville, eastward along the Palmer Lake divide, and extending into eastern Kansas. Figure 16 illustrates the integrated surface rainfall simulated by Tripoli for a 24-hour period starting at midnight. Throughout the nighttime, cooler air descends the mountain slopes and settled in the lower-lying terrain to the east. Over the plains, the presence of the cooler air beneath the warmer free air creates an inversion which is intense enough to inhibit most convection. As the sun rises, air near the ground is heated and an organized upslope circulation develops along both the eastern and western slopes of the Rocky Mountain barrier. The upslope flow glides upward along the barrier slopes beneath the capping inversion and generally carries moist air from the valley floors or the plains. The overlying capping inversion prevents the outbreak of cumulus clouds. Normally the first appearance of cumulus clouds occurs over the higher peaks where the capping inversion is thinnest and therefore most easily penetrated. These first cumuli usually appear between 9 and 10 in the morning. They rapidly grow into towering cumulus clouds which vent gases and aerosols transported by the organized slope flows from the lower-lying valleys and plains into the middle troposphere. By late morning light showers form in the towering cumuli. Being cold-based and continental cumulus clouds, precipitation is formed predominately by ice-phase processes. Heavily rimed graupel particles are the primary form of ice particle, though vapor-grown ice crystals and aggregates of ice crystals also contribute to the precipitation.

Between local noon and 2 P.M. the first cumulnimbi form. In response to convective heating, the shallow solenoidal field associated with surface heating of elevated terrain deepens through the entire depth of the troposphere. As a result of the interaction between the deep convection and the prevailing southwesterly flow aloft, a line of cumulonimbi (Cb) begin to propagate eastward (see Fig. 12). Clouds along the western slopes are suppressed by the solenoidal field modified by deep convection so that mainly towering cumuli prevail. Low-level air feeding the Cb's has its origins along the eastern slopes. Mid-level air feeding the downdrafts in the cells, however, has its origins

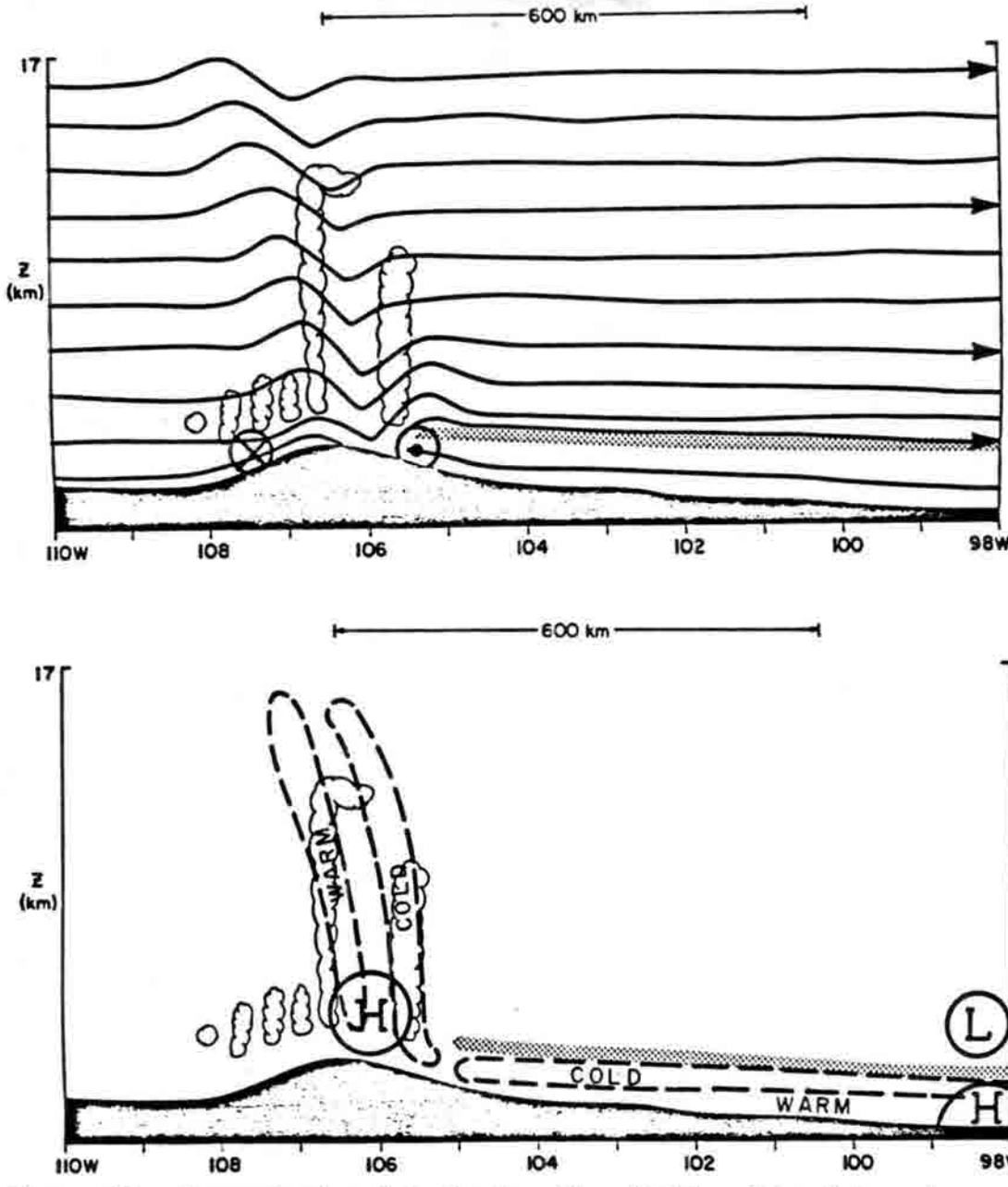


Figure 11. Conceptual model showing flow field and position of convective elements at time that deep convection forms. The surface topography is depicted by the black shading. The vertical axis is height in km above mean sea level (MSL) and the horizontal axis is west longitude. The stippled line represents the position of the plains inversion. Regions of cloud are indicated. Part (a) depicts the flow field with ground relative streamlines. Circles depict flow perturbation normal to plane. Part (b) depicts the pressure and temperature response. Pressure centers are depicted by solid closed contours and temperature by dashed contours. The length scale of 600 km (2L ) is indicated. (From Tripoli, 1986.)

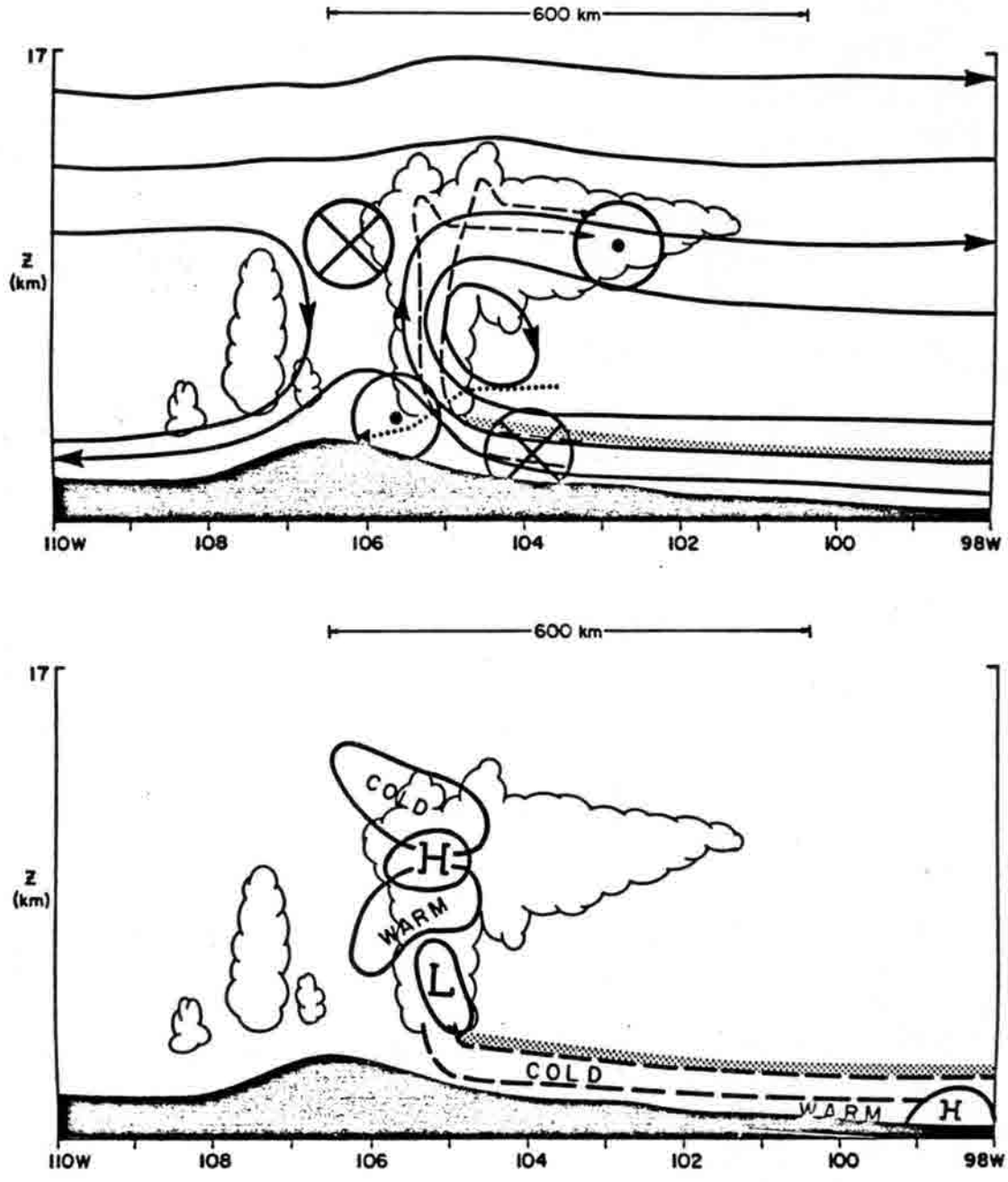


Figure 12. Same as Figure 11, except for Stage 3. Also flow is storm relative flow. Individual parcel paths are given by dashed (updraft) and dotted (downdraft) lines. (From Tripoli, 1986.)

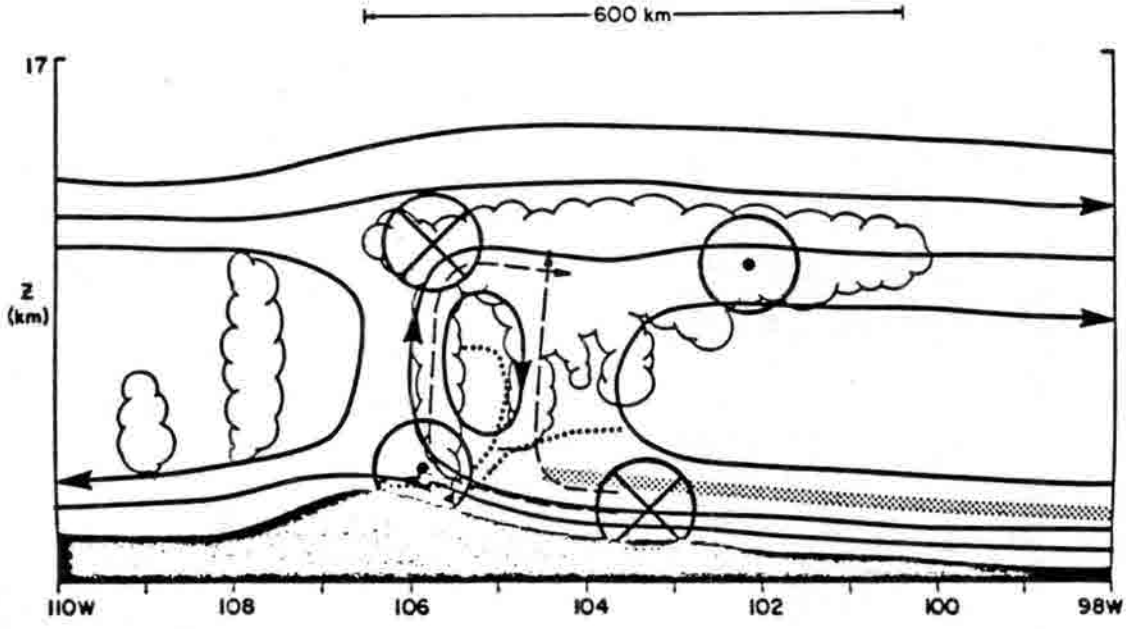


a.

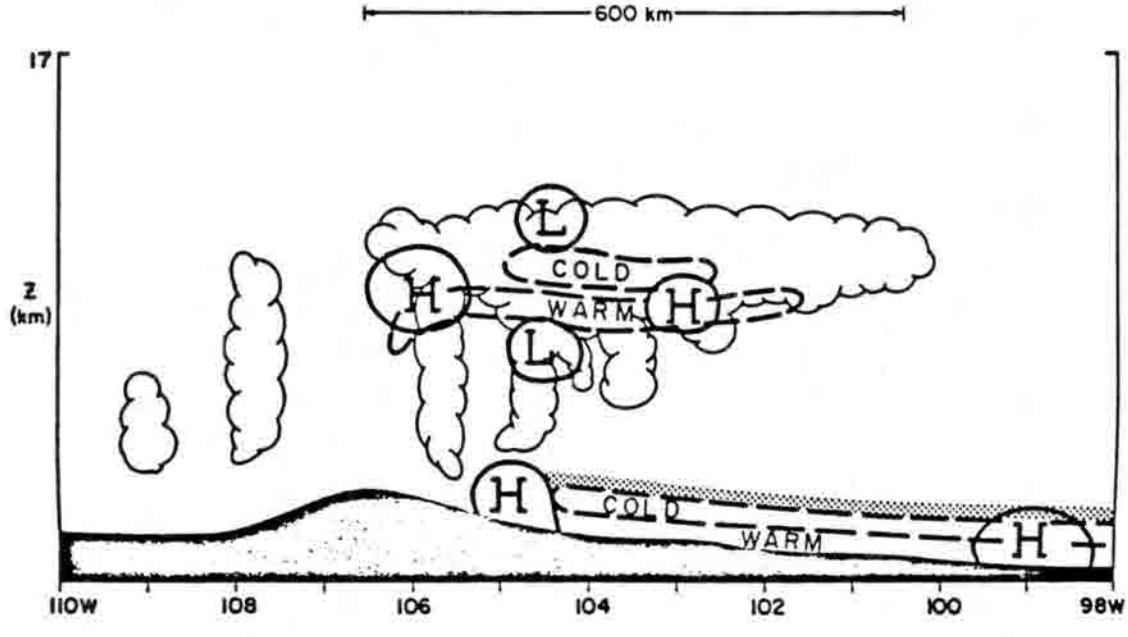


b.

Figure 13. Same as Figure 12, except for Stage 4. (From Tripoli, 1986.)

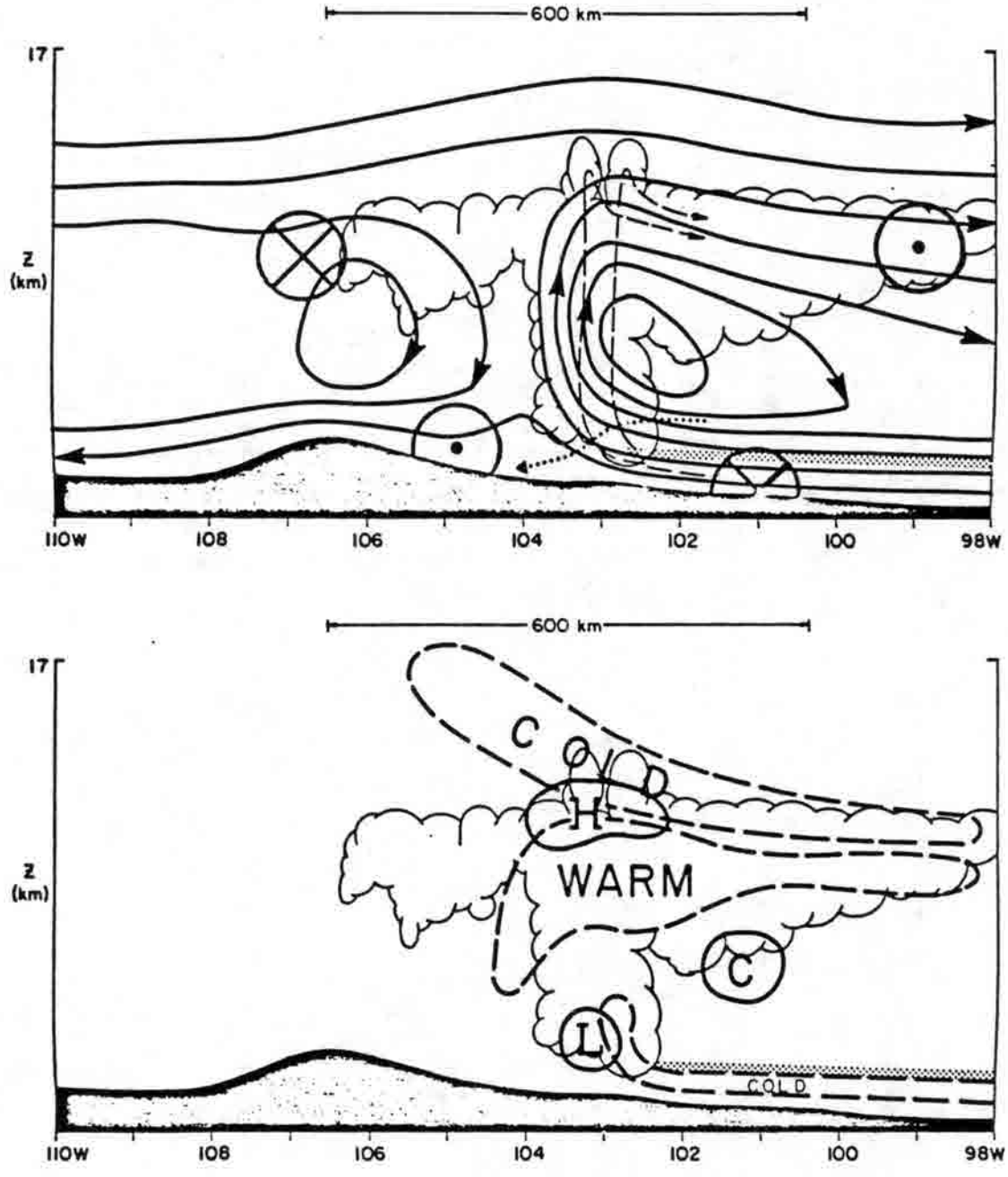


Figure 14. Same as Figure 13, except for Stage 5. (From Tripoli, 1986.)

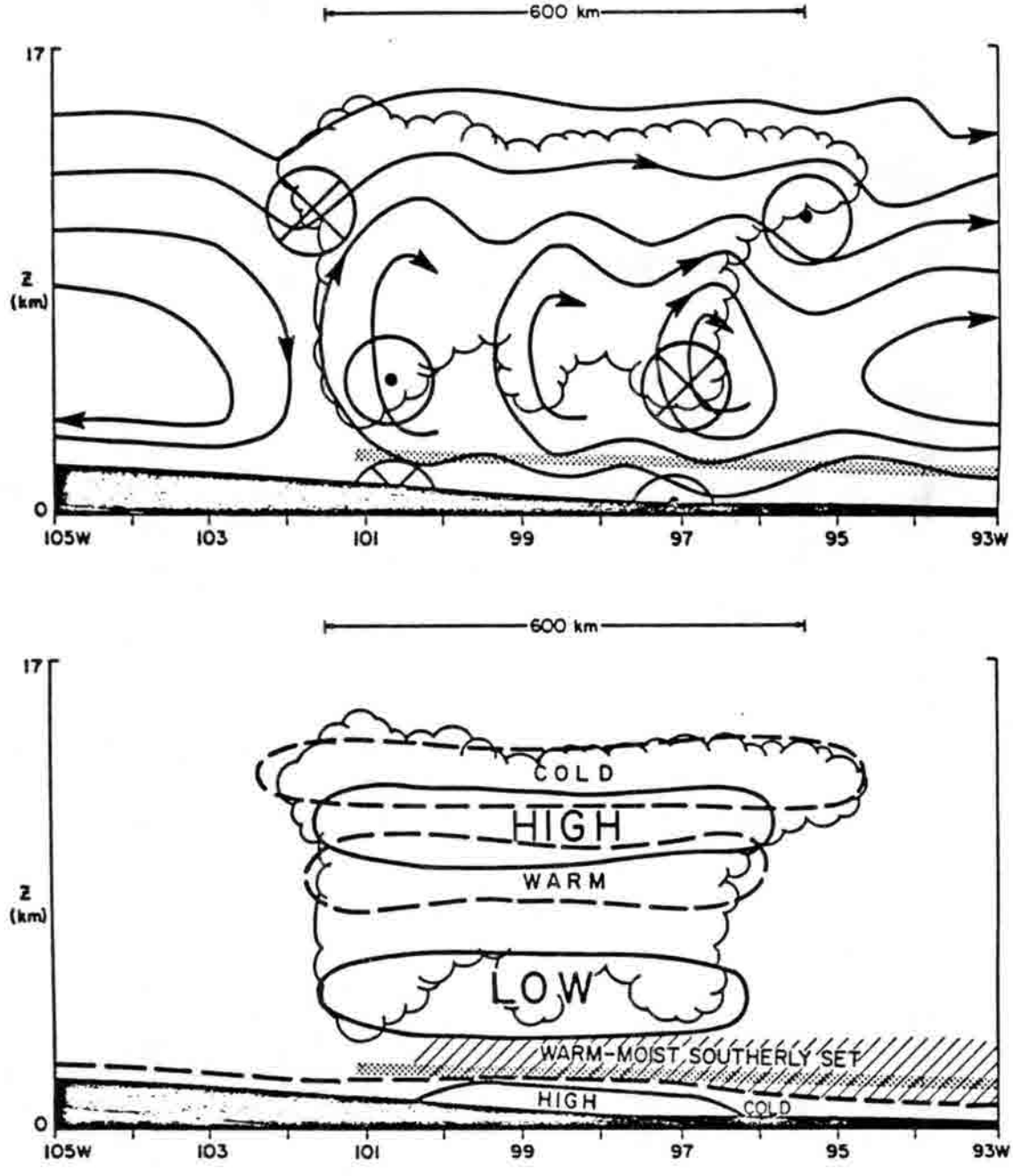


Figure 15. Same as Figure 14, except for Stage 6. Also, the region of the low level southerly jet is hatched. (From Tripoli, 1986.)

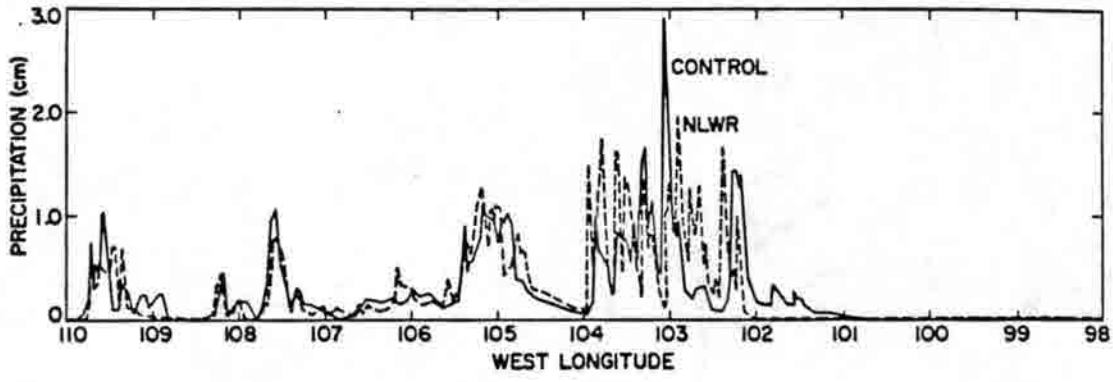


Figure 16. Accumulated precipitation in cm (vertical axis) versus horizontal location W longitude (horizontal axis). Curves for control case and NLWR case drawn. (From Tripoli, 1986.)

along the western slopes. The Cb's can be characterized as ordinary Cb's with PE's probably in the 25–45% range.

Between 4 and 6 P.M., typically the line of Cb's propagates off the mountains onto the plains. At the juncture between the steeply sloping mountains and the shallow sloping plains, the Cb's enter a zone of suppressed convection (see Fig. 13). Mainly dissipating Cb's prevail which are characterized by downdrafts and light to moderate rainfall. Fig. 16 illustrates the consequences of the suppressed convection on surface rainfall. On many occasions the Cb's are not able to survive the zone of suppressed convection and dissipate altogether. The fact that many of the convective clouds are dissipating or at least characterized by predominately downdrafts may have bearing on acid deposition and the quality of water precipitating along the Front Range. First of all, the air feeding the convective cells along the eastern slopes of the Rockies primarily has its origins in the highly urbanized Denver basin region extending from Colorado Springs to Fort Collins. During the lifecycle of the ordinary Cb's, there is plenty of opportunity for the gaseous and aerosol pollutants to be scavenged by the cloud system. As the clouds enter the suppression zone, the clouds collapse by creating evaporating downdrafts through much of the cloud layer, and evaporating precipitation elements in the dry sub-cloud layer. As the precipitation elements evaporate, any acids which may have formed in them now becomes more concentrated. Furthermore, as the cloud droplets, ice crystals, and raindrops partially evaporate, phoretic scavenging of aerosols is enhanced. Thus any sub-micron aerosol in the Front Range region will readily be scavenged by the partially-evaporating precipitation elements. One would thus expect the most acidic rainfall to occur in the suppressed zone of convection over the most populous portion of the state.

On many occasions convective cells can survive the suppression zone along the Front Range and enter a region where mesoscale ascent and moister air combine to favor intensification of the convective cells. It is in this region that the most intense Cb's in Colorado form and the largest amount of precipitation falls. Occasionally the Cb's are severe supercells and multicell storms which exhibit relatively low PE's. A great deal of the water condensed in their updrafts is convected into anvil clouds or evaporated in deep convective downdrafts. When a moist low-level jet resides over eastern Colorado and western Kansas, the intense Cb's may join in the formation of a large mesoscale convective system (see Fig. 15 or Fig. 8). Under these conditions Colorado may be an exporter of its pollution and acid rain since much of the pollutant exhaused in anvil clouds may settle out in the more stratiform rainfall of an MCC lying over Kansas or Nebraska.

Of course the particular scenario outlined here does not occur all the time during the summer in Colorado. Occasionally the ridge over Colorado may become so strong that the flow may be very weak through much of the depth of the troposphere. Under these conditions, convective cells do not propagate off the mountains and instead can remain anchored to the higher terrain. If the airmass at low levels is very moist, heavy-raining Cb's can form and sometimes these evolve to the scale of MCC's. Such storms can be the source of flash floods and may produce periods of steady, stratiform rainfall for 18 hours or longer. The Big Thompson flood was one example of such a storm. Because these storms form in relatively weak wind shear they are very efficient rain producers with PE's probably in excess of 85%. During their extended lifetime air feeding the storm may have its origins along the polluted eastern slope and/or the western slope. Such storms may be major contributors to acid precipitation, although the concentration of acid per drop may be low owing to the reduced evaporation in the moist subcloud layer.

## CONCLUDING REMARKS

This chapter has been a review of cloud scavenging processes, convective cloud types, and summertime cloud climatology for Colorado in terms of their impact on cloud venting and acid deposition

in Colorado. The discussion is largely descriptive in nature since little can be said about the quantitative details of cloud venting or of acid deposition, in general, or in Colorado specifically. Many of my comments regarding acid deposition in Colorado are quite speculative. They at best can be considered educated guesses based on the author's experience in modeling and observational analysis of convective storms in Colorado.


## ACKNOWLEDGEMENTS

Any original research reported here has been supported by the National Science Foundation under Grant ATM–8512480, the Air Force Geophysics Laboratory Contract F19628–84–C–0005, and Battelle Contract B–M2922–A–E to ASTeR, Inc. Mrs. Brenda Thompson and Nancy Duprey graciously typed the manuscript. Special thanks to Mike Moran for his careful editing of the manuscript.


## REFERENCES


Borys, R.D., P.J. DeMott, E.E. Hindman, and D. Feng, 1983. The significance of snow crystal and mountain-surface riming to the removal of atmospheric trace constituents from cold clouds. In Precipitation Scavenging, Dry Deposition, and Resuspension. Vol. 1, Precipitation Scavenging. H.R. Pruppacher, R.G. Semonin and W.G.N. Slinn, coordinators. Elsevier Science Publishing Co., Inc., New York, 181–189.

Braham, R.R., 1952. The water and energy budgets of the thunderstorm and their relation to thunderstorm development. *J. Meteor.*, **9**, 227–242.

Browning, K.A., 1965. Some inferences about the updraft within a severe local storm. *J. Atmos. Sci.*, **22**, 669–677.

Byers, H.R., and R.R. Braham, 1949. The Thunderstorm. U.S. Weather Bureau, Washington, D.C., 287 pp.

Ching, J., 1982. The role of convective clouds in venting ozone from the mixed layer. Preprints, 3rd Joint Conf. Applications of Air Pollution Meterology, January 12–15, San Antonio, TX. Amer. Meteor. Soc.

Chisholm, A.S., and J.H. Renick, 1972. The kinematics of multicell and supercell hailstorms. Alberta Hail Studies, Research Council of Alberta Hail Studies, Rep. 72-2, 24-32, 53 pp.

Cotton, W.R., and R.A. Anthes, 1987. The Dynamics of Clouds and Precipitating Mesosocale Systems. To be published by Academic Press.

Foote, G.B., and H.W. Frank, 1983. Case study of a hailstorm in Colorado. Part III: Airflow from triple-Doppler measurements. *J. Atmos. Sci.*, **40**, 686–707.

Foote, G.B., and C.G. Wade, 1982. Case study of a hailstorm in Colorado. Part I: Radar echo structure and evolution. *J. Atmos. Sci.*, **39**, 2828–2846.

Klemp, J.B., and R.B. Wilhelmson, 1978a. The simulation of three-dimensional convective storm dynamics. *J. Atmos. Sci.*, **35**, 1070–1096.

Klemp, J.B., and R.B. Wilhelmson, 1978b. Simulations of right- and left-moving storms produced through storm splitting. *J. Atmos. Sci.*, **35**, 1097–1110.

Knupp, K.R., 1985. Precipitation convective downdraft structure: A synthesis of observations and modeling. Ph.D. dissertation, Colorado State University, Dept. of Atmospheric Science, Fort Collins, CO 80523.

Lamb, D., D. Mitchell, and R. Blumenstein, 1986. Snow chemistry in relation to precipitation growth forms. Conf. Cloud Physics, September 22–26, Snowmass, CO. Amer. Meteor. Soc., 77–80.

Lin, M.-S., 1986. The evolution and structure of composite meso-alpha-scale convective complexes. Ph.D. dissertation, Colorado State University, Dept. of Atmospheric Science, Fort Collins, CO 80523, 245 pp.

Lyons, W.A., R.H. Calby, and C.S. Keen, 1986. The impact of mesoscale convective precipitation systems on regional visibility and oxidant distributions during presistent elevated pollution episodes. *J. Clim. Appl. Meteor.* (submitted).

Marwitz, J.D., 1972. Precipitation efficiency of thunderstorms on the high plains. *J. de Rech. Atmos.*, **6**, 367–370.

McAnelly, R.L., and W.R. Cotton, 1986. Meso-$\beta$-scale characteristics of an episode of meso-$\alpha$-scale convective complexes. *Mon. Wea. Rev.*, **114**, PLEASE PROVIDE PAGE NUMBERS. THANKS.

Newton, C.W., 1966. Circulations in large sheared cumulonimbus. *Tellus*, **18**, 699-713.

Newton, C.W., and H.R. Newton, 1959. Dynamical interactions between large convective clouds and environment with vertical shear. *J. Meteor.*, **16**, 483–496.

Schmidt, J.M., 1985. Structure and evolution of a squall line with an embedded supercell. M.S. thesis, Colorado State University, Dept. of Atmospheric Science, Fort Collins, CO 80523, 141 pp.

Scott, B.C., 1981. Sulfate washout ratios in winter storms. *J. Atmos. Sci.*, **20**, 619–625.

Slinn, W.G.N., and J.M. Hales, 1971. A reevaluation of the role of thermophoresis as a mechanism of in- and below-cloud scavenging. *J. Atmos. Sci.*, **28**, 1465–1471.

Tripoli, G.J., 1986. A numerical investigation of an orogenic mesoscale convective system. Ph.D. dissertation, Colorado State University, Dept. of Atmospheric Science, Fort Collins, CO 80523. (Also, Atmospheric Science Paper No. 401.)

Weisman, M.L., and J.B. Klemp, 1984. The structure and classification of numerically simulated convective storms in directionally varying wind shears. *Mon. Wea. Rev.*, **112**, 2479–2498.

# The Feasibility of the Chemical Element Balance Applied to Regional-Scale Source Apportionment

John G. Watson
Norman F. Robinson
Desert Research Institute
P.O. Box 60220
Reno, Nevada 89506

Harold S. Javitz
SRI International
333 Ravenswood Avenue
Menlo Park, California 94025

August 15, 1986

**Abstract**

A numerical simulation test is applied to a receptor model analysis similar to that applied to a source apportionment study in Colorado. This test consists of applying the modeling method to data which have been randomized in proportion to their expected variability or measurement uncertainty. The results of this testing show that the apportionment of three contributing source regions can be accomplished with uncertainties of 25 to 65%, given expected uncertainties of the model input data.

## INTRODUCTION

Receptor models, such as the Chemical Mass Balance (CMB), Factor Analysis (FA), and Multiple Linear Regression (MLR), have been proposed for apportioning airborne pollutant concentrations by source (Gordon, 1980; Cooper and Watson, 1980; Watson, 1984a). These models depend on the differentiation among pollutant properties found in the emissions from pollution sources.

It has been proposed that the air in different regions of the United States and Europe contains particles with chemical profiles that are unique enough and constant enough to allow the identification (Navarre, et al., 1981; Rahn, 1982; Rahn, et al., 1982a & b; Rahn and Lowenthal, 1983, 1984a, 1985; Husain, et al., 1984; Thurston, 1982) and quantification (Rahn and Lowenthal, 1984, 1985; Webber, et al., 1985) of their contributions to receptors by using receptor models. For successful apportionment, it is necessary that the regional source profiles differ sufficiently from each other, when their natural intrinsic variability is taken into account (Kneip, et al., 1983; Rahn and Lowenthal, 1984b; Thurston and Laird, 1985).

Borys, et al. (1986) present the results from an application of the Effective Variance Chemical Mass Balance (Watson, et al., 1984) and Multiple Linear Regression (Kleinman, et al., 1980) models to receptor measurements of ambient aerosol at the Storm Peak Laboratory in the Colorado Rockies.

Borys, et al. derived their smelter source profiles from eight daily samples taken at Underhill, Vermont (which they determined to be representative of nonferrous smelters in southern Ontario and Quebec); their coal-fired power plant profile from Rahn and Lowenthal's (1985) Lower Midwest source profile; and their southern California source profile from the San Francisco Bay area data acquired by John, et al. (1973). Data derived from twenty-seven of sixty-one HIVOL samples, taken during the winter of 1984–85 at a mountain-top site in northwestern Colorado through a 10 $\mu$m SA-321A inlet (McFarland, et al., 1984) and analyzed by instrumental neutron activation (INAA), were submitted to the CMB receptor model using the selenium mass balance variation of Rahn and Lowenthal (1984, 1985). The concentrations of many measured species in the remaining samples were less than detection limits. Sulfate concentrations were linearly regressed on the source contributions calculated by the CMB. This modeling attributed averages of 67±10 percent of the sulfate to regions containing coal-fired power plants, 27±4 percent to regions containing smelter, and 6±4 percent to regions in California. Borys, et al. (1986) recognize that "even though we believe that these signatures are substantially correct, they should all be updated by direct measurements in the source regions."

Even if the regional source profiles are correct, they are still quite variable. Rahn and Lowenthal (1984, 1985) cite typical variabilities on the order of 30 to 40% for their regional source profiles. Watson, et al. (1986) recently examined annual and seasonal averages of fine particle chemical composition data from a variety of regional-scale studies in eleven western states and found variabilities on the order of ±100%. The tolerance of receptor models to these variabilities needs to be determined in order to assess their validity.

Watson (1979) first applied such numerical simulation testing to the CMB model, and later tests of a similar nature have been conducted by Currie, et al. (1984), Watson and Robinson (1984), Watson, et al. (1985, 1986), Ito, et al. (1986), and Javitz and Watson (1986). These tests have generally shown that receptor models can tolerate substantial amounts of random variability in model input data, when the contributing sources are properly identified and when the source profiles are sufficiently different. The exact amount of input data variability which is tolerable depends on the degree of multi-collinearity among source profiles, the number of source categories into which individual sources or source-dominated sub-regions are grouped, and the relative contributions of the contributing sources.

Javitz and Watson (1986) describe the most extensively developed and quality assured numerical simulation testing procedure which has been used to date. One of the examples submitted to that testing procedure by Javitz and Watson (1986) is very similar to that of Borys, et al. (1986). This example is published here, in the open literature for the first time, to lend credance to the western regional apportionment of acidic aerosol in Colorado reported by Borys, et al. (1986).

The objectives of this report are:

- To briefly describe the numerical simulation testing method.
- To report the results of applying this testing to the regional source profiles of Rahn and Lowenthal (1985).
- To identify further research needed to obtain more specific regional source profiles for the apportionment of gases, particles, and wet deposition quality at receptor areas in the western United States.

## TESTING PROCEDURE

The numerical simulation test applied to the effective variance solution to the chemical mass balance receptor model is described by Javitz and Watson (1986) and consists of the following steps:

1. List all likely sources and expected contributions.
2. Obtain likely emissions compositions in terms of all quantifiable species.
3. Set the true source contributions and true source compositions at expected values. In these tests, the true values were drawn from specified log-normal distributions of the source contributions and source compositions.
4. Generate 100 receptor concentrations (labeled "true") for the elements Se, Zn, Sb, Mn, V, As and In.
5. Add a random amount (plus or minus) to the true concentration to simulate measurement uncertainty.
6. Apply the CMB receptor model to each randomized data set using the means and standard deviations of the distributions from which the source compositions used to generate the concentrations were drawn.
7. Calculate a series of performance measures which compare the model-calculated source contributions to the true source contributions.

The performance measure presented in the following tables is the ratio of the average absolute error of estimation (AAE) to the average of the 100 true source contributions. The AAE is defined as the average of the absolute differences between the calculated and true source contributions for the 100 cases.

Other performance measures that have been used in the literature include the average maximum ratio, the root-mean-square error, and the range of absolute errors defined by Javitz and Watson (1986) and Watson, et al. (1986).

The AAE ratio performance measure is reported here because it attaches relatively more importance to large absolute errors of estimation than the average maximum ratio, without being as sensitive to single large deviations as the root-mean-square error and the range of absolute errors. The AAE performance measure only indicates the relative acceptability of the agreement between estimated and true source contributions. Scatterplots were also prepared to more fully illustrate the agreement between the true and calculated source contributions, and these results are reported in Javitz and Watson (1986). This testing method and the performance measures it produces are applicable to both the CMB allocation of primary species to sources and to the linear regression of secondary species, or effects such as visibility reduction, on the primary source contributions.

## INPUT DATA

Table 1 contains the regional source profiles reported by Rahn and Lowenthal (1985). They have been re-normalized to an arbitrary mass concentration in each regional source sample of 10 $\mu g/m^3$. To obtain species concentrations as a fraction of primary particle mass, it has also been assumed that the average selenium concentration for each regional source sample was 1 $\mu g/m^3$. Rahn and Lowenthal (1985) originally calculated their regional source profiles with respect to selenium, but they note that "this selection was arbitrary, for both theory and actual experiment show that different elements in the denominator are mathematically equivalent." This normalization to the

primary mass concentration as opposed to a tracer species allows the data of Rahn and Lowenthal (1984, 1985) and Borys, et al. (1986) to be more readily compared with those of other researchers. It also allows the model-testing software to impose physical limits (i.e., the simulated ambient concentration of a single species can never exceed the mass concentration at the receptor) on the randomization process.

The secondary species fractions were selected such that Rahn and Lowenthal's average sulfate concentrations of 3.2 $\mu g/m^3$ for the summer and winter of 1982 at Underhill, Vermont, would be approximated when the average primary regional source contributions are those stated in Table 1. These average primary regional source contributions also approximate the averages found by Rahn and Lowenthal for the 132 samples taken at Underhill, Vermont. The regional source compositions in Table 2 also assume that primary sulfate, nitrate, ammonium, and the secondary nitrate are negligible. The secondary ammonium fraction of the primary mass was selected to maintain a stoichiometric ratio to sulfate under the assumptions that all sulfate is present as ammonium sulfate.

Although several of the other references cited above provide regional source profiles that may be equally valid, the one proposed by Rahn and Lowenthal (1985) contains the largest number of species and the largest number of samples. It is, therefore, the most appropriate selection for testing to ascertain the feasibility of regional-scale receptor modeling at this time. The upper midwest and southern Ontario regional profiles are also the same ones used by Borys, et al. (1986).

Rahn and Lowenthal (1984, 1985) report standard deviations of the regional source compositions on the order of 30 to 40% and of the ambient concentrations in the range of 10 to 20%. These are the most appropriate parametric cases for examination in the model tests.

## RESULTS

Tables 2 and 3 summarize the AAE ratios for simple (3 sources) and complex (5 sources) regional-scale scenarios a function of coefficient of variation (CV) in the source profile and receptor input data. Source profile uncertainties were systematically increased from 0%, to 25%, to 50%, and to 100%. Two levels of receptor uncertainty, 10% and 20%, were examined for each level of source profile uncertainty. The AAE ratios reported in these tables were each derived from 100 simulations using the mean source profiles and source contributions reported in Table 1.

The "acceptable" value of an AAE ratio really depends on the purposes of the modeling, and this type of analysis cannot pre-judge those purposes. These tables are useful, however, in determining how much variability in the input data can be tolerated for a given level of uncertainty in model output. The following observations are relevant:

- A three-source regional apportionment with the given species is much more accurate than a five source apportionment. For example, the 25% source CV and 10% receptor CV NENG source is apportioned with a 12% AAE ratio in the three source case while the corresponding five source AAE ratio is 46%. This is caused by much higher multi-collinearity in the five-source case and argues for combining similar source profiles into a broader source category.

- The AAE ratio varies substantially among source categories. In the three-source tests, NENG is always apportioned more accurately than the other source types. LMWS is always apportioned less accurately. This occurs both because of multi-collinearity and because of the different source contributions. Watson, et al. (1986) show that small average numerical values of source contributions are often apportioned less accurately than large ones.

Rahn and Lowenthal have also performed numerical simulations similar to those reported here. They report (personal communication) "acceptable" results up to 50% source profile CV. The

Table 1

REGIONAL SOURCE PROFILES AND AVERAGE CONTRIBUTIONS

| Aerosol Property | Fraction of Species in Each Source[a] | | | | |
|---|---|---|---|---|---|
| | New England (NENG) | Central East Coast (CEC) | Lower Midwest (LMW) | Upper Midwest (UMW) | Southern Ontario (SONT) |
| Se | 0.0001 | 0.0001 | 0.0001 | 0.0001 | 0.0001 |
| Zn | 0.0032 | 0.0029 | 0.00053 | 0.0024 | 0.0029 |
| Sb | 0.000046 | 0.000114 | 0.0000148 | 0.000043 | 0.000031 |
| Mn[b] | 0.00094 | 0.00037 | 0.000110 | 0.00067 | 0.00044 |
| V[b] | 0.00116 | 0.0027 | 0.000016 | 0.000083 | 0.00044 |
| As | 0.0000136 | 0.000074 | 0.000023 | 0.000149 | 0.00028 |
| In | 0.0000006 | 0.00000046 | 0.0000001 | 0.00000045 | 0.0000095 |
| Other | 0.9944174 | 0.99374154 | 0.9992061 | 0.99655455 | 0.9957995 |
| | Average Primary Contributions ($\mu g/m^3$) | | | | |
| Simple Case | 4.0 | 0.0 | 5.0 | 0.0 | 1.0 |
| Complex Case | 2.0 | 2.0 | 3.0 | 2.0 | 1.0 |

[a] Taken from Rahn and Lowenthal (1985), Table 1 and normalized to a 10 $\mu g/m^3$ regional source sample assuming the average Se concentration in each source region is equal to 1 $\mu g/m^3$. This is equivalent to dividing Rahn and Lowenthal's (1985) values by 10,000.

[b] Non-Crustal

Table 2

CMB MODEL PERFORMANCE IN THE SIMPLE REGIONAL SCENARIO

| Source Profile CV(%) | Meas Error CV(%) | Inter-Source Correl. | AAE of CMB-Estimated Source Contribution as a Percentage of True Source Contribution | | |
|---|---|---|---|---|---|
| | | | NENG | LMWS | SONT |
| 0 | 0 | 0.0 | 0 | 0 | 0 |
| 25 | 10 | 0.0 | 12 | 29 | 20 |
| 25 | 20 | 0.0 | 16 | 43 | 26 |
| 50 | 10 | 0.0 | 25 | 66 | 40 |
| 50 | 20 | 0.0 | 22 | 62 | 37 |
| 100 | 10 | 0.0 | 46 | 95 | 66 |
| 100 | 20 | 0.0 | 40 | 91 | 51 |

Table 3

CMB MODEL PERFORMANCE IN THE COMPLEX REGIONAL SCENARIO

| Source Profile CV(%) | Meas Error CV(%) | Inter-Source Correl. | AAE of CMB-Estimated Source Contribution as a Percentage of True Source Contribution | | | | |
|---|---|---|---|---|---|---|---|
| | | | NENG | LMWS | SONT | CEC | UMWS |
| 0 | 0 | 0.0 | 0 | 0 | 0 | 0 | 0 |
| 25 | 10 | 0.0 | 46 | 63 | 20 | 27 | 37 |
| 25 | 20 | 0.0 | 51 | 81 | 32 | 33 | 53 |
| 50 | 10 | 0.0 | 75 | 98 | 32 | 40 | 68 |
| 50 | 20 | 0.0 | 74 | 87 | 49 | 50 | 75 |
| 100 | 10 | 0.0 | 146 | 140 | 63 | 69 | 134 |
| 100 | 20 | 0.0 | 114 | 156 | 69 | 63 | 110 |

difference between Rahn and Lowenthal's results and those reported here appears to be attributable to a difference in the CMB algorithm employed: their CMB routine removes regional sources that are initially allocated negative contributions whereas the CMB routine employed in this study does not. The more acceptable performance measures they obtained indicate that the bias induced by source removal is more than compensated for by an increase in precision and, therefore, argues for the inclusion of source removal procedures in the future application of CMB models to regional scenarios.

## SUMMARY, CONCLUSIONS AND RECOMMENDATIONS

A general procedure for performing numerical simulation testing of receptor models was applied to allocation of regional aerosols similar to that of Borys, et al. (1986). The CMB model allocated the contributions of three to five regional sources to a regional aerosol to within an average absolute error of 50% when the CV of the source profiles was 25% and the CV of measurement error was 10%.

The numerical simulations reported here demonstrate that if a 50% uncertainty is tolerable for decision-making purposes, and in these particular allocation efforts, the measurement requirements for the CMB model can be met as follows:

- For the eastern regional aerosol, measure Se, Zn, Sb, non-crustal Mn, non-crustal V, As, and In.
- Have a coefficient of variation of receptor measurements of no more than 10% (i.e., with 95% confidence the measured concentration of a species at the receptor is no less than 80% of the true concentration or more than 125% of the true concentration).
- Have a coefficient of variation of the source profiles of no more than 25% (i.e., with 95% confidence the estimated source profile of a species is no less than 50% of the true species fraction or more than 200% of the true species fraction).

These measurement requirements appear to have been marginally met by Borys, et al. (1986), thereby lending credance to their conclusions.

Of the measurement requirements, the most difficult to guarantee is the one relating to the CV of the source profile. This variation might be reduced by a number of measurement and estimation strategies: (1) measuring the specific source region that is likely to affect the receptor rather than a similar source region in a different location; (2) using a fractionation model to predict the changes that will occur in the regional source profile during transport and in the sample collection process at the receptor; (3) forming linear combinations of source profiles when two or more sources with slightly different profiles are in a source type; and (4) additional measurements of source properties.

The measurement requirements found in these simulations are not necessarily indicative of the requirements that would exist in other situations. In a more complicated region with more sources, the measurement requirements might be much more stringent. On the other hand, if more species were available that were unique to specific sources, then the requirements on the coefficients of variation of the source profile and ambient measurement errors might be much more lenient. Measurement requirements must be determined case by case.

Further work in western regional-scale receptor modeling should include the following activities:

- Compilation of fine particle data bases from western source regions from which regional source profiles might be derived.

- Measurement of chemical (particles and gases) and physical (particles) composition in both source and receptor areas. Emphasis should be given to those species which reduce multicollinearities in source profiles.
- Additional numerical simulation testing as well as model–model, model–tracer, and model–ambient intercomparisons to validate receptor model results.
- Application of receptor model source apportionment methods to a wider geographical scale in the west.

## ACKNOWLEDGEMENTS

This research was supported by the Electric Power Research Institute, Palo Alto, California. Sponsorship of this work does not signify that the contents necessarily reflect the views and policies of EPRI. Careful review and recommendations were provided by J. Guertin of the Electric Power Research Institute.

## REFERENCES

Borys, R.D., D.H. Lowenthal, and K.A. Rahn, 1986. Contributions of smelters and other sources to pollution sulfate at a mountain top site in northwestern Colorado. Presented at the CIRA Workshop on Acid Deposition in Colorado, August 13–15, 1986, Pingree Park Campus. Cooperative Institute for Research in the Atmosphere, Colorado State University, Fort Collins, CO.

Cooper, J.A., and J.G. Watson, 1980. Receptor oriented methods of air particulate source apportionment. *J. Air Pollution Control Assoc.*, **30**, 1116.

Currie, L.A., R.W. Gerlach, C.W. Lewis, W.D. Balfour, J.A. Cooper, S.L. Dattner, R.T. DeCesar, G.E. Gordon, S.L. Heisler, P.K. Hopke, J.J. Shah, G.D. Thurston, and H.J. Williamson, 1984. Interlaboratory comparison of source apportionment procedures: Results for simulated data sets. *Atmos. Environ.*, **18**, 1517.

Gordon, G.E., 1980. Receptor models. *Environ. Sci. Tech.*, **14**, 792.

Husain, L., J.W. Webber, E. Canelli, V.A. Dutkiewicz, and J.A. Halstead, 1984. Mn/V ratio as a tracer of aerosol sulfate transport. *Atmos. Environ.*, **18**, 1059.

Ito, K., T.J. Kneip, and P.J. Lioy, 1986. The effects of number of samples and random error on the factor analysis/multiple linear regression (FA/MR) receptor modeling technique. *Atmos. Environ.*, **20**, 1433.

Javitz, H.S., and J.G. Watson, 1986. Feasibility study of receptor modeling for apportioning utility contributions to air constituents, deposition quality and light extinction. Draft report for the Electric Power Research Institute prepared by SRI International, Menlo Park, CA.

John, W., R. Kaifer, K. Rahn, and J. Wesolowski, 1973. Trace element concentrations in aerosols from the San Francisco Bay area. *Atmos. Environ.*, **7**, 107.

Kleinman, M.T., B.S. Pasternack, M. Eisenbud, and J.T. Kneip, 1980. Identifying and estimating the relative importance of sources of airborne particulates. *Environ. Sci. Tech.*, **14**, 62.

Kneip, T.J., P.J. Lioy, and G.T. Wolff, 1983. A critical review of Kenneth Rahn's elemental tracer acid rain studies. *Environ. Forum*, **2**, 9.

McFarland, A.R., C.A. Ortiz, and R.W. Bertch, 1984. A 10 $\mu$m cutpoint size selective inlet for hi-vol samplers. *J. Air Pollution Control Assoc.*, **34**, 544.

Navarree, J.L., P. Priest, and Ronneau, 1981. Relations between sulfur and heavy elements in rural atmospheres. *Atmos. Environ.*, **15**, 221.

Rahn, K.A., 1982. Elemental tracers and sources of atmospheric acidity for the Northeast – A statement of new evidence. *Environ. Forum*, May, p. 27.

Rahn, K.A., D.H. Lowenthal, and N.F. Lewis, 1982a. Elemental tracers and source areas of pollution aerosol in Narrangansett, Rhode Island. Report of the Center for Atmospheric Chemistry Studies, Graduate School of Oceanography, University of Rhode Island, Narragansett, RI.

Rahn, K.A., N.F. Lewis, and D.H. Lowenthal, 1982b. Elemental tracers of Canadian smelter aerosol transported into the Northeastern United States. *Receptor Models Applied to Contemporary Pollution Problems*, Air Pollution Control Association, Pittsburgh, PA.

Rahn, K.A., and D.H. Lowenthal, 1983. The promise of elemental tracers as indicators of source areas of pollution aerosol in the Eastern United states. *Trace Substances in Environmental Health–XVII*, D.D. Hemphill (ed.), University of Missouri, Columbia, MO.

Rahn, K.A., and D.H. Lowenthal, 1984a. Elemental tracers of distant regional pollution aerosols. *Science*, **223**, 132.

Rahn, K.A., and D.H. Lowenthal, 1984b. Comment on erasure of Midwestern Mn/V signature in an area of high vanadium concentration. *J. Air Pollution Control Assoc.*, **34**, 548.

Rahn, K.A., and D.H. Lowenthal, 1985. Pollution aerosol in the Northeast: Northeastern–Midwestern contributions. *Science*, **228**, 275.

Thurston, G.D., J.D. Spengler, and P.J. Samson, 1982. An assessment of the relationship between regional pollution transport and trace elements using wind trajectory analysis. *Receptor Models Applied to Contemporary Pollution Problems*, Air Pollution Control Association, Pittsburgh, PA.

Thurston, G.D., and N.M. Laird, 1985. Tracing aerosol pollution. *Science*(Letters), **227**, 1406.

Tuncel, S.G., I. Olmez, J.R. Parrington, G.E. Gordon, and R.K. Stevens, 1985. Composition of fine particle regional sulfate component in Shenandoah Valley. *Environ. Sci. Tech.*, **19**, 529.

Watson, J.G., 1979. Chemical elemental balance receptor model methodology for assessing the sources of fine and total suspended particulate matter in Portland, OR. Ph.D. dissertation, Oregon Graduate Center, Beaverton, OR.

Watson, J.G., 1984a. Overview of receptor model principles. *J. Air Pollution Control Assoc.*, **34**, 620.

Watson, J.G., J.A. Cooper, and J.J. Huntzicker, 1984. The effective variance weighting for least squares calculations applied to the mass balance receptor model. *Atmos. Environ.*, **18**, 1347–1355.

Watson, J.G., A.W. Gertler, G.H. Prowell, J.C. Chow, S.V. Hering, L.W. Richards, and D.S. Blumenthal, 1985. Causes of secondary aerosol in the San Joaquin Valley determined from the WOGA aerosol data base. Desert Research Institute Report #6687.4D2 prepared for the Western Oil and Gas Association, Reno, NV.

Watson, J.G., J.C. Chow, and N.F. Robinson, 1986. Western State Acid Deposition Project Phase I: Volume 4 – An Evaluation of Ambient Aerosol Chemistry in the Western United States. Systems Applications Document No. SYSAPP-86-129, San Rafael, CA.

Webber, J.S., V.A. Dutkiewicz, and L. Husain, 1985. Identification of submicrometer coal fly ash in a high-sulfate episode at Whiteface Mountain, New York. *Atmos. Environ.*, **19**, 285.

# Mesoscale Influences on Long-Range Pollutant Transport

Roger A. Pielke[1,2], Moti Segal[1],
Raymond W. Arritt[2], and Michael D. Moran[1]

[1]Department of Atmospheric Science and
[2]Cooperative Institute for Research in the Atmosphere
Colorado State University
Fort Collins, Colorado 80523

August 15, 1986

**Abstract**

**An overview analysis of mesoscale and microscale influences on atmospheric transport and dispersion and of the non-representativeness of standard rawinsonde observations is used to highlight the serious limitations of current diagnostic long-range transport models.**

## INTRODUCTION

In the absence of the release and continuous monitoring of conservative tracers from all possible source regions of pollution which could impact Colorado, one has to rely on trajectory estimates based on the available upper air meteorological observational data (i.e. rawindsonde data). Unfortunately, these data are only routinely available from the standard synoptic observing network which has the following characteristics:

1. observations are made routinely only every 12 hours (0000 GMT and 1200 GMT);
2. observations are made with a typical horizontal spatial resolution of
   a. about 250 km over the central portion of the United States
   b. about 450 km over north-central Canada
   c. at the best about 1000 km over much of the Gulf of Mexico and the western Atlantic Ocean, with even larger gaps over the eastern Pacific Ocean;
3. observations are made at standard pressure heights (1000 mb, 850 mb, 700 mb, 500 mb, 300 mb and 200 mb) plus several other so-called significant pressure levels where a substantial change of one or more of the meteorological parameters with height is observed.

The upper-air observational data, therefore, have substantial limitations because of the coarse temporal and spatial resolution of the measurements. With the existing temporal and spatial coverage of the upper-air network, unless these observations are representative of the area out to about one half the distance between adjacent rawinsondes and for the six-hour period on either side of the observation time, errors of representativeness will occur.

When atmospheric research programs have been carried out which have had an upper-air sounding component with greater spatial and temporal resolution than the standard upper-air network, it

has been found that the representativeness of rawinsonde observations extends over larger areas at heights which are well above the planetary boundary layer (PBL) than at heights within the PBL itself. Similarly, measurements made well above complex terrain are more representative than those made at or close to the surface or close to the terrain. Surface observations, which have a one-hour temporal resolution, are strongly influenced by local effects and, therefore, are seldom representative enough of the surrounding area to be useful in trajectory assessments. In addition, particularly when the PBL is stably stratified, surface winds are not even representative of the winds a short distance above the surface.

The position of a pollutant parcel as it moves away from its source can be estimated from the equations

$$\begin{aligned} x(t+\delta t) &= x(t) + \tilde{u}(t)\delta t = x(t) + [u_0(t) + u'(t) + u''(t)]\delta t, \\ y(t+\delta t) &= y(t) + \tilde{v}(t)\delta t = y(t) + [v_0(t) + v'(t) + v''(t)]\delta t, \\ z(t+\delta t) &= z(t) + \tilde{w}(t)\delta t = z(t) + [w_0(t) + w'(t) + w''(t)]\delta t, \end{aligned} \tag{1}$$

where $x(t)$, $y(t)$, and $z(t)$ represent the parcel's initial position and $x(t+\delta t)$, $y(t+\delta t)$ and $z(t+\delta t)$ are its location after a time period $\delta t$. The wind components $u_0$ and $v_0$ represent horizontal gradient wind flow above the PBL with the corresponding vertical motion, $w_0$, resulting from the spatial distribution of $u_0$ and $v_0$ at any time. Within the PBL, frictional retardation reduces the wind speed and turns the wind at these heights towards lower pressure. Values of $u_0$, $v_0$ and $w_0$ are typically estimated from analyses of the synoptic observational data, and are therefore referred to as synoptic wind components. Synoptic-scale motions in mid-latitudes have horizontal spatial scales of several thousand kilometers or more. The wind components $u'$, $v'$ and $w'$ represent mesoscale deviations from the synoptic wind. The mesoscale wind components deviate significantly from gradient wind balance throughout the atmosphere, but the pressure distribution which drives these winds is close to hydrostatic balance. Mesoscale motions have horizontal spatial scales in mid-latitudes of a few kilometers up to several hundred kilometers. The microscale wind components $u''$, $v''$ and $w''$, the remaining part of the total wind, represent the nonhydrostatic flow with horizontal spatial scales of a few kilometers or less (this flow includes turbulent motions).

In mathematical terminology, the synoptic wind $(u_0, v_0)$ can be defined as

$$u_0 = \int_t^{t+\delta t} \int_x^{x+\delta x} \int_y^{y+\delta y} \int_p^{p-\delta p} \tilde{u}\, dp\, dy\, dx\, dt/(\delta t)(\delta x)(\delta y)(\delta p) \tag{2}$$

$$v_0 = \int_t^{t+\delta t} \int_x^{x+\delta x} \int_y^{y+\delta y} \int_p^{p-\delta p} \tilde{v}\, dp\, dy\, dx\, dt/(\delta t)(\delta x)(\delta y)(\delta p) \tag{3}$$

where the distances $\delta x$ and $\delta y$ represent a large enough spatial scale such that the gradient wind approximation is valid, $\delta p$ is the distance between standard pressure heights on a constant pressure surface grid, and $\tilde{u}$ and $\tilde{v}$ are the components of the actual horizontal wind. The synoptic vertical motion $w_0$, as mentioned above, is diagnosed from the spatial distribution of $u_0$ and $v_0$.

Within the PBL it is well known that often

$$|u'| \simeq |u_0|;\ |v'| \simeq |v_0|;\ |w'| \gg |w_0|;\ |u''| \simeq |u_0|;\ |v''| \simeq |v_0|;\ |w''| \gg |w_0|.$$

Values of $|u''|$, $|v''|$ and $|w''|$ are even larger when the PBL is convective. Above the PBL, however, $|u''|$, $|v''|$ and $|w''|$ are usually much smaller than the synoptic wind components except at locations such as in the vicinity of thunderstorms, at cloud tops, over mountain barriers, and near and in the polar and subtropical jet streams.

Because of our inability to measure specific values of $u''$, $v''$ and $w''$ from the synoptic rawinsonde network, the general procedure to use (1) in order to determine the movement and spread of pollutant parcels requires the random selection of different values of $u''$, $v''$ and $w''$ from probability distributions whose means, standard deviations, and higher-order statistical moments are determined from our understanding of microscale motions. The spread of pollutants due to microscale motions is referred to as *turbulent diffusion*. The spread of pollutants as a result of some of the pollutant moving into volumes with different synoptic ($u_0$, $v_0$ and $w_0$) and mesoscale ($u'$, $v'$, $w'$) winds is called *differential transport*. The sum of *turbulent diffusion* and *differential transport* is called *dispersion*. In terms of the trajectory of a pollutant plume from its source, therefore, dispersion can, under a range of atmospheric conditions, cause a plume to split apart and move in more than one direction.

The configuration of the synoptic rawinsonde network does not permit resolution of the mesoscale wind field ($u'$, $v'$, $w'$), although this scale of motion often tends to occur in organized circulations. Examples of mesoscale flows include those associated with synoptically-induced mesoscale systems such as squall lines, arctic lows, mesoscale convective complexes, and jet streaks, and with terrain-induced mesoscale systems such as sea- and land-breezes, mountain-valley winds, and lake-effect storms. Since these atmospheric features have well-defined circulations, it is not necessary to represent mesoscale motions with the stochastic parameterizations employed for the microscale wind components. However, as discussed in the next section, existing long-range-transport (LRT) trajectory models generally ignore these mesoscale winds.

## ASSESSMENT OF ROUTINE TRAJECTORY MODELS

To illustrate the limitations of current long-range trajectory models, two LRT models which have been applied by Takacs, et al. (1985) will be interpreted in the context of (1). The two models are a moist isentropic trajectory analysis model (MITA) and the Air Resources Laboratory (ARL) trajectory model. With respect to the discussion in the Introduction, these models have the following general characteristics:

MITA:

i) effects due to mesoscale and microscale motions (i.e., $u'$, $v'$, $w'$, and $u''$, $v''$, $w''$, respectively) are ignored. In addition, values of wind velocity obtained from the synoptic rawinsonde network (defined in this paper as $u_0^*$, $v_0^*$ and $w_0^*$) are only estimates of $u_0$, $v_0$ and $w_0$ because of the limited spatial sampling capability of the rawinsondes.

ii) a physically consistent representation of estimated synoptic vertical velocity, $w_0^*$, is obtained as long as $\theta_w$ (the wet-bulb potential temperature) increases monotonically with height.

ARL:

i) [same as (i) above]

ii) synoptic vertical velocity, $w_0^*$, is ignored

iii) a vertically averaged wind value of $u_0^*$ and $v_0^*$ in the PBL is assumed to be representative of the mean horizontal advective velocity.

In order to discuss the *minimum* error that can result due to the first assumption under the MITA model above, let

$$\begin{aligned}
\tilde{u} &= u_0 + u' + u'' = u_0^* + u' + u'' + \epsilon_u = u_0^* + \epsilon_u' + \epsilon_u'' + \epsilon_u, \\
\tilde{v} &= v_0 + v' + v'' = v_0^* + v' + v'' + \epsilon_v = v_0^* + \epsilon_v' + \epsilon_v'' + \epsilon_v, \\
\tilde{w} &= w_0 + w' + w'' = w_0^* + w' + w'' + \epsilon_w = w_0^* + \epsilon_w' + \epsilon_w'' + \epsilon_w,
\end{aligned} \tag{4}$$

where $\tilde{u}$, $\tilde{v}$ and $\tilde{w}$ are the true winds at any point in space. The synoptic wind components $u_0^*$, $v_0^*$ and $w_0^*$ are what are obtained from the MITA model. The error introduced because of the imperfect representation of $u_0$, $v_0$ and $w_0$ by the rawinsonde network is given by $\epsilon_u$, $\epsilon_v$ and $\epsilon_w$, while $\epsilon_u'$, $\epsilon_v'$, $\epsilon_w'$, $\epsilon_u''$, $\epsilon_v''$, and $\epsilon_w''$ denote the errors that would be introduced by neglecting the mesoscale and microscale wind fields, respectively.

If we assume for this error analysis that both mesoscale and microscale motions are normally distributed and are independent of one another, then one standard deviation on either side of $u_0^*$, $v_0^*$ and $w_0^*$ represents a reasonable estimate of one source of the error due to approximating the true wind by the rawinsonde-deduced synoptic wind. Therefore, likely ranges for $\tilde{u}$, $\tilde{v}$ and $\tilde{w}$ (denoted by the angle brackets around $\tilde{u}$, $\tilde{v}$ and $\tilde{w}$) can be expressed as

$$\begin{aligned}
< \tilde{u} > &= u_0^* \pm \sigma_u' \pm \sigma_u'' + \epsilon_u, \\
< \tilde{v} > &= v_0^* \pm \sigma_v' \pm \sigma_v'' + \epsilon_v, \\
< \tilde{w} > &= w_0^* \pm \sigma_w' \pm \sigma_w'' + \epsilon_w,
\end{aligned} \tag{5}$$

where $\sigma_u'$ is the standard deviation of the mesoscale $u$-component, $\sigma_u''$ is the standard deviation of the microscale $u$-component, and so on. An estimate of the error due to approximating the true wind by the observed synoptic wind can be made once values of the synoptic-wind-component standard deviations representative of the rawinsonde-network measurement errors $\epsilon_u$, $\epsilon_v$ and $\epsilon_w$ are known.

Gifford (1982) has summarized much of what is known concerning the horizontal dispersion of a plume after long travel times. Among the characteristics of such longer-term dispersion is the phenomenon that the wider a plume is, the faster it spreads. The reason is that dispersion results not only from three-dimensional turbulent diffusion imposed on a constant mean wind field (such as is represented in a Gaussian plume model), but also from larger-scale spatial variations in the mean wind which cause differential transport and a resultant spread of the mean plume. Figure 1, reproduced from Gifford's paper, shows how the expected lateral dispersion[1] increases with time. Table 1 shows several representative values. When the winds change spatially due to such features as well-defined mesoscale systems, the dispersion will be even larger.

As mentioned earlier, the rawinsonde network samples the wind field only at a series of points and over a short period of time. Estimates of $u_0$ and $v_0$ determined in this fashion are not likely to be accurate [see (2) and (3)]. The influence of this lack of representativeness of the observed synoptic wind is represented by $\epsilon_u$, $\epsilon_v$ and $\epsilon_w$ in (5). As an example of a *minimum estimate* of the error, suppose that the wind measurement has the correct speed but is off by 10° in direction (and that this error exists throughout the period of the trajectory, i.e., $\epsilon_u$ and $\epsilon_v$ are equivalent to a 10° error). Resulting errors in the calculated trajectory are shown in Table 2 for two wind speeds. Thus using Table 1, the *minimum* error in horizontal trajectory position in fair weather due to the effects

[1] which is probably a minimum since the measurement data were likely collected under fair weather conditions with an absence of especially turbulent systems such as thunderstorms.

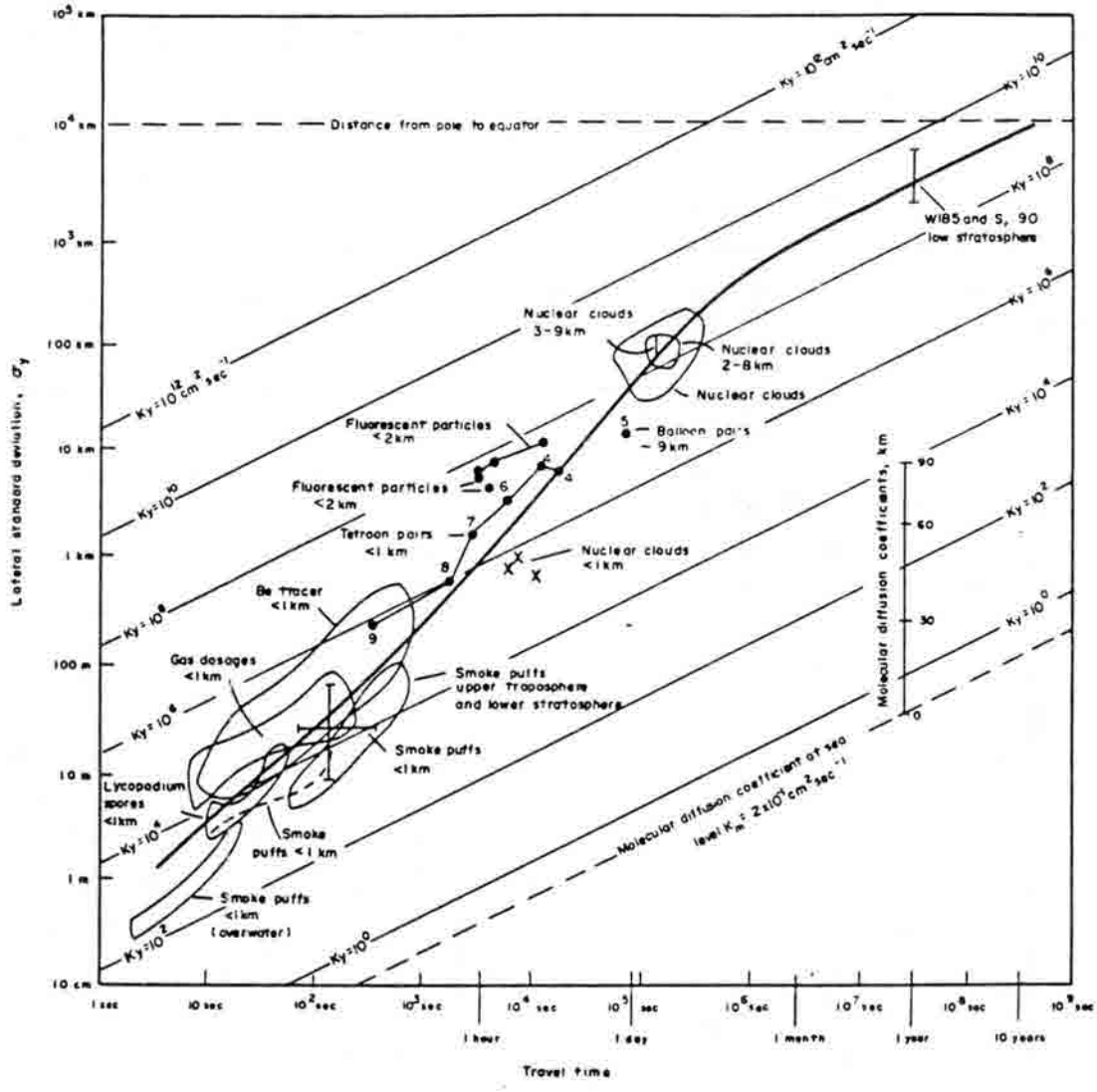


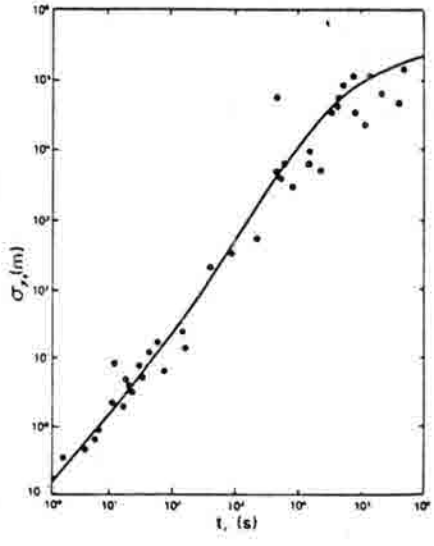


Figure 1. Estimates of the lateral standard deviation of a plume (a) from a variety of sources including stratospheric data and; (b) from tropospheric diffusion data (from Gifford, 1982).

Table 1. Growth of lateral plume spread with travel time.

| travel time of plume | standard deviation of lateral displacement |
|---|---|
| ~ 3 hours | 10 km |
| ~ 30 hours | 100 km |

Table 2. Trajectory positional error due to a small directional (10°) error in specifying the synoptic wind field.

| synoptic wind speed | displacement after 24 hours | error after 24 hours | displacement after 48 hours | error after 48 hours |
|---|---|---|---|---|
| 10 $ms^{-1}$ | 864 km | 152 km | 1728 km | 304 km |
| 20 $ms^{-1}$ | 1728 km | 304 km | 3456 km | 608 km |

of turbulent diffusion and differential advection alone is about 80 km after 24 hours and 160 km after 48 hours. To this number must be added the error due to the lack of representativeness of the estimated synoptic wind such as was given in Table 2. The maximum error is much larger. For instance, thunderstorms in the vicinity of a parcel can introduce very large values of $\sigma'_w$ and $\sigma''_w$. Lyons, et al. (1986), for example, have documented the occurrence of substantial venting and deposition of sulfates by organized mesoscale convective cloud systems in the eastern U.S. They suggest, for the situation which they studied, that about two-thirds of the airborne sulfate was not wet deposited but instead was transported vertically to altitudes as high as the tropopause.

Using a Lagrangian model calculation for a specific LRT episode, Eliassen, et al. (1982) found that a model run using the observed 850 mb winds, as contrasted with a solution in which the 850 mb winds were backed (i.e., rotated counter-clockwise) by 15° and reduced in speed by 10 percent, resulted in different ozone concentration predictions. The differences (from Fig. 6 of their paper) were in excess of 25 percent for 9 of their 31 comparison times. They attributed the differences to the fact that the wind trajectories stayed north of a region of large pollution emissions.

The errors associated with the ARL model will include those of the MITA model plus those associated with the neglect of $w_0^*$ and the averaging of the horizontal synoptic wind, $u_0^*$ and $v_0^*$, with height. As shown, for instance, by Syrakov, et al. (1983) using a simple, barotropic, stationary PBL model, stratification within the PBL and vertical motion in the upper PBL have a substantial influence on plume transport. However, in the convective PBL, $w_0$, and usually $w'$, are often much smaller in magnitude than $w''$ (and hence, $\epsilon''_w$). Therefore, the assumption of vertical transfer of pollution only by turbulence, and not by mean vertical motion, is quite realistic. A well-mixed PBL in terms of pollution concentration under this situation is reasonable, and the errors associated with the ARL model formulation should not be large. In the stable PBL, however, $w''$ is expected to be generally small and perhaps of the same order of magnitude as $w_0$ and $w'$ except in the vicinity of rough terrain or along coastlines. Thus the neglect of the latter two quantities will be more serious.

The assumption of a *well-mixed velocity profile* even in the convective PBL, however, is not usually observed, even under ideal conditions (e.g., see Pielke and Mahrer, 1975). We can illustrate the likely error introduced by using this assumption with the geostrophic relation, i.e., $\vec{V}_g = (g/f)\vec{k} \times \nabla_p z$. Using the ideal gas law and the hydrostatic equation, after differentiating with respect to pressure, the geostrophic relation yields

$$\frac{\partial \vec{V}_g}{\partial ln p} = -\frac{R}{f}\vec{k} \times \nabla_p T, \tag{6}$$

so that a horizontal temperature gradient on the synoptic scale within the PBL would be expected to produce a velocity shear in the PBL, unless the convective mixing is extreme. Using (6), an average horizontal temperature gradient of 5°C per 200 km between 1000 and 850 mb, for instance, would result in a change of geostrophic wind speed of 11.7 $ms^{-1}$ between those two levels. The direction of the wind with height, of course, can also change if the temperature gradient changes direction with height (even causing 180° wind direction reversals with height).

## CONCLUSIONS

An overview discussion of existing long-range trajectory models has shown that these tools lack realistic representations of the true wind field, and therefore cannot, in general, provide realistic, detailed estimates of air pracel trajectories. In lieu of wind observations with extremely high spatial and temporal resolution, a numerical meteorological model based on fundamental physical principles in conjunction with and assimilating all available observations (including satellite imagery)

is required in order to obtain a more representative estimate of the actual mean wind and thermodynamic fields and their natural spatial and temporal variability. Such a model would have to have high spatial and temporal resolution, and be able to represent the statistics of boundary-layer processes and convective cloud activity in a realistic fashion. As shown, for example, by Warner, et al. (1983), a dynamic model is able to diagnose atmospheric transport more accurately than a kinematic model because of its ability to provide for realistic, nonlinear variations of the wind field in space and time. Johnson (1983, p. 572) summarizes a number of the physical improvements which are needed. A quantification of the errors introduced in (4) is also impossible in the absence of a model with a realistic treatment of the PBL and with both mesoscale and convective cloud physics. This approach will require substantial additional research and development support.

Finally, a procedure to statistically relate acidic deposition to antecedent meteorological conditions should be examined. A suggested procedure is outlined below:

1. Catalog the estimated path of the pollutant with respect to the synoptic classification scheme suggested in Pielke (1982). The purpose of categorizing synoptic weather patterns in this fashion is that such features as chemical transformation characteristics, precipitation intensity, and PBL moisture and pollutant concentration will likely be related to these categories.

2. Relate the observed wet (and dry, if available) acidic deposition to these synoptic categories and to all available meteorological variables from the time of deposition backwards 48 hours using multiple linear regression. This analysis would include the emission source inventory and the estimated trajectory path. This approach is analogous to the method of Model Output Statistics (MOS) developed and applied by the NWS Techniques Development Lab except that observed data rather than model forecasts are used, and supplemental information (e.g., the source emission inventory) is included. This approach is currently being evaluated for the western United States by H. Iyer and W. Malm (National Park Service, personal communication, 1986).

It is our opinion that the statistical evaluation of the relation between observed acidic deposition and meteorological conditions (including estimated trajectory paths) will not only help to delineate source regions, but will also elucidate the interrelationship between synoptic category, local meteorological conditions and the emission inventory. This type of approach has been used successfully to forecast one-hour ozone concentrations in the northeastern United States by Clark and Karl (1982). In that study 77 percent of the predictions were within 40 percent of the observed values while about one-half were within 20 percent of the measured ozone values. In addition, the authors concluded that prognostic and climatological *meteorological variables alone* accounted for much of the day-to-day and site-to-site variations of the daily maximum one-hour average ozone concentrations. A similar analysis for wet and dry acidic deposition seems warranted.

## ACKNOWLEDGEMENTS

This paper was originally prepared by R. A. Pielke for the Wisconsin Department of Natural Resources (WDNR) as a contractors report entitled "An Assessment of the Trajectory Contractor's Methodology," 1983. It was modified for the purposes of the CIRA workshop. Besides the WDNR, support for this work was provided by EPRI contract No. RP-1630-53 and NPS project No. NA81RAH00001. Paul Koziar of WDNR is acknowledged for his support of the contractor study. Dallas McDonald and Loretta Wilson competently handled the preparation of the manuscript.

## REFERENCES


Clark, T.L., and T.R. Karl, 1982. Application of prognostic meteorological variables to forecasts of daily maximum one-hour ozone concentrations in the Northeastern United States. *J. Appl. Meteor.*, **21**, 1662–1671.

Eliassen, A., O. Hov, I.S.A. Isaksen, J. Saltbones, and F. Stordal, 1982. A Lagrangian long-range transport model with atmospheric boundary layer chemistry. *J. Appl. Meteor.*, **21**, 1645–1661.

Gifford, F.A., 1982. Horizontal diffusion in the atmosphere: a Lagrangian-dynamical theory. *Atmos. Environ.*, **16**, 505–512.

Johnson, W.B., 1983. Interregional exchanges of air pollution: model types and applications. *J. Air Pollu. Contr. Assoc.*, **33**, 563–574.

Lyons, W.A., R.H. Calby, and C.S. Keen, 1986. The impact of mesoscale convective systems on regional visibility and oxidant distributions during persistent elevated pollution episodes. *J. Clim. Appl. Meteor.*, **25**, 1518–1531.

Pielke, R.A., 1982. The role of mesoscale numerical models in very-short-range forecasting. In Nowcasting, K. Browning, ed., Academic Press, New York, 207–221.

Pielke, R.A., and Y. Mahrer, 1975. Representation of the heated planetary boundary layer in mesoscale models with coarse vertical resolution. *J. Atmos. Sci.*, **32**, 2288–2308.

Syrakov, D., G. Djolov, and D. Yordanov, 1983. Incorporation of planetary boundary layer dynamics in a numerical model of long-range air-pollutant transport. *Boundary-Layer Meteor.*, **26**, 1–14.

Takacs, J.F., D.B. Smith, and L.G. Lebowitz, 1985. Wisconsin Acid Deposition Trajectory Analysis Research Program. Report prepared for Dairyland Power Cooperative, La Crosse, Wisconsin, on behalf of the Wisconsin Acid Deposition Joint Technical Review Committee.

Warner, T.T., R.R. Fizz, and N.L. Seaman, 1983. A comparison of two types of atmospheric transport models – use of observed winds versus dynamically predicted winds. *J. Clim. Appl. Meteor.*, **22**, 394–406.

# Appendix A
# LIST OF ATTENDEES

Ray Arritt
Department of Atmospheric Science
Colorado State University
Fort Collins, CO 80523

Sumner Barr
Los Alamos Scientific Laboratory
Los Alamos, NM 87545

David Bigelow
Natural Resources Ecology Lab
Colorado State University
Fort Collins, CO 80523

Randy Borys
Department of Atmospheric Science
Colorado State University
Fort Collins, CO 80523

Patrick Burns
Department of Mechanical Engineering
Colorado State University
Fort Collins, CO 80523

Willard R. Chappell
Center for Environmental Science
University of Colorado at Denver
Denver, CO 80202

Mark Christon
Department of Mechanical Engineering
Colorado State University
Fort Collins, CO 80523

William Cotton
Department of Atmospheric Science
Colorado State University
Fort Collins, CO 80523

Dennis Fitz
AeroVironment, Inc.
825 Myrtle Avenue
Monrovia, CA 91016-3424

Douglas Fox
U.S. Forest Service
Rocky Mountain Experiment Station
240 W. Prospect Street
Fort Collins, CO 80521

James Gibson
Natural Resources Ecology Lab
Colorado State University
Fort Collins, CO 80523

David Greenland
Department of Geography
Campus Box 260
University of Colorado
Boulder, CO 80309-0260

William R. Jacobi
Department of Plant Pathology
and Weed Science
Colorado State University
Fort Collins, CO 80523

M. Iggy Litaor
Institute of Arctic and
Alpine Research
Campus Box 450
University of Colorado
Boulder, CO 80309-0450

William E. Marlatt
Department of Earth Resources
Colorado State University
Fort Collins, CO 80523

Mike Moran
Department of Atmospheric Science
Colorado State University
Fort Collins, CO 80523

Ralph Morris
Systems Applications, Inc.
101 Lucas Valley Road
San Rafael, CA 94903

Richard Olsen
Western Confiers Research Co-Op
200 S.W. 35th Street
Corvallis, OR 97333

Robert Pearson
Public Service Company
of Colorado
P.O. Box 840
Denver, CO 80201

James Purdom
NOAA/NESDIS/CIRA
Colorado State University
Fort Collins, CO 80523

Robert Sievers
Department of Chemistry
Campus Box 215
University of Colorado
Boulder, CO 80309-0215

Richard Sommerfeld
Rocky Mountain Forest and Range
Experiment Station
240 W. Prospect
Fort Collins, CO 80526

Don Stedman
Department of Chemistry
University of Denver
Denver, CO 80208

Larry Svoboda
U.S. E.P.A. Region VIII
999 18th Street
One Denver Place, Suite 1300
Denver, CO 80202-2413

John G. Watson
Atmospheric Sciences Center
Desert Research Institute
P.O. Box 60220
Reno, NV 89506

Birgit Wolff
National Center for Vehicle
Emission Control and Safety
205 Gibbons Building
Colorado State University
Fort Collins, CO 80523

Robert Yuhenke
Environmental Defense Fund
1405 Arapahoe Avenue
Boulder, CO 80302